PhD Thesis

Development of inks for tissue engineering of the dentoalveolar region through bioprinting

Mehdi Salar Amoli

Supervisor:
Prof. Dr. Veerle Bloemen
Co-supervisor:
Prof. Dr. Reinhilde Jacobs

Examination Committee:
Prof. Dr. Toon van Waterschoot
Prof. Dr. Ivo Lambrichts
Prof. Dr. Maria Cadenas de Llano Perula
Prof. Dr. Annabel Braem
Prof. Dr. Arn Mignon
Prof. Dr. Carlos Domingues Mota
Mr. Philippe Demoyer

Dissertation presented in partial fulfilment of the requirements for the degree of Doctor of Engineering Technology (PhD)

May 2023





OMFS
IMPATH

KU LEUVEN

GROUP T LEUVEN CAMPUS

Acknowledgements

I would like to express my deepest gratitude towards supervisors, colleagues, in addition to friends and family who supported me during this incredible journey. I would like to start by my supervisors, Prof. Veerle Bloemen, for her generous and caring support throughout my PhD, as well as her attention to detail coupled with her outlook on broader picture of the research direction reflected in her advice to me, and for guiding me in developing my ideas and on implementing them, and Prof. Reinhilde Jacobs, for her continues thoughtful support, valuable insights on my research, wisdom offered regarding the process, in addition to her attention to ensure my research is performed methodically and accurately.

I am grateful to Dr. Mostafa EzEldeen, whose knowledge, advice and suggestions have been instrumental since the early days of my PhD to the end, and to Dr. Resmi Anand, who was always available to generously offer her support as well as scientific expertise, and for incredible fruitful brainstorming talks we had.

I am thankful to my supervisory committee, Prof. Ivo Lambrichts, Prof. Maria Cadenas, Prof. Eleonora Ferraris and Mr. Philippe Demoyer, for the yearly meetings and discussions during which I had the pleasure of receiving valuable feedback on my research and my directions.

I am also thankful to the additional members of my examination committee, Prof. Carlos Mota for agreeing to join my committee and offering his valuable expertise, Prof. Arn Mignon, not only for joining my examination committee, but also for generously offering his valuable input and expertise on the chemistry during my PhD, Prof. Annabel Braem for joining my examination committee, and for the fruitful collaborations we've had, and to Prof. Toon Van Waterschoot for agreeing to chair my defence.

I also appreciate my friends and colleagues Paulo Alexandre Amorim, Hannah Agten, Sadegh Mousavi , Mahsa Esmailpour and Merve Kubra Aktan, for all their support, as well as collaborations and discussions we've had, and I am thankful to all members of the Skeletal Biology and Engineering (SBE) research center, the BioFabrication and Tissue Engineering (BioFaTe) research group, and the OMFS-IMPATH research group, including PhD students, postdocs, as well as

technicians and managers, for all the discussions, suggestions, and help they provided during the course of my PhD.

To my parents Hossein Salar Amoli and Parvin Bagheri, for their love, motivation and support throughout my academic career.

Abstract

Oral health issues in the dentoalveolar region are considered to have a significant impact on the individual's quality of life. Consequently, a range of treatment options have been developed to address complications in this region. However, certain shortcomings of these treatments have resulted in the exploration of regenerative strategies and tissue engineering approaches aimed at reconstructing tissue structures in this region. Within the tissue engineering approaches, the emerging technique of bioprinting, capable of potentially addressing limitations of traditional tissue engineering strategies, has recently gained widespread attention. This is because bioprinting has an enhanced potential to fabricate tissue analogues in a robust manner and with a high degree of geometrical resemblance to natural tissue by incorporating multiple biomaterials, cell types and biological factors within the manufacturing process.

Still, the application of bioprinting in dentoalveolar tissue engineering is a relatively unexplored field of study. The limited, recent research performed on this topic focuses mainly on the development of biomaterials and solutions to address the inherent heterogeneity within the dentoalveolar tissues. The aim of the research presented here is to combine both and to develop biomaterial-based strategies capable of being utilized in bioprinting and addressing heterogeneities such as the localized differentiation in dental pulp, the gradient structure of periodontal ligament interfacing bone and cementum, as well as the layered structure of the alveolar bone. In particular, this thesis focuses on the development of novel biomaterials which could be used as biomaterial inks, bioinks and drug delivery systems to bioprint constructs, and which are able to recapitulate the dentoalveolar structures.

To achieve this, first, an overview of the materials used for this application was made, highlighting the current demands in this field of research. Next, hydrogels based on chitosan and poly n-isopropylacrylamide were developed, and their ability to be used in the fabrication process, and to support viability of dental pulp stem cells was demonstrated. Being based on tunable chemistries, these biomaterials create a basis for the development of bioinks with variable

physical and mechanical properties for different tissues in the dentoalveolar region.

Addressing the heterogeneity in the dentoalveolar region could, aside from the development of suitable bioinks, further benefit from delivery of biological cues such as growth factors. As a result, a part of this thesis was dedicated to the development of microgels capable of delivering molecules within tissue engineering strategies. It was demonstrated that these microgels are capable of loading and sustained release of small molecules, and that they could be integrated in bioinks without having any negative impact on their printability.

Overall, the biomaterials developed in this thesis provide a solid basis for the fabrication of constructs through bioprinting which would be able to address the physical, mechanical and biological heterogeneity of the inherently complex dentoalveolar region.

Samenvatting

Mondgezondheidsproblemen in het dentoalveolaire gebied worden geacht een aanzienlijke invloed te hebben op de levenskwaliteit van het individu. Daarom is er een reeks behandelingsopties ontwikkeld om complicaties in dit gebied aan te pakken. Bepaalde tekortkomingen van deze behandelingen hebben echter geleid tot de verkenning van regeneratieve strategieën en weefselbouwkunde gericht op het reconstrueren van weefselstructuren in deze regio. Binnen de weefselbouwkunde heeft de opkomende bioprinttechnologie, die mogelijk in staat is de beperkingen van traditionele weefselbouwkunde aan te pakken, onlangs brede aandacht gekregen. Dit komt omdat bioprinten een groter potentieel heeft om weefselanalogen te vervaardigen op een robuuste manier en met een hoge mate van geometrische gelijkenis aan natuurlijk weefsel, door meerdere biomaterialen, celtypen en biologische factoren in het fabricageproces op te nemen.

Toch is de toepassing van bioprinten in dentoalveolaire weefselbouwkunde een relatief onontgonnen studiegebied. Het beperkte, recente onderzoek dat over dit onderwerp is uitgevoerd, richt zich voornamelijk op de ontwikkeling van biomaterialen en het vinden van oplossingen om de inherente heterogeniteit binnen de dentoalveolaire weefsels aan te pakken. Het doel van het hier gepresenteerde onderzoek is om beide benaderingen te combineren en strategieën te ontwikkelen die gebaseerd zijn op biomaterialen en die gebruikt kunnen worden bij bioprinten om die heterogeniteiten, zoals de gelokaliseerde differentiatie in tandpulp, de gradiëntstructuur van parodontaal ligament dat bot en cement verbindt, evenals de gelaagde structuur van het alveolaire bot, in rekening te brengen. Specifiek richt dit proefschrift zich op de ontwikkeling van nieuwe biomaterialen die kunnen worden gebruikt als biomateriaalinkten, bioinkten en medicijnafgiftesystemen voor geprinte implantaten, en die in staat zijn de dentoalveolaire structuren te recapituleren.

Om dit te bereiken, werd eerst een overzicht gemaakt van de materialen die reeds voor deze toepassing worden gebruikt, waarbij de huidige noden in dit onderzoeksgebied worden belicht. Vervolgens werden hydrogels ontwikkeld op basis van chitosan en poly-n-

isopropylacrylamide. Hun vermogen om te worden gebruikt in het fabricageproces en hun vermogen om tandpulpstamcellen te ondersteunen, werd aangetoond. Deze biomaterialen zijn gebaseerd op aanpasbare chemie en vormen een basis voor de ontwikkeling van bio-inkten met variabele fysische en mechanische eigenschappen voor verschillende weefsels in het dentoalveolaire gebied.

Het aanpakken van de heterogeniteit in het dentoalveolaire gebied zou, afgezien van de ontwikkeling van geschikte bio-inkten, verder kunnen profiteren van het incorporeren van biologische signalen zoals groeifactoren. Als gevolg hiervan was een deel van dit proefschrift gewijd aan de ontwikkeling van microgels die in staat zijn om moleculen af te leveren wanneer ze gebruikt worden voor weefselbouwkunde. Er werd aangetoond dat deze microgels in staat zijn om kleine moleculen op te slaan en langdurig vrij te geven, en dat ze kunnen worden geïntegreerd in bio-inkten zonder enige negatieve invloed op hun printbaarheid.

Over het algemeen bieden de biomaterialen die in dit proefschrift zijn ontwikkeld een solide basis voor de fabricage van implantaten door middel van bioprinten en zouden ze in staat zijn om de fysieke, mechanische en biologische heterogeniteit van het inherent complexe dentoalveolaire gebied aan te pakken.

List of Abbreviations

ANOVA	Analysis of Variance
APS	Ammonium persulfate
ASCs	Adipose derived stem cells
BMP	Bone morphogenetic protein
CAGR	Compound annual growth rate
CBCT	Cone beam computed tomography
CSR	Controlled shear rate
CT	Computed tomography
DLS	Dynamic light scattering
DMP	Dentin matrix protein
DMSO	Dimethyl sulfoxide
DPSCs	Dental pulp stem cells
DSPP	Dentin sialophosphoprotein
ECM	Extracellular matrix
FBS	Fetal bovine serum
FGF	Fibroblast growth factor
FTIR	Fourier Transform Infrared Spectroscopy
GAG	Glycosaminoglycan
gelMA	Gelatin methacrylate
GMSCs	Gingival mesenchymal stem cells
GPTMS	3-Glycidyloxypropyl trimethoxysilane
HA	Hyaluronic acid
HUVECs	Human umbilical vein endothelial cells
IGF	Insulin-like growth factor
iPSCs	Induced pluripotent stem cells
LAP	Lithium phenyl-2,4,6 trimethylbenzoylphosphintae
LCST	Lower critical solution temperature
LIFT	Laser induced forward transfer
LVE	Linear viscoelastic envelope
MA	Maleic anhydride
MA-C	Maleic anhydride grafted chitosan
MBA	Methylene bisacrylamide
MC	Methylcellulose
MEM	Minimum essential medium
MRI	Magnetic resonance imaging

MSC	Mesenchymal stem cells
NMR	Nuclear Magnetic Resonance
OPN	Osteopontin
PBS	Phosphate buffered saline
PCL	Polycaprolactone
PDGF	Platelet derived growth factors
PDI	Polydispersity index
PDL	Periodontal ligament
PDLSCs	Periodontal ligament stem cells
PEG	Poly (ethylene glycol)
PEGDMA	Poly(ethylene glycol) dimethacrylate
pHEMA	Poly hydroxyethyl methacrylate
PLA	Poly lactic acid
PLGA	Poly lactic-co-glycolic acid
pNIPAM	poly (N-isopropylacrylamide)
SCAPs	Stem cells from apical papilla
SDS	Sodium Dodecyl Sulfate
SEM	Scanning electron microscopy
SMC	Smooth muscle cells
SMDCs	Skeletal muscle derived cells
TEMED	Tetramethylethylenediamine
TGF-β	Transforming growth factor beta
VEGF	Vascular endothelial growth factor
VPTT	Volume phase transition temperature

Table of contents

CHAPTER 1. INTRODUCTION: TISSUE ENGINEERING OF THE DENTOALVEOLAR REGION THROUGH BIOPRINTING 1

Chapter Summary 2

1.1 General background 3
1.2 Bioink requirements for dentoalveolar tissue engineering 8
1.2.1 General requirements for a bioink material 8
1.2.2 Requirements of bioinks for dental pulp regeneration 9
1.2.3 Requirements of bioinks for dentin regeneration 11
1.2.4 Requirements of bioinks for periodontal ligament regeneration 11
1.2.5 Requirements of bioinks for alveolar bone regeneration 12
1.3 Bioinks 13
1.3.1 Natural polymers 16
1.3.1.1 Collagen based materials 16
1.3.1.2 Hyaluronic acid-based materials 19
1.3.1.3 Fibrin-based materials 21
1.3.1.4 Alginate-based materials 22
1.3.2 Synthetic polymers 23
1.4 Cells and growth factors 28
1.4.1 Cell types 29
1.4.1.1 Dental Pulp Stem Cells 29
1.4.1.2 Periodontal Ligament Stem Cells 29
1.4.1.3 Stem Cells from Apical Papilla (SCAPs) 30
1.4.1.4 Human Umbilical Vein Endothelial Cells (HUVECs) 30
1.4.2 Growth factors 30
1.4.2.1 Platelet derived growth factors (PDGF) 31
1.4.2.2 Insulin-like growth factor (IGF) 31
1.4.2.3 Transforming growth factor beta (TGF-β) 32
1.4.2.4 Fibroblast growth factor (FGF) 33
1.5 Delivery of growth factors 33
1.5.1 Scaffold-based systems 35
1.5.2 Micro/nano particles 36
1.5.3 Combined systems 36
1.6 Conclusions 37
1.7 References 38

CHAPTER 2. AIMS 57

2.1 Background 58
2.2 Overall aim 59
2.3 Specific chapter aims 59
2.3.1 Objective 1 (Chapter 3): Development and assessment of a chitosan based copolymer for bioprinting 59

2.3.2 Objective 2 (Chapter 4): Assessment of a pNIPAM based copolymer for bioprinting 59
2.3.3 Objective 3 (chapter 5): Development of a tunable thermo-sensitive bioink 60
2.3.4 Objective 4 (Chapter 6): Development of a delivery system for use in bioinks 60
2.3.5 Objective 5 (Chapter 7): preliminary assessment of encapsulating microgels in bioinks 60
2.3.6 Discussion 61
2.3.7 Valorization 61
2.4 References 61

CHAPTER 3. THE DEVELOPMENT OF A 3D PRINTABLE CHITOSAN-BASED COPOLYMER WITH TUNABLE PROPERTIES FOR DENTOALVEOLAR REGENERATION 63

Chapter summary 64
3.1 Introduction 65
3.2 Materials and methods 67
3.2.1 Materials 67
3.2.2 Preparation of hydrogels 67
3.2.2.1 Synthesis of maleic anhydride grafted chitosan (MA-C) 67
3.2.2.2 Preparation of genipin crosslinked MA-C/gelatin copolymers 67
3.2.3 Physico-chemical characterization 68
3.2.3.1 Fourier transform infrared spectroscopy 68
3.2.3.2 Proton nuclear magnetic resonance (^{1}H NMR) 68
3.2.3.3 Measurement of the crosslinking degree 68
3.2.3.4 Estimation of unreacted genipin 69
3.2.4 3D printing and physical characterizations of the scaffold 69
3.2.4.1 Evaluation of printing fidelity 69
3.2.4.2 Evaluation of the linear viscoelasticity of the material 70
3.2.4.3 Evaluation of surface morphology 70
3.2.4.4 Swelling and degradation studies 71
3.2.5 Evaluation of cellular response 71
3.2.5.1 Evaluation of cell viability through live/dead assay 71
3.2.5.2 AlamarBlue assay 72
3.2.5.3 DNA quantification 72
3.2.5.4 Statistical analysis 73
3.3 Results 73
3.3.1 Synthesis of MA-C 73
3.3.2 Physico-chemical characterization 73
3.3.2.1 Fourier transform infrared spectroscopy 73
3.3.2.2 Measurement of the degree of crosslinking in MA-C-gelatin copolymer 75
3.3.2.3 Estimation of unreacted genipin 76

3.3.3 3D printing and physical characterizations of the scaffold 77
3.3.3.1 Evaluation of printing fidelity 77
3.3.3.2 Evaluation of linear viscoelasticity 78
3.3.3.3 Swelling and degradation studies 80
3.3.3.4 Evaluation of surface morphology 81
3.3.4 Cellular response 82
3.3.4.1 Live/Dead assay 82
3.3.4.2 AlamarBlue assay 83
3.3.4.3 DNA quantification 84
3.4 Discussion 84
3.5 Conclusion 88
3.6 References 88

CHAPTER 4. DEVELOPMENT OF 3D PRINTED PNIPAM-CHITOSAN SCAFFOLDS FOR DENTOALVEOLAR TISSUE ENGINEERING 93

Chapter summary 94
4.1 Introduction 95
4.2 Materials and Methods 96
4.2.1 Materials 96
4.2.2 Methods 97
4.2.2.1 Sol-gel synthesis of chitosan-pNIPAM copolymer 97
4.2.2.2 Fourier transform infrared spectroscopy (FTIR) 97
4.2.2.3 3D printability of the scaffolds 98
4.2.2.4 Evaluation of degradation and swelling 98
4.2.2.5 Evaluation of surface morphology 99
4.2.2.6 Cell viability 99
4.2.2.7 Statistical analysis 100
4.3 Results 100
4.3.1 Sol-gel synthesis and characterization of pNIPAM-chitosan copolymer 100
4.3.2 Evaluation of printability 102
4.3.3 Evaluation of degradation and swelling 103
4.3.4 Evaluation of surface morphology 104
4.3.5 Evaluation of cell viability 105
4.4 Discussion 106
4.5 Conclusion 108
4.6 References 108

CHAPTER 5. DEVELOPMENT OF A THERMO-RESPONSIVE, PNIPAM-BASED BIOINK FOR TISSUE ENGINEERING OF DENTOALVEOLAR REGION THROUGH BIOPRINTING 113

Chapter summary 114
5.1 Introduction 115
5.2 Materials and Methods 118
5.2.1 Materials 118

5.2.2 Methods 118
5.2.2.1 Synthesis of pNIPAM-methylcellulose (MC-pNIPAM) ... 118
5.2.2.2 Methacrylation of MC-pNIPAM 119
5.2.2.3 Fourier Transform Infrared Spectroscopy (FTIR) 119
5.2.2.4 Proton Nuclear Magnetic Resonance (^{1}H NMR) 119
5.2.2.5 Evaluation of the LCST and critical gel formation concentration 120
5.2.2.6 Evaluation of water release 120
5.2.2.7 Hydrolytic degradation 121
5.2.2.8 Printability 121
5.2.2.9 Evaluation of cell viability 121
5.2.2.10 Statistical analysis 122
5.3 Results 122
5.3.1 Structural characterization 122
5.3.2 Evaluation of the LCST and gel formation 125
5.3.3 Evaluation of water release 127
5.3.4 Evaluation of hydrolytic degradation 127
5.3.5 Printability 128
5.3.6 Evaluation of hydrogel toxicity 129
5.4 Discussion 129
5.5 Conclusion 132
5.6 References 132

CHAPTER 6. DEVELOPMENT AND CHARACTERIZATION OF COLLOIDAL PNIPAM-BASED MICROGELS FOR DRUG DELIVERY IN DENTOALVEOLAR TISSUE ENGINEERING STRATEGIES 137

Chapter summary 138
6.1 Introduction 139
6.2 Materials and Methods 142
6.2.1 Materials 142
6.2.2 Methods 142
6.2.2.1 Synthesis of microgels 142
6.2.2.2 Structural characterization 143
6.2.2.3 Evaluation of volume phase transition temperature (VPTT) 143
6.2.2.4 Evaluation of microgel size in PBS 144
6.2.2.5 Evaluation of drug loading in the microgels 144
6.2.2.6 Evaluation of drug release from the microgels 145
6.2.2.7 Evaluation of microgel toxicity 145
6.2.2.8 DNA quantification 146
6.2.2.9 Statistical analysis 146
6.3 Results 146
6.3.1 Structural characterization 147
6.3.2 Evaluation of volume phase transition temperature (VPTT) 149
6.3.3 Evaluation of microgel size 150

6.3.4 Evaluation of drug loading in the microgels 151
6.3.5 Evaluation of drug release from the microgels 152
6.3.6 Evaluation of microgel toxicity 153
6.3.7 DNA quantification 154
6.4 Discussion *154*
6.5 Conclusion *157*
6.6 References *158*

CHAPTER 7. ENCAPSULATION OF PNIPAM-METHYLCELLULOSE MICROGELS IN GELMA AIMED AT BIOPRINTING DENTOALVEOLAR TISSUES: PRELIMINARY VALIDATIONS 165

Chapter summary 166

7.1 Introduction *167*
7.2 Materials and methods *170*
7.2.1 Materials 170
7.2.2 Methods 170
7.2.2.1 Synthesis of gelMA 170
7.2.2.2 Synthesis of microgels 171
7.2.2.3 Proton nuclear magnetic resonance 171
7.2.2.4 Evaluation of printability 171
7.2.2.5 Evaluation of microgel cytotoxicity 172
7.2.2.6 Differentiation study 173
7.2.2.7 Alizarin red staining 174
7.2.2.8 Quantitative real time polymerase chain reaction 174
7.2.2.9 Statistical analysis 175
7.3 Results *175*
7.3.1 GelMA synthesis 175
7.3.2 Evaluation of printability following microgel encapsulation 176
7.3.3 Evaluation of microgel cytotoxicity 177
7.3.4 Evaluation of DPSCs differentiation through alizarin red assay 178
7.3.5 Evaluation of DPSCs differentiation through qPCR 179
7.4 Discussion *180*
7.5 Conclusion *181*
7.6 References *182*

CHAPTER 8. GENERAL DISCUSSION 187

8.1 General discussion *188*
8.2 Conclusions and future perspectives *193*
8.3 References *198*

CHAPTER 9. VALORIZATION POTENTIAL OF THE RESEARCH 203

Chapter summary 204

9.1 Introduction *205*
9.2 Products and solutions *206*
9.3 Market *207*

9.4 Exploitation strategy....208
9.5 Challenges and competitors....209
9.6 Economic/social value....210
9.7 Valorization roadmap....211
9.8 References....212

CURRICULUM VITAE....215

List of figures

Figure 1.1. schematic representation of the dentoalveolar complex composed of a range of tissues (image obtained from https://smart.servier.com/) 4

Figure 1.2. An overview of a tissue engineering process highlighting bioprinting as a promising fabrication technique (figure made using elements from https://smart.servier.com/) 5

Figure 1.3. Most widespread bioprinting technologies (a) extrusion-based bioprinting (b) inkjet bioprinting and (c) light-based bioprinting through LIFT (figure made using adobe illustrator) 7

Figure 1.4. Schematic representation of cellular structures in dental pulp, image obtained from [54] 10

Figure 1.5. schematic representation of the structure of alveolar bone, image obtained from Bartold et al. 2019 [74] 13

Figure 1.6. different strategies for delivery of drugs and biomolecules within tissue engineering approaches. A) encapsulation of drugs within porous scaffolds, B) delivery of molecules through micro/nano particles and C) loading of drugs onto particles, loaded within tissue engineering systems such as hydrogels (figure made using biorender.com) 34

Figure 3.1. A) FTIR spectra of chitosan (top) and synthesized MA-C (bottom). B) ^{1}H NMR spectrum of maleic anhydride (top) and MA-C (bottom) in D2O, C) confirmation of crosslinking through FTIR analysis, the area between dashed lines represents peaks corresponding to primary amine groups. D) Measurement of crosslinking degree through ninhydrin assay (n=3). 75

Figure 3.2. The amount of unreacted genipin based on the crosslinking time. 77

Figure 3.3. A) computer aided design, arrows represent lines used for measurements in table 3.1 B) Printability of different gelatin, chitosan MA and genipin concentrations. 5 layer constructs, scale bar 5 mm 78

Figure 3.4. Mechanical spectra of gelatin/chitosan MA with low (0.5 wt.%) and high (2.5 wt.%) genipin contents, representative graph for three samples (A) hybrid hydrogel blends at the 3D printing temperature of 20 °C and (B) the chemical hydrogels at the physiological temperature of 37 °C. 79

Figure 3.5. A) swelling rate of printed hydrogel scaffolds B) Hydrolytic degradation rate of printed hydrogel scaffolds 81

Figure 3.6. Scanning electron microscopy of the cross-section of 3D printed hydrogels A) 0.5 wt% genipin, 200x B) 0.5 wt% genipin 500x C) 2.5 wt% genipin 200x D) 2.5 wt% genipin 500x 81

Figure 3.7. Viability of cells seeded on gels with different genipin concentrations, green represents live cells, red represents dead cells and blue represents cell nucleus, control sample represents cells cultured on a 2D surface.....82

Figure 3.8. A) AlamarBlue readings analyzed at day 1, 3, and 7 B) DNA concentration relative to hydrogel volume, analyzed at day 1, 3, and 7. Results shown as average +/- standard deviation, (n=3), ns shows no significant difference, * stands for difference ($p<0.05$), ** stands for difference ($p<0.01$), and **** stands for difference ($p<0.0001$), control sample consists of cells cultured on a 2D surface.....83

Figure 4.1. FTIR characterization of pNIPAM, chitosan and the copolymer with different ratios of constituents 101

Figure 4.2. A) Evaluation of print fidelity by measurement of perimeter ratio B) Evaluation of print fidelity by calculating the pr value C) evaluation of print resolution by measuring the area between the lines and D) printability in 3D.....102

Figure 4.3. A) Rate of scaffold hydrolytic degradation in water at 37 °C B) Rate of scaffold swelling at 37 °C.....104

Figure 4.4. Surface morphology of the scaffolds obtained through SEM 104

Figure 4.5. A) Live/dead viability assay of DPSCs seeded on the scaffolds and B) DNA quantification of DPSCs 105

Figure 5.1. FTIR spectra of methylcellulose, pNIPAM, MC-pNIPAM copolymer, and methacrylated MC-pNIPAM 124

Figure 5.2. ^{1}H NMR of methylcellulose, MC-pNIPAM and methacrylated MC-pNIPAM in DMSO.....125

Figure 5.3. Measurement of turbidity of the methacrylated MC-pNIPAM solution (n=3) 126

Figure 5.4. Demonstration of thermal gelation of the methacrylated MC-pNIPAM copolymer through vial tilting 126

Figure 5.5. Swelling rates of A. MC:pNIPAM 4:1, B. MC:pNIPAM 1:1 and C. MC:pNIPAM 1:4 in PBS.....127

Figure 5.6. Hydrolytic degradation of methacrylated MC-pNIPAM 127

Figure 5.7. A) Evaluation of perimeter ratio as a measure of strand fidelity, B) measurement of circularity factor as a measure of two-dimensional accuracy and C) printability in 3D.....128

Figure 5.8. Dental pulp stem cells encapsulated in methacrylated MC-pNIPAM with a MC:pNIPAM ratio of 1:1. 129

Figure 6.1. Structural characterization A. FTIR spectra and B. 1H NMR spectra of methylcellulose, pNIPAM and the microgels 148

Figure 6.2. A. VPTT of the microgels in DI water, B. VPTT of the microgels in PBS, and C. Half normal probability plot of the magnitude of different effects on VPTT, the red line has a slope of 1 and the blue light has a slope equal to Lenth's PSE 149

Figure 6.3. A. Size distribution of various microgel formulations suspended in PBS at 37 °C and B. Half normal probability plot of the effect estimates determining parameters with highest impact on microgel size, the red line has a slope of 1 and the blue light has a slope equal to Lenth's PSE 150

Figure 6.4. A. Loading of genipin onto different microgel formulations, n=3 B. Half-normal probability plot of the effect of different parameters on drug loading, the red line has a slope of 1 and the blue light has a slope equal to Lenth's PSE 151

Figure 6.5. Release of genipin from different microgel formulations into PBS at 37 °C A) cumulative release over time and B) comparison of release from different microgel formulations after 7 days 152

Figure 6.6. Viability of cells cultured for 7 days in presence of different microgel formulations, green color represent live cells, red color represent dead cells. Scale bar 500 µm.....153

Figure 6.7. DNA content of cells cultured for 7 days in presence of different microgel formulations (n=3).....154

Figure 7.1. 1H NMR spectra of top: gelatin and bottom: gelMA 176

Figure 7.2. Printability of microgel encapsulated gelMA. A) analysis of the perimeter ratio B) analysis of the circularity factor and C) printing of gelMA encapsulating microgels loaded with fluorescent sulforhodamine B.....177

Figure 7.3. Evaluation of the possible cytotoxicity of microgels through A) Live/dead assay, and B) DNA quantification (n=3).....178

Figure 7.4. Expression of OPN, DMP-1 and DSPP analyzed through qPCR after 21 days of culture 179

Figure 7.5. A) Alizarin red staining of cells cultured in differentiation medium, control samples cultured in base medium, and samples cultured in genipin supplemented medium for 21 days, and B) quantification of the alizarin red results. Scale bar 200 µm 179

Figure 8.1. Schematic representation of suggestive approaches for further utilization of the strategies developed in this thesis towards addressing the complexities in tissue engineering of the dentoalveolar region, the top picture represents a suggestive strategy for pulp-dentin regeneration, followed by alveolar bone and periodontal ligament. Abbreviations: pNIPAM: poly n-isopropylacrylamide, VEGF: vascular endothelial growth factor, DPSC: dental pulp stem cell, hUVEC: human umbilical vein endothelial cell, TGF: transforming growth factor, PDGF: platelet derived growth factor, SCAP: stem cells from apical papilla, IGF: insulin like growth factor, PDLSC: periodontal

ligament stem cell, MA-C: maleic grafted chitosan (figure elements obtained from smart.servier.com, and biorender.com).....197

Figure 9.1. Number of studies involving bioprinting from year 2000 to 2019, obtained from [12].....207

Figure 9.2. Suggested steps for valorization, completed steps are shown in green, steps that need to be taken are shown in blue 212

List of schemes

Scheme 3.1. Schematic representation showing the synthesis of maleic anhydride grafted chitosan, and copolymerization with gelatin through crosslinking with genipin. A) maleic anhydride reaction with methanol B) reaction of monomethyl maleate with pyridine C) overall reaction of MA-C synthesis D) synthesis of genipin crosslinked MA-C-gelatin copolymer.....74

Scheme 4.1. Schematic representation of the proposed reaction for synthesis of pNIPAM-chitosan copolymer.....100

Scheme 5.1. Schematic representation of the reaction of methylcellulose and pNIPAM, along with modification with methacrylic anhydride.....123

Scheme 6.1. Schematic representation of the reaction of NIPAM and methylcellulose, and synthesis of pNIPAM-methylcellulose copolymer.....147

Scheme 7.1. Synthesis of gelatin methacrylate through reaction with methacrylic anhydride.....175

List of tables

Table 1.1. Overview of the research on bioprinting of dental pulp, periodontal ligament and dentoalveolar bone. 14

Table 1.2. An overview of some candidate materials with potential to be used in bioprinting for pulp-dentin, along with cell types and biological cues useful for the purpose. 26

Table 1.3. An overview of some candidate materials with potential to be used in bioprinting for periodontal ligament and alveolar bone, along with cell types and biological cues useful for the purpose. 27

Table 3.1. Measurement of strand width in samples containing 1.5 %(w/v) MA-C, 3 %(w/v) gelatin and varying amounts of genipin. Line numbers correspond to different lines within a single printed shape, the lines are presented in the schematic in figure 3.3.A 78

Table 4.1. Different formulations used for sol-gel synthesis of hydrogels 97

Table 6.1. Composition of different microgel formulations. 143

Table 6.2. Analysis of the effect of different parameters on the loading capacity of the studied microgels. The most significant effect estimate is marked by *. 152

Table 7.1. Primer sequences 175

Chapter 1. Introduction: Tissue engineering of the dentoalveolar region through bioprinting

This chapter is adapted from:

"Materials for Dentoalveolar Bioprinting: Current State of the Art"

Mehdi Salar Amoli [a,b], Mostafa EzEldeen [b,c], Reinhilde Jacobs [b,d] , Veerle Bloemen [a,e]
[a] Surface and Interface Engineered Materials (SIEM), Campus Group T, KU Leuven, Andreas Vesaliusstraat 13, 3000 Leuven, Belgium
[b] OMFS IMPATH Research Group, Faculty of Medicine, Department of Imaging and Pathology, KU Leuven and Oral and Maxillofacial Surgery, University Hospitals Leuven, Kapucijnenvoer 33, 3000 Leuven, Belgium
[c] Department of Oral Health Sciences, KU Leuven and Paediatric Dentistry and Special Dental Care, University Hospitals Leuven, Kapucijnenvoer 33, 3000 Leuven, Belgium
[d] Department of Dental Medicine, Karolinska Institutet, Stockholm, Sweden
[e] Prometheus, Division of Skeletal Tissue Engineering Leuven, KU Leuven, Leuven, Belgium

Published in Biomedicines, 2022; 10, 71

Chapter Summary

Although current treatments can successfully address a wide range of complications in the dentoalveolar region, they often still suffer from drawbacks and limitations, resulting in sub-optimal treatments for specific problems such as tooth loss in pediatric patients. As a result, significant progress has been made in the last decades in the field of tissue engineering aiming at restoring damaged tissues via a regenerative approach. Yet, the translation into a clinical product is still challenging. Novel technologies such as bioprinting have been developed to solve some of the shortcomings faced in traditional tissue engineering approaches. Using automated bioprinting techniques allows for the precise placement of cells, biological molecules, materials, as well as for geometrical patient specific design of produced biological scaffolds. Recently, bioprinting has also been introduced into the field of dentoalveolar tissue engineering. However, the dentoalveolar region is a complex tissue structure composed of a range of tissues with heterogeneous physicomechanical and biological properties. Consequently, the choice of a suitable material to encapsulate cells in the development of so-called bioinks for bioprinting dentoalveolar tissues, and strategies to address the biological heterogeneity of these structures, are still challenges faced in the field. This chapter therefore aims to provide an overview of the current state of the art, by discussing the main bioprinting technologies available, the progress of the research on materials used for dentoalveolar bioprinting, and strategies useful for addressing the inherent heterogeneity of these tissue structures.

1.1 General background

Oral health is considered as an integrated part of general health [1] posing a major health burden for many countries [2]. Periodontitis, a condition which can lead to bone resorption and eventually tooth loss [3], is the sixth most common human disease with a high global prevalence of 45–50 % [4]. While inequities still exist in the burden of oral disease worldwide, the prevalence rate of elderly people (65–74 years) having lost all their natural teeth varies from 5% to 51% in Europe, undermining the patients quality of life significantly [5]. Apart from periodontitis, missing teeth can also be caused by dental trauma, caries, pulp necrosis, tooth agenesis, tumor resection and/or cyst removal [6].

While there are ample treatment options to intervene, slow down or stop the pathological process, eventual tooth and bone loss are deterministic and characterized by a lack of dentoalveolar regenerative capacity [7]. The current gold standard for treatment of tooth loss is the use of dental implants. Apart from dealing with a non-biological replacement, there is an age-related aspect hampering implant placement in children, where the osseointegration of the implant may prevent the natural process of concomitant bone growth with tooth eruption [8]. While techniques such as tooth autotransplantation, involving surgical repositioning of a tooth from one position to another, have addressed the issue well. Yet, the technique is still limited by challenges such as stringent patient selection with regards to age, donor tooth and root length, suitability of recipient site, presence of sufficient alveolar bone support, and the orthodontic requirement of tooth extraction [9–13].

The challenges associated with current treatment options have led to the exploration of regenerative strategies, aiming to develop biological substitutes that can restore, maintain or improve the function of tissues [14]. In the field of tissue engineering, a subfield of regenerative medicine, the aim is to fabricate such a tissue analogue by combining principles of life sciences and engineering [15]. This could potentially offer a sustainable solution to complications such as alveolar ridge resorption, tooth loss, condylar resorption, and craniofacial defects.

Several tissue engineering approaches have been explored for the regeneration of dentoalveolar tissues. As a first step, regeneration of the pulp-dentin complex has been the focus [16] by using scaffolds based on natural polymers such as collagen [17], synthetic polymers such as poly lactic acid (PLA) [18], or through injectable hydrogels [19]. Other strategies have been implemented to regenerate periodontium tissues, including the incorporation of guided tissue/bone regeneration membranes [20], and several natural/synthetic scaffolds or transplantation strategies have been explored for the regeneration of impacted bone [21]. While these efforts have been promising, there are still challenges associated with the lack of tissue formation, the possibility of immunological rejection, the difficulty of delivering required growth factors efficiently, the inability to control the type of formed tissue, the possible shortage of cells in the defect area and a lack of microvasculature formation [20–25].

However, the main challenge rises from the fact that the dentoalveolar complex is a hybrid organ composition. As shown in figure 1.1, it is made of highly specialized nerves and mechanoreceptors, ligaments, enamel, dentin, root, cementum, and bone. Current regenerative practices are focused on regenerating individual tissues without addressing specific physical, mechanical and biological heterogeneities and thus, they fail to mimic and to regenerate such complex tissue architectures.

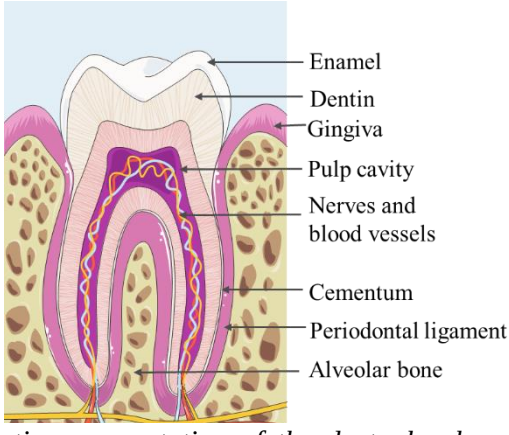

Figure 1.1. schematic representation of the dentoalveolar complex composed of a range of tissues (image obtained from https://smart.servier.com/)

Aiming to solve some of these challenges, bioprinting is an emerging technique which allows for the production of patient specific implants through an automated process of fabrication, enhancing the ability to control cell positioning and increasing the possibility of upscaling, while improving the outcome by reducing the variability, and increasing robustness. A schematic overview of tissue engineering and the role of bioprinting in the process is presented in figure 1.2.

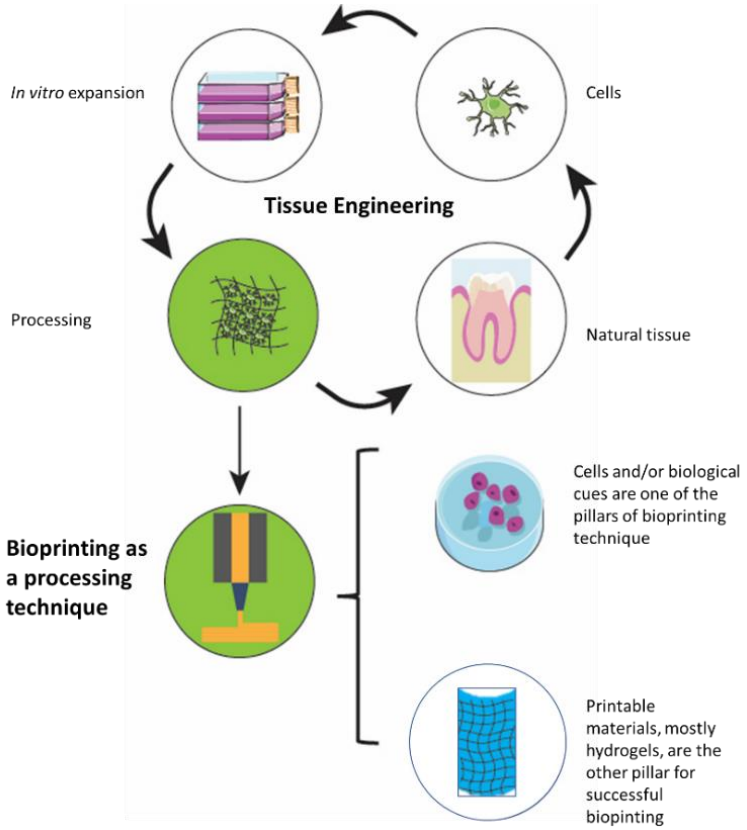

Figure 1.2. An overview of a tissue engineering process highlighting bioprinting as a promising fabrication technique (figure made using elements from https://smart.servier.com/)

Being a 3D fabrication method based on computer aided designs, bioprinting aims to use 3D designs retrieved from computed tomography (CT), cone beam computed tomography (CBCT) or magnetic resonance imaging (MRI), and presents the opportunity to produce patient-specific constructs addressing specific needs of

individuals, in addition to facilitating direct placement of different biomolecules, cells and scaffold materials, known as bioinks, in desired locations [26]. Additionally, the possibility to use different bioinks in one process enhances the ability to mimic the complexities of the natural tissue. This ability has been represented in bioprinting of vasculature using coaxial nozzles and carbon nanotube reinforced alginate [27] or by using sacrificial Pluronic F127 [28], in bioprinting of nerve conduits using novel stereolithographic techniques [29], or in development of liver models for drug testing [30].

While research on bioprinting in the field of dentoalveolar region is still in its early stages, this enhanced ability to replicate natural structures has resulted in hope to address several specific clinical conditions. Dental carries is one of these conditions, affecting two billion people worldwide [31]. Current treatments, such as pulpectomy followed by root canal filling, removes the vital pulp tissue, resulting in a possibility for periodontal lesions, root fracture and eventually tooth loss [32,33], and traditional tissue engineering techniques cannot closely mimic the complex structure of the pulp [34]. Furthermore, treatments for periodontitis are time consuming, can be undermined by pre-existing conditions such as diabetes or cardiovascular disease, and most importantly, are not successful in 20-30 % of cases. Furthermore, Restoring lost tissue (bone & periodontal ligament interface) after periodontitis is challenging and is limited to small size defects [3]. Consequently, tissue engineering has been suggested to recreate a functioning periodontal tissue, facing limited success due to variable results and difficulty in recapitulating the complex structure interfacing bone and cementum [35,36]. Moreover, alveolar bone loss caused by periodontitis, trauma, surgical interventions or other causes, is currently treated using bone grafts. While autografts are the gold standard for treatment of alveolar bone loss, they are limited by the availability of autologous tissue, donor site morbidity and potential related complications such as infections [37]. Alternative sources are also faced with challenges such as immune rejection or limited long term survival in xenografts [38,39], or limited integration with host tissue in cases of natural or synthetic grafts. This has resulted in the exploration of tissue engineering strategies which still require further innovations to effectively replicate the complexities of the alveolar

bone structures [40]. Consequently, different bioprinting technologies have been employed aiming to achieve clinical solutions for these issues.

Most widespread bioprinting technologies include extrusion bioprinting, inkjet bioprinting or light-based bioprinting. In the extrusion process, a filament of biomaterial is formed which will be placed on the substrate in a layer-by-layer manner, forming the 3D construct [41]. While in inkjet printing droplets of the material are formed through piezoelectric or thermal methods, and droplets are deposited on the substrate in a drop-on-demand fashion, resulting in formation of 3D tissue model [42]. Light based strategies encompass a range of solutions and modalities employing the energy of light to develop the 3D tissue models. These include strategies such as stereolithography bioprinting and digital light processing, where illumination of a cell encapsulated resin results in hydrogel formation, without or with use of photomasks, respectively [43][44], two photon polymerization where in a similar method direct writing in cell encapsulated hydrogel takes place [45], in addition to volumetric bioprinting where the illumination takes place in 3D resulting in a remarkably faster bioprinting process [46]. Laser induced forward transfer (LIFT) is another light-based technique where application of laser to a donor layer results in ejection of cell encapsulated droplets and formation of 3D constructs on the substrate [47].

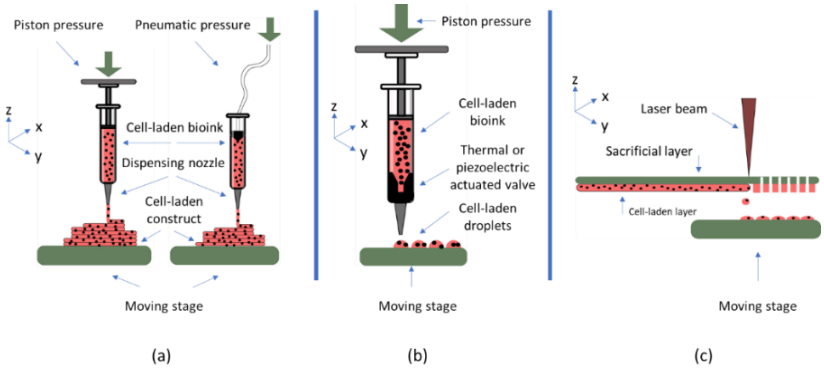

Figure 1.3. Most widespread bioprinting technologies (a) extrusion-based bioprinting (b) inkjet bioprinting and (c) light-based bioprinting through LIFT (figure made using adobe illustrator)

As bioprinting relies on cell and growth factor encapsulated biomaterials, there are several aspects affecting the success of this tissue engineering approach. First, the choice of materials to be used as the ink, has a significant impact on the outcome of the process. In addition to the materials used, delivery of specific biological factors can affect behavior of encapsulated cells to a significant degree, assisting in tackling the challenge of biological heterogeneity, specifically in complex areas such as the dentoalveolar region.
The next section will therefore describe the properties required for bioinks aimed at regeneration of specific tissues in the dentoalveolar region, followed by a detailed description of the materials that have been used as bioinks so far. Following this, an analysis of the delivery approaches capable of being used to deliver growth factors with the ability to induce specific cell behaviors in the dentoalveolar region will be presented.

1.2 Bioink requirements for dentoalveolar tissue engineering

1.2.1 General requirements for a bioink material

Bioinks are usually biomaterials encapsulating cells, which will then be deposited on a substrate via bioprinting strategies to form three dimensional constructs. Consequently, biomaterials used for this purpose must possess a range of biological and physicochemical properties, depending on the target tissue and the bioprinting modality used. In general, these materials are in direct contact with the cells. Therefore, one of the most important qualities they must possess is biocompatibility. In the context of bioprinting, biocompatibility encompasses both the absence of cell toxicity and the presence of cell adhesion cues. This is significantly influenced by the water content, facilitating the transfer of oxygen and nutrients to the cells [48]. Furthermore, these materials need to be biodegradable, as they need to be replaced by extracellular matrix components produced by the cells. As a result, it is important for the degradation profile of the tissue engineering constructs to match the regeneration rate of the extracellular matrix (ECM) by the cells [49]. Furthermore, mechanical properties, such as stiffness, must match those of the target tissue to provide a favorable environment for cellular activities [50]. Moreover,

the possibility of a rapid gelation is of extreme importance for the bioink to keep its shape upon deposition on the substrate [51].
In addition to these general requirements, each bioprinting modality imposes additional considerations on the choice of material. In extrusion-based bioprinting, the material needs to form a filament upon ejection from the nozzle. During the process, shear stress is applied to the cell encapsulating material introducing the possibility of damage to the cells, thus, properties such as shear thinning, and yield stress of the material must be considered [52]. While in extrusion-based bioprinting the viscosity of the material should be in the range of 3 to 6×10^8 mPa/s, the viscosity in inkjet printing has to be much lower and in the range of 3.5 to 12 mPa/s [53]. This is because in this technique, different methods such as thermal or piezoelectric actuation are used to produce droplets of the material, rather than filaments. Furthermore, bioinks for this printing modality need to have rheopectic properties rather than shear-thinning properties, meaning there needs to be an increase in viscosity upon application of shear force, leading to droplet formation. As for laser-based bioprinting, the bioink should be able to adhere sufficiently to the sacrificial layer and spread uniformly on it. Additionally, it needs to possess high viscoelasticity enabling the formation of material jets. The viscosity of the material used for this bioprinting modality is usually in the range of 1 to 300 mPa/s [53].
As the target tissue of the regeneration process has a significant effect on requirements of the bioink, and the modality chosen, the main characteristics of most important dentoalveolar tissues and required material properties for each tissue are described in the following sections.

1.2.2 Requirements of bioinks for dental pulp regeneration

Dental pulp is a connective tissue composed of cells embedded in a collagen-based ECM, 75 % of which is consisted of water, hence, encouraging the use of hydrogels as tissue engineering scaffolds. As demonstrated schematically in figure 1.4 obtained from [54], the pulp core, containing fibroblasts, is surrounded by a cell-rich zone accommodating dental pulp stem cells (DPSCs) along with fibroblasts. Surrounding this cell-rich zone, there is a cell free zone housing the capillary network along with nerves. Finally, in the interface with

dentin, lies the peripheral area of the pulp containing odontoblasts, differentiated from the stem cells in the cell-rich zone [55,56]. This heterogeneity within the cell types present in dental pulp must be taken into account when designing a bioink for this tissue. The most important parameter to consider in this regard would be the localized differentiation of the DPSCs in the interface with dentin, and presence of undifferentiated stem cells in the core [57].

Furthermore, the pulp tissue, consisting of collagen fibers, proteoglycans and cells, is the only soft tissue inside the tooth. This tissue exhibits a gel-like linear viscoelastic behavior with a storage modulus of approximately 100 Pa and a loss modulus of around 10 Pa. This tissue possesses a Young's modulus of 0.8 ± 0.4 kPa and a toughness value of 37.7 ± 19.1 kPa, along with a time-dependent stress relaxation caused by the viscoelasticity [58]. These mechanical properties have been known to have a significant effect on activities of DPSCs such as proliferation and differentiation, enabling control over cellular behavior in the tissue engineering construct [59]. Consequently, it is important for the hydrogels used for bioprinting strategies to represent these mechanical properties to create a favorable environment for the native cells to function and regenerate natural tissue.

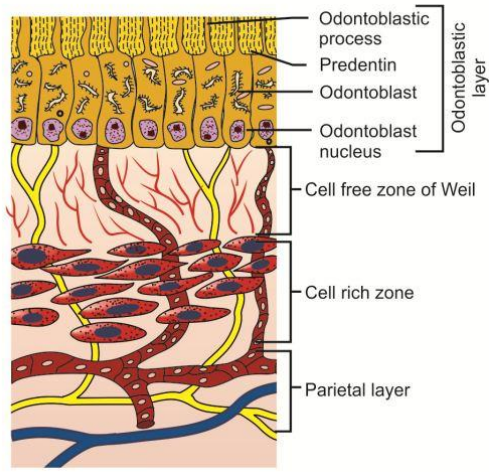

Figure 1.4. Schematic representation of cellular structures in dental pulp, image obtained from [54]

1.2.3 Requirements of bioinks for dentin regeneration

Odontoblasts present in the outer layer of the pulp have the principal function of producing dentin during tissue formation and tissue regeneration. Consequently, provided a favorable environment, stem cells in the dental pulp are capable of regenerating dentin tissue. However, this regeneration process could be enhanced by using scaffolds, and bioprinting enables the production of scaffolds closely resembling the complex structure of dentin. Dentin itself is a mineralized, tubular structure surrounding the pulp, and it is composed mainly of hydroxyapatite crystals [60]. It has a very complex structure with a range of properties depending on the location, the alignment of microtubules and the density of mineralization, with a Young's modulus ranging from 17 GPa in regions close to the pulp, to 42 GPa in center regions [61].

While dentin is deposited by odontoblasts, the microenvironment is known to have a significant effect on the behavior and activity of these cells. Consequently, replication of the tubules, their structure and their mechanical properties can have a significant effect on the success of the tissue engineering process [62]. For example, the microporosity of the material must allow the cells to extend their cytoplasm on the surface and regenerate the tissue. A pore size of approximately 300 μm is known to provide sufficient space for odontoblasts to regenerate dentin-like tissue [63].

1.2.4 Requirements of bioinks for periodontal ligament regeneration

Periodontal ligament (PDL) is a specialized and vascularized soft connective tissue, mainly composed of collagen fibers, surrounding the tooth and filling the space between the tooth and its socket in the alveolar bone. PDL is tasked with supporting the dental structure, providing sensory information and assisting in regeneration of damaged tissue, as well as with maintaining homeostasis in osteogenesis of alveolar bone. A wide variety of cell types are present in PDL, including fibroblasts, bone-related cells such as osteoblasts and osteoclasts, cementoblasts and cementoclasts, and periodontal

ligament stem cells (PDLSCs), which are used widely for tissue engineering of PDL and other dentoalveolar tissues [64].
The inherent complexity of the PDL tissue and its behavior in reaction to stress, along with differences in characterization techniques, have resulted in a range of analytical and experimental models to analyze the mechanical behavior of the material. These include the assumption of PDL as an isotropic homogeneous tissue with linear elastic properties, hyperelastic models, and viscoelastic models describing behaviors such as force-relaxation and hysteresis [65,66]. However, the non-linear time dependency of the PDL behavior with regard to tooth movement has been shown in several experimental studies [67]. While there are discrepancies in the reported literature with regard to the physical and mechanical properties of PDL [65,66], from a tissue engineering standpoint, the most important requirement is to ensure the regeneration of a functional support for the tooth, and to provide the proper environment for the stem cells to enable this regeneration. For this purpose, time-dependent viscoelasticity has been reported to best reflect the mechanical behavior of natural PDL. Such models have been developed and discussed in detail in various studies [68–70] and a Young's modulus of 5×10^6 N/m^2 and a Poisson's ratio of 0.45 have been experimentally detected for the PDL [71]. These properties such as mechanical loading and stiffness are known to have a significant effect in modulation of proliferation and differentiation of PDLSCs [72], where cell proliferation increased significantly with an increased stiffness in the range of 6 to 135 kPa, and a higher osteogenic differentiation was reported in stiff substrates [73]. Consequently, being mindful of these properties in a bioink is extremely important in efforts towards controlling the behavior of encapsulated or invading cells and the regeneration of a functional tissue.

1.2.5 Requirements of bioinks for alveolar bone regeneration

Alveolar bone is a flexible ridge of the jaw that incorporates tooth sockets and supports the dental structures. Alveolar bone is made up of several layers, and their differences should be considered in any tissue engineering effort aimed at these tissues. As shown in figure 1.5, obtained from [74], these layers are the periosteum, alveolar bone proper, cancellous bone and cortical bone [75]. This structure easily

responds to different stimuli such as tooth loss, usually in the form of resorption which can cause major challenges in other treatment strategies such as implant placement. Similar to other bones in the body, alveolar bone is highly mineralized with the majority of mineral content being semi-crystalline hydroxyapatite. Furthermore, 70% of its structure is composed of an organic matrix, the main component of which is collagen type I. It includes 2 to 5 % cells, mostly being bone lining cells, osteoblasts, osteoclasts and osteocytes [76].

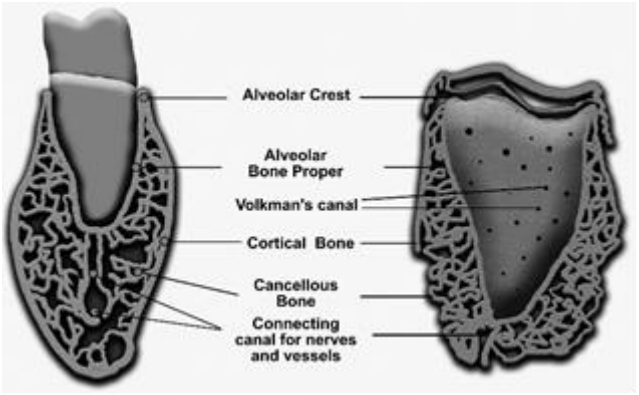

Figure 1.5. schematic representation of the structure of alveolar bone, image obtained from Bartold et al. 2019 [74]

Tissue engineering of the bones in the alveolar region requires consideration of their differences with other bones in the body in terms of their functional activities, including the load applied during physical activities of the face [77]. Consequently, the bioink needs to support the bioactivity of different cell types present, and account for differences in mechanical properties of different layers of the bone. The most important mechanical property to replicate is the Young's modulus, which is approximately 13.7×10^9 N/m^2 in high density alveolar bone and close to 0.9×10^9 N/m^2 in cancellous alveolar bone [71,78]. Moreover, a pore size of 150-500 μm has been known to facilitate bone tissue regeneration and formation of vasculature [79].

1.3 Bioinks

Hydrogels, a class of materials comprised of vast, water-encapsulating polymeric networks, are the most common class of materials used for bioprinting. This is due to their favorable properties which could meet

the general requirements for a bioink, including large water content resembling the natural ECM, support of cell attachment, growth and differentiation, in addition to biodegradability and viscoelastic properties [80,81]. Hydrogels used for bioprinting in the dentoalveolar region can be divided into two main categories, hydrogels based on natural polymers and synthetic polymers. Natural hydrogels used in this field could be further classified into hydrogels based on collagen, hyaluronic acid, fibrinogen and alginate. An overview of the materials used for bioprinting dentoalveolar tissues is presented in table 1.1, along with the modality used for bioprinting using these, and the nozzle size representing an estimate of the resolution of the bioprinted structures. The table also presents whether or not these materials have been used for *in vivo* experiments, demonstrating how far the research on these materials has gone towards potential clinical applications. The classes of materials are further discussed in detail in this section.

Table 1.1. Overview of the research on bioprinting of dental pulp, periodontal ligament and dentoalveolar bone.

Study	**Tissue**	**Bioprinting strategy**	**Material used**	**Nozzle size µm (Gauge)**	***in vivo ?***
Tian et al., 2021 [82]	Alveolar bone	Extrusion	sodium alginate + gelatin + nano hydroxyapatite	400 (22)	×
Amler et al., 2021 [83]	Alveolar bone	Stereolitography	gelatin methacrylate	N/A	×
Amler et al., 2021 [84]	Alveolar bone	Stereolitography	gelatin methacrylate + methacrylated hyaluronic acid	N/A	×
Walladbegi et al., 2020 [85]	Alveolar bone	Extrusion	β-TCP + nanofibrillated cellulose/alginate	Coaxial (inner-outer): 406–535 (22-18) 406–885 (22-16) 406-1295 (22-14)	×

Dubey et al., 2020 [86]	Alveolar bone	Inkjet	ECM-based hydrogel + self-assembling FEFEFKFK octapeptide + amorphous magnesium phosphates	N/A	✓
Chimene et al., 2020 [87]	Alveolar bone	Extrusion	gelatin methacrylate + kappa-carrageenan + nanosilicates	400 (22)	×
Ma et al., 2017 [88]	Alveolar bone	Inkjet	gelatin methacrylate + poly (ethylene glycol)	150 (30)	✓
Kuss et al., 2017 [89]	Alveolar bone	Extrusion	methacrylated hyaluronic acid + gelatin methacrylate	400 (22G)	×
Kang et al., 2016 [90]	Alveolar bone	Extrusion	gelatin + hyaluronic acid + fibrinogen + glycerol	300 (23G)	✓
Campos et al., 2016 [91]	Alveolar bone	Extrusion	collagen type I + agarose	600 (20)	×
Ono et al., 2021 [92]	Periodontal ligament	In-house - single cell printing	N/A	240 (26)	×
Lee et al., 2021 [93]	Periodontal ligament	Extrusion	collagen + FGF-2	400 (22G)	✓
Raveendran et al., 2019 [94]	Periodontal ligament	Extrusion	gelatin methacrylate	220 (25, 27)	×
Ma et al., 2015 [95]	Periodontal ligament	Inkjet	gelatin methacrylate + poly (ethylene glycol) dimethacrylate	150 (30)	×
Lin et al., 2021 [96]	Pulp-dentin	Extrusion	calcium silicate reinforced gelatin methacrylate	30 (150)	×
Han et al., 2021 [97]	Pulp-dentin	Extrusion	fibrinogen – gelatin - demineralized dentin matrix particles	300 (23)	×
Han et al., 2019 [57]	Pulp-dentin	Extrusion	fibrinogen + gelatin + hyaluronic acid + glycerol	300 (23)	×

Athirasala et al., 2018 [98]	Pulp-dentin	Extrusion	alginate + dentin matrix	450 (22)	×
Park et al., 2020 [99]vv	Dental pulp	Extrusion	BMP-mimetic peptide modified GelMA + gelatin + hyaluronic acid + glycerol	330 (23)	×
Campos et al., 2019 [100]	Dental pulp	Inkjet	agarose + collagen type I + fibrinogen	300 (23)	×
Betsch et al, 2018 [101]	Dental pulp / cornea / articular cartilage	Inkjet	agarose + collagen type I	300 (23)	×

1.3.1 Natural polymers

1.3.1.1 Collagen based materials

Collagen is one of the main components of the natural ECM, consequently, it has an excellent biocompatibility making it a very interesting option for different tissue engineering strategies. Moreover, it can form hydrogels at 37 ˚C and thus allows for the encapsulation of cells. In the dentoalveolar field, dental pulp stem cells (DPSCs) encapsulated in collagen type I and II have shown a viability of over 95 % [102]. However, its low mechanical properties have made it essential to explore the possibility of combining collagen with other materials, incorporating crosslinking modalities, or performing modifications on natural collagen in order to use it for bioprinting [103]. Through such modifications, collagen has been widely used in inkjet [104], extrusion-based [103], and laser-based [105] bioprinting for the regeneration of different tissues including skin [106], bone, cartilage tissue [107], cardiovascular [108], liver [109] and nervous tissues [110], in addition to the dentoalveolar tissues.

In dentoalveolar bioprinting, agarose was used by Campus et al., to increase the viscosity, and enhance the mechanical properties of collagen for inkjet bioprinting of alveolar bone, enabling bioprinting of

complex structures. While the increased agarose content reduced cell spreading, the increased stiffness resulted in a higher differentiation of mesenchymal stem cells (MSCs) [91]. However, a compressive modulus ranging from 18.1 ± 3.5 kPa to 89.1 ± 13.9 kPa, compared to natural bones 110 MPa, could potentially lead to complications in integration of the after implantation, especially in load bearing regions [91,111], highlighting the need to consider the incorporation of mechanically stronger materials such as thermoplastic polymers [112]. However, in a subsequent study, the same material, plus fibrinogen, was used for bioprinting of dental pulp [100]. The mechanical properties obtained for the material without fibrinogen [91], suggest the properties to be more suitable for regeneration of dental pulp than bone. Still, a storage modulus and loss modulus of approximately 280 and 20 Pa, respectively, are significantly higher than those of natural tissue, demonstrating room for improvement of the bioink in terms of physical properties. Interestingly, a co-culture of DPSCs and human umbilical vein endothelial cells (HUVECs) resulted in the formation of microvessels in the bioprinted structures within 14 days of *in vitro* culture, a very important requirement for regeneration approaches directed towards dental pulp [100].

While collagen in its native form is being used for bioprinting and tissue engineering strategies, the denatured form of the protein derived from its hydrolysis, gelatin, is used much more extensively. Retaining the RGD sequences present on collagen, gelatin is also highly biocompatible, in addition to the fact that it does not trigger an immune response and it is more cost-effective than collagen [113]. Furthermore, the need for a rapid and efficient crosslinking in the field of bioprinting has given rise to the use of a gelatin derivative called gelMA, which is gelatin functionalized with methacryloyl groups [114]. The possibility of encapsulating mouse dental pulp cells (OD-21) in gelMA has led to viabilities of over 80 % [115] and 90 % [116] in different studies. The reduced viability as compared to collagen can be attributed to the presence of photoinitiators, toxic by nature, and UV irradiation, as it was determined that increasing the crosslinking time could reduce the viability [115]. Furthermore, similar to collagen, encapsulation of DPSCs and HUVECs in the material has resulted in formation of vasculature [117].

One step beyond the studies only performing cell encapsulation, a combination of gelMA and poly(ethylene glycol) dimethacrylate (PEGDA) has been used in inkjet bioprinting for the regeneration of periodontal tissue. While incorporation of PEG resulted in enhanced control over droplet size, PDLSCs encapsulated in this material demonstrated a higher viability and spreading in higher gelMA concentrations [95], the same tradeoff observed in collagen combinations, which could potentially be addressed by incorporation of cell binding motifs to account for lack of bioactivity on PEG [118]. Further properties of this bioink were analyzed in a study aimed at regeneration of alveolar bone, where a stiffness in the range of 4.5 kPa to 23.5 kPa was observed and *in vivo* analysis resulted in bone formation within 6 weeks of implantation [88]. Still, a lack of further in-depth characterizations and the relatively rapid degradation of around 80 % in two weeks leads to questions about structural integrity in the long-term, showing room for further research.

In addition to inkjet, gelMA has also been used as the base material for extrusion-based bioprinting strategies in the dentoalveolar region. For this application, optimization of parameters such as polymer concentration, photoinitiator type and concentration, UV exposure time and printing parameters can have a significant effect on the outcome, as shown by Raveendran et al. [94]. However, limitations imposed by parameters such as polymer concentration lead to the need for exploration of complementary strategies, such as the use of polymeric support rather than increasing polymer concentration, as shown in the study by Kuss et al., where incorporation of polycaprolactone / hydroxyapatite resulted in a compressive modulus of around 50 MPa, much closer to natural bone than the compressive modulus of the pure hydrogel [89]. In addition to mechanical properties, strategies to induce angiogenesis are essential for the regeneration of functional tissues. While some studies have suggested a co-culture of HUVECs and region-specific stem cells [100,117], post processing by subjecting stromal vascular fraction cells encapsulated in bioprinted constructs to short-term hypoxia was shown by Kuss et al., to significantly enhance vascularization [89]. A comparison of these methods could potentially lead to a better understanding of the angiogenesis within the engineered constructs.

As described, there is widespread interest in using collagen-based materials for bioprinting strategies in the dentoalveolar tissue engineering. Still, a wide range of modifications remain unexplored in this field. The use of collagen derivatives such as methacrylated collagen which is photocrosslinkable [119], compositing collagen with molecules such as calcium phosphates [120], crosslinking of collagen [121] or printing along with stronger thermoplastic polymers [122] are some of these modifications, in addition to exploring options to exert control over physicomechanical properties of gelMA. These options could range from blending with viscosity enhancing materials such as gellan gum [123], relying on the inherent temperature behavior of gelMA [124], or compositing gelMA with materials such as calcium phosphates [125], or polysaccharides [126], to chemical modifications of gelatin with acrylamides [127], styrene groups [128], norbornene [129] etc. Incorporation of such strategies could present a path towards addressing some of the challenges faced in using collagen-based materials.

1.3.1.2 Hyaluronic acid-based materials

Hyaluronic acid (HA) is a glycosaminoglycan (GAG) abundant in the ECM of many soft tissues. As a result, it is biocompatible, biodegradable, does not trigger an immune response and is non thrombogenic. Possessing shear thinning properties in addition to these, hyaluronic acid has been used extensively in the field of tissue engineering and bioprinting [130–132]. However, similar to other natural based hydrogels, hyaluronic acid suffers from weak mechanical properties making it difficult to print stable constructs. Consequently, crosslinking or chemical modification is often required to ensure long lasting mechanical integrity, post-printing shape fidelity and controlled degradation behavior [48]. Such modifications have enabled the use of hyaluronic acid in bioprinting of bone, cartilage, vascular tissue amongst others [133,134].

In the field of dentoalveolar regeneration, materials based on hyaluronic acid have been used as cell-encapsulating hydrogels for the regeneration of both alveolar bone and pulp tissue with different strategies to augment its mechanical properties. Combining hyaluronic acid with a thiol derivative of gelatin (gelatin-DTPH) and crosslinking

with polyethylene glycol diacrylate, along with the use of polycaprolactone as support has been proposed for alveolar bone regeneration. The encapsulation did prove to be suitable as mineral deposition was observed within four weeks of *in vivo* implantation [135]. However, the lack of any physical and mechanical characterization makes it difficult to assess the role of different constituents of the material in cellular behavior. In a different strategy, a combination of hydrazide-modified hyaluronic acid with cellulose nanocrystals resulted in crosslinking between the functional groups of the two materials enhancing material stability. Encapsulation of both DPSCs and HUVECs leads to the formation of blood vessels within two weeks of *in vitro* culture [136]. This, along with a reported gelation time of 3 to 30 seconds, make the material a suitable option to be explored in bioprinting strategies as well. However, with a full degradation being achieved within 2 to 13 days, further research and optimization of the material might be required to increase its stability.

The step towards bioprinting using hyaluronic acid was first taken by combining hyaluronic acid with gelatin, fibrinogen and glycerol to produce a bioink for extrusion-based bioprinting aimed at alveolar bone regeneration, where the cell-laden hydrogel would be printed along with polycaprolactone support. Furthermore, the use of a sacrificial material, Pluronic F127, enhancing the precision of the printing was first reported [90]. Development of such a system encompassing the cell encapsulated hydrogel, mechanical support and sacrificial layers, could be considered a major step towards the development of clinically relevant tissue engineering constructs through bioprinting. In a strategy different from combining HA with other materials, modification of hyaluronic acid by methacryloyl groups and demonstrating its potential to be used along with gelMA and polycaprolactone for alveolar bone bioprinting was a major innovation in the study by Kuss et al. [89], showing the importance of slight chemical modifications and the use of hyaluronic acid derivatives in the success of bioprinting strategies.

To further enhance the use of hyaluronic acid in dentoalveolar bioprinting, the degradation rate, the viscoelastic profile and the mechanical stability of hyaluronic acid can potentially be tuned by controlling the molecular weight of hyaluronic acid, incorporating

other natural or synthetic polymers such as methyl cellulose [137], dextran, polyethylene glycol, and polycaprolactone [138], modifying the material through esterification or methacrylation [139], or crosslinking the available functional groups using different modifiers such as carbodiimides [140], or Schiff-base reactions [131].

1.3.1.3 Fibrin-based materials

Fibrin is a glycoprotein consisting of fibrinogen monomers and is known to have a critical role in blood clotting, inflammatory responses and wound healing. Consequently, fibrin can be a suitable candidate to act as an active scaffold enhancing cell adhesion and proliferation [141], and its hydrogels have been widely used in tissue engineering of different tissues [142–144] as well as in bioprinting strategies aimed at the regeneration of nervous tissue [142], skin [145], bone [146], vascular tissue [147], and dental tissue [57]. Fibrin has been reported to support differentiation of DPSCs into odontoblasts, and vascularization of dental tissues, making it a promising candidate for dentoalveolar tissue engineering [57]. However, challenges such as gel shrinkage, low mechanical stability and rapid degradation are faced in tissue engineering strategies using fibrin. To circumvent this, modification of fibrin and the synthesis of polyethylene glycol fibrinogen is one strategy resulting in a viability of over 85 % among encapsulated DPSCs. However, the storage modulus ranging from 140 Pa in pure fibrin gel to 3601 Pa in maximum PEG concentration is significantly higher than that of natural dental pulp [148], risking the possibility of full mineralization and bone formation rather than the regeneration of a functioning pulp tissue.

As mentioned in section 2, one of the most critical aspects of pulp-dentin tissue regeneration is the localized differentiation of DPSCs to odontoblasts at the interface of the pulp-dentin. A gradient of fibrin concentrations was used by Han et al. [57], leading to a compressive modulus ranging from 270 Pa to 400 Pa. As a result, differentiation to odontoblasts only happened in higher concentrations of fibrin, enabling the possibility of accomplishing a localized differentiation of DPSCs. While this achievement is a major step forward in the development of bioinks for pulp-dentin regeneration, challenges such as the internal pores size of 2 to 4 μm , which could negatively affect angiogenesis

and tissue formation [149], or the degradation rate of 30 to 60 % within 5 days, demonstrate the need for further optimization of the suggested bioink.
While fibrin has been used in combination with other materials, other methods such as chemical modification or incorporation of plasmin inhibitors such as laminin, have not been studied in the dentoalveolar field yet [143,150]. Through these modifications, further control over mechanical properties of the materials could be achieved which in turn, could lead to an enhanced control over cellular processes such as differentiation, enabling the achievement of localized differentiation within the scaffold, and combined with cells such as dental pulp stem cells, human umbilical cord stem cells, stem cells from apical papilla or endothelial cells, they can be of interest in research aiming to regenerate vascularized soft tissue such as dental pulp.

1.3.1.4 Alginate-based materials

Alginate is a biocompatible, non-immunogenic natural polymer capable of dissolving in water and forming hydrogels through ionic crosslinking, which has become very popular in the field of bioprinting. This interest is mainly due to the fact that the material properties such as compressive modulus, stiffness, or the gelation rate can be easily modified by optimizing the polymer density and crosslinking density [151]. However, the main disadvantage of alginate is its lack of biological cues preventing cells from adhering to the alginate, leading to cell death [152]. Several methods have been suggested to address this issue, including the combination with other materials, or modification with cell binding peptides such as the incorporation of RGD peptides or laminin sequences on its backbone [153]. For example, Bhoj et al. [154] made alginate cell friendly through modification with RGD sequences. Encapsulation of human umbilical cord stem cells and DPSCs in the gel resulted in high cell viability and proliferation presenting an injectable scaffold capable of regenerating pulp-like tissue [154]. A different strategy was suggested by Sevari et al. [155], who combined alginate with Matrigel®, a commercially available matrix containing collagen, laminin, as well as other biomolecules [156], and bioglass® for the regeneration of craniofacial tissues. As expected, encapsulation of DPSCs demonstrated that a

higher Matrigel concentration leads to better cell viability [155]. The similarity of the viability data in the two studies suggests both strategies to be acceptable from a biological point of view.
The satisfactory and tunable mechanical properties have led to a wide use for alginate in the field of bioprinting tissues such as bone or cartilage [157]. Furthermore, alginate has been widely used to bioprint vasculature in regenerative strategies [158], such as the study by Yu et al., where bioprinting of hollow tubular channels using alginate printed through coaxial nozzles was demonstrated [159]. However, so far, alginate has only been used in one study for extrusion-based bioprinting of the dentin-pulp complex. To augment the cellular response, soluble dentin matrix was combined with alginate, leading to differentiation of DPSCs to odontoblasts even without the use of additional growth factors [98]. While showing the promise of using natural tissue in bioink formulations, the complicated procedure of obtaining the dentin matrix, along with limited resources of the material, may hamper the use of this bioink in upscaling strategies as a step towards clinical applications.
This lack of bioprinting research using alginate in the dentoalveolar region, combined with opportunities presented by the tunability of alginate hydrogels and the feasibility of making them cell friendly, demonstrate a clear path towards further research using this material. Still, due to the soft nature of alginate, its usage without support from synthetic polymers is limited to soft tissues in the region, where the very high tunability of the properties could help addressing the complex mechanical requirements of tissues such as the periodontal ligament.

1.3.2 Synthetic polymers

While natural polymers are perfect materials for tissue engineering in terms of the biological response from the cells [160], batch-to-batch variability of physical, mechanical and biological properties turns the production of a reliable bioink based solely on natural polymers into a difficult task. Moreover, most natural polymers suffer from low mechanical properties, reducing their reliability in the printing procedure and their capacity to regenerate hard tissues such as bone [80]. On the other hand, synthetic polymers offer a high control over

different physicomechanical properties such as the compressive modulus or degradation rate. This is due to the tunable nature of their synthesis procedure, being build up from single blocks of monomers. Therefore, several synthetic polymers have been used in tissue engineering strategies to produce hydrogels with a reduced variability in their properties. However, one of the major challenge faced in the use of most synthetic polymers is to compensate for their lack of cell adhesion sites, resulting in the need to either incorporate such molecules on the polymer backbone, such as grafting of RGD peptides on the backbone of polycaprolactone (PCL) [161], or to combine them with natural polymers, where for example PCL has been blended with gelatin to enhance the cell response [162,163]. In the framework of bioprinting, synthetic polymers are incorporated with three main goals: (i) to enhance the physicomechanical properties of the constructs as part of the bioink, (ii) to improve the shape fidelity of printed constructs by acting as a frame for softer bioinks, and (iii) to provide extra functionalities such as sacrificial layers [164]. Several synthetic materials have been used for such functions including poly (hydroxyethyl methacrylate) (pHEMA), poly (ethylene glycol) (PEG), polycaprolactone (PCL), poloxamer 407 (pluronic F127), and poly (N-isopropylacrylamide) (pNIPAM).

A variety of synthetic polymers have been used to encapsulate cells for tissue engineering of dentoalveolar tissues. PEG is one of these polymers. However, it is incapable of forming 3D networks and thus, hydrogels. As a result, it requires modifications such as acrylation. PEG-diacrylate combined with fibrinogen has been used to encapsulate DPSCs with a cell viability of over 85 %, and a storage modulus ranging from 453 Pa to 3601 Pa. Similar to the study by Han et al., where a change in concentration was used to control differentiation [57], it was determined that increased mechanical properties, could lead to odontoblastic differentiation [148]. While this study did not include printing, it could evolve into bioprinting of pulp tissue with localized differentiation guided by material properties. Similarly, in a study using pNIPAM-chitosan-graphene oxide by Amiryaghoubi et al. [165], osteogenic differentiation of DPSCs was observed and attributed to the presence of graphene oxide [165], suggesting the possibility of using hydrogel composition as a trigger for differentiation behavior in

the dentoalveolar regeneration approaches. Moreover, synthetic materials have been used in a number of studies mentioned earlier in the field of bioprinting dentoalveolar tissues for different functionalities described. Polyethylene glycol diacrylate was used by Ma et al. as part of the bioink in two studies [88,95] to enhance the mechanical properties of the bioink. Polycaprolactone was used as mechanical support to stand as scaffold for cell-encapsulated bioinks by Han et al. [57] and Kang et al. [90]. Additionally, Pluronic F127 has been used by Kang et al., as a sacrificial layer for the bioprinted constructs [90].

Overall, it is clear that, while different classes of hydrogels, including both natural and synthetic hydrogels, can be used for tissue regeneration in the dentoalveolar region, often modifications or combinations of them are required for a successful bioprinting strategy. Table 1.2 and 1.3 present a summary of hydrogels that have been used to encapsulate cells for dentoalveolar tissue engineering strategies. This includes modifications and combinations of hydrogels of both natural and synthetic origins. Furthermore, the cell type encapsulated in the hydrogels, along with the reported viability is demonstrated in the table. Having demonstrated their capability for cell encapsulation, these hydrogels could be used for bioprinting strategies using different modalities with slight modifications to ensure suitability for the desired bioprinting technique. Furthermore, a list of biomaterials that have been used for bioprinting strategies aimed at other tissues, such as vascular tissue is provided. Considering similarity in the properties of these tissues with some requirements in the dentoalveolar region, such as the need for vascularization in pulp regeneration strategies, or certain similarities in properties of alveolar bone with other bone tissues in the body, these options could be applied to the field of dentoalveolar regeneration using appropriate cell types and growth factors. Some suggestions for cell types and growth factors that could be used in these strategies are also presented in table 1.2 and 1.3. The tables also present whether the indicated materials have been used in a bioprinting strategy, in addition to their ability to support cell viability and if they have been used in an *in vivo* setup.

Table 1.2. An overview of some candidate materials with potential to be used in bioprinting for pulp-dentin, along with cell types and biological cues useful for the purpose.

Ref.	Material	Targeted tissue	Cell types used	Bioprinted? (Tech)	Max cell viability (%)	Study duration (days)	*In vivo* ?	Suggestive tissue	Suggestive cell types	suggestive biological cues
[155]	alginate + matrigel + bioactive glass microparticles	pulp-dentin	DPSCs	No	80	21	×	pulp-dentin	dental pulp stem cells (DPSCs) [166][167] / stem cells from apical papilla (SCAPs) [168] / human umbilical vein endothelial cells (HUVECs) [169] / odontoblast-like cells / stem cells from human exfoliated deciduous teeth	vascular endothelial growth factor (VEGF) / nerve growth factor (NGF) / bone morphogenetic protein 7 (BMP-7) / platelet-derived growth factor (PDGF) (138)
[154]	RGD modified alginate	pulp-dentin	hUVEC + hDPSCs	No	N/A	14	×			
[148]	fibrin + polyethylene glycol	pulp-dentin	DPSCs	No	85	7	×			
[136]	hyaluronic acid + cellulose nanocrystals + platelet lysate	pulp-dentin	DPSCs	No	N/A	14	×			
[170]	gelatin norbornene + thyiolated gelatin	vascularized cardiac tissue	hUVEC + iPSC	L	94	7	×			
[171]	gelMA + gelatin + glycerol + hyaluronic acid	small blood vessels	hUVEC + SMCs	Ex	89.8	7	×			
[172]	alginate + type I collagen	microvasculature	hUVEC	IJ	N/A	3	✓			
[173]	RGD modified elastin-like protein hydrogel	neural tissue model	iPSCs + hUVEC	IJ	88.3	14	×			
[174]	alginate in nanoclay support bath	complex vascular structures	fb	Ex	94.3	7	×			
[175]	alginate + gelatin + carbon nanotubes	vessel constructs	fb	Ex	86.6	7	×			
[176]	alginate-methylcellulose	bioinks for gene delivery	MSCs	Ex	N/A	N/A	✓			
[177]	collagen type I	capillary network	SCAPs	L	N/A	N/A	×			

Footnote: abbreviations: DPSCs: Dental Pulp Stem Cells, hUVEC: human umbilical vein endothelial cells, SMC: smooth muscle cells, MSC: mesenchymal stem cells, fb: fibroblasts, SCAP: stem cells from apical papilla, iPSCs: human induced pluripotent stem cells

Table 1.3. An overview of some candidate materials with potential to be used in bioprinting for periodontal ligament and alveolar bone, along with cell types and biological cues useful for the purpose.

Ref.	Material	Targeted tissue	Cell types used	Bioprinted? (Tech)	Max cell viability (%)	Study duration (days)	*In vivo* ?	Suggestive tissue	Suggestive cell types	suggestive biological cues
[178]	alginate + sodium periodate	periodontal ligament	PDLSCs + GMSCs	No	59	28	✓	periodontal ligament	periodontal ligament stem cells (PDLSCs) [179] / gingival mesenchymal stem cells [178]	connective tissue growth factor (CTGF) + transforming growth factor-β3 (TGF-β3) [180] / transforming growth factor B1 (TGFB1)
[181]	gelatin + fibrinogen + hyaluronic acid + glycerol + PCL support	anisotropic cartilage	MSCs	Ex	75	21	✓			
[182]	pluronic + alginate	liver model	hepG2/C3A	Ex	N/A	7	×			
[183]	decellularized tendon extracellular matrix	tendon tissue	NIH 3T3	Ex	≈ 85	3	×			
[184]	methacryloyl-polyethylenglycol dimethacrylate	muscle and tendon tissues	SMDCs + tenocytes	IJ	95	<1	×			
[185]	hyaluronic acid + gelatin + fibrinogen + polyurethane support	muscle tendon unit	C2C12 + NIH/3T3	Ex	80	7	×			
[186]	gelMA, collagen methacrylate, fibronectin, laminin	cardiac muscle	hiPSCs	Ex	N/A	13	×			
[187]	collagen + fibrinogen + alginate	multilayered vascular tissue constructs	hUVECs	Ex	N/A	5	×			
[188]	chitosan + chitosan-hyaluronic acid	bone tissue	MC3T3-E1	Ex	95	9	×			
[135]	hyaluronic acid + polycaprolactone	alveolar bone	osteoblasts	No	75	7	✓			
[194]	gelatin + hyaluronic acid + fibrinogen + glycerol + hydroxyapatite + aprotinin	prevascularized bone tissue	MSCs + hUVECs	IJ	90	<1	✓			
[195]	alginate + gelatin + glycerol	bone tissue	MSCs	Ex	≈ 85	7	×			

[196]	gelatin - ureido-pyrimidinone – tyramine	complex structures	MSCs	Ex	90	1	×	alveolar bone	dental pulp stem cells (DPSCs) [189] / human umbilical vein endothelial cells (HUVECs)[190] / bone marrow mesenchymal stem cells (BMSCs) [191] / osteoblast cell precursor MC3T3-E1 [192]	periostin + TGF-β [193] transforming growth factor–β3 (TGFβ3), bone + morphogenetic protein 4 (BMP4) [181] / basic fibroblast growth factor (bFGF) / vascular endothelial growth factor (VEGF)
[51]	oligo(poly[ethylene glycol] fumarate) + gelatin	bone and nerve	MC3T3-E1	Ex	N/A	7	×			
[197]	blood plasma + alginate + methylcellulose + calcium phosphate cement support	bone tissue	MSCs	Ex	75	<1	×			
[198]	collagen + β-Tricalcium phosphate	bone tissue	MC3T3-E1 pre- + hASCs	Ex	92	<1	×			
[199]	poly(ethylene glycol) dimethacrylate + acrylated GRGDS and MMP-sensitive peptides	bone and cartilage	hMSCs	IJ	≈ 88	1	×			
[200]	alginate + methylcellulose + laponite	bone tissue	MSCs	Ex	75	21	×			
[201]	carboxymethyl chitosan + amorphous calcium phosphate	bone tissue	MSCs	Ex	N/A	15	✓			

Footnote: abbreviations: DPSCs: Dental Pulp Stem Cells, hUVEC: human umbilical vein endothelial cells, SMC: smooth muscle cells, MSC: mesenchymal stem cells, fb: fibroblasts, SCAP: stem cells from apical papilla, iPSCs: human induced pluripotent stem cells, PDLSCs: periodontal ligament stem cells, GMSCs: gingival mesenchymal stem cells, SMDC: skeletal muscle derived cells, ASCs: adipose derived stem cells

1.4 Cells and growth factors

While the development of materials is of extreme importance for bioprinting, one should equally consider the appropriate cells and/or biological factors. These will be encapsulated inside the bioink and deposited through the described procedures. As demonstrated in table 1.2 and 1.3, a variety of cell types and growth factors have been used for dentoalveolar tissue engineering and can be used in bioprinting strategies for these tissues as well. This section will briefly introduce

the most widely used cell types, demonstrating their potential for use in tissue engineering of the dentoalveolar region.

1.4.1 Cell types

1.4.1.1 Dental Pulp Stem Cells

Dental pulp stem cells (DPSCs) are a type of stem cells present in the dental pulp core. They are derived from the ectoderm and demonstrate properties similar to mesenchymal stem cells, such as their stretched morphology, as well as their surface adherence, proliferation and ability to form colonies [202]. These cells are multipotent, meaning they can differentiate into several different lineages. This has led to their widespread use in dental tissue engineering [203], bone tissue engineering [204], neurology [205], vascular [206] and adipose tissue engineering [207]. Furthermore, DPSCs are known to maintain their differentiation abilities after long periods of cryopreservation, resulting in easier handling for tissue engineering applications [208]. The ability of DPSCs to differentiate into odontoblasts and osteoblasts, in addition to their relatively easy access, has made them very interesting in regeneration of craniofacial tissues [209]. High cell viability of DPSCs encapsulated in a range of biomaterials, and their differentiation capacity has been shown in different research projects presented in this chapter [57,99,155].

1.4.1.2 Periodontal Ligament Stem Cells

Periodontal ligament stem cells are another type of multipotent stem cells present in the dentoalveolar region and are found in the perivascular space of the periodontium. The properties of this cell type are similar to mesenchymal stem cells and many of the expressed markers are similar among the two. In addition, they have an ability to modulate the immune response through release of bioactive agents including resolvins [210,211]. PDLSCs have been known to differentiate into different lineages including cementoblasts, osteoblasts, chondroblasts, fibroblasts, endothelial cells, adipoblasts and myocytes [212,213]. They have been reported to be efficient in the regeneration of periodontal ligament along with other tissues in tissue

engineering and bioprinting strategies aimed at regeneration of the dentoalveolar region, as mentioned in previous sections of this chapter.

1.4.1.3 Stem Cells from Apical Papilla (SCAPs)

SCAPs are a group of multipotent stem cells originated from neural crest, and present in the apical papilla of immature permanent teeth. They are considered to be a type of mesenchymal stem cells [214]. Furthermore, these cells are known to be able to differentiate into osteoblast, odontoblasts, neural lineages, adipocytes and hepatocytes [215–217]. Additionally, they are known to have a higher proliferation rate compared to PDLSCs, and they present a low immunogenicity [168]. Such properties have resulted in use of SCAPs in regeneration strategies for pulp-dentin complex [218], for periodontal regeneration [219], for bone regeneration [220], and for strategies aimed at promoting angiogenesis [221]. Consequently, they can be considered as a suitable cell population for use within bioprinting strategies aimed at tissue engineering of the dentoalveolar region and have been used for this purpose in some of the studies described in previous sections .

1.4.1.4 Human Umbilical Vein Endothelial Cells (HUVECs)

HUVECs are primary cells derived from endothelial layer of the veins from the umbilical cord. They have a high potential in generating vasculature in tissue engineering approaches. For this purpose, HUVECs have been used for the engineering of functional vasculature in bioprinted constructs as shown in different sections of this chapter. In addition to bioprinted constructs, their potential to induce vasculature formation inside hydrogels has been demonstrated by Monteiro et al. [115] and Khayat et al. [117], which in turn has resulted in their use for further regeneration of living pulp tissue [169].

1.4.2 Growth factors

In order to regenerate a functional tissue, a range of cellular events need to be closely regulated, including mitogenesis, migration, metabolism and differentiation. Such processes are regulated by specific proteins called growth factors. These proteins often bind to receptors on the cell membrane, starting a signaling cascade which impacts cellular components and results in altered gene expression and hence, altered

behavior by the cells. A wide range of growth factors have been used for tissue regeneration in the dentoalveolar region and could be applied to the field of bioprinting these tissues. The most widely used options for these growth factors can be divided into four main classes, which are described in this section.

1.4.2.1 Platelet derived growth factors (PDGF)

PDGFs are a class of growth factors present in the serum and bone matrix, capable of affecting fibroblasts, smooth muscle cells and glia cells [222]. In addition to that, they are also known to affect the proliferation rate of osteoblasts stimulating bone formation [223]. Consequently, they are used for modulation of bone homeostasis and regeneration, in addition to soft tissue and wound healing [224]. In the field of dentoalveolar tissue engineering, PDGFs have been used to enhance proliferation of cells derived from periodontal ligament. In fact, expression of PDGF receptors on the damaged periodontal tissue is known to be critical in the healing process [225]. In addition, this family of growth factors has been used to control bone regeneration in strategies aimed at tissue engineering of dentoalveolar bone [226]. Aside from addressing challenges in the periodontal tissue, PDGF growth factors have also been used for regeneration of pulp-dentin tissue, demonstrating an impact on odontoblastic differentiation of dental pulp stem cells, enhancing the production of mineralized tissue resembling dentin *in vivo* [227]. Consequently, this class of biomolecules could be used to address a wide range of requirements within the tissue engineering strategies aimed at dentoalveolar regeneration.

1.4.2.2 Insulin-like growth factor (IGF)

The insulin-like growth factors are a family of proteins with high resemblance to insulin in their chain structure, and they are known to be critical in development and regeneration of a range of tissues [228], and consequently, they have been widely used in studies aimed at the dentoalveolar regeneration. For this, it has been shown that this family of growth factors could enhance cell viability of the periodontal fibroblasts significantly, due to their effect in inhibiting apoptosis [229]. Furthermore, localized delivery of these growth factors through

their incorporation in dextran-gelatin microspheres has been reported by Chen et al., to have a positive impact on the regeneration of periodontal tissue [230]. In addition, IGFs are known to enhance osteogenic ability of SCAPs, and PDLSCs, in addition to enhancing their proliferation [228,231]. Aside from these two cell types, IGFs are also known to affect proliferation of DPSCs, in addition to enhancing their osteogenic and odontogenic differentiation [232]. This wide impact on a range of dentoalveolar cells and tissues demonstrates the suitability of this growth factor family for incorporation in tissue engineering strategies aimed at this region, where they could modulate a range of properties including wound healing, cell proliferation and cell differentiation.

1.4.2.3 Transforming growth factor beta (TGF-β)

The transforming growth factor beta family is a family of dimeric proteins known to impact proliferation and differentiation of a range of cell types, consequently affecting tissue development, regeneration and homeostasis to a large extent [233,234]. This family of growth factors is present in dental pulp, periodontal ligament and alveolar bone [235], and is known to enhance matrix deposition by odontoblasts, and to induce differentiation of DPSCs [236]. As a result of this significant impact, these growth factors have been widely used in efforts towards regeneration of the dentoalveolar structures. Encapsulation of these growth factors in microspheres of poly lactic co glycolic acid is an example of these efforts, where an enhancement of dentin matrix production was observed, along with differentiation of DPSCs to odontoblast like cells [237]. Furthermore, culture of periodontal ligament cells in the presence of TGF-β demonstrated its effect on increasing the mitogenic potential of these cells [235,238]. Furthermore, encapsulation of growth factors from this family in bioinks is already reported for tissue engineering of cartilage [181] and bone [193] tissues, suggesting the suitability of these growth factors to be used within bioprinting strategies aimed at dentoalveolar tissue engineering.

1.4.2.4 Fibroblast growth factor (FGF)

Fibroblast growth factors are a family of polypeptides with a closely related structure. They are known to play an important role in regulating a range of developmental processes and thus, have an important role in embryonic development [239]. Having mitogenic and angiogenic potential, these heparin binding growth factors are known to affect wound healing, angiogenesis, and tissue formation [240]. These properties have been demonstrated in the dentoalveolar region, by affecting wound healing of periodontal ligament *in vivo* [241]. In addition, their impact on bone formation and bone regeneration is well known, and they have been incorporated in tissue engineering strategies for this purpose [242], and also in tissue engineering strategies aimed at alveolar bone [243]. In addition to these tissues, FDFs are known to modulate the behavior of human dental pulp cells. An increase in proliferation and migration of HDPCs is observed when cultured in the presence of FGFs, while the presence of these growth factors suppresses mineral deposition by these cells [244]. Due to these properties, growth factors of the FGF family are potent factors to modulate tissue regeneration within tissue engineering and bioengineering applications aimed at dentoalveolar regeneration.

1.5 Delivery of growth factors

While biomaterials, including hydrogels, provide a favorable environment for the viability and metabolic activity of stem cells, a higher degree of control over cellular activities, including proliferation and differentiation, is required to be able to mimic complex architectures of natural tissues [245]. As a result, advanced tissue engineering strategies, often take advantage of drugs, growth factors and other biomolecules to stimulate cellular behavior and tissue regeneration [246,247]. However, such biomolecules usually suffer from a short half-life, and their activity is dependent on the dosage. Furthermore, over-concentration of such molecules can lead to undesired consequences such as uncontrolled tissue formation, inflammation, or cytotoxicity [248]. Consequently, a range of drug delivery systems have been developed to be incorporated within tissue engineering strategies, addressing the demand for further control over

cell behavior, in addition to further control over inflammatory responses of the surrounding tissues [249]. Such delivery systems can be both stimuli-responsive systems, where the release of drugs or growth factors upon application of certain triggers is required, and sustained-release systems, where prolonged presence of these molecules within a specific area is desired. Trigger-based systems can either be activated by enzymes, such as strategies aimed at skin regeneration in treatment of chronic wounds [250], by pH, such as bone regeneration efforts where the local acidic pH at the defect site can be used as a stimuli for drug release [251], temperature, where temperature-sensitive materials have been used in tissue engineering of vascular tissues [252], or redox-responsive systems, where the inflammation in defect area results in increased production of reactive oxygen species, and these species can act as a trigger to release therapeutics [253]. In addition, within tissue engineering strategies, significant effort has been put into prolonging the release of drugs and growth factors, as the availability of such molecules over specific periods of time is of interest, and a burst release of entire growth factor or drug is often unwanted. Some of the main strategies used for sustained release of drugs and biomolecules within tissue engineering strategies, shown in figure 1.6, are presented in this section.

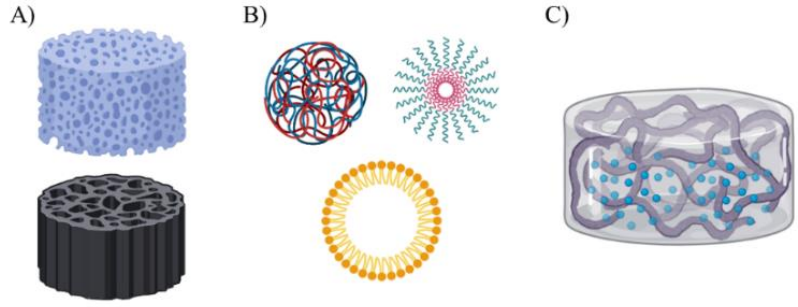

Figure 1.6. different strategies for delivery of drugs and biomolecules within tissue engineering approaches. A) encapsulation of drugs within porous scaffolds, B) delivery of molecules through micro/nano particles and C) loading of drugs onto particles, loaded within tissue engineering systems such as hydrogels (figure made using biorender.com)

1.5.1 Scaffold-based systems

Scaffold-based systems use the biomaterial incorporated within the tissue engineering strategy as a vehicle for the delivery of drugs and growth factors. Such biomaterials are porous scaffolds, produced through different methods such as solvent casting, electrospinning, 3D printing, etc. These scaffolds can be based on ceramics, metals, thermoplastic polymers, as well as hydrogels, and are usually produced with a controlled degree of porosity, which allows for the incorporation of drugs and their release upon diffusion from the pores. This system has been applied to tricalcium phosphate scaffolds used for bone regeneration, capable of releasing bone morphogenetic protein 2 (BMP-2) [254], and the success of tricalcium phosphate loaded with Platelet-derived growth factor in bone formation has been demonstrated in clinical trials [255,256]. Furthermore, degradable polymers such as poly lactic acid (PLA) or poly lactic-co-glycolic acid (PLGA) have been extensively studied for the purpose of drug release, due to the controllable degradation rate enabling sustained release of the drugs upon scaffold degradation. For example, PLA has been loaded with brain-derived neurotrophic factor for neural regeneration [257], and PLGA has been loaded with BMP-2 for bone regeneration [258].

In addition to solid scaffolds, hydrogels of both synthetic and natural origin have been widely used for the delivery of drugs and growth factors within tissue engineering strategies. Drugs and biomolecules are trapped within the polymeric network of the hydrogels, and the high water content reduces the possibility of drug denaturation or aggregation caused by the presence of organic solvents. Furthermore, crosslinking of the hydrogel network, and its physical properties (e.g. degradation rate) enable a wide control over the release kinetics of the encapsulated molecules. These properties were used to induce angiogenesis, by encapsulating vascular endothelial growth factor (VEGF) in alginate hydrogels [259], and using fibrin hydrogels for the delivery of heparin [260].

1.5.2 Micro/nano particles

Systems composed of nanoparticles ranging in size from less than ten to one hundred nano meters, and microparticles ranging from a few hundreds of nanometers to hundreds of micrometers, have been used extensively for the delivery of drugs and growth factors within regenerative strategies [261]. Such particles are usually either lipid-based [262], polymer-based [263] or inorganic [264]. Among those, particles of a nano-scale size offer advantages when penetration of the particles into deeper tissues is required. However, there is the possibility of cellular uptake, the risk of which is lower with micro particles. Additionally, the larger size of micro particles allows for incorporation of a larger amount of drug which potentially enhances the period of release, in addition to allowing for incorporation of larger drugs such as proteins and macromolecules.
Among these particles, polymeric micro/nanoparticles are some of the most versatile options, due to the high degree of control over polymer structure, crosslinking and the particle form, which translates into higher control over the release kinetics. For example, PLGA has been used for the delivery and release of Insulin [265], VEGF [266], and BMP-2 [267]. Natural polymers such as chitosan and gelatin have also been used to develop microparticles capable of delivering and releasing BMP-2 [268] and IGF-1 [269], respectively.

1.5.3 Combined systems

While each of the systems described offer advantages with regards to the delivery of growth factors and drugs to the tissue engineering site, they also each suffer from shortcomings. As tissue engineering requires a site-specific release of molecules, particle-based systems might suffer from inaccurate localization, caused by particles leaching to other areas [248]. On the other hand, scaffold-based release systems also face challenges. A first challenge is the design of biomaterials, as they would need to take into account both, the requirements for tissue regeneration, and the requirements for drug release kinetics. Additionally, it is quite challenging to incorporate multiple drugs and growth factors within a single scaffold architecture, as each drug will require specific physical properties such as degradation rate or porosity

to modulate its release [248,261]. As a result of these requirements, a combination of particle-based systems with scaffold-based systems has been proposed. This approach allows for designing delivery vehicles specifically designed for the required molecule and offers freedom in spatial requirements of the drug release, in addition to the incorporation of multiple drugs and biomolecules.

Success of this approach has been demonstrated by encapsulation of bovine serum albumin in PLGA microparticles and encapsulation of the particles in crosslinked gelatin scaffolds, resulting in a sustained release over 30 days [270]. Furthermore, particle loaded hydrogels have been used for the delivery of a variety of drugs and biomolecules including doxorubicin loaded in liposomes [271], Fluvastatin loaded in n-isopropylacrylamide (NIPAM) [272], quercetin in poly-D,L-lactideco-glycolide nanoparticles [273], among others. Following this success in efficient controlled delivery of drugs, this approach has also been applied to tissue engineering strategies, for example where IGF-1 was encapsulated in PLGA nanoparticles, which were in turn encapsulated in polypropylene glycol and polyethylene glycol hydrogels for tissue engineering of cardiac tissues [274], or the incorporation of basic fibroblast growth factor (bFGF) and BMP-7 loaded chitosan microparticles encapsulated in gellan xanthan gels for bone regeneration [275]. These examples demonstrate advantages of combined systems over individual approaches for the efficient delivery of drugs and biomolecules.

1.6 Conclusions

Regenerative medicine has opened new horizons for the field of dentoalveolar treatments when traditional treatments are faced with shortcomings. Such clinical applications can range from treatment of dental caries, to regeneration of periodontal tissue and alveolar bone. Yet, the clinical translation of tissue regeneration strategies is hitherto limited. Some of the hurdles include the failure of recapitulating complex tissue architectures as well as the variability in the process. These limitations often lead to a biological outcome which is not clinically relevant. However, with bioprinting, significant hope has been generated that some of these challenges could be overcome. Still, the role of bioprinting is to provide a platform as a robust scaffold

fabrication technology, possibly enabling tissue engineering of more complex structures. However, the alveolar region is a heterogeneous system consisting of multiple tissues with each having its own physical, mechanical and biological properties. One of the key aspects in developing bioprinting strategies for dentoalveolar tissue regeneration through bioprinting is the choice of appropriate biomaterials for the formulation of bioinks. A wide range of materials have been suggested to be used in bioprinting dentoalveolar tissues. While from a biological point of view natural polymers seem to be a suitable choice for bioprinting, they suffer from a weak mechanical strength, variability among different batches, and a limited control over physicomechanical properties. This highlights the need for further modifications and/or combinations of these polymers with synthetic polymers to achieve viable strategies for the regeneration of these tissues. While a range of biomaterials, or their combinations, could readily be applied to the field of dentoalveolar bioprinting as demonstrated in tables 3 and 4, a bioink based on natural or synthetic materials with adjustable physical and mechanical properties, capable of being used for a variety of dentoalveolar tissues is still lacking. In addition, strategies to address the biological heterogeneity of the region are still needed to be developed. This could be performed developing mechanisms to efficiently deliver growth factors and signaling molecules within the bioinks at specific locations, and hence, enabling addressing the complexity in tissue engineering strategies.

1.7 References

1 Petersen PE. "World Health Organization global policy for improvement of oral health - World Health Assembly 2007". Int Dent J. 2008 Jun 1;58(3):115–21.
2. "Political Declaration of the High-Level Meeting of the General Assembly on the Prevention and Control of Non-Communicable Diseases : draft resolution /". 2011 Sep;13 p.
3. Shaddox LM, Walker CB. "Treating chronic periodontitis: current status, challenges, and future directions.". Clin Cosmet Investig Dent. 2010;2:79–91.
4. Kassebaum NJ, Bernabé E, Dahiya M, Bhandari B, Murray CJL, Marcenes W. "Global burden of severe periodontitis in 1990-2010: a systematic review and meta-regression.". J Dent Res. 2014 Nov;93(11):1045–53.
5. "WHO/Europe | Disease prevention - Oral health" [Internet]. [cited 2020 Jul 28].
6. Al-Ani AH, Antoun JS, Thomson WM, Merriman TR, Farella M. "Hypodontia: An Update on Its Etiology, Classification, and Clinical Management.". Biomed Res Int. 2017;2017:9378325.

7. Khodakaram-Tafti A, Mehrabani D, Shaterzadeh-Yazdi H, Zamiri B, Omidi M. "Tissue Engineering in Maxillary Bone Defects". World J Plast Surg. 2018 Jan;7(1):3–11.
8. Hanif A, Qureshi S, Sheikh Z, Rashid H. "Complications in implant dentistry". Eur J Dent. 2017;11(1):135–40.
9. Martin K, Nathwani S, Bunyan R. "Autotransplantation of teeth: an evidence-based approach.". Br Dent J. 2018 Jun;224(11):861–4.
10. Denys D, Shahbazian M, Jacobs R, Laenen A, Wyatt J, Vinckier F, Willems G. "Importance of root development in autotransplantations: a retrospective study of 137 teeth with a follow-up period varying from 1 week to 14 years.". Eur J Orthod. 2013 Oct;35(5):680–8.
11. Gupta S, Goel M, Sachdeva G, Sharma B, Malhotra D. "Autotransplantation". J Conserv Dent. 2015;18(6):500–3.
12. Shahbazian M, Wyatt J, Willems G, Jacobs R. "Clinical application of a stereolithographic tooth replica and surgical guide in tooth autotransplantation". Virtual Phys Prototyp. 2012 Sep 1;7(3):211–8.
13. EzEldeen M, Wyatt J, Al-Rimawi A, Coucke W, Shaheen E, Lambrichts I, Willems G, Politis C, Jacobs R. "Use of CBCT Guidance for Tooth Autotransplantation in Children.". J Dent Res. 2019 Apr;98(4):406–13.
14. Langer R, Vacanti J. "Advances in tissue engineering". J Pediatr Surg. 2016;51(1):8–12.
15. Langer R, Vacanti JP. "Tissue engineering.". Science. 1993 May;260(5110):920–6.
16. Na S, Zhang H, Huang F, Wang W, Ding Y, Li D, Jin Y. "Regeneration of dental pulp/dentine complex with a three-dimensional and scaffold-free stem-cell sheet-derived pellet.". J Tissue Eng Regen Med. 2016 Mar;10(3):261–70.
17. Kim NR, Lee DH, Chung PH, Yang HC. "Distinct differentiation properties of human dental pulp cells on collagen, gelatin, and chitosan scaffolds.". Oral Surg Oral Med Oral Pathol Oral Radiol Endod. 2009 Nov;108(5):e94-100.
18. Cordeiro MM, Dong Z, Kaneko T, Zhang Z, Miyazawa M, Shi S, Smith AJ, Nör JE. "Dental pulp tissue engineering with stem cells from exfoliated deciduous teeth.". J Endod. 2008 Aug;34(8):962–9.
19. Galler KM, Hartgerink JD, Cavender AC, Schmalz G, D'Souza RN. "A customized self-assembling peptide hydrogel for dental pulp tissue engineering.". Tissue Eng Part A. 2012 Jan;18(1–2):176–84.
20. Chen FM, Zhang J, Zhang M, An Y, Chen F, Wu ZF. "A review on endogenous regenerative technology in periodontal regenerative medicine". Biomaterials. 2010;31(31):7892–927.
21. Smith BT, Shum J, Wong M, Mikos AG, Young S. "Bone Tissue Engineering Challenges in Oral & Maxillofacial Surgery.". Adv Exp Med Biol. 2015;881:57–78.
22. Kim SG, Zheng Y, Zhou J, Chen M, Embree MC, Song K, Jiang N, Mao JJ. "Dentin and dental pulp regeneration by the patient's endogenous cells". Endod Top. 2013 Mar;28(1):106–17.
23. Abou Neel EA, Chrzanowski W, Salih VM, Kim HW, Knowles JC. "Tissue engineering in dentistry". J Dent. 2014 Aug 1 [cited 2020 Feb 18];42(8):915–28.
24. Galler KM, Eidt A, Schmalz G. "Cell-free Approaches for Dental Pulp Tissue Engineering". J Endod. 2014 Apr 1;40(4):S41–5.
25. Scantlebury T, Ambruster J. "The Development of Guided Regeneration: Making the Impossible Possible and the Unpredictable Predictable". J Evid

Based Dent Pract. 2012;12(3, Supplement):101–17.
26. Jammalamadaka U, Tappa K. "Recent Advances in Biomaterials for 3D Printing and Tissue Engineering.". J Funct Biomater. 2018 Mar;9(1).
27. Dolati F, Yu Y, Zhang Y, De Jesus AM, Sander EA, Ozbolat IT. "In vitro evaluation of carbon-nanotube-reinforced bioprintable vascular conduits.". Nanotechnology. 2014 Apr;25(14):145101.
28. Kolesky DB, Truby RL, Gladman AS, Busbee TA, Homan KA, Lewis JA. "3D bioprinting of vascularized, heterogeneous cell-laden tissue constructs.". Adv Mater. 2014 May;26(19):3124–30.
29. Pateman CJ, Harding AJ, Glen A, Taylor CS, Christmas CR, Robinson PP, Rimmer S, Boissonade FM, Claeyssens F, Haycock JW. "Nerve guides manufactured from photocurable polymers to aid peripheral nerve repair.". Biomaterials. 2015 May;49:77–89.
30. Chang R, Emami K, Wu H, Sun W. "Biofabrication of a three-dimensional liver micro-organ as an in vitro drug metabolism model.". Biofabrication. 2010 Dec;2(4):45004.
31. "Oral health" [Internet]. 2023 [cited 2023 Apr 24].
32. Nakashima M, Iohara K, Murakami M, Nakamura H, Sato Y, Ariji Y, Matsushita K. "Pulp regeneration by transplantation of dental pulp stem cells in pulpitis: a pilot clinical study". Stem Cell Res Ther. 2017;8(1):61.
33. Sritharan A. "Discuss That The Coronal Seal Is More Important Than The Apical Seal For Endodontic Success". Aust Endod J. 2002 Dec 1;28(3):112–5.
34. Han J, Kim DS, Jang H, Kim HR, Kang HW. "Bioprinting of three-dimensional dentin-pulp complex with local differentiation of human dental pulp stem cells.". J Tissue Eng. 2019;10:2041731419845849.
35. Wu C, Zhou Y, Lin C, Chang J, Xiao Y. "Strontium-containing mesoporous bioactive glass scaffolds with improved osteogenic/cementogenic differentiation of periodontal ligament cells for periodontal tissue engineering". Acta Biomater. 2012;8(10):3805–15.
36. Iwata T, Yamato M, Ishikawa I, Ando T, Okano T. "Tissue Engineering in Periodontal Tissue". Anat Rec. 2014 Jan 1;297(1):16–25.
37. Silva FMS, Cortez ALV, Moreira RWF, Mazzonetto R. "Complications of intraoral donor site for bone grafting prior to implant placement.". Implant Dent. 2006 Dec;15(4):420–6.
38. Lutz R, Berger-Fink S, Stockmann P, Neukam FW, Schlegel KA. "Sinus floor augmentation with autogenous bone vs. a bovine-derived xenograft – a 5-year retrospective study". Clin Oral Implants Res. 2015 Jun 1;26(6):644–8.
39. Klijn RJ, Meijer GJ, Bronkhorst EM, Jansen JA. "A meta-analysis of histomorphometric results and graft healing time of various biomaterials compared to autologous bone used as sinus floor augmentation material in humans.". Tissue Eng Part B Rev. 2010 Oct;16(5):493–507.
40. Pilipchuk SP, Plonka AB, Monje A, Taut AD, Lanis A, Kang B, Giannobile W V. "Tissue engineering for bone regeneration and osseointegration in the oral cavity.". Dent Mater. 2015 Apr;31(4):317–38.
41. Arslan-Yildiz A, El Assal R, Chen P, Guven S, Inci F, Demirci U. "Towards artificial tissue models: past, present, and future of 3D bioprinting.". Biofabrication. 2016 Mar;8(1):14103.
42. Boland T, Xu T, Damon B, Cui X. "Application of inkjet printing to tissue engineering". Biotechnol J. 2006 Sep 1;1(9):910–7.
43. Grigoryan B, Sazer DW, Avila A, Albritton JL, Padhye A, Ta AH, Greenfield

PT, Gibbons DL, Miller JS. "Development, characterization, and applications of multi-material stereolithography bioprinting". Sci Rep. 2021;11(1):3171.
44. Goodarzi Hosseinabadi H, Dogan E, Miri AK, Ionov L. "Digital Light Processing Bioprinting Advances for Microtissue Models". ACS Biomater Sci Eng. 2022 Apr 11;8(4):1381–95.
45. Kumar H, Kim K. "Stereolithography 3D Bioprinting.". Methods Mol Biol. 2020;2140:93–108.
46. Bernal PN, Delrot P, Loterie D, Li Y, Malda J, Moser C, Levato R. "Volumetric Bioprinting of Complex Living-Tissue Constructs within Seconds". Adv Mater. 2019 Oct 1;31(42):1904209.
47. Guillotin B, Catros S, Guillemot F. "Laser Assisted Bio-printing (LAB) of Cells and Bio-materials Based on Laser Induced Forward Transfer (LIFT) BT - Laser Technology in Biomimetics: Basics and Applications". In: Schmidt V, Belegratis MR, editors. Berlin, Heidelberg: Springer Berlin Heidelberg; 2013. p. 193–209.
48. Hospodiuk M, Dey M, Sosnoski D, Ozbolat IT. "The bioink: A comprehensive review on bioprintable materials". Biotechnol Adv. 2017;35(2):217–39.
49. Murphy S V, Atala A. "3D bioprinting of tissues and organs.". Nat Biotechnol. 2014 Aug;32(8):773–85.
50. Freeman F, Kelly D. "Tuning Alginate Bioink Stiffness and Composition for Controlled Growth Factor Delivery and to Spatially Direct MSC Fate within Bioprinted Tissues". Sci Rep. 2017 Dec;7.
51. Liu X, Gaihre B, George MN, Miller AL 2nd, Xu H, Waletzki BE, Lu L. "3D bioprinting of oligo(poly[ethylene glycol] fumarate) for bone and nerve tissue engineering.". J Biomed Mater Res A. 2020 May;
52. Amorim PA, d'Ávila MA, Anand R, Moldenaers P, Van Puyvelde P, Bloemen V. "Insights on shear rheology of inks for extrusion-based 3D bioprinting". Bioprinting. 2021;22:e00129.
53. Mandrycky C, Wang Z, Kim K, Kim DH. "3D bioprinting for engineering complex tissues". Biotechnol Adv. 2016;34(4):422–34.
54. Garg N. "Chapter-03 Structure of Teeth". Textbook of Operative Dentistry. 2013. p. 18–32.
55. Sloan AJ. "Chapter 29 - Biology of the Dentin-Pulp Complex". In: Vishwakarma A, Sharpe P, Shi S, Ramalingam MBTSCB and TE in DS, editors. Boston: Academic Press; 2015. p. 371–8.
56. Abbass MMS, El-Rashidy AA, Sadek KM, Moshy S El, Radwan IA, Rady D, Dörfer CE, Fawzy El-Sayed KM. "Hydrogels and Dentin-Pulp Complex Regeneration: From the Benchtop to Clinical Translation". Polymers (Basel). 2020 Dec 9;12(12):2935.
57. Han J, Kim DS, Jang H, Kim HRHW, Kang HW, Shaddox LM, Walker CB, Schiffman EL, Velly AM, Look JO, Hodges JS, Swift JQ, Decker KL, Anderson QN, Templeton RB, Lenton PA, Kang W, Fricton JR, Amrollahi P, et al. "Bioprinting of three-dimensional dentin-pulp complex with local differentiation of human dental pulp stem cells.". Kahveci MU, editor. J Tissue Eng. 2017/10/03. 2019 Mar 10;10(3):2041731419845849.
58. Erisken C, Kalyon DM, Zhou J, Kim SG, Mao JJ. "Viscoelastic Properties of Dental Pulp Tissue and Ramifications on Biomaterial Development for Pulp Regeneration.". J Endod. 2015 Oct;41(10):1711–7.
59. Liu N, Zhou M, Zhang Q, Zhang T, Tian T, Ma Q, Xue C, Lin S, Cai X. "Stiffness regulates the proliferation and osteogenic/odontogenic

differentiation of human dental pulp stem cells via the WNT signalling pathway". Cell Prolif. 2018 Apr 1;51(2):e12435.
60. Bouillaguet S. "BIOLOGICAL RISKS OF RESIN-BASED MATERIALS TO THE DENTIN-PULP COMPLEX.". Crit Rev oral Biol Med an Off Publ Am Assoc Oral Biol. 2004 Jan;15(1):47–60.
61. Zhang YR, Du W, Zhou XD, Yu HY. "Review of research on the mechanical properties of the human tooth". Int J Oral Sci. 2014 Jun;6(2):61–9.
62. Panseri S, Montesi M, Dozio SM, Savini E, Tampieri A, Sandri M. "Biomimetic Scaffold with Aligned Microporosity Designed for Dentin Regeneration " [Internet]. Vol. 4, Frontiers in Bioengineering and Biotechnology . 2016. p. 48.
63. AbdulQader ST, Rahman IA, Thirumulu KP, Ismail H, Mahmood Z. "Effect of biphasic calcium phosphate scaffold porosities on odontogenic differentiation of human dental pulp cells.". J Biomater Appl. 2016 Apr;30(9):1300–11.
64. Dean R. "The Periodontal Ligament: Development, Anatomy and Function". Oral Health Dent Manag. 2017;2017:1–7.
65. Fill TS, Toogood RW, Major PW, Carey JP. "Analytically determined mechanical properties of, and models for the periodontal ligament: Critical review of literature". J Biomech. 2012;45(1):9–16.
66. Fill TS, Carey JP, Toogood RW, Major PW. "Experimentally determined mechanical properties of, and models for, the periodontal ligament: critical review of current literature". J Dent Biomech. 2011/04/05. 2011;2011:312980.
67. Dorow C, Krstin N, Sander FG. "Experiments to Determine the Material Properties of the Periodontal Ligament". J Orofac Orthop / Fortschritte der Kieferorthopädie. 2002;63(2):94–104.
68. Qian L, Todo M, Morita Y, Matsushita Y, Koyano K. "Deformation analysis of the periodontium considering the viscoelasticity of the periodontal ligament". Dent Mater. 2009;25(10):1285–92.
69. Natali AN, Pavan PG, Carniel EL, Dorow C. "Viscoelastic Response of the Periodontal Ligament: An Experimental–Numerical Analysis". Connect Tissue Res. 2004 Jan;45(4–5):222–30.
70. Wang CY, Su MZ, Chang HH, Chiang YC, Tao SH, Cheng JH, Fuh LJ, Lin CP. "Tension-compression viscoelastic behaviors of the periodontal ligament". J Formos Med Assoc. 2012;111(9):471–81.
71. Mestrović S, Slaj M, Rajić P. "Finite element method analysis of the tooth movement induced by orthodontic forces.". Coll Antropol. 2003;27 Suppl 2:17–21.
72. Jin SS, He DQ, Wang Y, Zhang T, Yu HJ, Li ZX, Zhu LS, Zhou YH, Liu Y. "Mechanical force modulates periodontal ligament stem cell characteristics during bone remodelling via TRPV4". Cell Prolif. 2020 Oct 1;53(10):e12912.
73. Liu N, Zhou M, Zhang Q, Yong L, Zhang T, Tian T, Ma Q, Lin S, Zhu B, Cai X. "Effect of substrate stiffness on proliferation and differentiation of periodontal ligament stem cells". Cell Prolif. 2018/07/24. 2018 Oct;51(5):e12478–e12478.
74. Bartold M, Gronthos S, Haynes D, Ivanovski S. "Mesenchymal stem cells and biologic factors leading to bone formation". J Clin Periodontol. 2019 Jun 1;46(S21):12–32.
75. Gorrel C, Andersson S, Verhaert L. "Chapter 4 - Anatomy of the teeth and periodontium". In: Gorrel C, Andersson S, Verhaert LBTVD for the GP

(Second E, editors. W.B. Saunders; 2013. p. 37–41.
76. Goudouri OM, Kontonasaki E, Boccaccini AR. "17 - Layered scaffolds for periodontal regeneration". In: Tayebi L, Moharamzadeh KBTB for O and DTE, editors. Woodhead Publishing; 2017. p. 279–95.
77. Almasoud NN, Tanneru N, Marei HF. "Alveolar bone density and its clinical implication in the placement of dental implants and orthodontic mini-implants". Saudi Med J. 2016 Jun;37(6):684–9.
78. Park HS, Lee YJ, Jeong SH, Kwon TG. "Density of the alveolar and basal bones of the maxilla and the mandible". Am J Orthod Dentofac Orthop. 2008;133(1):30–7.
79. Scaglione S, Giannoni P, Bianchini P, Sandri M, Marotta R, Firpo G, Valbusa U, Tampieri A, Diaspro A, Bianco P, Quarto R. "Order versus Disorder: in vivo bone formation within osteoconductive scaffolds.". Sci Rep. 2012;2:274.
80. Gungor-Ozkerim PS, Inci I, Zhang YS, Khademhosseini A, Dokmeci MR. "Bioinks for 3D bioprinting: an overview". Biomater Sci. 2018 May 1;6(5):915–46.
81. Chen DXB. "Biomaterials for Bioprinting BT - Extrusion Bioprinting of Scaffolds for Tissue Engineering Applications". In: Chen DXB, editor. Cham: Springer International Publishing; 2019. p. 33–48.
82. Tian Y, Liu M, Liu Y, Shi C, Wang Y, Liu T, Huang Y, Zhong P, Dai J, Liu X. "The performance of 3D bioscaffolding based on a human periodontal ligament stem cell printing technique". J Biomed Mater Res Part A. 2021 Oct 5;109(n/a):1209–19.
83. Amler AK, Dinkelborg PH, Schlauch D, Spinnen J, Stich S, Lauster R, Sittinger M, Nahles S, Heiland M, Kloke L, Rendenbach C, Beck-Broichsitter B, Dehne T. "Comparison of the Translational Potential of Human Mesenchymal Progenitor Cells from Different Bone Entities for Autologous 3D Bioprinted Bone Grafts". Int J Mol Sci. 2021 Jan 14;22(2):796.
84. Amler AK, Thomas A, Tüzüner S, Lam T, Geiger MA, Kreuder AE, Palmer C, Nahles S, Lauster R, Kloke L. "3D bioprinting of tissue-specific osteoblasts and endothelial cells to model the human jawbone". Sci Rep. 2021 Mar 1;11(1):4876.
85. Walladbegi J, Schaefer C, Pernevik E, Sämfors S, Kjeller G, Gatenholm P, Sándor GK, Rasmusson L. "Three-Dimensional Bioprinting Using a Coaxial Needle with Viscous Inks in Bone Tissue Engineering - An In vitro Study". Ann Maxillofac Surg. 2020/12/23. 2020;10(2):370–6.
86. Dubey N, Ferreira JA, Malda J, Bhaduri SB, Bottino MC. "Extracellular Matrix/Amorphous Magnesium Phosphate Bioink for 3D Bioprinting of Craniomaxillofacial Bone Tissue.". ACS Appl Mater Interfaces. 2020 May;12(21):23752–63.
87. Chimene D, Miller L, Cross LM, Jaiswal MK, Singh I, Gaharwar AK. "Nanoengineered Osteoinductive Bioink for 3D Bioprinting Bone Tissue". ACS Appl Mater Interfaces. 2020 Apr 8;12(14):15976–88.
88. Ma Y, Ji Y, Zhong T, Wan W, Yang Q, Li A, Zhang X, Lin M. "Bioprinting-Based PDLSC-ECM Screening for in Vivo Repair of Alveolar Bone Defect Using Cell-Laden, Injectable and Photocrosslinkable Hydrogels". ACS Biomater Sci Eng. 2017 Dec 11;3(12):3534–45.
89. Kuss MA, Harms R, Wu S, Wang Y, Untrauer JB, Carlson MA, Duan B. "Short-term hypoxic preconditioning promotes prevascularization in 3D bioprinted bone constructs with stromal vascular fraction derived cells". RSC Adv. 2017;7(47):29312–20.

90. Kang HW, Lee SJ, Ko IK, Kengla C, Yoo JJ, Atala A. "A 3D bioprinting system to produce human-scale tissue constructs with structural integrity". Nat Biotechnol. 2016;34(3):312–9.
91. Duarte Campos DF, Blaeser A, Buellesbach K, Sen KS, Xun W, Tillmann W, Fischer H. "Bioprinting Organotypic Hydrogels with Improved Mesenchymal Stem Cell Remodeling and Mineralization Properties for Bone Tissue Engineering.". Adv Healthc Mater. 2016 Jun;5(11):1336–45.
92. Ono T, Tomokiyo A, Ipposhi K, Yamashita K, Alhasan MA, Miyazaki Y, Kunitomi Y, Tsuchiya A, Ishikawa K, Maeda H. "Generation of biohybrid implants using a multipotent human periodontal ligament cell line and bioactive core materials". J Cell Physiol. 2021 Sep 1;236(9):6742–53.
93. Lee UL, Yun S, Cao HL, Ahn G, Shim JH, Woo SH, Choung PH. "Bioprinting on 3D Printed Titanium Scaffolds for Periodontal Ligament Regeneration". Cells. 2021 May 28;10(6):1337.
94. Thattaruparambil Raveendran N, Vaquette C, Meinert C, Samuel Ipe D, Ivanovski S. "Optimization of 3D bioprinting of periodontal ligament cells". Dent Mater. 2019 Dec 1 [cited 2020 Feb 11];35(12):1683–94.
95. Ma Y, Ji Y, Huang G, Ling K, Zhang X, Xu F. "Bioprinting 3D cell-laden hydrogel microarray for screening human periodontal ligament stem cell response to extracellular matrix.". Biofabrication. 2015 Dec;7(4):44105.
96. Lin YT, Hsu TT, Liu YW, Kao CT, Huang TH. "Bidirectional Differentiation of Human-Derived Stem Cells Induced by Biomimetic Calcium Silicate-Reinforced Gelatin Methacrylate Bioink for Odontogenic Regeneration". Vol. 9, Biomedicines . 2021.
97. Han J, Jeong W, Kim MK, Nam SH, Park EK, Kang HW. "Demineralized Dentin Matrix Particle-Based Bio-Ink for Patient-Specific Shaped 3D Dental Tissue Regeneration". Polymers (Basel). 2021 Apr 15;13(8):1294.
98. Athirasala A, Tahayeri A, Thrivikraman G, Franca CM, Monteiro N, Tran V, Ferracane J, Bertassoni LE, França CM, Monteiro N, Tran V, Ferracane J, Bertassoni LE. "A dentin-derived hydrogel bioink for 3D bioprinting of cell laden scaffolds for regenerative dentistry.". Biofabrication. 2018 Jan;10(2):24101.
99. Park JH, Gillispie GJ, Copus JS, Zhang W, Atala A, Yoo JJ, Yelick PC, Lee SJ. "The effect of BMP-mimetic peptide tethering bioinks on the differentiation of dental pulp stem cells (DPSCs) in 3D bioprinted dental constructs". Biofabrication. 2020;12(3):35029.
100. Duarte Campos DF, Zhang S, Kreimendahl F, Kopf M, Fischer H, Vogt M, Blaeser A, Apel C, Esteves-Oliveira M, Köpf M, Fischer H, Vogt M, Blaeser A, Apel C, Esteves-Oliveira M. "Hand-held bioprinting for de novo vascular formation applicable to dental pulp regeneration.". Connect Tissue Res. 2019 Jul;61(2):1–11.
101. Betsch M, Cristian C, Lin YY, Blaeser A, Schöneberg J, Vogt M, Buhl EM, Fischer H, Duarte Campos DF. "Incorporating 4D into Bioprinting: Real-Time Magnetically Directed Collagen Fiber Alignment for Generating Complex Multilayered Tissues". Adv Healthc Mater. 2018 Nov 1;7(21):1800894.
102. Yao L, Flynn N. "Dental pulp stem cell-derived chondrogenic cells demonstrate differential cell motility in type I and type II collagen hydrogels.". Spine J. 2018 Jun;18(6):1070–80.
103. Osidak E, Kozhukhov I, Osidak M, Domogatsky S. "Collagen as Bioink for Bioprinting: A Comprehensive Review". Int J Bioprinting. 2020 Apr 22;6.

104. Marques CF, Diogo GS, Pina S, Oliveira JM, Silva TH, Reis RL. "Collagen-based bioinks for hard tissue engineering applications: a comprehensive review.". J Mater Sci Mater Med. 2019 Mar;30(3):32.
105. Koch L, Deiwick A, Schlie S, Michael S, Gruene M, Coger V, Zychlinski D, Schambach A, Reimers K, Vogt PM, Chichkov B. "Skin tissue generation by laser cell printing.". Biotechnol Bioeng. 2012 Jul;109(7):1855–63.
106. Shi Y, Xing TL, Zhang HB, Yin RX, Yang SM, Wei J, Zhang WJ. "Tyrosinase-doped bioink for 3D bioprinting of living skin constructs.". Biomed Mater. 2018 Mar;13(3):35008.
107. Kim WJ, Yun HS, Kim GH. "An innovative cell-laden α-TCP/collagen scaffold fabricated using a two-step printing process for potential application in regenerating hard tissues". Sci Rep. 2017 Jun 9;7(1):3181.
108. Lee A, Hudson AR, Shiwarski DJ, Tashman JW, Hinton TJ, Yerneni S, Bliley JM, Campbell PG, Feinberg AW. "3D bioprinting of collagen to rebuild components of the human heart". Science (80-). 2019 Aug 2;365(6452):482 LP – 487.
109. Mazzocchi A, Devarasetty M, Huntwork R, Soker S, Skardal A. "Optimization of collagen type I-hyaluronan hybrid bioink for 3D bioprinted liver microenvironments.". Biofabrication. 2018 Oct;11(1):15003.
110. Lee YB, Polio S, Lee W, Dai G, Menon L, Carroll RS, Yoo SS. "Bio-printing of collagen and VEGF-releasing fibrin gel scaffolds for neural stem cell culture". Exp Neurol. 2010;223(2):645–52.
111. Prasadh S, Wong RCW. "Unraveling the mechanical strength of biomaterials used as a bone scaffold in oral and maxillofacial defects". Oral Sci Int. 2018;15(2):48–55.
112. Yang GH, Kim M, Kim G. "Additive-manufactured polycaprolactone scaffold consisting of innovatively designed microsized spiral struts for hard tissue regeneration". Biofabrication. 2016;9(1):15005.
113. Jaipan P, Nguyen A, Narayan RJ. "Gelatin-based hydrogels for biomedical applications". MRS Commun. 2017/10/03. 2017;7(3):416–26.
114. Sun M, Sun X, Wang Z, Guo S, Yu G, Yang H. "Synthesis and Properties of Gelatin Methacryloyl (GelMA) Hydrogels and Their Recent Applications in Load-Bearing Tissue". Polymers (Basel). 2018 Nov 21;10(11):1290.
115. Monteiro N, Thrivikraman G, Athirasala A, Tahayeri A, França CM, Ferracane JL, Bertassoni LE. "Photopolymerization of cell-laden gelatin methacryloyl hydrogels using a dental curing light for regenerative dentistry.". Dent Mater. 2018 Mar;34(3):389–99.
116. Athirasala A, Lins F, Tahayeri A, Hinds M, Smith AJ, Sedgley C, Ferracane J, Bertassoni LE. "A Novel Strategy to Engineer Pre-Vascularized Full-Length Dental Pulp-like Tissue Constructs". Sci Rep. 2017;7(1):3323.
117. Khayat A, Monteiro N, Smith EE, Pagni S, Zhang W, Khademhosseini A, Yelick PC. "GelMA-Encapsulated hDPSCs and HUVECs for Dental Pulp Regeneration.". J Dent Res. 2017 Feb;96(2):192–9.
118. Zhan H, Löwik DWPM. "A Hybrid Peptide Amphiphile Fiber PEG Hydrogel Matrix for 3D Cell Culture". Adv Funct Mater. 2019 Apr 1;29(16):1808505.
119. Brinkman WT, Nagapudi K, Thomas BS, Chaikof EL. "Photo-Cross-Linking of Type I Collagen Gels in the Presence of Smooth Muscle Cells: Mechanical Properties, Cell Viability, and Function". Biomacromolecules. 2003 Jul 1;4(4):890–5.
120. Lawson AC, Czernuszka JT. "Collagen-calcium phosphate composites". Proc Inst Mech Eng Part H J Eng Med. 1998 Jun 1;212(6):413–25.

121. Davidenko N, Schuster CF, Bax D V, Raynal N, Farndale RW, Best SM, Cameron RE. "Control of crosslinking for tailoring collagen-based scaffolds stability and mechanics". Acta Biomater. 2015/07/26. 2015 Oct;25:131–42.
122. Sanjairaj V, Vialli N, Fuh J, Lu WF. "Conductive Collagen/PPy-b-PCL hydrogel for bioprinting of neural tissue constructs". Int J Bioprinting. 2019 Jul 11;5.
123. Melchels FPW, Dhert WJA, Hutmacher DW, Malda J. "Development and characterisation of a new bioink for additive tissue manufacturing". J Mater Chem B. 2014;2(16):2282–9.
124. Billiet T, Gevaert E, De Schryver T, Cornelissen M, Dubruel P. "The 3D printing of gelatin methacrylamide cell-laden tissue-engineered constructs with high cell viability.". Biomaterials. 2014 Jan;35(1):49–62.
125. Zuo Y, Liu X, Wei D, Sun J, Xiao W, Zhao H, Guo L, Wei Q, Fan H, Zhang X. "Photo-cross-linkable methacrylated gelatin and hydroxyapatite hybrid hydrogel for modularly engineering biomimetic osteon.". ACS Appl Mater Interfaces. 2015 May;7(19):10386–94.
126. Wang H, Zhou L, Liao J, Tan Y, Ouyang K, Ning C, Ni G, Tan G. "Cell-laden photocrosslinked GelMA-DexMA copolymer hydrogels with tunable mechanical properties for tissue engineering.". J Mater Sci Mater Med. 2014 Sep;25(9):2173–83.
127. Billiet T, Van Gasse B, Gevaert E, Cornelissen M, Martins JC, Dubruel P. "Quantitative contrasts in the photopolymerization of acrylamide and methacrylamide-functionalized gelatin hydrogel building blocks.". Macromol Biosci. 2013 Nov;13(11):1531–45.
128. Hoshikawa A, Nakayama Y, Matsuda T, Oda H, Nakamura K, Mabuchi K. "Encapsulation of chondrocytes in photopolymerizable styrenated gelatin for cartilage tissue engineering.". Tissue Eng. 2006 Aug;12(8):2333–41.
129. Mũnoz Z, Shih H, Lin CC. "Gelatin hydrogels formed by orthogonal thiol–norbornene photochemistry for cell encapsulation". Biomater Sci. 2014;2(8):1063–72.
130. Anand R, Salar Amoli M, Huysecom AS, Amorim PA, Agten H, Geris L, Bloemen V. "A tunable gelatin-hyaluronan dialdehyde/methacryloyl gelatin interpenetrating polymer network hydrogel for additive tissue manufacturing.". Biomed Mater. 2022 Jun;17(4).
131. Lin CY, Peng HH, Chen MH, Sun JS, Liu TY, Chen MH. "In situ forming hydrogel composed of hyaluronate and polygalacturonic acid for prevention of peridural fibrosis". J Mater Sci Mater Med. 2015;26(4):168.
132. Highley CB, Prestwich GD, Burdick JA. "Recent advances in hyaluronic acid hydrogels for biomedical applications". Curr Opin Biotechnol. 2016;40:35–40.
133. Pescosolido L, Schuurman W, Malda J, Matricardi P, Alhaique F, Coviello T, van Weeren PR, Dhert WJA, Hennink WE, Vermonden T. "Hyaluronic Acid and Dextran-Based Semi-IPN Hydrogels as Biomaterials for Bioprinting". Biomacromolecules. 2011 May 9;12(5):1831–8.
134. Skardal A, Zhang J, Prestwich GD. "Bioprinting vessel-like constructs using hyaluronan hydrogels crosslinked with tetrahedral polyethylene glycol tetracrylates". Biomaterials. 2010;31(24):6173–81.
135. Hamlet SM, Vaquette C, Shah A, Hutmacher DW, Ivanovski S. "3-Dimensional functionalized polycaprolactone-hyaluronic acid hydrogel constructs for bone tissue engineering.". J Clin Periodontol. 2017 Apr;44(4):428–37.

136. Silva CR, Babo PS, Gulino M, Costa L, Oliveira JM, Silva-Correia J, Domingues RMA, Reis RL, Gomes ME. "Injectable and tunable hyaluronic acid hydrogels releasing chemotactic and angiogenic growth factors for endodontic regeneration.". Acta Biomater. 2018 Sep;77:155–71.
137. Law N, Doney B, Glover H, Qin Y, Aman ZM, Sercombe TB, Liew LJ, Dilley RJ, Doyle BJ. "Characterisation of hyaluronic acid methylcellulose hydrogels for 3D bioprinting". J Mech Behav Biomed Mater. 2018;77:389–99.
138. Petta D, D'Amora U, Ambrosio L, Grijpma DW, Eglin D, D'Este M. "Hyaluronic acid as a bioink for extrusion-based 3D printing.". Biofabrication. 2020 May;12(3):32001.
139. Radhakrishnan J, Subramanian A, Krishnan UM, Sethuraman S. "Injectable and 3D Bioprinted Polysaccharide Hydrogels: From Cartilage to Osteochondral Tissue Engineering". Biomacromolecules. 2017 Jan 9;18(1):1–26.
140. Khunmanee S, Jeong Y, Park H. "Crosslinking method of hyaluronic-based hydrogel for biomedical applications". J Tissue Eng. 2017 Sep 6;8:2041731417726464–2041731417726464.
141. Ye Q, Zünd G, Benedikt P, Jockenhoevel S, Hoerstrup SP, Sakyama S, Hubbell JA, Turina M. "Fibrin gel as a three dimensional matrix in cardiovascular tissue engineering.". Eur J cardio-thoracic Surg Off J Eur Assoc Cardio-thoracic Surg. 2000 May;17(5):587–91.
142. England S, Rajaram A, Schreyer DJ, Chen X. "Bioprinted fibrin-factor XIII-hyaluronate hydrogel scaffolds with encapsulated Schwann cells and their in vitro characterization for use in nerve regeneration". Bioprinting. 2017;5:1–9.
143. Dikovsky D, Bianco-Peled H, Seliktar D. "The effect of structural alterations of PEG-fibrinogen hydrogel scaffolds on 3-D cellular morphology and cellular migration.". Biomaterials. 2006 Mar;27(8):1496–506.
144. Ahmed TAE, Dare E V, Hincke M. "Fibrin: a versatile scaffold for tissue engineering applications.". Tissue Eng Part B Rev. 2008 Jun;14(2):199–215.
145. Hakam MS, Imani R, Abolfathi N, Fakhrzadeh H, Sharifi AM. "Evaluation of fibrin-gelatin hydrogel as biopaper for application in skin bioprinting: An in-vitro study.". Biomed Mater Eng. 2016;27(6):669–82.
146. Chiesa I, De Maria C, Lapomarda A, Fortunato GM, Montemurro F, Di Gesù R, Tuan RS, Vozzi G, Gottardi R. "Endothelial cells support osteogenesis in an in vitro vascularized bone model developed by 3D bioprinting.". Biofabrication. 2020 Feb;12(2):25013.
147. Cui X, Boland T. "Human microvasculature fabrication using thermal inkjet printing technology.". Biomaterials. 2009 Oct;30(31):6221–7.
148. Lu Q, Pandya M, Rufaihah AJ, Rosa V, Tong HJ, Seliktar D, Toh WS. "Modulation of Dental Pulp Stem Cell Odontogenesis in a Tunable PEG-Fibrinogen Hydrogel System.". Stem Cells Int. 2015;2015:525367.
149. Mastrullo V, Cathery W, Velliou E, Madeddu P, Campagnolo P. "Angiogenesis in Tissue Engineering: As Nature Intended? ". Vol. 8, Frontiers in Bioengineering and Biotechnology . 2020. p. 188.
150. Kjaergard HK, Weis-Fogh US. "Important factors influencing the strength of autologous fibrin glue; the fibrin concentration and reaction time--comparison of strength with commercial fibrin glue.". Eur Surg Res Eur Chir Forschung Rech Chir Eur. 1994;26(5):273–6.
151. Szekalska M, Puciłowska A, Szymańska E, Ciosek P, Winnicka K. "Alginate: Current Use and Future Perspectives in Pharmaceutical and Biomedical Applications". Kahveci MU, editor. Int J Polym Sci. 2016;2016:7697031.

152. Lee KY, Mooney DJ. "Alginate: Properties and biomedical applications". Prog Polym Sci. 2012;37(1):106–26.
153. Sandvig I, Karstensen K, Rokstad AM, Aachmann FL, Formo K, Sandvig A, Skjåk-Bræk G, Strand BL. "RGD-peptide modified alginate by a chemoenzymatic strategy for tissue engineering applications.". J Biomed Mater Res A. 2015 Mar;103(3):896–906.
154. Bhoj M, Zhang C, Green DW. "A First Step in De Novo Synthesis of a Living Pulp Tissue Replacement Using Dental Pulp MSCs and Tissue Growth Factors, Encapsulated within a Bioinspired Alginate Hydrogel.". J Endod. 2015 Jul;41(7):1100–7.
155. Sevari SP, Shahnazi F, Chen C, Mitchell JC, Ansari S, Moshaverinia A. "Bioactive glass-containing hydrogel delivery system for osteogenic differentiation of human dental pulp stem cells.". J Biomed Mater Res A. 2020 Mar;108(3):557–64.
156. Conboy I, Freimer J, Weisenstein L, Liu Y, Mehdipour M, Gathwala R. "6.13 Tissue Engineering of Muscle Tissue☆". In: Ducheyne PBTCBII, editor. Oxford: Elsevier; 2017. p. 216–35.
157. Wüst S, Godla ME, Müller R, Hofmann S. "Tunable hydrogel composite with two-step processing in combination with innovative hardware upgrade for cell-based three-dimensional bioprinting.". Acta Biomater. 2014 Feb;10(2):630–40.
158. Jia W, Gungor-Ozkerim PS, Zhang YS, Yue K, Zhu K, Liu W, Pi Q, Byambaa B, Dokmeci MR, Shin SR, Khademhosseini A. "Direct 3D bioprinting of perfusable vascular constructs using a blend bioink.". Biomaterials. 2016 Nov;106:58–68.
159. Yu Y, Zhang Y, Martin JA, Ozbolat IT. "Evaluation of cell viability and functionality in vessel-like bioprintable cell-laden tubular channels.". J Biomech Eng. 2013 Sep;135(9):91011.
160. Sell S, Wolfe P, Garg K, McCool J, Rodriguez I, Bowlin G. "The Use of Natural Polymers in Tissue Engineering: A Focus on Electrospun Extracellular Matrix Analogues". Polymers (Basel). 2010 Dec 1;2:522–53.
161. Gabriel M, van Nieuw Amerongen GP, Van Hinsbergh VWM, Amerongen AVVN, Zentner A. "Direct grafting of RGD-motif-containing peptide on the surface of polycaprolactone films.". J Biomater Sci Polym Ed. 2006;17(5):567–77.
162. Duymaz BT, Erdiler FB, Alan T, Aydogdu MO, Inan AT, Ekren N, Uzun M, Sahin YM, Bulus E, Oktar FN, Selvi SS, ToksoyOner E, Kilic O, Bostan MS, Eroglu MS, Gunduz O. "3D bio-printing of levan/polycaprolactone/gelatin blends for bone tissue engineering: Characterization of the cellular behavior". Eur Polym J. 2019;119:426–37.
163. Hersel U, Dahmen C, Kessler H. "RGD modified polymers: biomaterials for stimulated cell adhesion and beyond". Biomaterials. 2003;24(24):4385–415.
164. Wang X. "Advanced Polymers for Three-Dimensional (3D) Organ Bioprinting". Micromachines. 2019 Nov 25;10(12):814.
165. Amiryaghoubi N, Noroozi Pesyan N, Fathi M, Omidi Y. "Injectable thermosensitive hybrid hydrogel containing graphene oxide and chitosan as dental pulp stem cells scaffold for bone tissue engineering". Int J Biol Macromol. 2020;162:1338–57.
166. Qu T, Liu X. "Nano-structured gelatin/bioactive glass hybrid scaffolds for the enhancement of odontogenic differentiation of human dental pulp stem cells". J Mater Chem B. 2013;1(37):4764–72.

167. Casagrande L, Cordeiro MM, Nör SA, Nör JE. "Dental pulp stem cells in regenerative dentistry.". Odontology. 2011 Jan;99(1):1–7.
168. Kang J, Fan W, Deng Q, He H, Huang F. "Stem Cells from the Apical Papilla: A Promising Source for Stem Cell-Based Therapy". Piva E, editor. Biomed Res Int. 2019;2019:6104738.
169. Cao Y, Gong Y, Liu L, Zhou Y, Fang X, Zhang C, Li Y, Li J. "The use of human umbilical vein endothelial cells (HUVECs) as an in vitro model to assess the toxicity of nanoparticles to endothelium: a review.". J Appl Toxicol. 2017 Dec;37(12):1359–69.
170. Yu C, Miller KL, Schimelman J, Wang P, Zhu W, Ma X, Tang M, You S, Lakshmipathy D, He F, Chen S. "A sequential 3D bioprinting and orthogonal bioconjugation approach for precision tissue engineering.". Biomaterials. 2020 Nov;258:120294.
171. Xu L, Varkey M, Jorgensen A, Ju J, Jin Q, Park JH, Fu Y, Zhang G, Ke D, Zhao W, Hou R, Atala A. "Bioprinting small diameter blood vessel constructs with an endothelial and smooth muscle cell bilayer in a single step.". Biofabrication. 2020 Jul;12(4):45012.
172. Yao R, Alkhawtani A, Chen R, Luan J, Xu M. "Rapid and efficient in vivo angiogenesis directed by electro-assisted bioprinting of alginate/collagen microspheres with human umbilical vein endothelial cell coating layer". Int J Bioprinting. 2019 Jun 24;5:3.
173. Duarte Campos DF, Lindsay CD, Roth JG, LeSavage BL, Seymour AJ, Krajina BA, Ribeiro R, Costa PF, Blaeser A, Heilshorn SC. "Bioprinting Cell- and Spheroid-Laden Protein-Engineered Hydrogels as Tissue-on-Chip Platforms.". Front Bioeng Biotechnol. 2020;8:374.
174. Afghah F, Altunbek M, Dikyol C, Koc B. "Preparation and characterization of nanoclay-hydrogel composite support-bath for bioprinting of complex structures.". Sci Rep. 2020 Mar;10(1):5257.
175. Li L, Qin S, Peng J, Chen A, Nie Y, Liu T, Song K. "Engineering gelatin-based alginate/carbon nanotubes blend bioink for direct 3D printing of vessel constructs.". Int J Biol Macromol. 2020 Feb;145:262–71.
176. Gonzalez-Fernandez T, Rathan S, Hobbs C, Pitacco P, Freeman FE, Cunniffe GM, Dunne NJ, McCarthy HO, Nicolosi V, O'Brien FJ, Kelly DJ. "Pore-forming bioinks to enable spatio-temporally defined gene delivery in bioprinted tissues.". J Control Release. 2019 May;301:13–27.
177. Kérourédan O, Bourget JM, Rémy M, Crauste-Manciet S, Kalisky J, Catros S, Thébaud NB, Devillard R. "Micropatterning of endothelial cells to create a capillary-like network with defined architecture by laser-assisted bioprinting.". J Mater Sci Mater Med. 2019 Feb;30(2):28.
178. Moshaverinia A, Chen C, Akiyama K, Xu X, Chee WWL, Schricker SR, Shi S. "Encapsulated dental-derived mesenchymal stem cells in an injectable and biodegradable scaffold for applications in bone tissue engineering.". J Biomed Mater Res A. 2013 Nov;101(11):3285–94.
179. Yang Z, Jin F, Zhang X, Ma D, Han C, Huo N, Wang Y, Zhang Y, Lin Z, Jin Y. "Tissue Engineering of Cementum/Periodontal-Ligament Complex Using a Novel Three-Dimensional Pellet Cultivation System for Human Periodontal Ligament Stem Cells". Tissue Eng Part C Methods. 2009 Jun 12;15(4):571–81.
180. Sun B, Lian M, Han Y, Mo X, Jiang W, Qiao Z, Dai K. "A 3D-Bioprinted dual growth factor-releasing intervertebral disc scaffold induces nucleus pulposus and annulus fibrosus reconstruction". Bioact Mater. 2021;6(1):179–

90.
181. Sun Y, You Y, Jiang W, Wang B, Wu Q, Dai K. "3D bioprinting dual-factor releasing and gradient-structured constructs ready to implant for anisotropic cartilage regeneration.". Sci Adv. 2020 Sep;6(37).
182. Gori M, Giannitelli SM, Torre M, Mozetic P, Abbruzzese F, Trombetta M, Traversa E, Moroni L, Rainer A. "Biofabrication of Hepatic Constructs by 3D Bioprinting of a Cell-Laden Thermogel: An Effective Tool to Assess Drug-Induced Hepatotoxic Response.". Adv Healthc Mater. 2020 Sep;e2001163.
183. Toprakhisar B, Nadernezhad A, Bakirci E, Khani N, Skvortsov GA, Koc B. "Development of Bioink from Decellularized Tendon Extracellular Matrix for 3D Bioprinting". Macromol Biosci. 2018 Oct 1;18(10):1800024.
184. Laternser S, Keller H, Leupin O, Rausch M, Graf-Hausner U, Rimann M. "A Novel Microplate 3D Bioprinting Platform for the Engineering of Muscle and Tendon Tissues". SLAS Technol. 2018/06/12. 2018 Dec;23(6):599–613.
185. Merceron TK, Burt M, Seol YJ, Kang HW, Lee SJ, Yoo JJ, Atala A. "A 3D bioprinted complex structure for engineering the muscle-tendon unit.". Biofabrication. 2015 Jun;7(3):35003.
186. Kupfer ME, Lin WH, Ravikumar V, Qiu K, Wang L, Gao L, Bhuiyan DB, Lenz M, Ai J, Mahutga RR, Townsend D, Zhang J, McAlpine MC, Tolkacheva EG, Ogle BM. "In Situ Expansion, Differentiation, and Electromechanical Coupling of Human Cardiac Muscle in a 3D Bioprinted, Chambered Organoid.". Circ Res. 2020 Jul;127(2):207–24.
187. Attalla R, Puersten E, Jain N, Selvaganapathy PR. "3D bioprinting of heterogeneous bi- and tri-layered hollow channels within gel scaffolds using scalable multi-axial microfluidic extrusion nozzle.". Biofabrication. 2018 Dec;11(1):15012.
188. Demirtaş TT, Irmak G, Gümüşderelioğlu M. "A bioprintable form of chitosan hydrogel for bone tissue engineering.". Biofabrication. 2017 Jul;9(3):35003.
189. Wongsupa N, Nuntanaranont T, Kamolmattayakul S, Thuaksuban N. "Assessment of bone regeneration of a tissue-engineered bone complex using human dental pulp stem cells/poly(ε-caprolactone)-biphasic calcium phosphate scaffold constructs in rabbit calvarial defects". J Mater Sci Mater Med. 2017;28(5):77.
190. Pandula PKCP, Samaranayake LP, Jin LJ, Zhang CF. "Human umbilical vein endothelial cells synergize osteo/odontogenic differentiation of periodontal ligament stem cells in 3D cell sheets.". J Periodontal Res. 2014 Jun;49(3):299–306.
191. Walmsley GG, Ransom RC, Zielins ER, Leavitt T, Flacco JS, Hu MS, Lee AS, Longaker MT, Wan DC. "Stem Cells in Bone Regeneration". Stem cell Rev reports. 2016 Oct;12(5):524–9.
192. Ding X, Li X, Li C, Qi M, Zhang Z, Sun X, Wang L, Zhou Y. "Chitosan/Dextran Hydrogel Constructs Containing Strontium-Doped Hydroxyapatite with Enhanced Osteogenic Potential in Rat Cranium". ACS Biomater Sci Eng. 2019 Sep 9;5(9):4574–86.
193. YANG WS, Kim W, Ahn JY, Lee J, Ko DW, Park S, Kim JY, Jang CH, Lim JM, Kim G. "A New Bioink Derived from Neonatal Chicken Bone Marrow Cells and its 3D-Bioprinted Niche for Osteogenic Stimulators". ACS Appl Mater Interfaces. 2020 Sep 18;
194. Rukavina P, Koch F, Wehrle M, Tröndle K, Björn Stark G, Koltay P, Zimmermann S, Zengerle R, Lampert F, Strassburg S, Finkenzeller G, Simunovic F. "In vivo evaluation of bioprinted prevascularized bone tissue".

Biotechnol Bioeng. 2020 Aug 4;n/a(n/a).
195. Zhang J, Wehrle E, Adamek P, Paul GR, Qin XH, Rubert M, Müller R. "Optimization of mechanical stiffness and cell density of 3D bioprinted cell-laden scaffolds improves extracellular matrix mineralization and cellular organization for bone tissue engineering". Acta Biomater. 2020;114:307–22.
196. He H, Li D, Lin Z, Peng L, Yang J, Wu M, Cheng D, Pan H, Ruan C. "Temperature-programmable and enzymatically solidifiable gelatin-based bioinks enable facile extrusion bioprinting.". Biofabrication. 2020 Jul;12(4):45003.
197. Ahlfeld T, Cubo-Mateo N, Cometta S, Guduric V, Vater C, Bernhardt A, Akkineni AR, Lode A, Gelinsky M. "A Novel Plasma-Based Bioink Stimulates Cell Proliferation and Differentiation in Bioprinted, Mineralized Constructs". ACS Appl Mater Interfaces. 2020 Mar 18;12(11):12557–72.
198. Kim W, Kim G. "Collagen/bioceramic-based composite bioink to fabricate a porous 3D hASCs-laden structure for bone tissue regeneration.". Biofabrication. 2019 Nov;12(1):15007.
199. Gao G, Yonezawa T, Hubbell K, Dai G, Cui X. "Inkjet-bioprinted acrylated peptides and PEG hydrogel with human mesenchymal stem cells promote robust bone and cartilage formation with minimal printhead clogging". Biotechnol J. 2015 Oct 1;10(10):1568–77.
200. Ahlfeld T, Cidonio G, Kilian D, Duin S, Akkineni AR, Dawson JI, Yang S, Lode A, Oreffo ROC, Gelinsky M. "Development of a clay based bioink for 3D cell printing for skeletal application.". Biofabrication. 2017 Jul;9(3):34103.
201. Zhao C, Qazvini NT, Sadati M, Zeng Z, Huang S, De La Lastra AL, Zhang L, Feng Y, Liu W, Huang B, Zhang B, Dai Z, Shen Y, Wang X, Luo W, Liu B, Lei Y, Ye Z, Zhao L, et al. "A pH-Triggered, Self-Assembled, and Bioprintable Hybrid Hydrogel Scaffold for Mesenchymal Stem Cell Based Bone Tissue Engineering.". ACS Appl Mater Interfaces. 2019 Mar;11(9):8749–62.
202. Lan X, Sun Z, Chu C, Boltze J, Li S. "Dental Pulp Stem Cells: An Attractive Alternative for Cell Therapy in Ischemic Stroke " [Internet]. Vol. 10, Frontiers in Neurology . 2019.
203. Kodonas K, Gogos C, Papadimitriou S, Kouzi-Koliakou K, Tziafas D. "Experimental Formation of Dentin-like Structure in the Root Canal Implant Model Using Cryopreserved Swine Dental Pulp Progenitor Cells". J Endod. 2012;38(7):913–9.
204. Graziano A, d'Aquino R, Laino G, Papaccio G. "Dental pulp stem cells: a promising tool for bone regeneration.". Stem Cell Rev. 2008;4(1):21–6.
205. Arthur A, Rychkov G, Shi S, Koblar SA, Gronthos S. "Adult human dental pulp stem cells differentiate toward functionally active neurons under appropriate environmental cues.". Stem Cells. 2008 Jul;26(7):1787–95.
206. Iohara K, Zheng L, Wake H, Ito M, Nabekura J, Wakita H, Nakamura H, Into T, Matsushita K, Nakashima M. "A novel stem cell source for vasculogenesis in ischemia: subfraction of side population cells from dental pulp.". Stem Cells. 2008 Sep;26(9):2408–18.
207. Tamaoki N, Takahashi K, Tanaka T, Ichisaka T, Aoki H, Takeda-Kawaguchi T, Iida K, Kunisada T, Shibata T, Yamanaka S, Tezuka K. "Dental pulp cells for induced pluripotent stem cell banking.". J Dent Res. 2010 Aug;89(8):773–8.
208. Zhang W, Walboomers XF, Shi S, Fan M, Jansen JA. "Multilineage

Differentiation Potential of Stem Cells Derived from Human Dental Pulp after Cryopreservation". Tissue Eng. 2006 Oct 1;12(10):2813–23.
209. Potdar PD, Jethmalani YD. "Human dental pulp stem cells: Applications in future regenerative medicine". World J Stem Cells. 2015 Jun 26;7(5):839–51.
210. Cianci E, Recchiuti A, Trubiani O, Diomede F, Marchisio M, Miscia S, Colas RA, Dalli J, Serhan CN, Romano M. "Human Periodontal Stem Cells Release Specialized Proresolving Mediators and Carry Immunomodulatory and Prohealing Properties Regulated by Lipoxins.". Stem Cells Transl Med. 2016 Jan;5(1):20–32.
211. Zhu W, Liang M. "Periodontal ligament stem cells: current status, concerns, and future prospects.". Stem Cells Int. 2015;2015:972313.
212. Seo BM, Miura M, Gronthos S, Bartold PM, Batouli S, Brahim J, Young M, Robey PG, Wang CY, Shi S. "Investigation of multipotent postnatal stem cells from human periodontal ligament.". Lancet (London, England). 2004 Jul;364(9429):149–55.
213. Zhang J, An Y, Gao LN, Zhang YJ, Jin Y, Chen FM. "The effect of aging on the pluripotential capacity and regenerative potential of human periodontal ligament stem cells.". Biomaterials. 2012 Oct;33(29):6974–86.
214. Ikeda E, Hirose M, Kotobuki N, Shimaoka H, Tadokoro M, Maeda M, Hayashi Y, Kirita T, Ohgushi H. "Osteogenic differentiation of human dental papilla mesenchymal cells". Biochem Biophys Res Commun. 2006;342(4):1257–62.
215. Sonoyama W, Liu Y, Yamaza T, Tuan RS, Wang S, Shi S, Huang GTJ. "Characterization of the Apical Papilla and Its Residing Stem Cells from Human Immature Permanent Teeth: A Pilot Study". J Endod. 2008;34(2):166–71.
216. Kim BC, Jun SM, Kim SY, Kwon YD, Choe SC, Kim EC, Lee JH, Kim J, Suh JKF, Hwang YS. "Engineering three dimensional micro nerve tissue using postnatal stem cells from human dental apical papilla". Biotechnol Bioeng. 2017 Apr 1;114(4):903–14.
217. Abe S, Hamada K, Miura M, Yamaguchi S. "Neural crest stem cell property of apical pulp cells derived from human developing tooth". Cell Biol Int. 2012 Oct 1;36(10):927–36.
218. Huang GTJ, Yamaza T, Shea LD, Djouad F, Kuhn NZ, Tuan RS, Shi S. "Stem/Progenitor Cell–Mediated De Novo Regeneration of Dental Pulp with Newly Deposited Continuous Layer of Dentin in an In Vivo Model". Tissue Eng Part A. 2009 Sep 8;16(2):605–15.
219. Li G, Han N, Zhang X, Yang H, Cao Y, Wang S, Fan Z. "Local Injection of Allogeneic Stem Cells from Apical Papilla Enhanced Periodontal Tissue Regeneration in Minipig Model of Periodontitis". Wada K, editor. Biomed Res Int. 2018;2018:3960798.
220. Abe S, Yamaguchi S, Watanabe A, Hamada K, Amagasa T. "Hard tissue regeneration capacity of apical pulp derived cells (APDCs) from human tooth with immature apex". Biochem Biophys Res Commun. 2008;371(1):90–3.
221. Bakopoulou A, Kritis A, Andreadis D, Papachristou E, Leyhausen G, Koidis P, Geurtsen W, Tsiftsoglou A. "Angiogenic Potential and Secretome of Human Apical Papilla Mesenchymal Stem Cells in Various Stress Microenvironments". Stem Cells Dev. 2015 Jul 23;24(21):2496–512.
222. Andrae J, Gallini R, Betsholtz C. "Role of platelet-derived growth factors in physiology and medicine.". Genes Dev. 2008 May;22(10):1276–312.
223. Graves DT, Cochran DL. "Periodontal regeneration with polypeptide growth

factors". Curr Opin Periodontol. 1994;178–86.
224. Hollinger JO, Hart CE, Hirsch SN, Lynch S, Friedlaender GE. "Recombinant Human Platelet-Derived Growth Factor: Biology and Clinical Applications". JBJS. 2008;90(Supplement_1).
225. Javed F, Al-Askar M, Al-Rasheed A, Al-Hezaimi K. "Significance of the platelet-derived growth factor in periodontal tissue regeneration". Arch Oral Biol. 2011;56(12):1476–84.
226. Kaigler D, Avila G, Wisner-Lynch L, Nevins ML, Nevins M, Rasperini G, Lynch SE, Giannobile W V. "Platelet-derived growth factor applications in periodontal and peri-implant bone regeneration.". Expert Opin Biol Ther. 2011 Mar;11(3):375–85.
227. Zhang M, Jiang F, Zhang X, Wang S, Jin Y, Zhang W, Jiang X. "The Effects of Platelet-Derived Growth Factor-BB on Human Dental Pulp Stem Cells Mediated Dentin-Pulp Complex Regeneration.". Stem Cells Transl Med. 2017 Dec;6(12):2126–34.
228. Yu Y, Mu J, Fan Z, Lei G, Yan M, Wang S, Tang C, Wang Z, Yu J, Zhang G. "Insulin-like growth factor 1 enhances the proliferation and osteogenic differentiation of human periodontal ligament stem cells via ERK and JNK MAPK pathways". Histochem Cell Biol. 2012;137(4):513–25.
229. Han X, Amar S. "IGF-1 signaling enhances cell survival in periodontal ligament fibroblasts vs. gingival fibroblasts.". J Dent Res. 2003 Jun;82(6):454–9.
230. Chen F ming, Zhao Y min, Wu H, Deng Z hong, Wang Q tao, Zhou W, Liu Q, Dong G ying, Li K, Wu Z fen, Jin Y. "Enhancement of periodontal tissue regeneration by locally controlled delivery of insulin-like growth factor-I from dextran–co-gelatin microspheres". J Control Release. 2006;114(2):209–22.
231. Wang S, Mu J, Fan Z, Yu Y, Yan M, Lei G, Tang C, Wang Z, Zheng Y, Yu J, Zhang G. "Insulin-like growth factor 1 can promote the osteogenic differentiation and osteogenesis of stem cells from apical papilla". Stem Cell Res. 2012;8(3):346–56.
232. Lv T, Wu Y, Mu C, Liu G, Yan M, Xu X, Wu H, Du J, Yu J, Mu J. "Insulin-like growth factor 1 promotes the proliferation and committed differentiation of human dental pulp stem cells through MAPK pathways". Arch Oral Biol. 2016;72:116–23.
233. Massagué J, Blain SW, Lo RS. "TGFβ Signaling in Growth Control, Cancer, and Heritable Disorders". Cell. 2000 Oct 13;103(2):295–309.
234. Dreyer MK. "CHAPTER 51 - Receptor–Ligand Recognition in the TGFβ Family as Suggested by the Crystal Structures of BMP-2–BR-IAec and TGFβ3–TR-IIec". In: Bradshaw RA, Dennis EABTH of CS, editors. Burlington: Academic Press; 2003. p. 289–92.
235. Fujii S, Maeda H, Tomokiyo A, Monnouchi S, Hori K, Wada N, Akamine A. "Effects of TGF-β1 on the proliferation and differentiation of human periodontal ligament cells and a human periodontal ligament stem/progenitor cell line". Cell Tissue Res. 2010;342(2):233–42.
236. Niwa T, Yamakoshi Y, Yamazaki H, Karakida T, Chiba R, Hu JCC, Nagano T, Yamamoto R, Simmer JP, Margolis HC, Gomi K. "The dynamics of TGF-β in dental pulp, odontoblasts and dentin". Sci Rep. 2018;8(1):4450.
237. Mathieu S, Jeanneau C, Sheibat-Othman N, Kalaji N, Fessi H, About I. "Usefulness of Controlled Release of Growth Factors in Investigating the Early Events of Dentin-pulp Regeneration". J Endod. 2013;39(2):228–35.

238. Oates TW, Rouse CA, Cochran DL. "Mitogenic Effects of Growth Factors on Human Periodontal Ligament Cells In Vitro". J Periodontol. 1993 Feb 1;64(2):142–8.
239. Itoh N, Ornitz DM. "Fibroblast growth factors: from molecular evolution to roles in development, metabolism and disease". J Biochem. 2011 Feb 1;149(2):121–30.
240. Akita S, Akino K, Hirano A. "Basic Fibroblast Growth Factor in Scarless Wound Healing.". Vol. 2, Advances in wound care. United States; 2013. p. 44–9.
241. Murakami S, Takayama S, Ikezawa K, Shimabukuro Y, Kitamura M, Nozaki T, Terashima A, Asano T, Okada H. "Regeneration of periodontal tissues by basic fibroblast growth factor.". J Periodontal Res. 1999 Oct;34(7):425–30.
242. Zhao W, Li Y, Zhou A, Chen X, Li K, Chen S, Qiao B, Jiang D. "Controlled release of basic fibroblast growth factor from a peptide biomaterial for bone regeneration.". R Soc open Sci. 2020 Apr;7(4):191830.
243. Kinoshita Y, Matsuo M, Todoki K, Ozono S, Fukuoka S, Tsuzuki H, Nakamura M, Tomihata K, Shimamoto T, Ikada Y. "Alveolar bone regeneration using absorbable poly(L-lactide-co-ε-caprolactone)/β-tricalcium phosphate membrane and gelatin sponge incorporating basic fibroblast growth factor". Int J Oral Maxillofac Surg. 2008;37(3):275–81.
244. Shimabukuro Y, Ueda M, Ozasa M, Anzai J, Takedachi M, Yanagita M, Ito M, Hashikawa T, Yamada S, Murakami S. "Fibroblast Growth Factor–2 Regulates the Cell Function of Human Dental Pulp Cells". J Endod. 2009;35(11):1529–35.
245. Qu M, Jiang X, Zhou X, Wang C, Wu Q, Ren L, Zhu J, Zhu S, Tebon P, Sun W, Khademhosseini A. "Stimuli-Responsive Delivery of Growth Factors for Tissue Engineering". Adv Healthc Mater. 2020 Apr 1;9(7):1901714.
246. Tada S, Kitajima T, Ito Y. "Design and synthesis of binding growth factors.". Int J Mol Sci. 2012;13(5):6053–72.
247. Whitaker MJ, Quirk RA, Howdle SM, Shakesheff KM. "Growth factor release from tissue engineering scaffolds.". J Pharm Pharmacol. 2001 Nov;53(11):1427–37.
248. Rambhia KJ, Ma PX. "Controlled drug release for tissue engineering". J Control Release. 2015/08/29. 2015 Dec 10;219:119–28.
249. Ekenseair AK, Kasper FK, Mikos AG. "Perspectives on the interface of drug delivery and tissue engineering". Adv Drug Deliv Rev. 2012/09/20. 2013 Jan;65(1):89–92.
250. Kim SE, Lee PW, Pokorski JK. "Biologically Triggered Delivery of EGF from Polymer Fiber Patches.". ACS Macro Lett. 2017;6(6):593–7.
251. Gan Q, Zhu J, Yuan Y, Liu H, Zhu Y, Liu C. "A proton-responsive ensemble using mesocellular foam supports capped with N,O-carboxymethyl chitosan for controlled release of bioactive proteins.". J Mater Chem B. 2015 Mar;3(11):2281–5.
252. Adibfar A, Amoabediny G, Baghaban Eslaminejad M, Mohamadi J, Bagheri F, Zandieh Doulabi B. "VEGF delivery by smart polymeric PNIPAM nanoparticles affects both osteogenic and angiogenic capacities of human bone marrow stem cells.". Mater Sci Eng C Mater Biol Appl. 2018 Dec;93:790–9.
253. Gong T, Liu T, Zhang L, Ye W, Guo X, Wang L, Quan L, Pan C. "Design Redox-Sensitive Drug-Loaded Nanofibers for Bone Reconstruction". ACS Biomater Sci Eng. 2018 Jan 8;4(1):240–7.

254. Takahashi T, Tominaga T, Watabe N, Yokobori AT, Sasada H, Yoshimoto T. "Use of porous hydroxyapatite graft containing recombinant human bone morphogenetic protein-2 for cervical fusion in a caprine model". J Neurosurg Spine. 1999;90(2):224–30.
255. Deshpande A, Koudale SB, Bhongade ML. "A comparative evaluation of rhPDGF-BB + β-TCP and subepithelial connective tissue graft for the treatment of multiple gingival recession defects in humans.". Int J Periodontics Restorative Dent. 2014;34(2):241–9.
256. McGuire MK, Scheyer ET, Schupbach P. "Growth Factor–Mediated Treatment of Recession Defects: A Randomized Controlled Trial and Histologic and Microcomputed Tomography Examination". J Periodontol. 2009 Apr 1;80(4):550–64.
257. Patist CM, Mulder MB, Gautier SE, Maquet V, Jérôme R, Oudega M. "Freeze-dried poly(d,l-lactic acid) macroporous guidance scaffolds impregnated with brain-derived neurotrophic factor in the transected adult rat thoracic spinal cord". Biomaterials. 2004;25(9):1569–82.
258. Fu YC, Nie H, Ho ML, Wang CK, Wang CH. "Optimized bone regeneration based on sustained release from three-dimensional fibrous PLGA/HAp composite scaffolds loaded with BMP-2". Biotechnol Bioeng. 2008 Mar 1;99(4):996–1006.
259. Silva EA, Mooney DJ. "Effects of VEGF temporal and spatial presentation on angiogenesis". Biomaterials. 2010;31(6):1235–41.
260. Sakiyama-Elbert SE, Hubbell JA. "Development of fibrin derivatives for controlled release of heparin-binding growth factors". J Control Release. 2000;65(3):389–402.
261. Atienza-Roca P, Cui X, Hooper GJ, Woodfield TBF, Lim KS. "Growth Factor Delivery Systems for Tissue Engineering and Regenerative Medicine BT - Cutting-Edge Enabling Technologies for Regenerative Medicine". In: Chun HJ, Park CH, Kwon IK, Khang G, editors. Singapore: Springer Singapore; 2018. p. 245–69.
262. García-Pinel B, Porras-Alcalá C, Ortega-Rodríguez A, Sarabia F, Prados J, Melguizo C, López-Romero JM. "Lipid-Based Nanoparticles: Application and Recent Advances in Cancer Treatment.". Nanomater (Basel, Switzerland). 2019 Apr;9(4).
263. Zielińska A, Carreiró F, Oliveira AM, Neves A, Pires B, Venkatesh DN, Durazzo A, Lucarini M, Eder P, Silva AM, Santini A, Souto EB. "Polymeric Nanoparticles: Production, Characterization, Toxicology and Ecotoxicology.". Molecules. 2020 Aug;25(16).
264. Paul W, Sharma CP. "13 - Inorganic nanoparticles for targeted drug delivery". In: Sharma CPBTB of MIM (Second E, editor. Woodhead Publishing Series in Biomaterials. Woodhead Publishing; 2020. p. 333–73.
265. Eley JG, Mathew P. "Preparation and release characteristics of insulin and insulin-like growth factor-one from polymer nanoparticles". J Microencapsul. 2007 Jan 1;24(3):225–34.
266. Golub JS, Kim Y tae, Duvall CL, Bellamkonda R V, Gupta D, Lin AS, Weiss D, Robert Taylor W, Guldberg RE. "Sustained VEGF delivery via PLGA nanoparticles promotes vascular growth.". Am J Physiol Heart Circ Physiol. 2010 Jun;298(6):H1959-65.
267. Del Castillo-Santaella T, Ortega-Oller I, Padial-Molina M, O'Valle F, Galindo-Moreno P, Jódar-Reyes AB, Peula-García JM. "Formulation, Colloidal Characterization, and In Vitro Biological Effect of BMP-2 Loaded

PLGA Nanoparticles for Bone Regeneration.". Pharmaceutics. 2019 Aug;11(8).
268. Wang Z, Wang K, Lu X, Li M, Liu H, Xie C, Meng F, Jiang O, Li C, Zhi W. "BMP-2 encapsulated polysaccharide nanoparticle modified biphasic calcium phosphate scaffolds for bone tissue regeneration.". J Biomed Mater Res A. 2015 Apr;103(4):1520–32.
269. Xu X, Capito RM, Spector M. "Delivery of plasmid IGF-1 to chondrocytes via cationized gelatin nanoparticles". J Biomed Mater Res Part A. 2008 Jan 1;84A(1):73–83.
270. Asghar W, Islam M, Wadajkar AS, Wan Y, Ilyas A, Nguyen KT, Iqbal SM. "PLGA Micro- and Nanoparticles Loaded Into Gelatin Scaffold for Controlled Drug Release". IEEE Trans Nanotechnol. 2012;11(3):546–53.
271. López-Noriega A, Hastings CL, Ozbakir B, O'Donnell KE, O'Brien FJ, Storm G, Hennink WE, Duffy GP, Ruiz-Hernández E. "Hyperthermia-Induced Drug Delivery from Thermosensitive Liposomes Encapsulated in an Injectable Hydrogel for Local Chemotherapy". Adv Healthc Mater. 2014 Jun 1;3(6):854–9.
272. McGillicuddy FC, Lynch I, Rochev YA, Burke M, Dawson KA, Gallagher WM, Keenan AK. "Novel "plum pudding" gels as potential drug-eluting stent coatings: Controlled release of fluvastatin". J Biomed Mater Res Part A. 2006 Dec 15;79A(4):923–33.
273. Bennet D, Marimuthu M, Kim S, An J. "Dual drug-loaded nanoparticles on self-integrated scaffold for controlled delivery.". Int J Nanomedicine. 2012;7:3399–419.
274. Karam JP, Muscari C, Sindji L, Bastiat G, Bonafè F, Venier-Julienne MC, Montero-Menei NC. "Pharmacologically active microcarriers associated with thermosensitive hydrogel as a growth factor releasing biomimetic 3D scaffold for cardiac tissue-engineering". J Control Release. 2014;192:82–94.
275. Dyondi D, Webster TJ, Banerjee R. "A nanoparticulate injectable hydrogel as a tissue engineering scaffold for multiple growth factor delivery for bone regeneration.". Int J Nanomedicine. 2013;8:47–59.

Chapter 2. Aims

2.1 Background

As demonstrated in detail in the introduction of this thesis, tissue engineering strategies have created hope in addressing certain complications in the dentoalveolar region when traditional treatments are faced with challenges.

While bioprinting enhances the ability of tissue engineering strategies in addressing tissue heterogeneities, this level of complexity requires versatile and tunable biomaterials capable of replicating a range of physical and mechanical properties, as well as strategies to address the biological heterogeneity within the tissues in order to develop biologically relevant tissue analogues. Such heterogeneities are present in the dentoalveolar region on different levels. First, a range of different tissues including both hard tissues and soft tissues are present in this composition, with each of them imposing different requirements for tissue engineering scaffolds [1]. For example, dental pulp is a viscoelastic tissue structure, the properties of which are closely mimicked by natural hydrogels [2,3]. While being a soft tissue similar to the dental pulp, periodontal ligament has a totally different structure and its properties have been studied using different models including viscoelastic or hyperelastic, or linear elastic models [4,5]. In addition to these, dentin and alveolar bone are hard tissues composed mainly of a mineral matrix [6]. In addition to the presence of this range of tissues, there is a wide range of heterogeneity in physicomechanical and biological properties within each of these tissues. Still, research on bioprinting dentoalveolar tissues is still in its early stages, and considering the physical, mechanical and biological complexities in this region, further research is required to enable replication of such heterogeneous structures.

With the focus of this thesis being on the development of biomaterials for bioprinting the heterogeneous dentoalveolar region, this chapter will outline the aims pursued throughout this thesis, starting by a description of the general aims, followed by specific aims of each chapter.

2.2 Overall aim

The overall aim of this thesis is to develop strategies that could address the complexities present in tissue engineering of the dentoalveolar region. This is performed in two main categories, the first one being through developing versatile materials as biomaterial inks and bioinks, suitable for tissue engineering of this region through bioprinting, and the second category, by manufacturing delivery systems for the delivery of drugs and molecules within the printing strategies. The research performed to achieve this aim, is organized in this thesis in the following chapters. The subobjectives 1 to 3 lead to development of biomaterial inks and bioinks based on tunable chemistries to achieve this goal, and subobjectives 4 and 5 discuss the development of microgels for biomolecule delivery within bioprinting strategies. these two sections combined will demonstrate a platform capable of being used to replicate heterogeneities in the field of dentoalveolar bioprinting.

2.3 Specific chapter aims

2.3.1 Objective 1 (Chapter 3): Development and assessment of a chitosan based copolymer for bioprinting

Chapter 3 is entitled “The development of a 3D printable chitosan-based copolymer with tunable properties for dentoalveolar regeneration”. In this chapter, the aim was to employ the antibacterial properties of chitosan and hence, to synthesize a water-soluble derivative of chitosan, maleic grafted chitosan, combine it with gelatin and genipin, and evaluate its suitability for 3D printing of scaffolds aimed at tissue engineering in the dentoalveolar region. It was hypothesized that the proposed modification could lead to a 3D printable, biocompatible chitosan-based biomaterial ink suitable for tissue engineering through subsequent seeding of dental pulp stem cells onto the scaffold.

2.3.2 Objective 2 (Chapter 4): Assessment of a pNIPAM based copolymer for bioprinting

Chapter 4 of this thesis, “Development of 3D printed pNIPAM-chitosan scaffolds for dentoalveolar tissue engineering”, aimed to

introduce a thermo-sensitive, synthetic polymer, poly n-isopropylacrylamide (pNIPAM) to the chitosan backbone, and to assess the resulting chitosan-based copolymer for its use in bioprinting strategies aimed at tissue engineering of the dentoalveolar region.

2.3.3 Objective 3 (Chapter 5): Development of a tunable thermo-sensitive bioink

"Development of a pNIPAM-based temperature sensitive bioink able to encapsulate cells for 3D bioprinting of the dentoalveolar region" is the fifth Chapter in this thesis, and it aimed to address issues preventing biomaterials developed in previous chapters to encapsulate cells, such as rapid gelation. It was hypothesized that incorporation of pNIPAM and control over its water release by copolymerization with methylcellulose could potentially result in the development of a bioprintable biomaterial capable of encapsulating cells and suitable for dentoalveolar bioprinting strategies. Being based on a synthetic tunable chemistry, it was hypothesized that this bioink could be used to replicate a range of physical and mechanical properties within these tissues.

2.3.4 Objective 4 (Chapter 6): Development of a delivery system for use in bioinks

The general aim of chapter 6, entitled "The development and characterization of colloidal pNIPAM-based microgels for drug delivery in dentoalveolar tissue", was to develop a versatile strategy capable of delivering a range of drugs and growth factors within tissue engineering strategies aimed at the dentoalveolar region. For this purpose, it was hypothesized that microgels of pNIPAM-methycellulose copolymer could be suitable options for this purpose, hence, their development and systemic characterization was the main goal of this chapter.

2.3.5 Objective 5 (Chapter 7): preliminary assessment of encapsulating microgels in bioinks

Chapter 7 , "Incorporation of pNIPAM-based microgels in gelMA to control cellular differentiation", aimed to perform preliminary verifications towards the final goal of encapsulating growth factors

within the developed microgels and their use in bioprinting strategies. These preliminary verifications included evaluation of dental pulp stem cell (DPSC) differentiation through qPCR and alizarin red staining, and synthesis of gelMA as a candidate for encapsulation of microgels, considering the widespread use of gelMA demonstrating the applicability of the microgels for a range of bioprinting applications.

2.3.6 Discussion

Chapter 8 is dedicated to a discussion of the impact of this thesis on the field of bioprinting dentoalveolar tissues, and suggestion of further research which is required to advance towards the clinical stage.

2.3.7 Valorization

In the final chapter, it will be outlined how the content of this thesis could be valorized, enabling further research within the community of researchers working on the topic.

2.4 References

1. Amoli M, EzEldeen M, Jacobs R, Bloemen V, Salar Amoli M, EzEldeen M, Jacobs R, Bloemen V. "Materials for Dentoalveolar Bioprinting: Current State of the Art". Biomed . 2022 Dec 30;10(1):71.
2. Garg N. "Chapter-03 Structure of Teeth". Textbook of Operative Dentistry. 2013. p. 18–32.
3. Sloan AJ. "Chapter 29 - Biology of the Dentin-Pulp Complex". In: Vishwakarma A, Sharpe P, Shi S, Ramalingam MBTSCB and TE in DS, editors. Boston: Academic Press; 2015. p. 371–8.
4. Fill TS, Toogood RW, Major PW, Carey JP. "Analytically determined mechanical properties of, and models for the periodontal ligament: Critical review of literature". J Biomech. 2012;45(1):9–16.
5. Fill TS, Carey JP, Toogood RW, Major PW. "Experimentally determined mechanical properties of, and models for, the periodontal ligament: critical review of current literature". J Dent Biomech. 2011/04/05. 2011;2011:312980.
6. Gorrel C, Andersson S, Verhaert L. "Chapter 4 - Anatomy of the teeth and periodontium". In: Gorrel C, Andersson S, Verhaert LBTVD for the GP (Second E, editors. W.B. Saunders; 2013. p. 37–41.

Chapter 3. The development of a 3D printable chitosan-based copolymer with tunable properties for dentoalveolar regeneration

This chapter is adapted from:

"The development of a 3D printable chitosan-based copolymer with tunable properties for dentoalveolar regeneration"

Mehdi Salar Amoli [a,b], Resmi Anand [a,c,d], Mostafa EzEldeen [b,e], Paulo Alexandre Amorim [a,c], Liesbet Geris [c, f, g], Reinhilde Jacobs [b,h] , Veerle Bloemen [a,c]
[a] Materials Technology TC, Campus Group T, KU Leuven, Andreas Vesaliusstraat 13, 3000 Leuven, Belgium
[b] OMFS IMPATH Research Group, Faculty of Medicine, Department of Imaging and Pathology, KU Leuven and Oral and Maxillofacial Surgery, University Hospitals Leuven, Kapucijnenvoer 33, 3000 Leuven, Belgium
[c] Prometheus, Division of Skeletal Tissue Engineering Leuven, KU Leuven, Leuven, Belgium
[d] Inter University Centre for Biomedical Research and Super Speciality Hospital, Mahatma Gandhi University Campus at Thalappady, Kottayam, Kerala-686009, India
[e] Department of Oral Health Sciences, KU Leuven and Paediatric Dentistry and Special Dental Care, University Hospitals Leuven, Kapucijnenvoer 33, 3000 Leuven, Belgium
[f] Biomechanics Research Unit GIGA-R In Silico Medicine, Université de Liege, Quartier Hôpital, Avenue de l'Hôpital 11, Liège, Belgium
[g] Biomechanics Section, KU Leuven, Celestijnenlaan 300C (2419), Leuven, Belgium
[h] Department of Dental Medicine, Karolinska Institutet, Stockholm, Sweden

Published in Carbohydrate Polymers, 2022;289:119441

Chapter summary

Dentoalveolar tissue engineering is an emerging yet challenging field, considering the lack of suitable materials and difficulty to produce patient-specific hydrogel scaffolds. This chapter aims to produce a 3D printable and tunable biomaterial by copolymerizing a synthesized water-soluble chitosan derivative called maleic anhydride grafted chitosan (MA-C) with gelatin using genipin, a natural crosslinking agent. Development of the MA-C and the copolymer was analyzed through Fourier Transform Infrared Spectroscopy (FTIR) and Nuclear Magnetic Resonance (NMR). Further characterization of the material through evaluation of 3D printing, viscoelastic properties, degradation, and swelling demonstrated the ability to fabricate scaffolds with controlled physical properties based on pre-determined designs. The MA-C-gelatin copolymer demonstrated excellent biocompatibility, which was verified by analyzing the viability, growth and proliferation of human dental pulp stem cells seeded on MA-C-gelatin constructs through live/dead, alamarBlue and DNA quantification assays. The presented findings of scaffold fabrication, biocompatibility and tunability, suggest that the proposed material might be a suitable candidate for dentoalveolar tissue engineering, while further research is required to achieve this goal.

3.1 Introduction

Dentoalveolar tissue loss affects millions of people around the world undermining their quality of life, by impacting both oral function and facial esthetics [1,2]. The limited regenerative capacity of the dentoalveolar tissues [3] is currently approached by oral surgical procedures such as dental implants or even tooth autotransplantation. While these treatments have come a long way, associated challenges such as the inability of implant placement in paediatric patients, or donor shortage for autotransplantation [4,5] may give rise to a demand for regenerative procedures. Consequently, tissue engineering has been proposed to address alveolar ridge resorption, tooth loss, condylar resorption, and craniofacial defects more effectively [6].

Within the tissue engineering strategies, the choice of the scaffold material is of significant importance and a wide range of material classes have been suggested as scaffolds for engineering soft tissues, including natural and synthetic polymers, hydrogels or bioceramics [7]. In particular, hydrogels have gained special interest due to their high water content and their resemblance of the natural extracellular matrix (ECM) [8]. However, it is rather challenging to produce precisely shaped constructs using traditional techniques with hydrogels. Consequently, 3D printing has been introduced as a novel method enabling the production of pre-designed scaffolds using hydrogels in their native form, called biomaterial inks, without any further processing [9]

Chitosan, a polysaccharide originated from chitin, can form hydrogels capable of interacting electrostatically with glycosaminoglycans (GAGs) distributed in natural ECM and thus, supporting the activity of cell attachment molecules and cytokines [10,11]. Furthermore, it is known to have an excellent biocompatibility, biodegradability and to possess antimicrobial properties [12], making it a suitable candidate for tissue engineering strategies. However, the insolubility of chitosan in neutral pH is a major disadvantage limiting the use of its hydrogels in any application requiring direct contact of cells with the material [13]. To overcome this, an interesting approach would be to synthesize chitosan derivatives capable of being dissolved in a neutral pH.

While there are many suggested strategies to synthesize water-soluble chitosan, including modification of chitosan with styrene groups , azido groups [14], methacryloyl groups [15], etc., modification of chitosan with carboxylic groups through reaction with maleic anhydride (MA) is of particular interest due to the fast and effective procedure resulting in a sufficiently water-soluble chitosan derivative [16].

Furthermore, being biocompatible, non-immunogenic, and biodegradable [17], gelatin has been used in combination with chitosan-based materials in tissue engineering applications to enhance cellular attachment to the chitosan, in addition to augmenting its mechanical properties [18]. However, for material solutions to form stable hydrogels, crosslinking is needed. Genipin is a naturally derived crosslinker able to attach primary amine groups and thus, crosslink both chitosan and gelatin [19], in addition to chitosan derivatives where the primary amines are still available for reaction. It has shown to induce a relatively lower amount of toxicity to the cells compared to other crosslinkers such as glutaraldehyde [20]. Additionally, genipin is known to promote odontoblastic differentiation in dental pulp cells (DPCs) [21]. Furthermore, using genipin allows for control over the physical properties of the scaffolds such as degradability or swelling, through adjusting the crosslinking degree. As a result, genipin appears to be a suitable crosslinker for production of scaffolds aimed at dentoalveolar regeneration.

It is hypothesized in this chapter, that synthesis of a water-soluble chitosan derivative, maleic anhydride grafted chitosan (MA-C), in which the primary amines are available for further reactions such as crosslinking, and copolymerizing that with gelatin using genipin could produce a printable, tunable material for fabrication of hydrogel scaffolds for dentoalveolar regeneration, while avoiding the use of acetic acid usually required for incorporation of chitosan. The study in this chapter aimed to synthesize the MA-C, and combine it with gelatin and genipin to investigate its potential for 3D printing, and to perform several physical characterizations and *in vitro* biocompatibility tests to assess suitability of the material to act as a tissue engineering scaffold.

3.2 Materials and methods

3.2.1 Materials

Chitosan (molecular weight 190-310 kDa, deacetylation rate 75-85%), maleic anhydride (purity > 99%), pyridine (anhydrous, 99.8%), absolute ethanol, methanol (100%), glacial acetic acid, citric acid, NaOH, ninhydrin, tin(II) chloride dihydrate, glycine, gelatin (from porcine skin, 240-270 g bloom) were obtained from Sigma Aldrich (Overijse, Belgium). Genipin and AlamarBlue reagents were obtained from Challenge Bioproducts Co., Ltd (Taiwan), and Thermo Fisher Scientific (Brussels, Belgium), respectively.

3.2.2 Preparation of hydrogels

3.2.2.1 Synthesis of maleic anhydride grafted chitosan (MA-C)

MA-C was synthesized through a reported procedure [16] with slight modifications. Briefly, 1 g chitosan was dissolved in 50 ml 80 % (v/v) acetic acid and then mixed with 30 ml 100% methanol in a 250 ml two-neck round bottom flask under stirring at room temperature. 1 g maleic anhydride was separately dissolved in 20 ml 100% methanol, and the solution was mixed with 1 ml pyridine by dropwise addition of pyridine in an ice water bath. The ice-cold solution was added to the chitosan in a dropwise manner, and stirring was continued for 24 h at 65 ºC. Excess ethanol was added to the reaction mixture to precipitate the MA-C, which was then recovered by centrifugation at 155 RCF for 10 minutes (Hettich Universal 32R) at room temperature. MA-C was added to excess water (approx. 750 mL) and dialyzed against deionized water using dialysis tubing with a 12 kDa molecular cut off for 5 days at room temperature to remove residual small molecules such as unreacted maleic anhydride and acetic acid. The solution was then freeze-dried to obtain the MA-C.

3.2.2.2 Preparation of genipin crosslinked MA-C/gelatin copolymers

The genipin component was dissolved in PBS (pH 7.4) in 5 different ratios of 0.5, 1, 1.5, 2 and 2.5 (w/w) % (with regards to the polymer content in the final combination) by heating to 60 °C followed by

vortexing for 30 s. Gel components were made separately by adding gelatin and MA-C to PBS (pH 7.4) and mixed by stirring at 60 °C for 24 h to yield final concentrations of 1.5 %(w/v) gelatin and 1.5 %(w/v) MA-C for the first set and 3 %(w/v) gelatin and 1.5 %(w/v) MA-C for the second set, achieving these concentrations after combination with the genipin component. The two components (gel component and genipin) were mixed for 10 min, leading to 10 sets of combination. They were placed in a 37 ºC water bath for 24 h to crosslink.

3.2.3 Physico-chemical characterization

3.2.3.1 Fourier transform infrared spectroscopy

MA-C and unmodified chitosan were freeze dried and grinded to prepare the samples. The FTIR-ATR spectra of the samples were recorded using a Bruker Vertex 70 FTIR spectrometer with a Diamond Attenuated Total Reflection (ATR) accessory in the wavelength range of 400-4000 cm^{-1}. The analysis was performed with a resolution of 2 cm^{-1} and an average of 32 scans on 3 samples for each condition.

3.2.3.2 Proton nuclear magnetic resonance (^{1}H NMR)

The structure of the synthesized MA-C was confirmed using ^{1}H NMR recorded on a Bruker Avance III HD/400, using D_2O as the solvent.

3.2.3.3 Measurement of the crosslinking degree

The degree of crosslinking was measured using the ninhydrin assay for samples containing 3 %(w/v) gelatin and 1.5 %(w/v) MA-C. Ninhydrin solution containing ninhydrin and $SnCl.H_2O$ was made using the protocols described by Yan et al., 2010 and kept in a dark bottle at room temperature for further use. For each five genipin concentrations, samples were crosslinked with genipin for different periods of 1 h, 3 h, 6 h, 12 h and 24 h. At each timepoint, samples were collected, placed in -80 ºC freezer and lyophilized, along with non-crosslinked samples as a negative control. 5 mg of each lyophilized sample was added to 4 ml ninhydrin solution and incubated in 100 ºC water bath for 20 min, cooled down to room temperature and mixed with 25 ml 50 % isopropanol. Optical absorbance at 570 nm was measured using a spectrophotometer (Spectronic genesys 8, Thermofisher scientific).

The amount of free amino groups in the samples was proportional to the absorbance and was detected using a standard curve of different glycine concentrations in PBS solution (pH 7.4). The sample absorbance was compared with the absorbance of an uncrosslinked sample to evaluate the crosslinking degree.

3.2.3.4 Estimation of unreacted genipin

Samples containing 3 %(w/v) gelatin and 1.5 %(w/v) MA-C and different genipin concentrations were prepared. After 1, 3, 6, 12 and 24 h of crosslinking with different genipin concentrations, 1 mL of sample was immersed in 10 mL PBS (pH 7.4) and placed on a shaker. At different timepoints of 12, 24, 48 and 72 h after immersion in PBS, 1 mL of PBS was removed, mixed with 1 mL of 1 %(w/v) glycine solution in PBS and placed in 60 ºC water bath for 1 h. Optical absorbance at 578 nm was measured using a spectrophotometer. To determine the concentration of released genipin, a calibration curve of 1 %(w/v) glycine solution in PBS with different amounts of genipin was made and cumulative data of different extract times for each crosslinking timepoint were represented.

3.2.4 3D printing and physical characterizations of the scaffold

3.2.4.1 Evaluation of printing fidelity

Genipin crosslinked gels were transferred to a piston-driven printing cartridge of 7.29 mm diameter and circles of 20 mm diameter with grid infill, containing a distance of 0.5 mm between strands, were printed using a 3DDiscovery bioprinter (RegenHU, Switzerland). A 410 µm nozzle (22G) was used to print 5 layer constructs as circles with a diameter of 20 mm and a grid infill with grid distance of 5 mm. The flow rate was empirically defined to be able to generate filaments, and the printing speed was estimated as the nozzle diameter was constant. Printed samples were compared in terms of strand width, uniformity within each strand and among different strands using FIJI software [25]. Only printable gels, consisting of 3 %(w/v) gelatin, 1.5 %(w/v) MA-C, and 5 different genipin concentrations, were used for physico-chemical and scaffold characterizations.

3.2.4.2 Evaluation of the linear viscoelasticity of the material

The linear viscoelastic properties of the hybrid (physical and chemical) and chemical hydrogels were measured via small-amplitude shear rheometry using an Anton Paar Physica MCR 501 rotational rheometer as in Zuidema et al. [1]. The device was equipped with a parallel plate test geometry of 25 mm and a temperature-controlled solvent trap to minimize dehydration. The bottom plate of the rheometer was covered with sandpaper to avoid slippage. Samples of low (0.5 w/w%) and high (2.5 w/w%) genipin contents were prepared by casting the materials in the sol state into cylindrical molds and allowing them to gelate for 24h at 37°C. Due to the inherent crosslinking degree and the subsequent shrinkage of each of the studied compositions, gap heights were determined by applying similar normal forces to all the samples. All the measurements were performed in triplicate after allowing the samples to reach steady state at the corresponding testing temperature. First, strain-amplitude sweep measurements were performed within the range of 0.01 to 10 % strain at 20 °C (processing temperature) and 0.05 to 5 % strain at 37° C (physiological temperature) at an angular frequency of 10 rad.s^{-1} to determine the materials linear viscoelastic envelope (LVE). Next, the mechanical spectra of the materials at 20 and 37 °C were obtained via a frequency sweep in the LVE within the range of 0.1 to 100 rad.s^{-1} at 1 % strain. The results reported refer to measurements performed in controlled shear rate mode (CSR), in which the generated torque values are at least one order of magnitude larger than the lower threshold of the device in oscillation mode (0.01 μN.m). The shear equilibrium moduli of the hydrogels were taken as the corresponding storage modulus (G') at the lowest angular frequency of its respective mechanical spectrum. In this way, the size of the spatial correlation length from rheological measurements, known as the elastic blob, was determined.

3.2.4.3 Evaluation of surface morphology

The morphology of gels crosslinked with 2.5 %(w/w) and 0.5 %(w/w) genipin (maximum and minimum concentration used) was evaluated through scanning electron microscopy, using a Philips scanning electron microscope XL30 at 10 KV. For this purpose, 5 layer scaffolds

of 10 mm* 10 mm with grid infill and grid distance of 4 mm were printed, frozen at -20 °C for 24 h, freeze-dried, cut into vertical and horizontal planes and coated with 5 nm Platinum to observe the inner structure. SEM images were used to analyse the average pore size by performing measurements on the images of at least three samples using FIJI software [25].

3.2.4.4 Swelling and degradation studies

Gel formulations of 3 %(w/v) gelatin and 1.5 %(w/v) chitosan-MA with 5 different genipin concentrations were printed in shapes of cubes of dimensions 10x10x5 mm and grid distance of 4 mm. Samples were freeze dried, weighed, and incubated in PBS at 37 ºC. At 3, 6, 12, 24, 48 and 72 h, the samples were dried with a tissue paper and weighed again. The swelling was calculated following equation 3.1, where E_{sw} is the percentage of swelling, W_{sw} is the swollen weight and W_0 is the initial weight.

$$E_{sw} = \frac{W_{sw} - W_0}{W_0} \times 100 \qquad \text{Eq. 3.1}$$

To measure hydrolytic degradation, samples were prepared similarly, freeze dried after 1, 3, 5, 7 and 14 days, and weighed. The degradation was measured following equation 3.2, where R_d is the degradation rate, W_0 is the initial weight and W is the sample weight at each timepoint.

$$R_d = \frac{W_0 - W}{W_0} \times 100 \qquad \text{Eq. 3.2}$$

3.2.5 Evaluation of cellular response

3.2.5.1 Evaluation of cell viability through live/dead assay

Gelatin and MA-C were prepared to yield 3 %(w/v) and 1.5 %(w/v) gels, respectively. Solutions were mixed with 2.5 wt% and 0.5 wt% genipin (maximum and minimum concentrations) and placed in a 48 well plate to crosslink for 24 h at 37 ºC. Sterilization was performed by exposure to UV-C for 2 h.

Subculturing of cells was performed using the protocol described by Hilkens et al. [22]. A cell density of $1x10^4/cm^2$ hDPSCs (passage 11) was seeded on top of 150 µL crosslinked gels and immersed in DMEM supplemented with 1% FBS and 1% antibiotics. Live/Dead staining

was performed using Calcein Am and Ethidium homodimer (Live/Dead viability cytotoxicity kit, Invitrogen, Thermofisher Scientific) according to the manufacturer's protocol at day 1, 3 and 7. Hoechst 33342 staining was performed according to the manufacturer's protocol at the same timepoints. Control samples consisted of monolayers with an initial density of $1x10^4/cm^2$ and cultured in 48-well plates. Microscopic images for this study were subjected to non-linear modifications to remove background signal.

3.2.5.2 AlamarBlue assay

Cell seeded scaffolds were prepared in 48 well plates similar to samples for live/Dead assay. A 10 % (v/v) solution of alamarBlue reagent (Challenge Bioproducts Co., Ltd, Taiwan) in DMEM (supplemented with 1% FBS and 1% antibiotics) was prepared and added to each well. Well plates were incubated at 37 °C for 2 h. Three readings were performed for each well using 100 µL for each reading. Readings were performed at excitation and emission wavelengths of 540 and 590 nm, respectively. Negative controls consisting of wells with medium and wells covered with gels in the absence of cells were subtracted from sample readings. Positive control readings were performed on cells cultured in well plates.

3.2.5.3 DNA quantification

Cell seeded scaffolds were prepared in 48 well plates following the same protocol used for live/dead assay. At 1, 3, and 7 days, 500 µL of 2 mg/mL Pronase enzyme was added to the wells and incubated at 37 °C for 24 h to digest the gels. The enzyme was also added to cell-only samples. Digested gel containing DNA was removed and centrifuged at 15000 rpm for 10 min. Supernatant was removed, and 350 µL commercial RLT lysis buffer (Qiagen, Belgium) plus 1 %(v/v) B-mercapto-ethanol was added to the remaining mixture of cells and DNA to prepare the lysate. Quant-iTTM dsDNA HS reagent was diluted in Quant-iTTM dsDNA HS buffer (Quant-iT dsDNA Assay Kit, Thermofisher Scientific) with a 1:200 ratio. 5 µL of lysate was mixed with 195 µL of the working solution. Standards were prepared following the manufacturers protocol. Samples were transferred to Qubit tubes and readings were performed using Qubit fluorometer.

3.2.5.4 Statistical analysis

All experiments in all sections were performed in three independent replicates (n=3). Two-way ANOVA and Tukey's multiple comparisons test were performed using GraphPad Prism (version 8.0.0 for Windows, GraphPad Software, San Diego, California USA, www.graphpad.com) to analyse differences with regards to time and genipin concentration. The bar charts demonstrate mean ± standard deviation, while the FTIR, NMR and rheology graphs are representative figures from at least three measurements.

3.3 Results

3.3.1 Synthesis of MA-C

To produce malec grafted chitosan, an esterification reaction was performed between the chitosan and maleic anhydride. Firstly, maleic anhydride was dissolved in methanol, producing monomethyl maleate in a rapid, irreversible reaction [23] (Scheme 3.1.A).
Further reaction of monomethyl maleate with methanol would yield dimethyl maleate. However, that reaction is very slow and usually requires catalysers such as zeolite. At this step, pyridine was added to the reaction mixture to generate the functional groups required for reaction with the chitosan. Through the reaction of monomethyl maleate with pyridine (scheme 3.1.B), it undergoes an isomerization turning into monomethyl fumarate, a more reactive form that may then react with chitosan [24]. As appears in scheme 3.1.C, monomethyl fumarate produced in the second step reacts mainly with hydroxyl groups on the chitosan backbone through an esterification reaction. The copolymer resulting from genipin crosslinking of MA-C and gelatin is demonstrated in scheme 3.1.D.

3.3.2 Physico-chemical characterization

3.3.2.1 Fourier transform infrared spectroscopy

The FTIR analysis (figure 3.1.A) shows peaks appearing at 3000-3629, 2826-2987, 1715, 1564, 1383 and 959-1118 cm^{-1} corresponding to O-H/N-H, =C-H, C=O, C=C, C-N and C-O groups, the characteristic peaks aimed for. Further confirmation of the synthesis was performed

using ^{1}H NMR, as represented in figure 3.1.B. The ^{1}H NMR peaks appearing at 6.5 ppm and 6.8 ppm represent alkene groups present on maleic anhydride confirming the grafting of maleic anhydride on the chitosan backbone. The peak appearing at 6.8 ppm represents the alkene close to the ester group, and the peak appearing at 6.5 represents the alkene group close to the amine group. Considering that the peak at 6.8 ppm is significantly larger than the one at 6.5, it can be concluded that the modification has mostly taken place on the hydroxyl groups rather than the amine groups. Peak integration demonstrates 70.8 % of modification to have taken place at the hydroxyl groups of the chitosan.

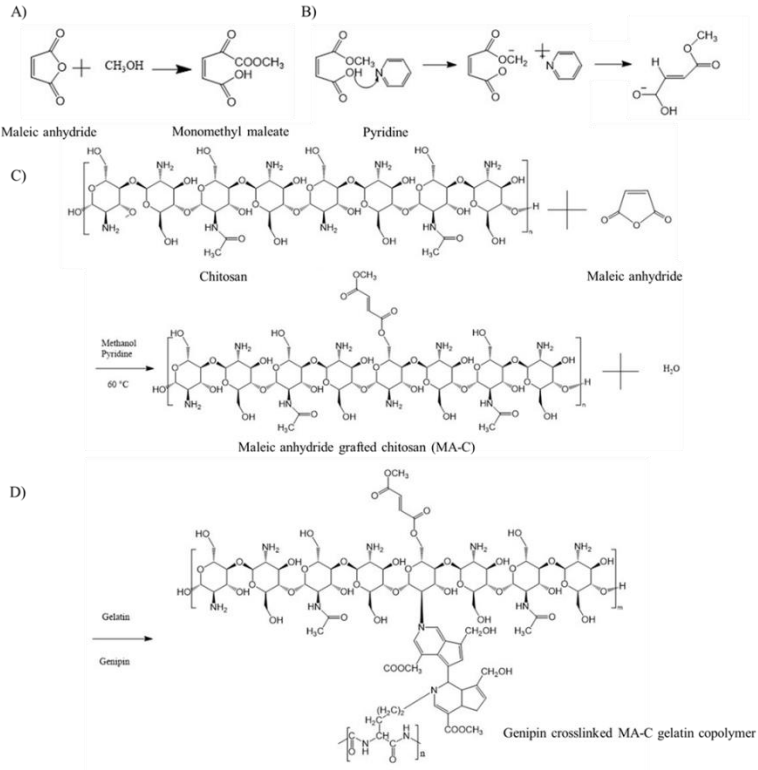

Scheme 3.1. Schematic representation showing the synthesis of maleic anhydride grafted chitosan, and copolymerization with gelatin through crosslinking with genipin. A) maleic anhydride reaction with methanol B) reaction of monomethyl maleate with pyridine C) overall reaction of MA-C synthesis D) synthesis of genipin crosslinked MA-C-gelatin copolymer (scheme made using chemdraw software)

3.3.2.2 Measurement of the degree of crosslinking in MA-C-gelatin copolymer

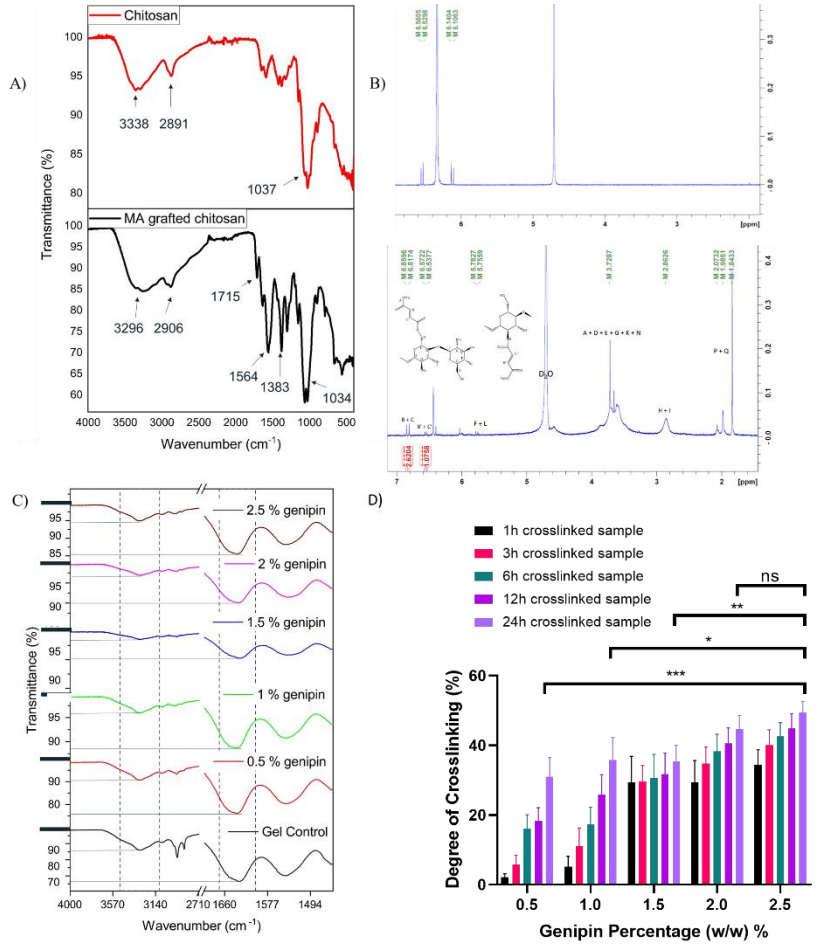

Figure 3.1. A) FTIR spectra of chitosan (top) and synthesized MA-C (bottom). B) ^{1}H NMR spectrum of maleic anhydride (top) and MA-C (bottom) in D2O, C) confirmation of crosslinking through FTIR analysis, the area between dashed lines represents peaks corresponding to primary amine groups. D) Measurement of crosslinking degree through ninhydrin assay (n=3).

Firstly, a confirmation of crosslinking was obtained using FTIR analysis, as indicated in figure 3.1.C. The control material represents non crosslinked MA-C and gelatin blend. The wide peak of 3400 –

3600 cm^{-1} represents an overlap of primary amine groups and hydroxyl groups. A reduction observed in the intensity of primary amine peaks in this range, mainly in samples crosslinked with more than 1 %(w/w) genipin, is a signal of efficient crosslinking. Similarly, the intensity of the N-H bending vibration of primary amines observed in the 1550-1650 cm^{-1} range is reduced significantly in the crosslinked samples, due to genipin reacting with primary amine groups [25]. Moreover, a very slight increase in the ratio of C=O/N-H peaks at the wavelengths of 1700 cm^{-1} and 1400 cm^{-1}, observed in the peaks, is mentioned to be a hallmark of genipin crosslinking [26].

Furthermore, the ninhydrin assay provides information on the percentage of free amine groups in the samples, thus, representing an estimate of the percentage of amine groups not involved in crosslinking reaction, from which the crosslinking degree can be calculated. As indicated in figure 3.1.D, higher crosslinking times leads to higher crosslinking degrees, however, the rate of increase in crosslinking degree is reduced as time goes by, due to more genipin being spent in the reaction. The ANOVA model shows a significant effect for both the effects of time and genipin concentration. Consequently, 2.5 wt% genipin leads to crosslinking degrees which are significantly higher than 0.5 wt% ($p \leq 0.001$), 1 wt% ($p \leq 0.05$) and 1.5 wt% ($p \leq 0.01$) genipin after 24 h of crosslinking, demonstrating ease of properties tunability by offering control over the crosslinking degree.

3.3.2.3 Estimation of unreacted genipin

Genipin is a crosslinker reacting with primary amine groups. Consequently, it is a favorable material for crosslinking of chitosan and gelatin. To ensure cytocompatibility of the resulting copolymer, it is vital to determine the amount of unreacted genipin released from the scaffolds. ANOVA shows a significant effect for both crosslinking time and genipin concentration on the amount of unreacted genipin ($p < 0.0001$). As demonstrated in figure 3.2, the amount of unreacted genipin released from scaffolds decreases significantly with an increase in crosslinking time, with the amount being close to 100 µg/mL after 24 h of crosslinking (significantly different from 1 h crosslinking time, $p<0.0001$), which would be the optimum amount shown not to induce any toxicity [21].

Furthermore, Tukey's multiple comparisons show a significant difference between samples crosslinked with 0.5 wt% genipin with those crosslinked with 2 wt% and 2.5 wt % genipin ($p \leq 0.05$) after 24 h, and with smaller variabilities in genipin concentration there are no significant differences. However, the remaining genipin is in the non-toxic region for all concentrations [21].

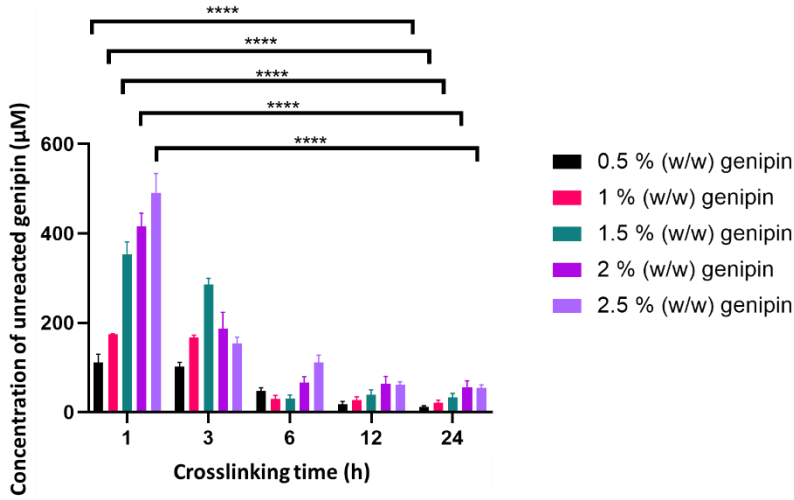

Figure 3.2. The amount of unreacted genipin based on the crosslinking time.

3.3.3 3D printing and physical characterizations of the scaffold

3.3.3.1 Evaluation of printing fidelity

To analyse the possibility of 3D printing scaffolds based on pre-determined designs using the proposed hydrogels, the printability of the materials was evaluated. Different combinations of gelatin, MA-C and genipin have been used for this purpose, and constructs printed with them can be seen in figure 3.3. Figure 3.3 demonstrates the hydrogels containing 1.5 %(w/v) MA-C and 3 %(w/v) gelatin yield much more accurate printed constructs representing the design, which was expected as gelatin is known to augment the mechanical properties of chitosan and thus, its ability to maintain its 3D structure [27]. This was also confirmed by measuring the strand width to evaluate

uniformity of the diameter of the printed strands at different locations on the sample. As shown in table 3.1, these measurements demonstrate that the variability in strand width is not significant, confirming uniformity across the printed constructs.

Table 3.1. Measurement of strand width in samples containing 1.5

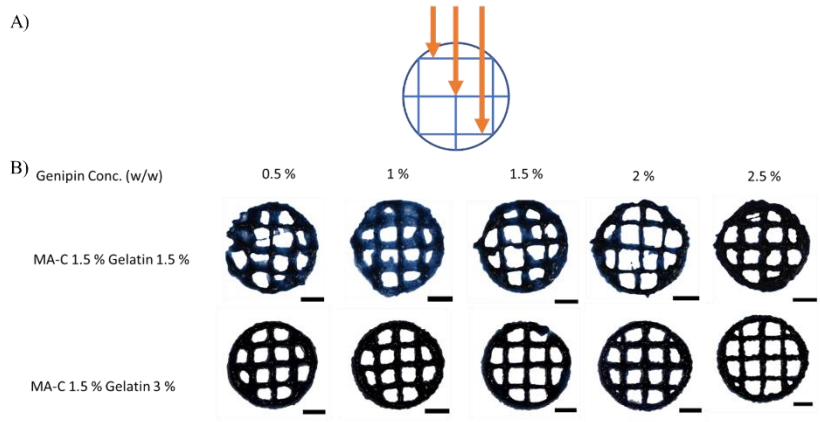

Figure 3.3. A) computer aided design, arrows represent lines used for measurements in table 3.1 B) Printability of different gelatin, chitosan MA and genipin concentrations. 5 layer constructs, scale bar 5 mm

%(w/v) MA-C, 3 %(w/v) gelatin and varying amounts of genipin. Line numbers correspond to different lines within a single printed shape, the lines are presented in the schematic in figure 3.3.A

MA-C 1.5 % Gelatin 3 %	**0.5 wt% genipin**	**1.0 wt% genipin**	**1.5 wt% genipin**	**2.0 wt% genipin**	**2.5 wt% genipin**
Line 1 (mm)	1.6 ± 0.1	1.6 ± 0.3	1.7 ± 0.1	1.8 ± 0.1	1.6 ± 0.1
Line 2 (mm)	1.7 ± 0.1	1.7 ± 0.2	1.7 ± 0.2	1.7 ± 0.1	1.6 ± 0.1
Line 3 (mm)	1.7 ± 0.2	1.8 ± 0.4	1.7 ± 0.3	1.8 ± 0.2	1.7 ± 0.1

3.3.3.2 Evaluation of linear viscoelasticity

Due to the viscoelastic character of the blend hydrogels, oscillatory shear measurements provide a representative description of their mechanical behavior at small deformations, in which the linear

viscoelasticity theory is held. Therefore, the mechanical spectra of the gelatin/chitosan MA crosslinked with low (0.5 wt.%) and high (2.5 wt.%) genipin concentrations were obtained via frequency sweep tests, as presented in Figure 3.4.

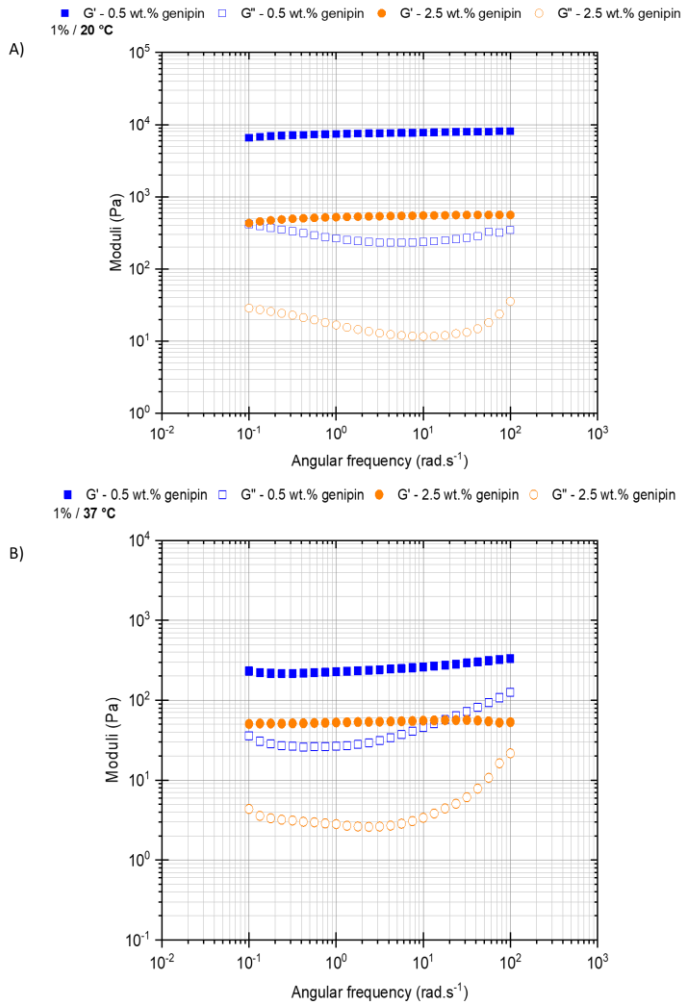

Figure 3.4. Mechanical spectra of gelatin/chitosan MA with low (0.5 wt.%) and high (2.5 wt.%) genipin contents, representative graph for three samples (A) hybrid hydrogel blends at the 3D printing temperature of 20 °C and (B) the chemical hydrogels at the physiological temperature of 37 °C.

In all the scenarios tested, the materials present higher magnitudes of G' over G" within a range of four orders of magnitude of angular frequencies. This result was expected as it reveals that conformational changes at both short and long length scales are hindered by the presence of gel networks. The strong frequency-independency of the moduli, as a consequence of their supramolecular structures, is a remarkable characteristic of the mechanical spectra of gels, such as the materials herein studied.

The mechanical spectra of both the hybrid and chemical gels revealed the existence of imperfect polymer networks due to the frequency dependency of their loss moduli. However, no evidence of terminal behavior (G' = G") was seen. In all the conditions, their mechanical spectra are situated in the rubbery plateau. The frequency dependency of the loss modulus suggests the presence of network defects such as dangling structures, branching and sol phase. This is probably attributed to the crosslinking conditions of the hydrogels applied in this work. Interestingly, the moduli of the hybrid hydrogels formulations with 2.5 w/w% and 0.5 w/w% genipin are shifted approximately one order of magnitude apart at 20 °C.

3.3.3.3 Swelling and degradation studies

Hydrogel swelling is an indicator of the water content of the hydrogel; thus, its measurement can be crucial in anticipating cellular response and mechanical behavior of the scaffold.

Figure 3.5.A shows that the swelling ratio ranges from 6 to 8 times depending on the crosslinker concentration. It is also noteworthy that the main water uptake takes place within 24 hours of scaffold placement in PBS due to the rapid penetration of the PBS into the material structure [28]. Two-way ANOVA showed significant effects of both time and genipin concentration on the swelling. Further multiple comparisons show significant differences in the swelling of all different comparisons of genipin concentrations ($p \leq 0.0001$), except for 0.5 versus 1 wt% and 1.5 versus 2 wt%.

Moreover, the degradation rate is of significant importance in tissue engineering allowing for natural tissue to regenerate and replace the scaffold. The rate of hydrolytic degradation of the printed scaffolds (figure 3.5.B) demonstrates the maximum degradation within 14 days

of immersion in PBS to be approximately 40%, and ANOVA analysis demonstrates the significant effect of both factors on degradation. However, after 7 days, differences in genipin concentration leads to significant differences among degradation rates of the samples ($p \leq 0.01$), except for comparisons among samples crosslinked with 0.5 wt% versus 1 wt% and 1.5 wt% versus 2 wt%.

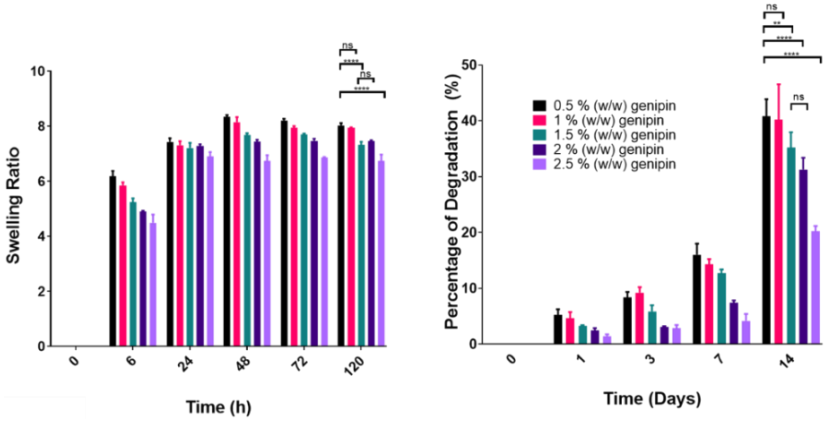

Figure 3.5. A) swelling rate of printed hydrogel scaffolds B) Hydrolytic degradation rate of printed hydrogel scaffolds

3.3.3.4 Evaluation of surface morphology

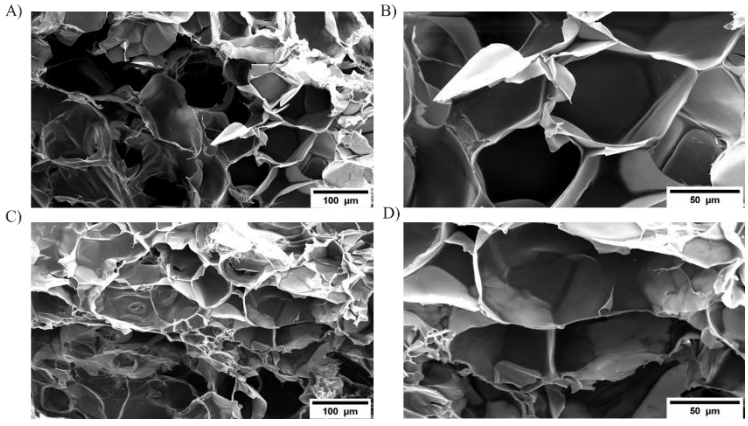

Figure 3.6. Scanning electron microscopy of the cross-section of 3D printed hydrogels A) 0.5 wt% genipin, 200x B) 0.5 wt% genipin 500x C) 2.5 wt% genipin 200x D) 2.5 wt% genipin 500x

The SEM images of the cross-section of the scaffolds prepared with 0.5 wt% and 2.5 wt% genipin are presented in figure 3.6. As the hydrogels in this study are used in the wet state, these images can offer insights into the effect of the crosslinker concentration on the pore size of the hydrogels. Both samples appear to have a large degree of porosity, confirming the swelling finding regarding the high water content. It appears that gels crosslinked with 0.5 wt% genipin have a larger pore diameter of an average of 86.3 ± 8.1 μm, while the pore diameter in gels crosslinked with 2.5 wt% genipin is in the range of 63.6 ± 6.8 μm.

3.3.4 Cellular response

3.3.4.1 Live/Dead assay

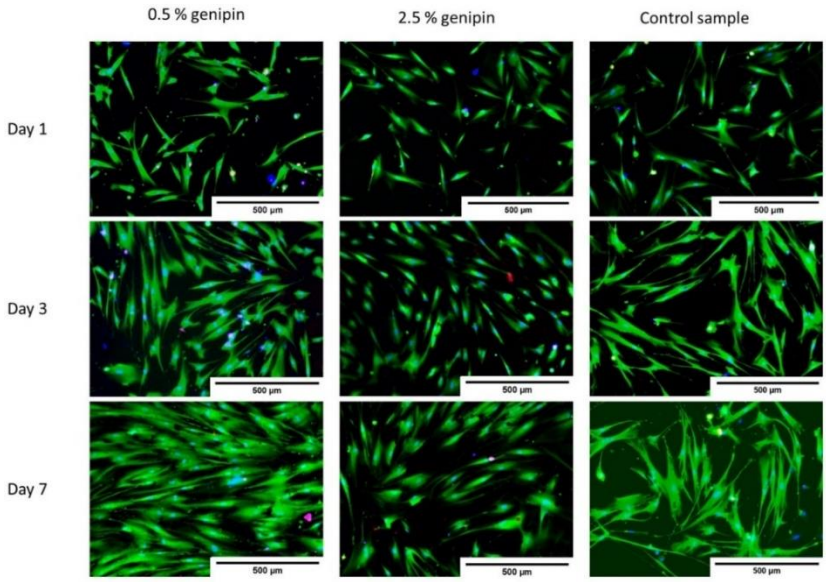

Figure 3.7. Viability of cells seeded on gels with different genipin concentrations, green represents live cells, red represents dead cells and blue represents cell nucleus, control sample represents cells cultured on a 2D surface.

The possible toxicity of the material on the cells can be viewed using live/dead staining. In this section, only gels containing 2.5 wt% and 0.5 wt% genipin were evaluated, representing the extreme concentrations. Results of the live/dead assay can be seen in figure 3.7. A qualitative

analysis of the pictures in all timepoints demonstrates that there is no visible difference in cell viability among cells cultured on the scaffolds and control samples with cells cultured on the well plates. Additionally, cells demonstrate the stretched form showing their adherence to the gel and exhibiting efficiency of the proposed hydrogel in supporting cell attachment and spreading.

3.3.4.2 AlamarBlue assay

AlamarBlue assay (figure 3.8.A) was performed to assess metabolic activity of the cells. ANOVA analysis shows a significant effect for both time and genipin concentration on the metabolic activity of the cells. After one day of culture, the sample with 2.5 wt% genipin shows a significantly higher metabolic activity compared to the sample with 0.5 wt% genipin, and the difference of 0.5 wt% with control samples are significant ($p < 0.05$). However, on day 3, the readings for all samples are significantly different from each other. After 7 days of culture, only the difference of the metabolic activity of cells cultured on scaffolds crosslinked with 0.5 wt% genipin is significantly different (higher) than the control ($p \leq 0.05$).

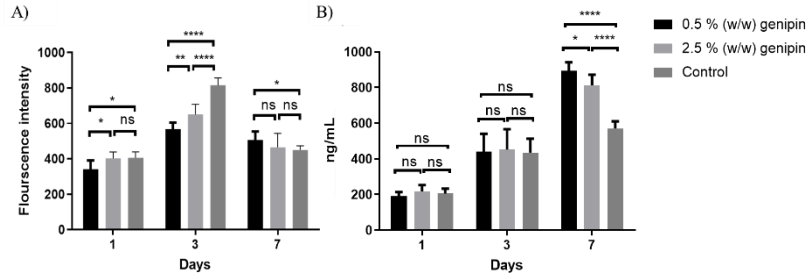

*Figure 3.8. A) AlamarBlue readings analyzed at day 1, 3, and 7 B) DNA concentration relative to hydrogel volume, analyzed at day 1, 3, and 7. Results shown as average +/- standard deviation, (n=3), ns shows no significant difference, * stands for difference (p<0.05), ** stands for difference (p<0.01), and **** stands for difference (p<0.0001), control sample consists of cells cultured on a 2D surface*

3.3.4.3 DNA quantification

A DNA quantification assay was performed to further investigate the effects on cell viability (figure 3.8.B). The DNA content almost tripled within 7 days. Similar to the results obtained through the alamarBlue assay, ANOVA analysis demonstrates both time and genipin concentration to have a significant effect on the DNA content. Additionally, while after 1 and 3 days of culture the difference of the DNA content in samples is not significantly different from the control group, the DNA content is significantly higher in scaffolds compared to the control group after 7 days of culture ($p \leq 0.0001$).

3.4 Discussion

The structure of chitosan (scheme 3.1.C), introduces a significant chance for formation of hydrogen bonds within the molecule structure, leading to a semi-crystalline structure that is not soluble in neutral pH [29]. At pH lower than 6.5, the amino groups in the structure get protonated leading to a weak repulsion force enabling the solubility. However, a low pH is considered a major disadvantage for biological purposes. Consequently, introducing hydrophilic groups in the structure is required leading to an increased solubility of chitosan in neutral pH. This was done using an esterification reaction with maleic anhydride, mediated by pyridine, as shown in scheme 3.1. The presence of ester groups leads to an increased polarity of the chitosan, in addition to decreased intramolecular hydrogen bonds, leading to an increased solubility in neutral pH. Confirmation of the reaction was achieved through FTIR and NMR analysis. In particular, the FTIR peak corresponding to C=C, observed at 1564 cm^{-1} demonstrates the success of modification considering these groups are only present on maleic anhydride and not on the chitosan backbone [30,31].

Furthermore, crosslinking of MA-C and gelatin using genipin was confirmed through FTIR and ninhydrin assay. Considering the synthesis procedure mainly engages the hydroxyl group on the chitosan backbone, leaving the majority of the amine groups free to react with genipin, the crosslinking degree was expected to be in the same range observed with similar materials. This is confirmed considering genipin crosslinked chitosan/gelatin films have been reported to result in 65%

crosslinking degree using 1.5% genipin [32]. Furthermore, the difference in crosslinking degree based on genipin concentration, can lead to a control over physical and mechanical properties of the scaffold through controlled crosslinking, assisting in production of tailor-made scaffolds for different applications. This method has been used previously to fabricate collagen-based scaffolds with controlled properties [33].

However, this genipin crosslinking could potentially result in toxicity of the copolymers for cultured cells. Being naturally derived, genipin has a lower cytotoxicity than other crosslinkers such as GPTMS ((3-Glycidyloxypropyl) trimethoxysilane) or glutaraldehyde [34]. Still, concentrations of over 1 mg/mL are known to be toxic to most cell types. However, the amount of released genipin from the copolymers was approximately 100 µg/mL after 24 h of crosslinking. This amount was determined in the literature to be non-toxic, and able to induce odontoblastic differentiation of DPCs [21].

Following development of the materials, the possibility of producing 3D printed scaffolds using the gels was demonstrated in gels prepared with 1.5 %(w/v) MA-C and 3 %(w/v) gelatin, with varying degrees of crosslinking. Additionally, mechanical properties including linear viscoelasticity, swelling and degradation of the hydrogels were evaluated. In the frequency sweep tests of the hydrogels the elastic and viscous responses given by the storage (G') and loss (G") moduli are monitored against the angular frequency of the applied sinusoidal oscillation. The storage modulus is a measure of the stored energy per oscillation cycle whereas the loss modulus (G") is a measure of dissipated energy as heat per cycle of sinusoidal deformation [35]. Thus, the mechanical spectra allow for the observation of the time-dependent mechanical behavior of the materials, within a relatively broad range of observation times. At 37°C, the gelatin chains are transitioning from random coil to a worm-like conformation as their sol-gel temperature is being approached [36]. The presence of these random coils at 37 °C favor the reaction of genipin molecules with the amine groups present in the lysine residues of the gelatin and chitosan chains, as those are more exposed at such molecular conformation [37]. The existence of an imperfect gel network is convenient in terms of both the 3D printing process and cell proliferation. An extremely

elastically dominated microstructure would result in filament rupture and an unfavorable environment for cell attachment and, thus, poorer viability and proliferation [38].

The shift of the moduli of the hybrid hydrogel formulations suggests that the high (2.5 wt.%) genipin concentration has a stronger influence in inhibiting the physical gelation of gelatin at temperatures below its sol-gel transition, such as 20 °C. Thus, the benefits of applying this blend in 3D printing are guaranteed. On the other hand, the observed difference in moduli at 37 °C is likely related to the aforementioned chemical gelation conditions used in this study. Chemical gelation of gelatin and chitosan in presence of genipin is reported to be substantially more effective at slightly higher temperatures [25]. However, the lower storage modulus seen for the 2.5 wt.% could be associated with polymerization of genipin molecules as previously reported [37], resulting in longer crosslinks and, thus, a weaker gel due to excess of genipin. Therefore, we estimate the spatial correlation length of the materials from rheological measurements, which is known as the size of the elastic blob. This spatial correlation length gives us an estimate size of the elastic active network chains. The size of the elastic blob (ξel) is given by Eq. 3.3 and 3.4 [39]:

$$G' = \rho_{el} k_B T \qquad \text{Eq. 3.3}$$

$$\xi_{el} = (\rho_{el})^{-\frac{1}{3}} \qquad \text{Eq. 3.4}$$

Taking G' at 0.1 rad.s^{-1} at 37 °C so that G' ≈ 200 Pa and 50 Pa for the 0.5 and 2.5 w/w%, genipin concentration formulations respectively, the size of the elastic blob of the blend hydrogels can be estimated from Eq. 1 and 2, where k_B is the Boltzmann constant, T is the absolute temperature and ρ_{el} is the density of the elastic blob. As hypothesized before, the size of the elastic blobs of the chemical 2.5 w/w% genipin crosslinked hydrogel is approximately 30% greater than the 0.5 w/w% counterpart, suggesting interpolymerization of genipin molecules.

In addition to the viscoelastic properties, the hydrogel swelling was measured, and the percentage observed is higher compared to other chitosan-based materials, with a combination of chitosan, gelatin and bioglass resulting in swelling of approximately 1.6 times [40]. While

the presence of bioglass in this study might have an effect on the swelling, a combination of chitosan and gelatin as a 2D film has resulted in a swelling ratio of approximately 3.5 in pH 7.4 [41]. The higher swelling observed is attributed to increased hydrophilicity of the synthesized water-soluble chitosan derivative. Similarly, a higher rate of degradation, where similar materials have a degradation in the range of 25 to 30 % [42] was observed. While the maleic anhydride grafting mainly takes place on the hydroxyl groups of the chitosan backbone, leaving majority of the amine groups free for reaction with genipin, the increased hydrophilicity in the synthesized material could potentially lead to increased hydrolytic degradation rates for the scaffolds. Together, the results of these analysis represent the crosslinker concentration as an effective tool to control the physical behavior of the scaffolds by controlling the crosslinking degree.

In addition to physico-mechanical properties, a critical property any tissue engineering scaffold must possess is biocompatibility, considered in this context as both, a lack of toxicity and on the other hand, a presence of cell adhesion cues. The results of the live/dead highlight for the first time that the MA-C does not have any adverse effect on the viability of hDPSCs, and the remaining genipin is non-toxic as expected [21]. These results were confirmed by the measurement of metabolic activity of the cells through an alamarBlue assay. The alamarBlue observations are in-line with other studies using genipin crosslinked chitosan where, similar to our obtained results, there is no vast difference in metabolic activity with regards to the genipin concentration after 7 days of culture [43]. Additionally, the overall reduction in alamarBlue readings at day 7 can be attributed to contact inhibition resulting from high proliferation of the cells, which can lead to reduced metabolic activity [44,45], while further in-depth analysis of the biological processes in the future could determine the exact cause of this behavior.

Furthermore, a DNA quantification was performed to further evaluate the cell viability. The increased DNA content on the scaffold as compared to the control groups. Can be attributed to the presence of a 3D environment including gelatin, providing a more favorable space for cell proliferation, an effect known to occur within 3D collagen scaffolds [46]. Similar behavior has been observed in other studies

incorporating gelatin and chitosan where a DNA content larger than the 2D control was considered as a sign of suitability of the scaffold for tissue engineering applications [47]. Furthermore, this is in line with the alamarBlue readings, as the DNA quantification demonstrates a much larger number of cells present in the scaffolds at day 7, hence, resulting in the possibility of contact inhibition and reduced metabolic activity. Taken together, these results confirm the absence of any toxicity, confirming the pattern obtained through live/dead analysis.

3.5 Conclusion

Through synthesis of maleic anhydride grafted chitosan (MA-C), a water-soluble derivative of chitosan was obtained which could be copolymerized with gelatin in the presence of genipin to yield a 3D printable hydrogel, capable of forming tissue engineering scaffolds. Being used for the first time as a tissue engineering scaffold, it was shown that neither the synthesized material, nor any of the crosslinker concentrations used, were toxic to hDPSCs. Moreover, as a range of physical properties might be needed for tissue engineering in the dentoalveolar region, it was demonstrated that these properties could be adequately tuned using different concentrations of genipin as crosslinker. Consequently, it can be concluded that the proposed material could be considered as a candidate for production of scaffolds for regeneration of soft tissues in the alveolar region, where tunability of the properties allowing for replicating the complex structures can be of extreme importance.

3.6 References

1. Kassebaum NJ, Bernabé E, Dahiya M, Bhandari B, Murray CJL, Marcenes W. “Global burden of severe periodontitis in 1990-2010: a systematic review and meta-regression.”. J Dent Res. 2014 Nov;93(11):1045–53.
2. Mack F, Schwahn C, Feine JS, Mundt T, Bernhardt O, John U, Kocher PT, Biffar R. “The impact of tooth loss on general health related to quality of life among elderly Pomeranians: results from the study of health in Pomerania (SHIP-O).”. Int J Prosthodont. 2005;18(5):414–9.
3. Khodakaram-Tafti A, Mehrabani D, Shaterzadeh-Yazdi H, Zamiri B, Omidi M. “Tissue Engineering in Maxillary Bone Defects”. World J Plast Surg. 2018 Jan;7(1):3–11.
4. Hanif A, Qureshi S, Sheikh Z, Rashid H. “Complications in implant dentistry”. Eur J Dent. 2017;11(1):135–40.
5. EzEldeen M, Wyatt J, Al-Rimawi A, Coucke W, Shaheen E, Lambrichts I,

Willems G, Politis C, Jacobs R. “Use of CBCT Guidance for Tooth Autotransplantation in Children.”. J Dent Res. 2019 Apr;98(4):406–13.
6. Abou Neel EA, Chrzanowski W, Salih VM, Kim HW, Knowles JC. “Tissue engineering in dentistry”. J Dent. 2014 Aug 1 [cited 2020 Feb 18];42(8):915–28.
7. Min LJ, Edgar TYS, Zicheng Z, Yee YW. “Chapter 6 – Biomaterials for Bioprinting”. In: Zhang LG, Fisher JP, Leong KWBT 3D B and N in TE and RM, editors. Academic Press; 2015. P. 129–48.
8. Lee JH, Kim HW. “Emerging properties of hydrogels in tissue engineering”. J Tissue Eng. 2018 Jan 1;9:2041731418768285.
9. Groll J, Burdick JA, Cho DW, Derby B, Gelinsky M, Heilshorn SC, Jüngst T, Malda J, Mironov VA, Nakayama K, Ovsianikov A, Sun W, Takeuchi S, Yoo JJ, Woodfield TBF. “A definition of bioinks and their distinction from biomaterial inks”. Biofabrication. 2018;11(1):13001.
10. Islam MM, Shahruzzaman M, Biswas S, Nurus Sakib M, Rashid TU. “Chitosan based bioactive materials in tissue engineering applications-A review”. Bioact Mater. 2020;5(1):164–83.
11. Ahmadi F, Oveisi Z, Samani SM, Amoozgar Z. “Chitosan based hydrogels: characteristics and pharmaceutical applications.”. Res Pharm Sci. 2015;10(1):1–16.
12. Seo JW, Shin SR, Lee MY, Cha JM, Min KH, Lee SC, Shin SY, Bae H. “Injectable hydrogel derived from chitosan with tunable mechanical properties via hybrid-crosslinking system”. Carbohydr Polym. 2021;251:117036.
13. Demirtaş TT, Irmak G, Gümüşderelioğlu M. “A bioprintable form of chitosan hydrogel for bone tissue engineering.”. Biofabrication. 2017 Jul;9(3):35003.
14. Rickett TA, Amoozgar Z, Tuchek CA, Park J, Yeo Y, Shi R. “Rapidly Photo-Cross-Linkable Chitosan Hydrogel for Peripheral Neurosurgeries”. Biomacromolecules. 2011 Jan;12(1):57–65.
15. Amsden BG, Sukarto A, Knight DK, Shapka SN. “Methacrylated glycol chitosan as a photopolymerizable biomaterial.”. Biomacromolecules. 2007 Dec;8(12):3758–66.
16. Fu Y, Xiao C. “A facile physical approach to make chitosan soluble in acid-free water”. Int J Biol Macromol. 2017;103:575–80.
17. Unal S, Arslan S, Karademir Yilmaz B, Kazan D, Oktar FN, Gunduz O. “Glioblastoma cell adhesion properties through bacterial cellulose nanocrystals in polycaprolactone/gelatin electrospun nanofibers”. Carbohydr Polym. 2020;233:115820.
18. Kumar P, Dehiya BS, Sindhu A. “Comparative study of chitosan and chitosan–gelatin scaffold for tissue engineering”. Int Nano Lett. 2017 Dec;7(4):285–90.
19. Maiz-Fernández S, Guaresti O, Pérez-Álvarez L, Ruiz-Rubio L, Gabilondo N, Vilas-Vilela JL, Lanceros-Mendez S. “β-Glycerol phosphate/genipin chitosan hydrogels: A comparative study of their properties and diclofenac delivery”. Carbohydr Polym. 2020;248:116811.
20. Kirchmajer DM, Watson CA, Ranson M, Panhuis M in het. “Gelapin, a degradable genipin cross-linked gelatin hydrogel”. RSC Adv. 2013;3(4):1073–81.
21. Kwon YS, Lim ES, Kim HM, Hwang YC, Lee KW, Min KS. “Genipin, a cross-linking agent, promotes odontogenic differentiation of human dental pulp cells.”. J Endod. 2015 Apr;41(4):501–7.

22. Hilkens P, Gervois P, Fanton Y, Vanormelingen J, Martens W, Struys T, Politis C, Lambrichts I, Bronckaers A. “Effect of isolation methodology on stem cell properties and multilineage differentiation potential of human dental pulp stem cells.”. Cell Tissue Res. 2013 Jul;353(1):65–78.
23. Induri S, Sengupta S, Basu JK. “A kinetic approach to the esterification of maleic anhydride with methanol on H-Y zeolite”. J Ind Eng Chem. 2010;16(3):467–73.
24. Karaman R, Dokmak G, Bader M, Hallak H, Khamis M, Scrano L, Bufo SA. “Prodrugs of fumarate esters for the treatment of psoriasis and multiple sclerosis—a computational approach”. J Mol Model. 2013;19(1):439–52.
25. Cui L, Jia J, Guo Y, Liu Y, Zhu P. “Preparation and characterization of IPN hydrogels composed of chitosan and gelatin cross-linked by genipin”. Carbohydr Polym. 2014;99:31–8.
26. Zhang Y, Wang QS, Yan K, Qi Y, Wang GF, Cui YL. “Preparation, characterization, and evaluation of genipin crosslinked chitosan/gelatin three-dimensional scaffolds for liver tissue engineering applications.”. J Biomed Mater Res A. 2016 Aug;104(8):1863–70.
27. Benbettaïeb N, Kurek M, Bornaz S, Debeaufort F. “Barrier, structural and mechanical properties of bovine gelatin-chitosan blend films related to biopolymer interactions.”. J Sci Food Agric. 2014 Sep;94(12):2409–19.
28. Ganji F, Vasheghani Farahani S, Vasheghani-Farahani E. “Theoretical Description of Hydrogel Swelling: A Review”. Iran Polym J. 2010 Apr 1;19:375–98.
29. Qin C, Li H, Xiao Q, Liu Y, Zhu J, Du Y. “Water-solubility of chitosan and its antimicrobial activity”. Carbohydr Polym. 2006;63(3):367–74.
30. Lavanya R, Gomathi T, Vijayalakshmi K, Saranya M, Sudha PN, Anil S. “Adsorptive removal of copper (II) and lead (II) using chitosan-g-maleic anhydride-g-methacrylic acid copolymer”. Int J Biol Macromol. 2017;104:1495–508.
31. Gopal Reddi MR, Gomathi T, Saranya M, Sudha PN. “Adsorption and kinetic studies on the removal of chromium and copper onto Chitosan-g-maliec anhydride-g-ethylene dimethacrylate”. Int J Biol Macromol. 2017;104:1578–85.
32. Koc FE, Altıncekic TG. “Investigation of gelatin/chitosan as potential biodegradable polymer films on swelling behavior and methylene blue release kinetics”. Polym Bull. 2020;
33. Davidenko N, Schuster CF, Bax D V, Raynal N, Farndale RW, Best SM, Cameron RE. “Control of crosslinking for tailoring collagen-based scaffolds stability and mechanics”. Acta Biomater. 2015/07/26. 2015 Oct;25:131–42.
34. Sung HW, Huang RN, Huang LL, Tsai CC. “In vitro evaluation of cytotoxicity of a naturally occurring cross-linking reagent for biological tissue fixation.”. J Biomater Sci Polym Ed. 1999;10(1):63–78.
35. Ferry 1912- JD. “Viscoelastic properties of polymers / [by] John D. Ferry” [Internet]. New York: Wiley; 1970.
36. Ross-Murphy SB. “Structure and rheology of gelatin gels: recent progress”. Polymer (Guildf). 1992;33(12):2622–7.
37. Butler MF, Ng YF, Pudney PDA. “Mechanism and kinetics of the crosslinking reaction between biopolymers containing primary amine groups and genipin”. J Polym Sci Part A Polym Chem. 2003 Dec 15;41(24):3941–53.
38. Amorim PA, d’Ávila MA, Anand R, Moldenaers P, Van Puyvelde P, Bloemen

V. “Insights on shear rheology of inks for extrusion-based 3D bioprinting”. Bioprinting. 2021;22:e00129.

39. Tsuji Y, Li X, Shibayama M. “Evaluation of Mesh Size in Model Polymer Networks Consisting of Tetra-Arm and Linear Poly(ethylene glycol)s”. Gels (Basel, Switzerland). 2018 May 25;4(2):50.
40. Maji K, Dasgupta S, Pramanik K, Bissoyi A. “Preparation and Evaluation of Gelatin-Chitosan-Nanobioglass 3D Porous Scaffold for Bone Tissue Engineering”. Jabbari E, editor. Int J Biomater. 2016;2016:9825659.
41. Ling X, Zu-yu Y, Chao Y, Hua-yue Z, Yu-min D. “Swelling studies of chitosan-gelatin films cross-linked by sulfate”. Wuhan Univ J Nat Sci. 2004;9(2):247–51.
42. Fischetti T, Celikkin N, Contessi Negrini N, Farè S, Swieszkowski W. “Tripolyphosphate-Crosslinked Chitosan/Gelatin Biocomposite Ink for 3D Printing of Uniaxial Scaffolds “ [Internet]. Vol. 8, Frontiers in Bioengineering and Biotechnology . 2020. P. 400.
43. Dimida S, Barca A, Cancelli N, De Benedictis V, Raucci MG, Demitri C. “Effects of Genipin Concentration on Cross-Linked Chitosan Scaffolds for Bone Tissue Engineering: Structural Characterization and Evidence of Biocompatibility Features”. Kawatsuki N, editor. Int J Polym Sci. 2017;2017:8410750.
44. Ng KW, Leong DTW, Hutmacher DW. “The Challenge to Measure Cell Proliferation in Two and Three Dimensions”. Tissue Eng. 2005 Jan 1;11(1–2):182–91.
45. Gallorini M, Zara S, Ricci A, Mangano FG, Cataldi A, Mangano C. “The Open Cell Form of 3D-Printed Titanium Improves Osteconductive Properties and Adhesion Behavior of Dental Pulp Stem Cells”. Vol. 14, Materials . 2021.
46. Jensen C, Teng Y. “Is It Time to Start Transitioning From 2D to 3D Cell Culture? “ [Internet]. Vol. 7, Frontiers in Molecular Biosciences . 2020. P. 33.
47. Gautam S, Chou CF, Dinda AK, Potdar PD, Mishra NC. “Fabrication and characterization of PCL/gelatin/chitosan ternary nanofibrous composite scaffold for tissue engineering applications”. J Mater Sci. 2014;49(3):1076–89.

Chapter 4. Development of 3D printed pNIPAM-chitosan scaffolds for dentoalveolar tissue engineering

Mehdi Salar Amoli [a,b], Resmi Anand [a,c,d], Mostafa EzEldeen [b,e], Reinhilde Jacobs [b,h], Veerle Bloemen [a,c]

[a] Materials Technology TC, Campus Group T, KU Leuven, Andreas Vesaliusstraat 13, 3000 Leuven, Belgium

[b] OMFS IMPATH Research Group, Faculty of Medicine, Department of Imaging and Pathology, KU Leuven and Oral and Maxillofacial Surgery, University Hospitals Leuven, Kapucijnenvoer 33, 3000 Leuven, Belgium

[c] Prometheus, Division of Skeletal Tissue Engineering Leuven, KU Leuven, Leuven, Belgium

[d] Inter University Centre for Biomedical Research and Super Speciality Hospital, Mahatma Gandhi University Campus at Thalappady, Kottayam, Kerala-686009, India

[e] Department of Oral Health Sciences, KU Leuven and Paediatric Dentistry and Special Dental Care, University Hospitals Leuven, Kapucijnenvoer 33, 3000 Leuven, Belgium

[h] Department of Dental Medicine, Karolinska Institutet, Stockholm, Sweden

Manuscript in preparation

Chapter summary

While available treatments have addressed a variety of complications in the dentoalveolar region, challenges associated with these treatments have resulted in exploration of tissue engineering approaches. In such strategies, scaffold fabrication and materials used to develop scaffolds have shown to be of paramount importance. This chapter focuses on the development of a copolymer of poly n-isopropylacrylamide (pNIPAM) and chitosan, used for 3D printing of scaffolds for dentoalveolar regeneration. Synthesized material was characterized by Fourier Transform Infrared Spectroscopy, and the possibility of printing was evaluated through different printability tests. The rate of degradation and swelling were analyzed through gravimetry, and surface morphology was characterized by scanning electron microscopy. Viability of dental pulp stem cells (DPSCs) seeded on the scaffolds was evaluated by a LIVE/DEAD analysis and DNA quantification. The results demonstrated successful copolymerization, and three formulations among different synthesized formulations were successfully 3D printed. Degradability of the material was confirmed and a swelling rate of approximately 1200 % was observed. Furthermore, initial assessment of DPSC viability demonstrated biocompatibility of the developed scaffolds. The results clearly indicate the proposed hydrogel as a candidate for fabrication of tissue engineering scaffolds for dentoalveolar tissue engineering through 3D printing.

4.1 Introduction

A wide range of available treatments have been used to address complications in the dentoalveolar region, such as the use of dental implants or tooth autotransplantation [1,2]. However, such treatments often suffer from challenges, resulting in exploration of regenerative strategies in this region, where the natural ability of the tissues for regeneration is limited [3,4]. Among these strategies, tissue engineering approaches using cells combined with scaffolds appear to be advantageous [5–7], however, several aspects of the scaffolds, including the materials used for scaffold development and the fabrication strategy need to be considered. The dentoalveolar region is a heterogeneous tissue structure composed of complex geometries [5,8], hence, it demands scaffold fabrication methods capable of addressing such structural heterogeneity. 3D printing has been proposed as a potential fabrication technology with capability to form scaffolds with pre-determined geometries for different tissue engineering applications [9].

However, materials which are compatible with the technology, and possess the desired properties to be used in tissue engineering, such as biocompatibility or biodegradability, are still an important area of research in the field [10]. A range of material classes have been used for 3D printing of scaffolds, including thermoplastic polymers [11], bioceramics [12], and hydrogels [9]. Among these, hydrogels of both natural and synthetic origin are favorable for tissue engineering applications, because of their high water content, which resembles the natural extracellular matrix (ECM), and allows for cell survival and proliferation [13]. Furthermore, hydrogels often possess physical and mechanical properties closer to natural soft tissues and hence, are more suitable for tissue engineering strategies aimed at such tissues [14]. Aside from these, degradation of this class of materials can be tuned to range from days to months, making them suitable for a variety of applications [15].

Among the wide range of materials used for the development of tissue engineering hydrogels, chitosan, a polysaccharide derived from chitin, is one of the most interesting and widely investigated options. This is due to its high biocompatibility, biodegradability, and antimicrobial

properties [16]. However, similar to other natural polymers, it suffers from low mechanical properties, and a limited control over its physicomechanical characteristics. Consequently, several approaches such as crosslinking or copolymerization with other polymers have been suggested to enhance its properties [17].

Among different approaches for modification of chitosan, copolymerization with poly n-isopropylacrylamide (pNIPAM) is known to enhance properties of chitosan, in addition to conferring additional properties such as thermosensitivity [18,19]. pNIPAM is a synthetic biocompatible polymer used in a variety of biomedical applications such as cell sheet engineering [20] or drug delivery [21]. Furthermore, being a synthetic polymer, pNIPAM offers significant opportunity for tuning different properties of hydrogels such as their mechanical properties, enhancing the possibility of application in 3D printing. While utilization of pNIPAM may cause some concerns regarding its biodegradability, its copolymerization with a natural polymer is known to result in degradable biomaterials as the natural component forms hydrogen bonds resulting in degradation of the polymer structure [22]. However, use of a pNIPAM-chitosan copolymer as tissue engineering scaffolds or in 3D printing strategies has not been previously reported.

Consequently, this chapter hypothesizes that copolymerization of pNIPAM and chitosan through a sol-gel synthesis in the presence of a crosslinker, methylene bisacrylamide (MBA), could potentially result in 3D printable hydrogels which could be freeze dried and used as tissue engineering scaffolds capable of supporting dental pulp stem cells (DPSCs).

4.2 Materials and Methods

4.2.1 Materials

N-isopropylacrylamide (NIPAM) (97 % purity), methylene-bis-acrylamide (MBA), chitosan (molecular weight 190-310 kDa, deacetylation rate 75-85%), glacial acetic acid, ammonium persulfate (APS), and tetramethylethylenediamine (TEMED) were obtained from Sigma Aldrich (Overijse, Belgium). Calcein AM, ethidium homodimer, phosphate buffered saline (PBS), Gibco minimum

essential alpha medium, gibco antibiotic-antimycotic, and Biowest fetal bovine serum (FBS) were obtained from ThermoFisher Scientific (Belgium).

4.2.2 Methods

4.2.2.1 Sol-gel synthesis of chitosan-pNIPAM copolymer

Chitosan was dissolved in 1 %(w/v) acetic acid in a round bottom flask at 60 °C overnight with a concentration of 25 mg/mL and cooled down to room temperature afterwards. The chitosan solution was purged with nitrogen, and an appropriate amount of NIPAM (according to table 3.1) was dissolved separately in 1.5 mL deionized water under nitrogen atmosphere. The NIPAM solution was added to the round bottom flask dropwise. Appropriate amounts of APS and MBA, according to table 3.1, were dissolved in 1 mL water under nitrogen atmosphere, and added to the reaction chamber in a dropwise manner. The solution was allowed to stir for 30 min to ensure complete mixing, and 25 µL TEMED was added to start the reaction. The reaction was allowed to continue until the gel was formed. The gels were dialyzed against deionized water for 3 days, with two water changes every day, using dialysis tubing with a 14 kDa molecular cutoff.

Table 4.1. Different formulations used for sol-gel synthesis of hydrogels

Chitosan/NIPAM ratio	APS (mol %)	MBA (mol %)	TEMED (µL)
1:1	4	0.5	25
1:2	4	0.5	25
1:3	4	0.5	25
1:1	4	1.25	25
1:2	4	1.25	25
1:3	4	1.25	25
1:1	4	2.45	25
1:2	4	2.45	25
1:3	4	2.45	25

4.2.2.2 Fourier transform infrared spectroscopy (FTIR)

The attenuated total reflection (ATR) FTIR spectra of the freeze-dried hydrogels were obtained using a Bruker Vertex 70 FTIR spectrometer,

in the wavelength range of 600-4000 cm^{-1}, with a resolution of 2 cm^{-1} and an average of 32 scans.

4.2.2.3 3D printability of the scaffolds

The possibility of 3D printing the hydrogels was evaluated using an extrusion bioprinter (3Ddiscovery, RegenHU, Switzerland). Gels were transferred to cartridges with a diameter of 7.29 mm, and several shapes for different analyses were printed using a 250 μm nozzle through a piston driven extrusion printing modality. To analyze one-dimensional shape fidelity, lines of 30 mm in length were printed, the perimeter of the lines was then measured and compared to the theoretical value. Additionally, to evaluate the two-dimensional accuracy of the print, squares were printed and a circularity factor (pr-value) was calculated as previously reported [23], where a value closer to 1 represents a more accurate print. Furthermore, the resolution of the prints was evaluated by printing lines with different distances ranging from 1 mm to 10 mm and the area between the lines was measured as an estimate of printing accuracy. The possibility of 3D printing was evaluated by printing cubes of 10 mm by 10 mm by 2.5 mm (L×W×H). Only samples capable of printing in 3D were selected for further tests.

4.2.2.4 Evaluation of degradation and swelling

Samples for studying the hydrolytic degradation were prepared through 3D printing cubes of 10 mm by 10 mm by 5 mm made from different hydrogel formulations. Printed samples were then freeze-dried (Alpha 1-2 LD plus, Martin Christ Freeze Dryers, Osterode, Germany), weighed and incubated in 5 mL deionized water at 37 °C for 1, 3, 5 and 7 days. At each timepoint, samples were removed, freeze-dried and weighed. The percentage of hydrolytic degradation was calculated through equation 4.1, in which W_0 is the initial weight, and W is the weight after incubation.

$$Degradation = \frac{W_0 - W}{W_0} \times 100 \qquad \text{Eqn 4.1}$$

For the swelling study, samples were prepared in the same way as the samples for the degradation study, except that they were not freeze-dried after incubation. Measurements for swelling were performed at 1, 3, 6, 24 and 72 hours after incubation and swelling was calculated

following equation 4.2, where W_0 is the initial weight and W_{sw} is the swollen weight.

$$Swelling = \frac{W_{sw} - W_0}{W_0} \times 100 \quad \text{Eqn 4.2}$$

4.2.2.5 Evaluation of surface morphology

To evaluate the surface morphology of the scaffolds, constructs of 10 mm by 10 mm by 5 mm with a grid infill and a distance of 2 mm between grids were printed and freeze-dried. The surface morphology of freeze-dried scaffolds was analyzed through scanning electron microscopy (SEM) using a Philips XL30 electron microscope at 10 KV.

4.2.2.6 Cell viability

Scaffolds of 0.7 mm by 0.7 mm by 0.5 mm, with a full infill were printed and freeze-dried to assess cell viability on the scaffolds. Scaffolds were then sterilized under UV-C for 2 hours. Dental pulp stem cells (DPSCs) were cultured according to a previously described protocol [24]. DPSCs at passage 11 were seeded on the scaffolds with a density of 10,000 cells/cm^2. Scaffolds were then immersed in αMEM supplemented with 1% FBS and 1% antibiotics (considered as the maintenance medium) with medium change every 2-3 days, and the viability of seeded cells was evaluated at day 1, 3, and 7 following the seeding. For this, Live/dead staining was used using Calcein AM and Ethidium homodimer (LIVE/DEAD viability cytotoxicity kit, Invitrogen, Thermofisher Scientific) according to manufacturer's protocol. Fluorescent imaging was performed (IX83 inverted microscope, Olympus Scientific Solutions, Tokyo, Japan) and images were subjected to non-linear modifications removing the background signal using Fiji ImageJ [25].

DNA quantification was performed to quantitatively assess the cell viability on the scaffolds. For this purpose, scaffolds seeded with DPSCs were prepared following the same protocol for live/dead assay. At each timepoint, medium covering the scaffolds was removed and cells were washed with PBS, 350 µL commercial RLT lysis buffer (Qiagen, Hilden, Germany) plus 1 %(v/v) β-mercapto-ethanol were added to the scaffolds, the samples were transferred to a

microcentrifuge tube and vortexed for 1 minute to prepare the lysate. Quant-iTTM dsDNA HS reagent was diluted in Quant-iTTM dsDNA HS buffer (Quant-iT dsDNA Assay Kit, Thermofisher Scientific, Belgium) with a 1:200 ratio to make the working solution. Next, 5 µL of lysate was mixed with 195 µL of the working solution, and readings were performed using a Qubit fluorometer.

4.2.2.7 Statistical analysis

All experiments in different sections were performed in triplicates (n=3). Analysis of Variance (ANOVA) followed by Tukey's post-hoc test were performed to assess statistical differences using Graphpad Prism (version 8.0.0 for Windows, GraphPad Software, San Diego, California USA, www.graphpad.com). A p-value of less than 0.05 was considered significant.

4.3 Results

4.3.1 Sol-gel synthesis and characterization of pNIPAM-chitosan copolymer

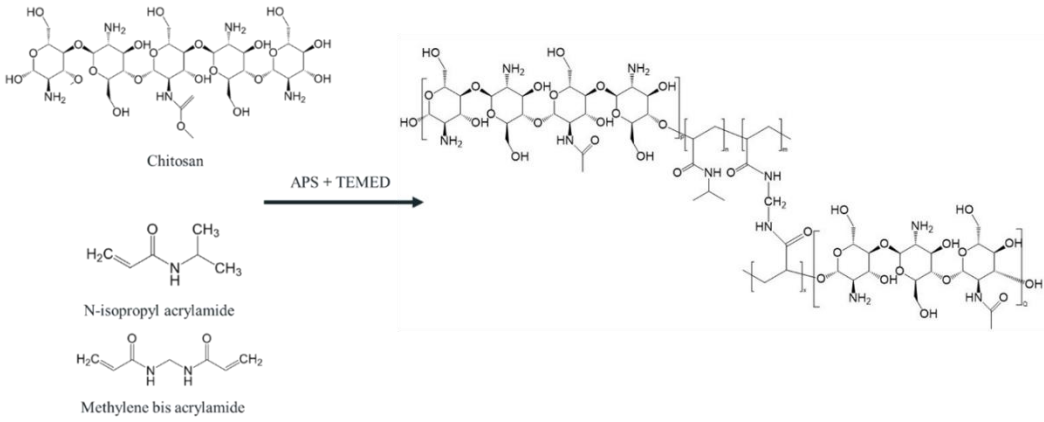

Scheme 4.1. Schematic representation of the proposed reaction for synthesis of pNIPAM-chitosan copolymer (scheme made using chemdraw software)

To synthesize hydrogels of pNIPAM-chitosan copolymer, different components, including chitosan, NIPAM and MBA were dissolved in 1 %(w/v) acetic acid. Addition of the radical initiator, APS, was followed by incorporation of TEMED, resulting in decomposition of APS through a redox reaction [26], making radicals available for initiation of the polymerization. Following addition of TEMED, and due to the presence of MBA, the hydrogel backbone rapidly started to form, as demonstrated in scheme 4.1. Among the 9 different combinations of constituents, 3 combinations, being samples with a chitosan:NIPAM ratio of 1:1, and the sample with a chitosan:NIPAM ratio of 1:2 and a crosslinker concentration of 0.5 mol% did not form a gel 24h after addition of TEMED. The other 5 formulations resulted in a crosslinked gel within 1 hour of TEMED addition.

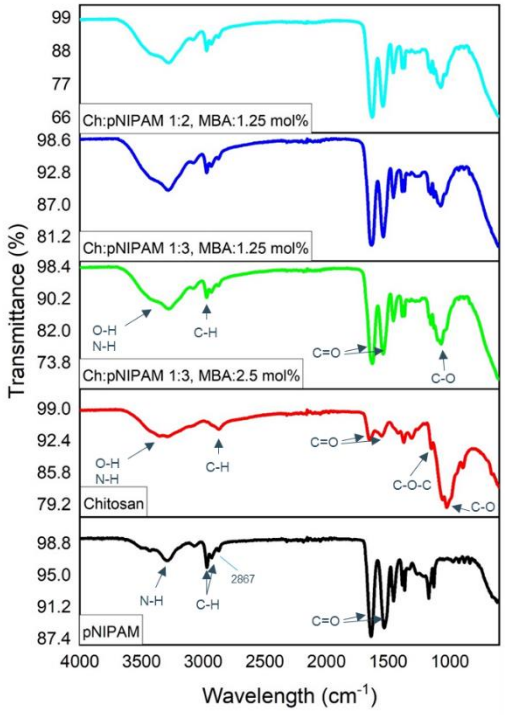

Figure 4.1. FTIR characterization of pNIPAM, chitosan and the copolymer with different ratios of constituents

Fourier transform infrared spectroscopy (FTIR) was used to characterize the synthesized copolymer. Figure 4.1 demonstrates the peaks corresponding to different functional groups of chitosan, pNIPAM and chitosan-pNIPAM copolymer. As demonstrated, the peak ranging from 3100 to 3500 cm^{-1} corresponds to OH/NH stretching vibration and it is intensified in the copolymer samples.. In addition to these, the presence of peaks attributed to amide I and amide II of pNIPAM at 1534 and 1636 cm^{-1}, along with the ether peak at 1077 cm^{-1} confirm the success of copolymerization [27–29].

4.3.2 Evaluation of printability

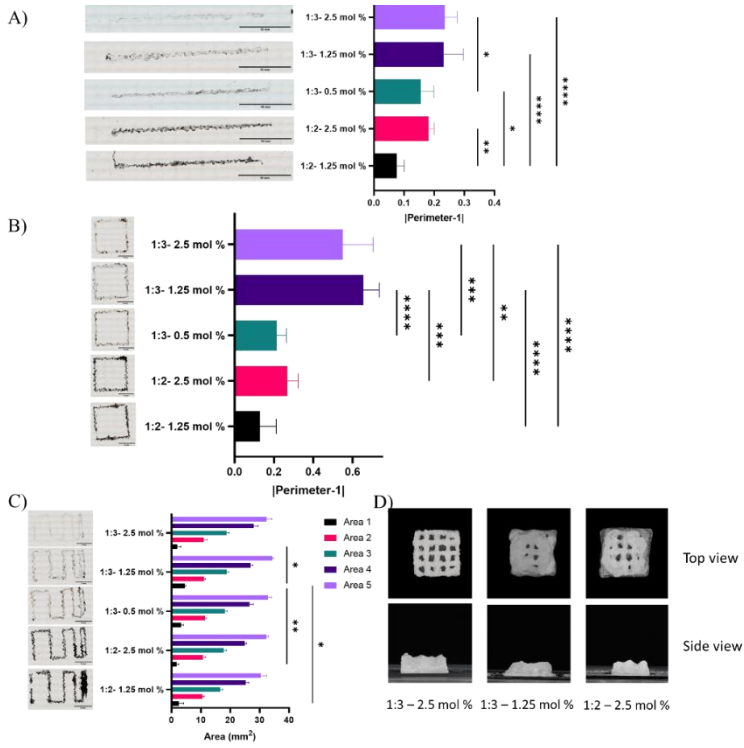

Figure 4.2. A) Evaluation of print fidelity by measurement of perimeter ratio B) Evaluation of print fidelity by calculating the pr value C) evaluation of print resolution by measuring the area between the lines and D) printability in 3D

The possibility of producing scaffolds of the synthesized hydrogel through 3D printing was evaluated by printing the synthesized gels on

an extrusion based bioprinter. As demonstrated in figure 4.2.A, the lines printed using different hydrogel formulations result in a range of fidelities, with the most accurate ones being the sample synthesized using a chitosan:NIPAM ratio of 1:2 and an MBA concentration of 1.25 mol%, followed by 1:3, 0.5 mol % and 1:2, 2.5 mol%. In terms of resolution, considered to be the smallest possible distance between two distinguishable lines, samples with a material ratio of 1:3 crosslinked with 1.25 mol% were the best options, as shown in figure 4.2.C. In terms of pr value, best results were obtained from samples synthesized with a chitosan:NIPAM ratio of 1:2, and 1.25 mol% crosslinker, along with 1:3, and 0.5 mol% crosslinker, as demonstrated in figure 4.2.B. However, printing in 3 dimensions was not possible with samples of 1:2, and 1.25 mol% and 1:3, and 0.5 mol %. As shown in figure 4.2.D, best shape fidelity in 3D was obtained from samples with a material ratio of 1:3 and a crosslinker concentration of 2.5 mol%.

4.3.3 Evaluation of degradation and swelling

Considering the importance of scaffold degradation in tissue engineering strategies, the hydrolytic degradation rate of produced scaffolds in 37 °C water was measured through gravimetry. As demonstrated in figure 4.3.A, degradation after 7 days ranges from approximately 25 % to 35 %, with the formulation synthesized with a ratio of 1:2 and an MBA concentration of 2.5 mol % having a significantly higher degradation compared to the other two formulations ($p < 0.05$). Furthermore, the 1:3, 1.25 mol% formulation and the 1:3, 2.5 mol% had a similar rate of degradation after one week. Additionally, the water content of the hydrogels can have a major impact on success of tissue engineering strategies. As presented in figure 4.3.B, the rate of swelling for all three hydrogel formulations was found to be approximately 12 times following one hour of immersion in deionized water. However, no significant differences among different samples were observed after one hour swelling. Furthermore, all the swelling took place in the first one hour of immersion, as no increase in the weight was observed in subsequent

timepoints. The rate presented in figure 4.3.B, seems to reduce after 3 days of immersion in water.

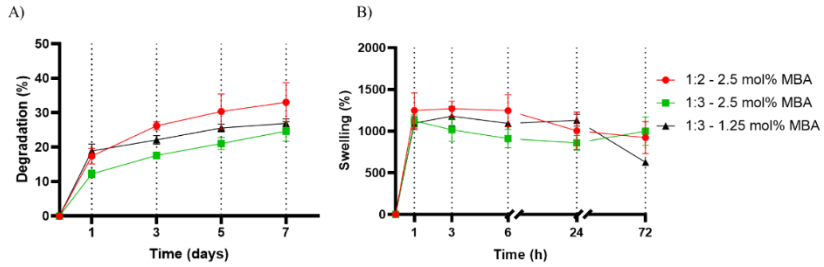

Figure 4.3. A) Rate of scaffold hydrolytic degradation in water at 37 °C B) Rate of scaffold swelling at 37 °C

4.3.4 Evaluation of surface morphology

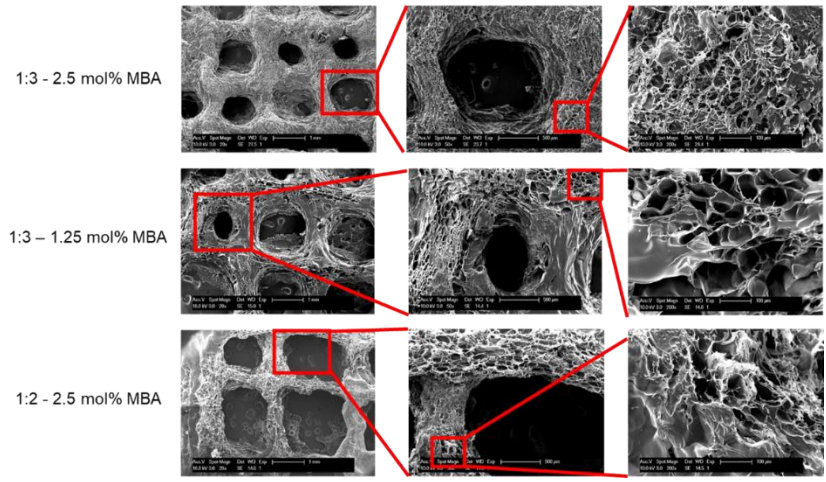

Figure 4.4. Surface morphology of the scaffolds obtained through SEM

The surface morphology of the 3D printed, freeze-dried scaffolds was evaluated through scanning electron microscopy (SEM). As shown in figure 4.4, all three formulations show a high degree of porosity. Among these the average pore size of samples synthesized with a ratio of 1:3 and a 1.25 mol % crosslinker was significantly larger than other samples, being on average $6.3 \times 10^3 \pm 176.6\ \mu m^2$, while this average was $3.7 \times 10^3 \pm 75.1\ \mu m^2$ for samples with a material ratio of 1:2 and

MBA concentration of 2.5 mol %, and $1.2 \times 10^3 \pm 118.1$ µm^2 for samples of 1:3 material ratio and 2.5 mol % crosslinker

4.3.5 Evaluation of cell viability

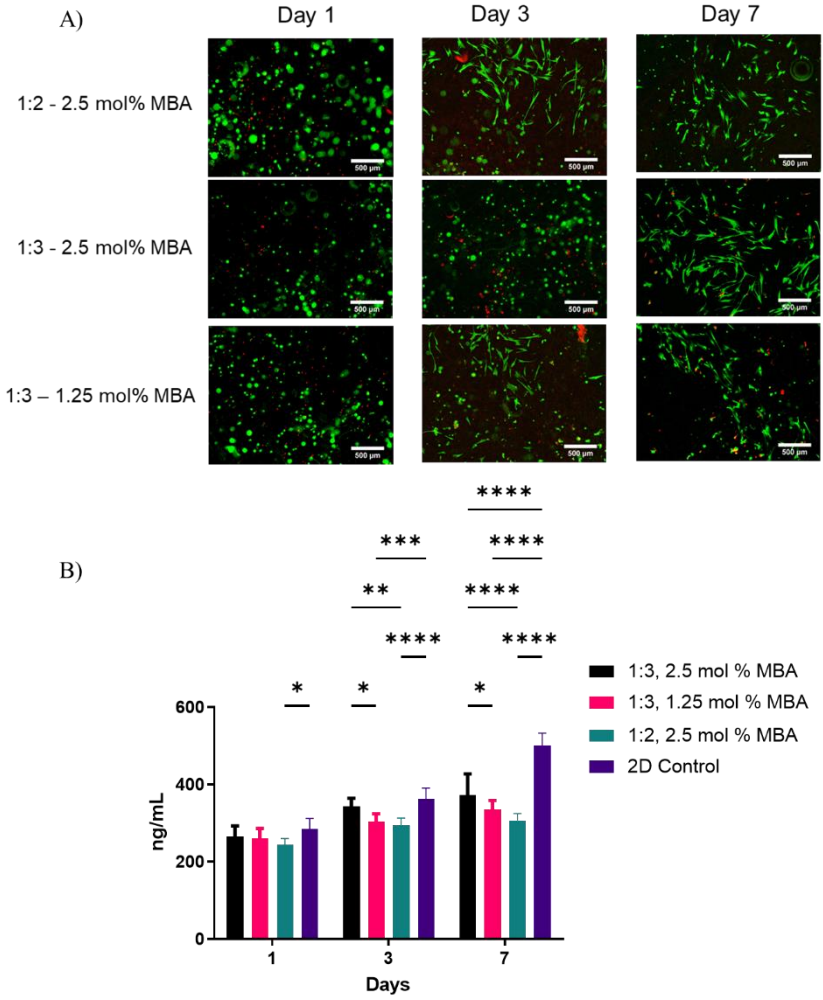

Figure 4.5. A) Live/dead viability assay of DPSCs seeded on the scaffolds and B) DNA quantification of DPSCs

To further evaluate suitability of the designed scaffolds for tissue engineering applications and assess any potential cytotoxicity, dental pulp stem cells (DPSCs) were seeded and cultured on the scaffolds.

The results of the live/dead viability assay demonstrated in figure 4.5.A show a much larger number of living cells compared to the dead cells, and no major differences can be observed among the three different hydrogel samples.
Additionally, to assess the cell viability in a quantitative manner, DNA quantification was performed on cells cultured on pNIPAM-chitosan scaffolds. The results, presented in figure 4.5.B, demonstrate capability of the scaffolds to support cell survival.

4.4 Discussion

In this study, hydrogels of pNIPAM-chitosan copolymer were synthesized through a one-step sol-gel polymerization reaction. Following the APS/TEMED reaction resulting in decomposition of APS, it can be hypothesized that the sulfate anion radicals, produced by decomposition of APS, react with hydroxyl groups of chitosan, producing alkoxy radicals which then initiate copolymerization of NIPAM [30], as demonstrated in scheme 4.1. Furthermore, presence of methylene bis acrylamide, results in the formation of crosslinks among polymer chains, leading to the development of hydrogels as the reaction proceeds. The hypothesis for the reaction was confirmed using FTIR, where the shifting of the peak at 3317 to 3423 cm^{-1} is reported to confirm reaction on the hydroxyl groups [31], in addition to the presence of the specific peaks correlating to both materials.
Following the synthesis 3D printing was performed to develop scaffolds using this material. Consequently, 3D printing of the developed hydrogels was analyzed. While it was possible to print all synthesized formulations using extrusion printing, the quality of the prints was significantly different in 2D. Moreover, only 3 formulations were printable in 3D. As it appears, a higher crosslinking degree resulting from both an increased amount of MBA, and an increased amount of NIPAM presenting a higher number of functional groups for crosslinking, results in an increased stability of the constructs enabling printing in 3D. As a result, considering the importance of printing in three dimensions for fabrication of tissue engineering scaffolds, formulations incapable of forming scaffolds in 3D were eliminated from further studies.

Being a synthetic polymer, pNIPAM alone is generally not considered as a degradable material [22], posing a challenge for tissue engineering applications using this material. However, copolymerization with natural polymers has been suggested as a method to induce biodegradability [32,33]. The efficiency of this method was confirmed through the results of this study, and the degradation behavior followed an expected trend, where a lower crosslinker concentration increased the rate of degradation [34]. Additionally, the rate of degradation is comparable to chitosan-based biomaterials, demonstrating the chitosan chains to be responsible for degradability of the copolymer [35].

Furthermore, the water content of the hydrogels was evaluated through a swelling study, where a swelling in the range of 1200 % was observed. This swelling rate is lower than reported swelling of pNIPAM in 20 °C [36], which could be attributed to the hydrophobic behavior of pNIPAM chains at 37 °C, however, it is well within the range observed in other chitosan-based scaffolds [37]. The slight reduction observed in the swelling rate after 72 hours can be attributed to the hydrolytic degradation of the hydrogels, affecting the swelling measurements which are also based on the measurement of the weight [38]. Additionally, all formulations resulted in a high porosity with pore areas ranging from 1.2×10^3 to 6.3×10^3 μm^2, which is of great importance for transport of nutrients and waste to and from the cells, in addition to facilitating tissue ingrowth following implantation [39]. Among the samples in this study, it was observed that a lower rate of crosslinking resulted in larger pores as they are composed of a less tightly held network. Still, the pore size observed is much larger than the reported pore size of pure pNIPAM, being approximately 3.5 μm in diameter [40], and it is much closer to reported pore size of chitosan-based materials [41]. This is likely due to the significant impact of chitosan on the increased hydrophilicity of the copolymer, resulting in larger pore sizes in aqueous environment [42].

Following the physical characterization of the produced scaffolds, their ability to support viability of dental pulp stem cells (DPSCs) was evaluated. A qualitative analysis of the live/dead results would suggest that the material is suitable for maintaining the cell viability following a 7-day culture in medium with 1% FBS. This is consistent with previously reported observations showing a lack of toxicity by

pNIPAM based films [43]. Quantitatively, the DNA quantification results presented in figure 4.5.B, demonstrate the capability of the scaffolds to support cell survival. However, the rate of proliferation is lower than the control sample cultured in 2D. A lower proliferation rate was expected considering the culture conditions, being in maintenance medium with a lower amount of FBS, and the higher rate in 2D culture is attributed to the culture plate coatings enhancing cell attachment. Additionally, the findings show that a larger number of cells are present on highly crosslinked scaffolds with a material ratio of 1:3, suggesting DPSCs prefer the increased mechanical properties. This behavior, and the effect of mechanical properties on behavior of DPSCs has been reported previously [44].

4.5 Conclusion

In this chapter, hydrogels based on a copolymer of pNIPAM and chitosan crosslinked with MBA were developed through sol-gel synthesis. It was demonstrated for the first time that these hydrogels could be used for fabrication of tissue engineering scaffolds for dentoalveolar regeneration through 3D printing. Further characterization of the hydrogels demonstrated degradability, and a high swelling rate and comparatively large pore sizes, qualities that are important for tissue engineering applications. In addition, DPSCs seeded on the scaffolds demonstrated viability of up to approximately 75 % after 7 days of culture. Taken together, results presented here suggest the proposed material and fabrication method as suitable for the development of scaffolds, while further research would be necessary to optimize the properties and achieve this goal. This research could include further optimization of the material for printing, evaluation of rheological properties, along with in-depth biological evaluation of the seeded cells.

4.6 References

1. Hanif A, Qureshi S, Sheikh Z, Rashid H. “Complications in implant dentistry”. Eur J Dent. 2017;11(1):135–40.
2. EzEldeen M, Wyatt J, Al-Rimawi A, Coucke W, Shaheen E, Lambrichts I, Willems G, Politis C, Jacobs R. “Use of CBCT Guidance for Tooth Autotransplantation in Children.”. J Dent Res. 2019 Apr;98(4):406–13.
3. Na S, Zhang H, Huang F, Wang W, Ding Y, Li D, Jin Y. “Regeneration of

dental pulp/dentine complex with a three-dimensional and scaffold-free stem-cell sheet-derived pellet.". J Tissue Eng Regen Med. 2016 Mar;10(3):261–70.
4. Khodakaram-Tafti A, Mehrabani D, Shaterzadeh-Yazdi H, Zamiri B, Omidi M. "Tissue Engineering in Maxillary Bone Defects". World J Plast Surg. 2018 Jan;7(1):3–11.
5. Abou Neel EA, Chrzanowski W, Salih VM, Kim HW, Knowles JC. "Tissue engineering in dentistry". J Dent. 2014 Aug 1 [cited 2020 Feb 18];42(8):915–28.
6. Chen FM, Zhang J, Zhang M, An Y, Chen F, Wu ZF. "A review on endogenous regenerative technology in periodontal regenerative medicine". Biomaterials. 2010;31(31):7892–927.
7. Kim NR, Lee DH, Chung PH, Yang HC. "Distinct differentiation properties of human dental pulp cells on collagen, gelatin, and chitosan scaffolds.". Oral Surg Oral Med Oral Pathol Oral Radiol Endod. 2009 Nov;108(5):e94-100.
8. Grawish ME, Grawish LM, Grawish HM, Grawish MM, El-Negoly SA. "Challenges of Engineering Biomimetic Dental and Paradental Tissues". Tissue Eng Regen Med. 2020;17(4):403–21.
9. Groll J, Burdick JA, Cho DW, Derby B, Gelinsky M, Heilshorn SC, Jüngst T, Malda J, Mironov VA, Nakayama K, Ovsianikov A, Sun W, Takeuchi S, Yoo JJ, Woodfield TBF. "A definition of bioinks and their distinction from biomaterial inks". Biofabrication. 2018;11(1):13001.
10. Do AV, Khorsand B, Geary SM, Salem AK. "3D Printing of Scaffolds for Tissue Regeneration Applications". Adv Healthc Mater. 2015 Aug 1;4(12):1742–62.
11. Cubo-Mateo N, Rodríguez-Lorenzo LM. "Design of Thermoplastic 3D-Printed Scaffolds for Bone Tissue Engineering: Influence of Parameters of "Hidden" Importance in the Physical Properties of Scaffolds". Vol. 12, Polymers . 2020.
12. Ma H, Feng C, Chang J, Wu C. "3D-printed bioceramic scaffolds: From bone tissue engineering to tumor therapy". Acta Biomater. 2018;79:37–59.
13. Lee JH, Kim HW. "Emerging properties of hydrogels in tissue engineering". J Tissue Eng. 2018 Jan 1;9:2041731418768285.
14. Erisken C, Kalyon DM, Zhou J, Kim SG, Mao JJ. "Viscoelastic Properties of Dental Pulp Tissue and Ramifications on Biomaterial Development for Pulp Regeneration.". J Endod. 2015 Oct;41(10):1711–7.
15. Browning MB, Cereceres SN, Luong PT, Cosgriff-Hernandez EM. "Determination of the in vivo degradation mechanism of PEGDA hydrogels.". J Biomed Mater Res A. 2014 Dec;102(12):4244–51.
16. Stoleru E, Dumitriu RP, Ailiesei GL, Yilmaz C, Brebu M. "Synthesis of Bioactive Materials by In Situ One-Step Direct Loading of Syzygium aromaticum Essential Oil into Chitosan-Based Hydrogels". Vol. 8, Gels . 2022.
17. Zarandona I, Bengoechea C, Álvarez-Castillo E, de la Caba K, Guerrero A, Guerrero P. "3D Printed Chitosan-Pectin Hydrogels: From Rheological Characterization to Scaffold Development and Assessment.". Gels (Basel, Switzerland). 2021 Oct;7(4).
18. Lai JY, Luo LJ. "Chitosan-g-poly(N-isopropylacrylamide) copolymers as delivery carriers for intracameral pilocarpine administration". Eur J Pharm Biopharm. 2017;113:140–8.
19. Bao H, Li L, Leong WC, Gan LH. "Thermo-Responsive Association of Chitosan-graft-Poly(N-isopropylacrylamide) in Aqueous Solutions". J Phys

Chem B. 2010 Aug 19;114(32):10666–73.
20. Kim H, Witt H, Oswald TA, Tarantola M. “Adhesion of Epithelial Cells to PNIPAm Treated Surfaces for Temperature-Controlled Cell-Sheet Harvesting”. ACS Appl Mater Interfaces. 2020 Jul 29;12(30):33516–29.
21. Lapeyre V, Ancla C, Catargi B, Ravaine V. “Glucose-responsive microgels with a core–shell structure”. J Colloid Interface Sci. 2008;327(2):316–23.
22. Patenaude M, Hoare T. “Injectable, Degradable Thermoresponsive Poly(N-isopropylacrylamide) Hydrogels”. ACS Macro Lett. 2012 Mar 20;1(3):409–13.
23. Ouyang L, Yao R, Zhao Y, Sun W. “Effect of bioink properties on printability and cell viability for 3D bioplotting of embryonic stem cells”. Biofabrication. 2016 Sep;8(3):035020.
24. Hilkens P, Gervois P, Fanton Y, Vanormelingen J, Martens W, Struys T, Politis C, Lambrichts I, Bronckaers A. “Effect of isolation methodology on stem cell properties and multilineage differentiation potential of human dental pulp stem cells.”. Cell Tissue Res. 2013 Jul;353(1):65–78.
25. Schindelin J, Arganda-Carreras I, Frise E, Kaynig V, Longair M, Pietzsch T, Preibisch S, Rueden C, Saalfeld S, Schmid B, Tinevez JY, White DJ, Hartenstein V, Eliceiri K, Tomancak P, Cardona A. “Fiji: an open-source platform for biological-image analysis”. Nat Methods. 2012;9(7):676–82.
26. Patras G, Qiao GG, Solomon DH. “On the mechanism of background silver staining during sodium dodecyl sulphate-polyacrylamide gel electrophoresis”. Electrophoresis. 1999 Jul 1;20(10):2039–45.
27. Lee JW, Jung MC, Park HD, Park KD, Ryu GH. “Synthesis and characterization of thermosensitive chitosan copolymer as a novel biomaterial”. J Biomater Sci Polym Ed. 2004 Jan 1;15(8):1065–79.
28. Chen JP, Cheng TH. “Thermo-Responsive Chitosan-graft-poly(N-isopropylacrylamide) Injectable Hydrogel for Cultivation of Chondrocytes and Meniscus Cells”. Macromol Biosci. 2006 Dec 8;6(12):1026–39.
29. Cheaburu-Yilmaz CN, Yilmaz O, Aydin Kose F, Bibire N. “Chitosan-Graft-Poly(N-Isopropylacrylamide)/PVA Cryogels as Carriers for Mucosal Delivery of Voriconazole”. Vol. 11, Polymers . 2019.
30. Duan C, Zhang D, Wang F, Zheng D, Jia L, Feng F, Liu Y, Wang Y, Tian K, Wang F, Zhang Q. “Chitosan-g-poly(N-isopropylacrylamide) based nanogels for tumor extracellular targeting”. Int J Pharm. 2011;409(1):252–9.
31. Qi M, Li G, Yu N, Meng Y, Liu X. “Synthesis of thermo-sensitive polyelectrolyte complex nanoparticles from CS-g-PNIPAM and SA-g-PNIPAM for controlled drug release”. Macromol Res. 2014;22(9):1004–11.
32. Eslahi N, Abdorahim M, Simchi A. “Smart Polymeric Hydrogels for Cartilage Tissue Engineering: A Review on the Chemistry and Biological Functions”. Biomacromolecules. 2016 Nov 14;17(11):3441–63.
33. Zou G, Shen J, Duan P, Xia X, Chen R, Jin B. “Temperature-Sensitive Poly(N-isopropylacrylamide)/Konjac Glucomannan/Graphene Oxide Composite Membranes with Improved Mechanical Property, Swelling Capability, and Degradability”. Sojoudi H, editor. Int J Polym Sci. 2018;2018:7906747.
34. You R, Xu Y, Liu G, Liu Y, Li X, Li M. “Regulating the degradation rate of silk fibroin films through changing the genipin crosslinking degree”. Polym Degrad Stab. 2014;109:226–32.
35. Dimida S, Barca A, Cancelli N, De Benedictis V, Raucci MG, Demitri C. “Effects of Genipin Concentration on Cross-Linked Chitosan Scaffolds for

Bone Tissue Engineering: Structural Characterization and Evidence of Biocompatibility Features". Kawatsuki N, editor. Int J Polym Sci. 2017;2017:8410750.

36. Martinez M V, Molina M, Barbero CA. "Poly(N-isopropylacrylamide) Cross-Linked Gels as Intrinsic Amphiphilic Materials: Swelling Properties Used to Build Novel Interphases". J Phys Chem B. 2018 Sep 27;122(38):9038–48.
37. Felfel RM, Gideon-Adeniyi MJ, Zakir Hossain KM, Roberts GAF, Grant DM. "Structural, mechanical and swelling characteristics of 3D scaffolds from chitosan-agarose blends". Carbohydr Polym. 2019;204:59–67.
38. Anand R, Salar Amoli M, Huysecom AS, Amorim PA, Agten H, Geris L, Bloemen V. "A tunable gelatin-hyaluronan dialdehyde/methacryloyl gelatin interpenetrating polymer network hydrogel for additive tissue manufacturing.". Biomed Mater. 2022 Jun;17(4).
39. Loh QL, Choong C. "Three-dimensional scaffolds for tissue engineering applications: role of porosity and pore size.". Tissue Eng Part B Rev. 2013 Dec;19(6):485–502.
40. Franke D, Gerlach G. "Studies on porosity in poly(N-isopropylacrylamide) hydrogels for fast-responsive piezoresistive microsensors". J Sensors Sens Syst. 2021;10(1):93–100.
41. Yan LP, Wang YJ, Ren L, Wu G, Caridade SG, Fan JB, Wang LY, Ji PH, Oliveira JM, Oliveira JT, Mano JF, Reis RL. "Genipin-cross-linked collagen/chitosan biomimetic scaffolds for articular cartilage tissue engineering applications.". J Biomed Mater Res A. 2010 Nov;95(2):465–75.
42. Wei D, Xiao W, Sun J, Zhong M, Guo L, Fan H, Zhang X. "A biocompatible hydrogel with improved stiffness and hydrophilicity for modular tissue engineering assembly". J Mater Chem B. 2015;3(14):2753–63.
43. Sanzari I, Buratti E, Huang R, Tusan CG, Dinelli F, Evans ND, Prodromakis T, Bertoldo M. "Poly(N-isopropylacrylamide) based thin microgel films for use in cell culture applications". Sci Rep. 2020;10(1):6126.
44. Liu N, Zhou M, Zhang Q, Zhang T, Tian T, Ma Q, Xue C, Lin S, Cai X. "Stiffness regulates the proliferation and osteogenic/odontogenic differentiation of human dental pulp stem cells via the WNT signalling pathway". Cell Prolif. 2018 Apr 1;51(2):e12435.

Chapter 5. Development of a thermo-responsive, pNIPAM-based bioink for tissue engineering of dentoalveolar region through bioprinting

Mehdi Salar Amoli [a,b], Thomas Van Laeken [a], Resmi Anand [a,c,d], Mostafa EzEldeen [b,e], Reinhilde Jacobs [b,f] , Veerle Bloemen [a,c]

[a] Materials Technology TC, Campus Group T, KU Leuven, Andreas Vesaliusstraat 13, 3000 Leuven, Belgium

[b] OMFS IMPATH Research Group, Faculty of Medicine, Department of Imaging and Pathology, KU Leuven and Oral and Maxillofacial Surgery, University Hospitals Leuven, Kapucijnenvoer 33, 3000 Leuven, Belgium

[c] Prometheus, Division of Skeletal Tissue Engineering Leuven, KU Leuven, Leuven, Belgium

[d] Inter University Centre for Biomedical Research and Super Speciality Hospital, Mahatma Gandhi University Campus at Thalappady, Kottayam, Kerala-686009, India

[e] Department of Oral Health Sciences, KU Leuven and Paediatric Dentistry and Special Dental Care, University Hospitals Leuven, Kapucijnenvoer 33, 3000 Leuven, Belgium

[f] Department of Dental Medicine, Karolinska Institutet, Stockholm, Sweden

Manuscript in preparation

Chapter summary

Certain shortcomings in available treatments for dentoalveolar complications have resulted in exploration of tissue engineering strategies. Within these strategies, bioprinting seems to be an interesting technology for development of tissue engineering constructs capable of addressing challenges faced in traditional approaches. However, majority of research in bioprinting perform the printing at temperatures lower than the physiological temperature due to limitations of the materials. This chapter aims to develop a 3D printable biocompatible copolymer through development of methacrylated methylcellulose pNIPAM, capable of printing at 37 ℃. The developed copolymer was analyzed through Fourier Transform Infrared Spectroscopy (FTIR) and proton Nuclear Magnetic Resonance (^{1}H NMR). Further characterization was performed by evaluating the lower critical solution temperature (LCST), critical gel concentration, water content at room temperature and 37 ℃, degradability of the material, followed by 3D printing and cell viability. Following confirmation of the copolymerization, the material demonstrated an LCST of 34 ℃, in addition to gel formation at concentrations of above 8 %(w/v). furthermore, the syneresis ranged from non-significant to 70 % depending on formulation, and printing was possible using formulations with a low syneresis. Furthermore, preliminary viability test demonstrated capability of the material to support viability of encapsulated dental pulp stem cells. Taken together, the present findings suggest the developed material might be a suitable candidate for dentoalveolar tissue engineering through bioprinting, while further research is required to assess the process in more depth.

5.1 Introduction

The limited regenerative capacity of the tissues in the dentoalveolar region [1], coupled with specific challenges associated with available treatments, such as inability in placement of implants in pediatric patients [2,3], have resulted in exploration of tissue engineering strategies addressing a range of conditions in this region [4,5]. Among these strategies, the emerging field of bioprinting has gained significant interest, due to the robust and replicable procedure enabling development of cell encapsulating tissue engineering scaffolds based on pre-determined designs [6].

Within the field of bioprinting, the choice of the material to be used as bioink is of extreme importance [7]. These materials, often belonging to the class of hydrogels, need to be printable and biodegradable, in addition to being able to encapsulate cells and support their viability and functionality [8,9]. Furthermore, these materials need to be combined with cells in the solution phase, and must be able to turn into printable gels in a relatively rapid process without having any negative impact on viability of the cells [10]. This is generally achieved through either physical gelation of the materials, via triggers such as temperature, ionic interactions [11], hydrogen bonding [12], or through pre-crosslinking of the materials with chemical crosslinkers [13].

The research using physical gelation of temperature sensitive materials for bioprinting is almost exclusively focused on gelatin [14,15]. This is because the solution of gelatin turns into a physical gel upon cooling, due to transformation of random coil chains to ordered triple helix structures where the interchain hydrogen bonds result in formation of the gel [16]. However, this can be considered a disadvantage, taking into account that cells encapsulated in the material would need to be incubated at low temperatures for specific periods of time, and the bioprinting process is performed at lower than physiological temperatures [17,18].

Consequently, a range of studies have focused on development of stimuli responsive biomaterials capable of being printed at 37 °C. Such studies have used materials such as combination of alginate and PLA nanofibers [19], alginate and gelatin [20], agarose and alginate [21], along with collagen-based materials [22]. However, each of these

combinations face specific challenges. Regarding the alginate-based materials, the main challenge rises from lack of any cell adhesion cues resulting in low viability of encapsulated cells [23]. The same challenge is present with agarose [24], while collagen results in a very high cell viability as it is the main component of the extracellular matrix. However, collagen-based materials suffer from drawbacks including a very high price limiting widespread application, relatively high batch to batch variability, and low mechanical properties [25], presenting challenges in its use in bioprinting applications.

Still, among the suggested strategies for development of bioinks suitable for bioprinting at 37 ℃, use of materials with inherent lower critical solution temperature (LCST) property is investigated in a very limited extent. Among such materials, poly-n-isopropylacrylamide (pNIPAM) is one of the most widely investigated materials suitable for a variety of applications including injectable scaffolds [26], drug delivery applications [27], along with other biomedical research applications such as cell sheet engineering [28].

The reason for the widespread application of pNIPAM is an LCST of around 32 ℃, meaning the materials turns from a solution state to a gel state at physiological temperature in aqueous solutions [29]. This transition takes place due to the transition of random coil polymer chain conformation to a globular structure upon application of temperature [30]. Below the LCST temperature, the random coil structure is exposed to the water molecules, with the amine side groups forming hydrogen bonds with water molecules. However, by introduction of energy in the form of heat, the increased entropy of water molecules at the isopropyl groups leads to a thermodynamically unstable state, resulting in expulsion of water molecules and collapse of the polymer chains into a globular state. This is represented by a free energy barrier favouring the random coil structure by 21 ± 9 kJ/mol at temperatures below the LCST, and a free energy barrier favouring the globular structure by 21 ± 8 kJ/mol above the LCST [31].

This LCST property has resulted in a widespread use of pNIPAM based materials in the field of tissue engineering. Injectable pNIPAM/hyaluronic acid hydrogels have been used to encapsulate mesenchymal stem cells along with drug delivery microparticles for cartilage tissue engineering [26]. Furthermore,

pNIPAM/hydroxyapatite scaffolds have been fabricated for bone tissue engineering [32]. In addition to bone and cartilage, pNIPAM based materials have been used for tissue engineering of intestinal crypts [33], skin and vascular grafts [34], cardiac tissue [35]. While pNIPAM has been used to a larger extent in tissue engineering, it has only been used recently in bioprinting strategies. This is represented in bioprinting pNIPAM based hydrogel at low temperatures on a heated printbed resulting in instant gelation of the material [36], characterization of pNIPAM gels for printing [37], along with development of a pNIPAM based bioink, along with printing at room temperature where the temperature sensitive property was used for increased mechanical properties following printing [38].

However, while pNIPAM is used widely in tissue engineering strategies, it often requires copolymerization or blending with other polymers, mainly natural polymers. This is due to certain disadvantages and challenges hindering its use within tissue engineering strategies. First major challenge is the large syneresis, or water release following phase transition and the accompanied precipitation of the polymer. Pure pNIPAM is known to release up to 85 % of its water content above the LCST [39], which affects both the cell viability and material properties, and prevents its application in strategies such as bioprinting. Furthermore, being a synthetic polymer, pNIPAM is not degradable, a property which is of extreme importance in tissue engineering strategies [40]. Additionally, the temperature-based gelation is reversible [41] and hence, not suitable for long term stability of the scaffolds, which prompts the need for further crosslinking of the printed constructs. Consequently, often copolymerization with other materials is required to induce the desired properties in the final material.

To address these challenges, several copolymerization strategies have been proposed. Copolymerizing pNIPAM with hyaluronic acid [26], gelatin [42], and alginate [43], which are capable of absorbing release water and preventing loss of water from the entire system, have been some of these approaches. However, copolymerization with cellulose [44] and methylcellulose [45] has been shown to be one of most effective approaches to control the syneresis of pNIPAM. Furthermore, this copolymerization results in development of biodegradable material

[45], and hence circumventing one of the important challenges in use of this material for tissue engineering and bioprinting applications. Still, for bioprinting, the material needs to be crosslinked permanently in order to be able to maintain its structure over long-term. For this purpose, photocrosslinking seems to be one of the most suitable options, due to the fast procedure and limited toxicity to cells [13]. However, for this, the material needs to possess photocrosslinkable side groups such as methacrylates. Methylcellulose includes a number of hydroxyl groups, capable of being used for introduction of photo reactive side groups [46].
Consequently, this chapter aims to develop a photocrosslinkable pNIPAM methylcellulose copolymer, capable of being used for bioprinting applications involving cell encapsulation at 37 °C, aimed at tissue engineering strategies of the dentoalveolar region.

5.2 Materials and Methods

5.2.1 Materials

N-isopropylacrylamide (NIPAM) (97% purity), methylcellulose (MC), ammonium persulfate (APS), tetramethylethyleendiamine (TEMED), methacrylic anhydride, lithium phenyl-2,4,6-trimethylbenzoylphosphintae (LAP) and deuterated dimethyl sulfoxide (DMSO-d_6) were purchased from Sigma Aldrich (Overijse, Belgium). Phosphate-buffered saline (PBS), Gibco minimum essential medium (MEM), and the Viability/Cytotoxicity Kit containing calcein AM and ethidium homodimer were purchased from ThermoFisher Scientific (Belgium).

5.2.2 Methods

5.2.2.1 Synthesis of pNIPAM-methylcellulose (MC-pNIPAM)

MC with a concentration of 3 %(w/v) was dissolved in 20 mL deionized water in a round bottom flask overnight and was purged with Argon. The solution was cooled down to below 10 °C. APS was dissolved in 2 mL deionized water with a concentration of 2 %(w/v) and was purged with argon. The APS solution was then added to the round bottom flask dropwise. NIPAM was dissolved separately in deionized water with ratios of 1:4, 1:1 and 1:4 with regards to MC.

NIPAM was then added to the reaction, followed by 200 µL of TEMED. The polymerization was carried out at temperatures below 10 °C for 3 hours under an Argon atmosphere to form the MC-pNIPAM copolymer. Next, the material was dialyzed against DI water for 5 days at room temperature, using dialysis membrane with 14 kDa molecular weight cutoff. The material was then freeze-dried (Christ Alpha 1-2 LD plus freeze drier) to obtain the final copolymer.

5.2.2.2 Methacrylation of MC-pNIPAM

Following synthesis of the copolymer, it was modified with methacrylic side groups. For this purpose, the freeze-dried MC-pNIPAM was dissolved in 20 mL phosphate buffer saline (PBS) with a 2 %(w/v) concentration. The pH was then adjusted to 9 by adding sodium hydroxide, and 200 %(w/w) methacrylic anhydride was added to the solution. During the methacrylation the pH was adjusted to 9 over 12 hours. The methacrylated MC-pNIPAM solution was dialyzed for 5 days against DI water with a 14 kDa molecular weight cutoff, with daily water change. Finally, the methacrylated MC-pNIPAM was freeze-dried to collect the methacrylated MC-pNIPAM.

5.2.2.3 Fourier Transform Infrared Spectroscopy (FTIR)

The FTIR-ATR spectra of the freeze-dried samples were recorded using an FTIR spectrometer (Vertex 70, Bruker, Massachusetts, USA) with a Diamond Attenuated Total Reflection (ATR) accessory, in the wavelength range of 400-4000 cm^{-1} with a resolution of 2 cm^{-1} and an average of 32 scans for each condition.

5.2.2.4 Proton Nuclear Magnetic Resonance (^{1}H NMR)

Structural characterization of the material was performed by obtaining ^{1}H-NMR spectra (Avance III HD-400 MHz, Bruker, Massachusetts, USA) using deuterated dimethyl sulfoxide (DMSO-d_6) as solvent, a 30° flip angle, a spectrometer frequency of 400 MHz and a spectral resolution of 0.15 Hz.

5.2.2.5 Evaluation of the LCST and critical gel formation concentration

To evaluate the LCST of the methacrylated MC-pNIPAM, the change in turbidity of the hydrogels was evaluated by first preparing a 20 mg/mL hydrogel of the copolymer in PBS and measuring the absorbance at a wavelength of 1000 nm using a spectrophotometer (Infinite 200 pro microplate reader, Tecan, Männedorf, Switzerland). The temperature of the hydrogels was increased from 30 ℃ to 40 ℃ in 1 ℃ increments, with a 20 minute wait time at each temperature to allow for stabilization.

To further evaluate the critical concentration at which increase in temperature results in gel formation rather than precipitation, different concentrations of methacrylated MC-pNIPAM in PBS were prepared, ranging from 40 mg/mL to 100 mg/mL, and 1 mL was transferred to an Eppendorf. The eppendorfs were then exposed to 37 ℃ environment, and gelation of the material was evaluated by a vial tilting method checking flow of the material visually.

5.2.2.6 Evaluation of water release

The water content of the hydrogels was evaluated through measurement of swelling at room temperature and 37 ℃, and the difference in two temperatures was considered as the amount of water release from the samples. To measure the swelling, hydrogels with a concentration of 100 mg copolymer in 1 mL of PBS were prepared for each of the samples including MC to pNIPAM ratios of 1:4, 1:1 and 4:1, mixed with 0.01 %(w/v) LAP, printed in the shape of grids of 1 cm by 1 cm with complete infill, crosslinked with UV for 1 minutes and freeze dried. The freeze-dried samples were weighed, and placed in PBS at 37 ℃ and room temperature. At different timepoints, including 1 h, 3 h, 6 h, 24 h, and 48 h, the samples were dried using a paper, weighed again, and the swelling was calculated following equation 5.1.

$$Swelling = \frac{W_{sw} - W_0}{W_0} \times 100 \qquad \text{Eqn. 5.1}$$

In the equation, W_0 is the initial weight, and W_{sw} is the weight at timepoint.

5.2.2.7 Hydrolytic degradation

To evaluate degradability of the materials, samples were prepared in the same manner as samples for the swelling measurement, freeze dried and weighed. The freeze-dried samples were then incubated in 5 mL DI water at 37 ℃ for 14 days. At different timepoint including 1, 3, 5, 7, and 14 days, samples were removed, freeze dried and weighed. The degradation at each timepoint was calculated using equation 5.2:

$$Degradation = \frac{W_0 - W}{W_0} \times 100 \qquad \text{Eqn. 5.2}$$

Were W_0 is the initial weight, and W is the weight at each timepoint.

5.2.2.8 Printability

To evaluate printability of the hydrogels at 37 ℃, methacrylated MC pNIPAM with MC to pNIPAM ratios of 1:4, 1:1 and 4:1 were dissolved in PBS at a concentration of 100 mg/mL. The hydrogels were then mixed with 0.01 %(w/v) LAP, moved to cartridge, and incubated at 37 ℃ for 10 min. Next, printability was evaluated on an extrusion bioprinter (3Ddiscovery, RegenHu, Villaz-Saint-Pierre, Switzerland), using a 400 µm heated nozzle. To analyze one-dimensional shape fidelity, lines of 3 cm were printed, the perimeter of the lines was then measured and compared to the theoretical value. Next, squares of 1 cm by 1 cm with an infill distance of 0.2 mm were printed to evaluate two-dimensional accuracy, and a circularity factor (Pr value) [47] was calculated, where a value of closer to 1 represents a more accurate print. Possibility of printing in 3D was evaluated by printing cubes of 1 cm by 1 cm with an infill distance of 2 mm, consisted of 10 layers.

5.2.2.9 Evaluation of cell viability

Possible cytotoxicity of the hydrogels was evaluated using dental pulp stem cells (DPSCs). For this purpose, DPSCs were cultured according to previously described protocol [48]. Hydrogels of MC:pNIPAM ratio 1:1 were prepared with a concentration of 100 mg/mL in PBS, and DPSCs with a concentration of 1 million/mL were encapsulated in the hydrogel at room temperature. The temperature was then increased to 37 ℃, and samples were crosslinked under UV for 1 min, before being immersed in α-MEM supplemented with 10 % FBS and 1 % antibiotics. Samples were placed in culture for 7 days, and at different

timepoints of 1, 3, and 7 days, Live/dead staining was performed using Calcein AM and Ethidium homodimer (Live/Dead viability cytotoxicity kit, Invitrogen, Thermofisher Scientific) according to manufacturer's protocol. Fluorescent imaging was performed (IX83 inverted microscope, Olympus scientific solutions, Tokyo, Japan) to assess viability of the encapsulated cells, and images were subjected to non-linear modifications removing the background signal.

5.2.2.10 Statistical analysis

All experiments in different sections were performed in triplicates. Analysis of Variance (ANOVA) followed by Tukey's post-hoc test were performed to assess differences using Graphpad Prism (version 8.0.0 for Windows, GraphPad Software, San Diego, California USA, www.graphpad.com).

5.3 Results

To synthesize the MC-pNIPAM, different constituents of the synthesis including methylcellulose, NIPAM and APS were dissolved in DI water and mixed until a homogeneous solution was obtained, and the temperature was decreased to below 10 ℃ to allow for formation of longer polymer chains. Next, TEMED was added to the system, resulting in a redox reaction with APS and providing free radicals initiating the free radical polymerization. Next, methacrylation of the copolymer took place at basic pH using methacrylic anhydride, resulting in substitution of remaining hydroxyl groups on methylcellulose with photoresponsive methacrylic groups. The synthesis procedure is schematically demonstrated in scheme 5.1.

5.3.1 Structural characterization

To evaluate the success of the copolymerization, FTIR and ^{1}H NMR characterizations were performed. The FTIR spectrum of methylcellulose, demonstrated in figure 5.1, shows peaks appearing at 1035 and 3450 cm^{-1}, corresponding to C-O stretching and vibration of hydroxyl groups, respectively. The spectrum for pNIPAM shows peaks appearing at 1543 and 1646 cm^{-1} which are attributed to N-H and C=O stretching. Furthermore, the copolymer demonstrates peaks

corresponding to groups present both on methylcellulose and on pNIPAM, demonstrating presence of both materials in the copolymer.

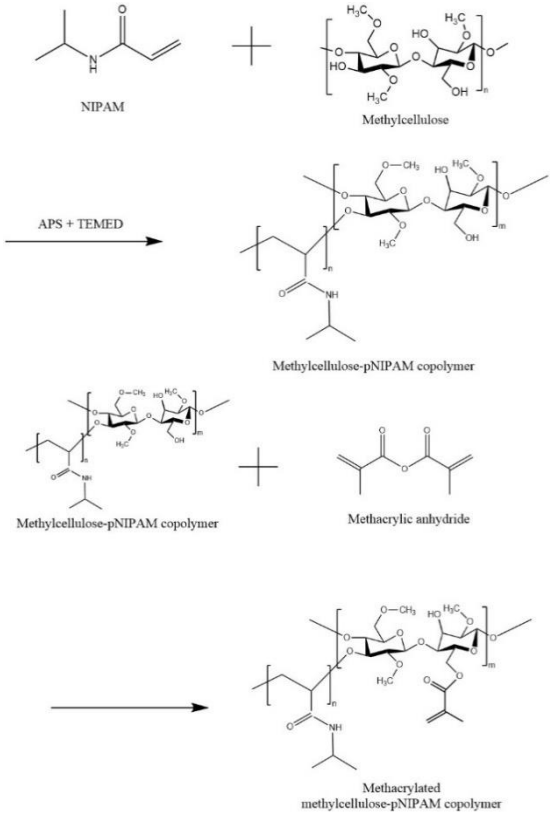

Scheme 5.1. Schematic representation of the reaction of methylcellulose and pNIPAM, along with modification with methacrylic anhydride (scheme made using chemdraw software)

To further analyze the chemical structure, ^{1}H NMR was performed on the samples. As demonstrated in figure 5.2, the methylcellulose spectrum represents peaks at 3.27 and 3.47 ppm corresponding to hydroxyl groups of methylcellulose. These peaks are also present on the spectrum corresponding to MC-pNIPAM, while the area under the peaks is reduced by approximately 40 %. The spectrum of methacrylated MC-pNIPAM represents a further 35.36 % decrease in the area under the peaks of the hydroxyl groups, and demonstrates the

peak at 1.85 ppm corresponding to methyl group of methacrylate, confirming modification with methacrylic anhydride.

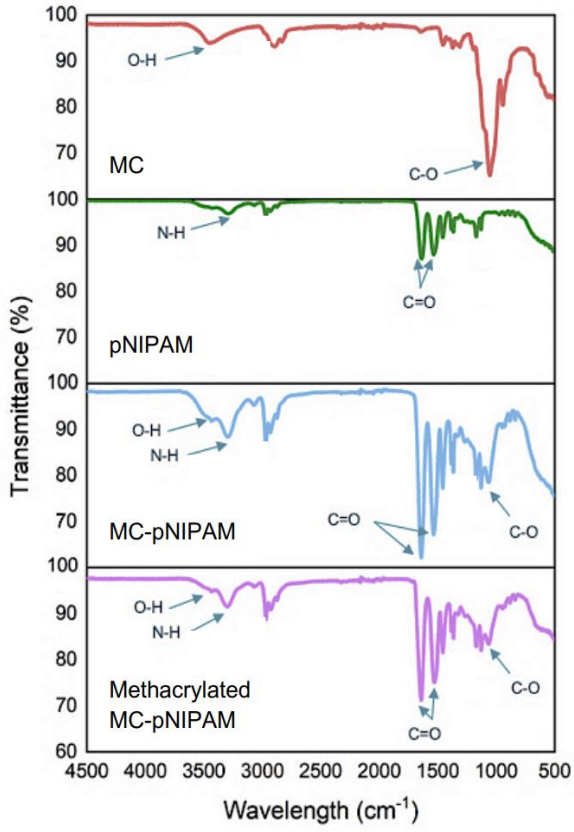

Figure 5.1. FTIR spectra of methylcellulose, pNIPAM, MC-pNIPAM copolymer, and methacrylated MC-pNIPAM

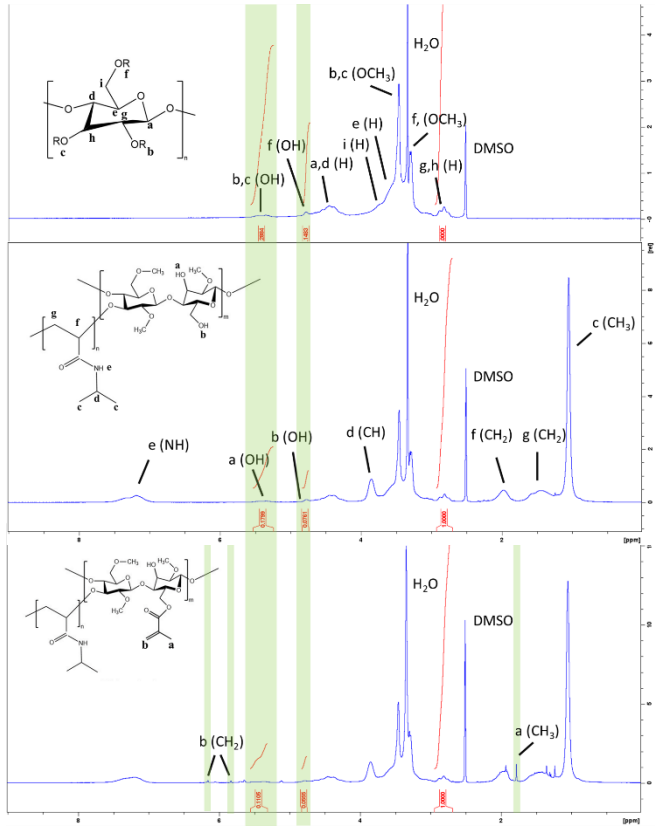

Figure 5.2. ^{1}H NMR of methylcellulose, MC-pNIPAM and methacrylated MC-pNIPAM in DMSO

5.3.2 Evaluation of the LCST and gel formation

To evaluate the LCST of the copolymer, turbidity of a low concentration of the copolymer synthesized with different ratios of MC:pNIPAM was evaluated at a range of temperatures. As demonstrated in figure 5.3, for high concentration of pNIPAM, the turbidity is relatively constant up to 33 °C, followed by a sharp increase up to 35 °C, after which it again reaches a plateau. However, the higher methylcellulose concentration results in stability of the turbidity up to a temperature of approximately 35 °C, while the sharp increase takes place at 36 °C. Consequently, the range of temperature sensitivity for

this material can be considered to be 33 ℃ to 36 ℃ depending on the copolymer ratio.

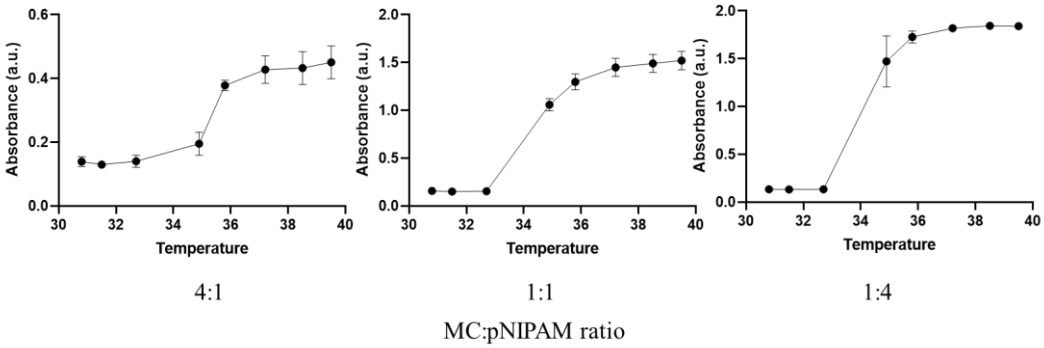

Figure 5.3. Measurement of turbidity of the methacrylated MC-pNIPAM solution (n=3)

Following this, possibility of thermal gelation of the material at 37 ℃ was evaluated by vial tilting method. As demonstrated in figure 5.4, higher NIPAM concentrations will lead to gelation at lower concentrations, as the samples synthesized with an MC to NIPAM ratio of 1:4 formed a gel at a concentration of 60 mg/mL. However, copolymers synthesized with all three ratios of NIPAM to MC demonstrated gelation at concentrations higher than 80 mg/mL.

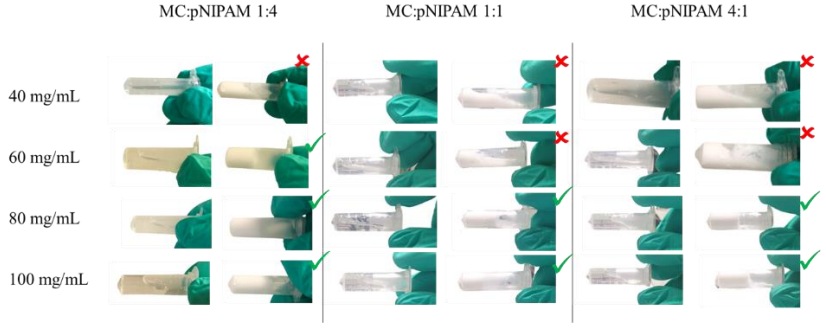

Figure 5.4 . Demonstration of thermal gelation of the methacrylated MC-pNIPAM copolymer through vial tilting

5.3.3 Evaluation of water release

Considering the water release from pNIPAM based materials, and its possible negative consequences in applications such as bioprinting, the water release was evaluated by measuring swelling at room temperature and 37 °C. As shown in figure 5.5, there is a significant difference in the rate of swelling between room temperature and 37 °C in samples consisting of an MC:NIPAM ratio of 1:4 ($p \leq 0.0001$), with the swelling being in the range of 1000 % at room temperature and below 400 % at 37 °C. This difference is not significant for samples synthesized with MC:pNIPAM ratios of 4:1 and 1:1, with the swelling being in the range of 800 % for both room temperature and 37 °C.

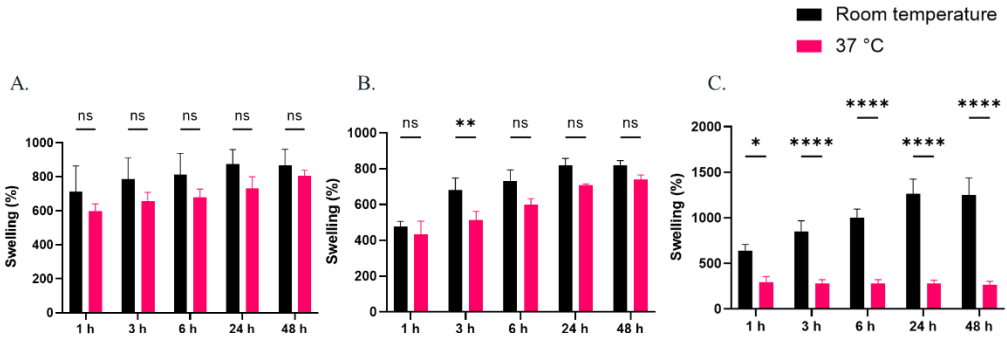

Figure 5.5. Swelling rates of A. MC:pNIPAM 4:1, B. MC:pNIPAM 1:1 and C. MC:pNIPAM 1:4 in PBS

5.3.4 Evaluation of hydrolytic degradation

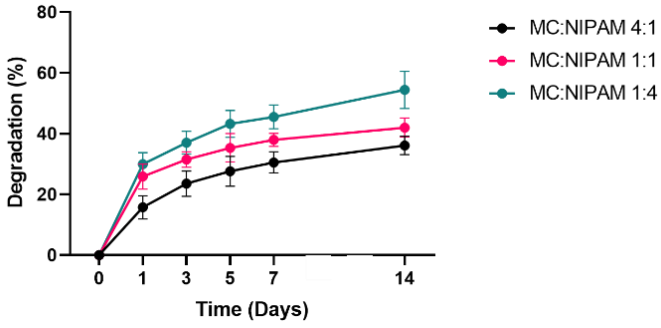

Figure 5.6. Hydrolytic degradation of methacrylated MC-pNIPAM

To evaluate degradability of the designed material, the rate of its hydrolytic degradation following printing and crosslinking was evaluated and is presented in figure 5.6. all three ratios of MC:NIPAM resulted in degradable polymers, with degradability being largest in the first days of *in vitro* evaluation. However, after two weeks, the degradation rate of samples consisting of a MC:NIPAM ratio of 1:4 is significantly larger than other samples ($p \leq 0.001$), whereas the difference among MC:NIPAM ratios of 1:1 and 4:1 is not significant. Furthermore, the degradation seems to be slower in samples consisting of a 4:1 MC to NIPAM ratio, as the degradation of this sample is significantly less than other samples in day 1 ($p \leq 0.05$).

5.3.5 Printability

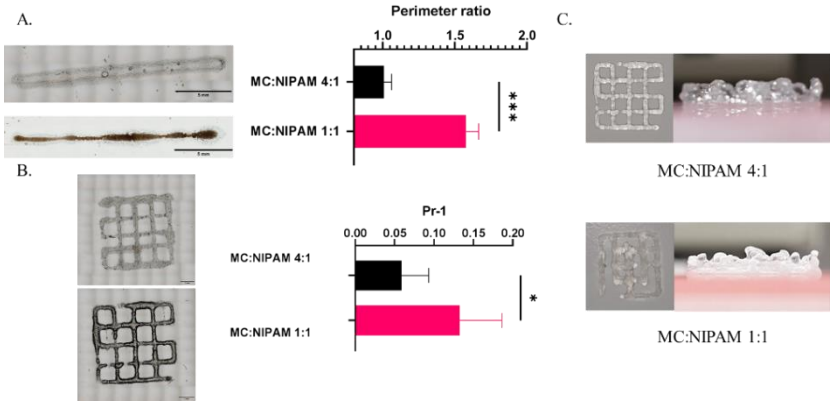

Figure 5.7. A) Evaluation of perimeter ratio as a measure of strand fidelity, B) measurement of circularity factor as a measure of two-dimensional accuracy and C) printability in 3D

To evaluate possibility of utilizing the synthesized hydrogels as bioinks, a printability test was performed by printing lines, squares and 3D constructs. These printability tests demonstrated MC:NIPAM ratio of 1:4 as not printable at 37 °C. Among the two remaining formulations, the formulation with a MC:NIPAM ratio of 4:1 resulted in more accurate prints. This is demonstrated in figure 5.7, where in section A, measurement of the accuracy of the printed lines compared to the theoretical design show a clear difference between the two

formulations ($p \leq 0.001$). this is also represented in figure 5.7.B, where the circularity factor is evaluated, in which values closer to one represent a more accurate print, where the difference of the two samples is still significant ($p \leq 0.05$). furthermore, both concentrations demonstrated capability of printing in 3D, as demonstrated in figure 5.7.C, where cubes of 10 layers were printed.

5.3.6 Evaluation of hydrogel toxicity

Considering the application of this material as bioink, biocompatibility of the material is of extreme importance. Consequently, the possibility of encapsulating cells in the proposed bioink was evaluated and viability of the cells was assessed by live/dead assay. As shown in figure 5.8, dental pulp stem cells encapsulated in methacrylated MC-pNIPAM with MC:pNIPAM ratio of 1:1 demonstrated a satisfactory viability, represented by the larger number of cells stained green compared to those stained red, after one week of encapsulation. Furthermore, the cells show an extended morphology exhibiting adhesion of the cells to the synthesized material.

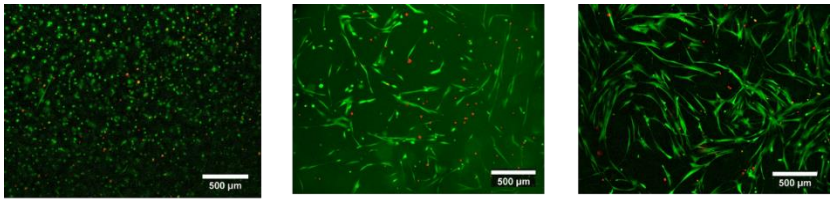

Figure 5.8. Dental pulp stem cells encapsulated in methacrylated MC-pNIPAM with a MC:pNIPAM ratio of 1:1.

5.4 Discussion

In this chapter, a copolymer of MC-pNIPAM was synthesized for use in bioprinting strategies aimed at tissue engineering of the dentoalveolar region. For this purpose, the copolymer was synthesized through a free radical polymerization at temperatures of below the LCST of pNIPAM. This results in formation of copolymer chains capable of forming macrogels upon rise of temperature to above the LCST [49]. As demonstrated in scheme 5.1, the synthesis starts by decomposition of APS through reaction with TEMED [50], providing

free radicals which attack the hydroxyl groups present on methylcellulose. These secondary radicals will then react with NIPAM to form the copolymer [51]. The synthesized copolymer was then modified with methacrylate side groups through reaction with methacrylic anhydride at pH 9 to induce photoactivity [52].

Following the synthesis, FTIR analysis demonstrated presence of peaks attributed to functional groups of both methylcellulose and pNIPAM on the copolymer, confirming presence of both groups in the copolymer. To further confirm formation of a copolymer rather than an interpenetrating network, ^{1}H NMR was performed. Following the synthesis procedure, it was hypothesized that both pNIPAM side chains and methacrylate groups react with hydroxyl groups on methylcellulose backbone. This was confirmed through a reduction in the area under the OH peaks of methylcellulose [53,54] after each step of the synthesis, as demonstrated in figure 5.2. Taken together, these characterizations confirmed formation of a methacrylated MC-pNIPAM copolymer through the proposed reaction.

Next, the LCST of the synthesized copolymer was measured through turbidity measurement. Pure pNIPAM is known to have an LCST of approximately 32 ℃ [55]. However, the critical temperature is known to be affected by environment of pNIPAM chains, including presence of hydrophilic side groups. Consequently, copolymers of pNIPAM are known to have different LCST values as the copolymerization can affect structure of the hydration of the monomers [56]. In this study, it was determined that copolymerization with methylcellulose increases the LCST by 2-3 ℃, and a higher methylcellulose content results in a higher LCST. Considering the LCST value for all copolymer ratios is still lower than the physiological temperature of 37 ℃, the resulting material would still be suitable for application of bioprinting at 37 ℃, as the material would supposedly have the gel form at this temperature. However, while phase transition of pNIPAM chains takes place at the LCST, formation of gels requires concentrations above a certain critical concentration. Below such concentration, high mobility of polymer chains caused by low entanglement of these chains results in formation or precipitates rather than gels as the water can easily exit the polymer structure [57]. While this is one of the limiting factors in application of pNIPAM based copolymers, due to the usually high

critical concentrations of 15 to 20 %(w/v) [58], the MC-pNIPAM copolymer synthesized demonstrated gelation at concentrations above 8 %(w/v) in all formulations, resulting in suitability of the synthesized material for applications such as bioprinting.

Furthermore, one of the challenges faced in application of pNIPAM based polymers in the biomedical field is the large syneresis, reported to be as high as 85 % for pure pNIPAM [59]. This was evaluated by comparing the swelling at room temperature and 37 °C. While the compositions including an MC to NIPAM ratio of 1:4 resulted in a very significant difference in swelling between the two temperatures, the formulations including a higher ratio of the relatively hydrophilic MC resulted in no significant difference in swelling among the two, suggesting these concentrations to be more suitable for tissue engineering applications. In addition to this, another property critical for tissue engineering applications is the degradability of the materials. While pNIPAM itself is known to be non-degradable [60], copolymerization is suggested to be a suitable method for development of degradable pNIPAM based materials [40]. This was further confirmed in this study by achieving degradation rates of up to 50 % depending on the formulation after two weeks. However, it was observed that MC:NIPAM ratio of 1:4 resulted in highest degradation, significantly larger from other formulations. This could be attributed to the crosslinking mechanism. Considering modification of methylcellulose hydroxyl groups with methacrylic groups, it could be concluded that a lower methylcellulose content results in lower degree of crosslinking, and hence, a higher rate of degradation. This behavior is also observed in other studies involving chemical crosslinking of methylcellulose, where lower rates of crosslinking result in high degradation rates [61].

In addition to these tests, the synthesized methacrylated MC-pNIPAM was tested for possibility of printing to assess suitability for 3D bioprinting. As demonstrated in figure 5.7, only formulations with a MC:NIPAM ratio of 4:1 and 1:1 were printable. Lack of printability in the 1:4 ratio could be attributed to the significant syneresis at temperatures above its LCST, where the applied pressure through the printing process results in expulsion of water from hydrogel network and precipitation of the polymer, preventing the hydrogel from being

printed. However, among the two formulations capable of being used for bioprinting, 4:1 resulted in more accurate prints at 37 °C, suggesting a higher methylcellulose content to be beneficial to the printability. In addition to this, capability of the synthesized material to support viability of encapsulated DPSCs was evaluated through live dead assay. For this purpose, the 1:1 MC:NIPAM ratio was selected and used to evaluate viability over 1 week *in vitro*. While the cells demonstrated a high viability in all timepoints, as observable by the larger number of green cells compared to red ones, at day 1 the cells showed a round morphology, while over 3 and 7 days they started to show the stretched morphology characteristic of the DPSCs. This could be caused by the process of cell adhesion governed by pNIPAM properties above the LCST. At temperatures higher than this critical temperature, pNIPAM is known to absorb proteins required for cell adhesion and trap such proteins within its chains, resulting in cell attachment [62]. Still, further analysis including DNA quantification, and metabolic activity assays are required to support these findings.

5.5 Conclusion

In this chapter, a free radical polymerization at low temperature was used to synthesize methylcellulose pNIPAM copolymer, followed by functionalization with methacrylate groups resulting in a thermoresponsive, photocrosslinkable copolymer. It was demonstrated that the material is capable of forming a physical gel at physiological temperatures, and except for formulation with a high pNIPAM content, other formulations could be used in printing process. Furthermore, it was demonstrated that the proposed material is biodegradable, and capable of supporting viability of dental pulp stem cells. While further experiments are required to support these findings, presented results suggest the developed material to be suitable as a bioink aimed at tissue engineering of the dentoalveolar tissue through bioprinting at 37 °C.

5.6 References

1. Khodakaram-Tafti A, Mehrabani D, Shaterzadeh-Yazdi H, Zamiri B, Omidi M. “Tissue Engineering in Maxillary Bone Defects”. World J Plast Surg. 2018 Jan;7(1):3–11.
2. Shaddox LM, Walker CB. “Treating chronic periodontitis: current status, challenges, and future directions.”. Clin Cosmet Investig Dent. 2010;2:79–91.

3. Hanif A, Qureshi S, Sheikh Z, Rashid H. “Complications in implant dentistry”. Eur J Dent. 2017;11(1):135–40.
4. Na S, Zhang H, Huang F, Wang W, Ding Y, Li D, Jin Y. “Regeneration of dental pulp/dentine complex with a three-dimensional and scaffold-free stem-cell sheet-derived pellet.”. J Tissue Eng Regen Med. 2016 Mar;10(3):261–70.
5. Cordeiro MM, Dong Z, Kaneko T, Zhang Z, Miyazawa M, Shi S, Smith AJ, Nör JE. “Dental pulp tissue engineering with stem cells from exfoliated deciduous teeth.”. J Endod. 2008 Aug;34(8):962–9.
6. Moroni L, Boland T, Burdick JA, De Maria C, Derby B, Forgacs G, Groll J, Li Q, Malda J, Mironov VA, Mota C, Nakamura M, Shu W, Takeuchi S, Woodfield TBF, Xu T, Yoo JJ, Vozzi G. “Biofabrication: A Guide to Technology and Terminology”. Trends Biotechnol. 2018 Apr 1;36(4):384–402.
7. Amoli M, EzEldeen M, Jacobs R, Bloemen V, Salar Amoli M, EzEldeen M, Jacobs R, Bloemen V. “Materials for Dentoalveolar Bioprinting: Current State of the Art”. Biomed . 2022 Dec 30;10(1):71.
8. Mandrycky C, Wang Z, Kim K, Kim DH. “3D bioprinting for engineering complex tissues”. Biotechnol Adv. 2016;34(4):422–34.
9. Murphy S V, Atala A. “3D bioprinting of tissues and organs.”. Nat Biotechnol. 2014 Aug;32(8):773–85.
10. Liu X, Gaihre B, George MN, Miller AL 2nd, Xu H, Waletzki BE, Lu L. “3D bioprinting of oligo(poly[ethylene glycol] fumarate) for bone and nerve tissue engineering.”. J Biomed Mater Res A. 2020 May;
11. Bruchet M, Melman A. “Fabrication of patterned calcium cross-linked alginate hydrogel films and coatings through reductive cation exchange”. Carbohydr Polym. 2015;131:57–64.
12. Dubbin K, Hori Y, Lewis KK, Heilshorn SC. “Dual-Stage Crosslinking of a Gel-Phase Bioink Improves Cell Viability and Homogeneity for 3D Bioprinting”. Adv Healthc Mater. 2016 Oct 1;5(19):2488–92.
13. GhavamiNejad A, Ashammakhi N, Wu XY, Khademhosseini A. “Crosslinking Strategies for 3D Bioprinting of Polymeric Hydrogels.”. Small. 2020 Sep;16(35):e2002931.
14. Ding H, Illsley NP, Chang RC. “3D Bioprinted GelMA Based Models for the Study of Trophoblast Cell Invasion”. Sci Rep. 2019;9(1):18854.
15. Aldana AA, Valente F, Dilley R, Doyle B. “Development of 3D bioprinted GelMA-alginate hydrogels with tunable mechanical properties”. Bioprinting. 2021;21:e00105.
16. Guo L, Colby RH, Lusignan CP, Howe AM. “Physical Gelation of Gelatin Studied with Rheo-Optics”. Macromolecules. 2003 Dec 1;36(26):10009–20.
17. Willing RP, Leopold AC. “Cellular expansion at low temperature as a cause of membrane lesions.”. Plant Physiol. 1983 Jan;71(1):118–21.
18. Shiozaki A, Yamazato Y, Kosuga T, Kudou M, Shoda K, Arita T, Konishi H, Komatsu S, Kubota T, Fujiwara H, Okamoto K, Marunaka Y, Otsuji E. “Effect of low temperature on the regulation of cell volume after hypotonic shock in gastric cancer cells.”. Int J Oncol. 2019 Oct;55(4):905–14.
19. Narayanan LK, Huebner P, Fisher MB, Spang JT, Starly B, Shirwaiker RA. “3D-Bioprinting of Polylactic Acid (PLA) Nanofiber–Alginate Hydrogel Bioink Containing Human Adipose-Derived Stem Cells”. ACS Biomater Sci Eng. 2016 Oct 10;2(10):1732–42.
20. Hafeez S, Ooi HW, Morgan FLC, Mota C, Dettin M, Van Blitterswijk C, Moroni L, Baker MB. “Viscoelastic Oxidized Alginates with Reversible

Imine Type Crosslinks: Self-Healing, Injectable, and Bioprintable Hydrogels". Vol. 4, Gels. 2018.
21. López-Marcial GR, Zeng AY, Osuna C, Dennis J, García JM, O'Connell GD. "Agarose-Based Hydrogels as Suitable Bioprinting Materials for Tissue Engineering". ACS Biomater Sci Eng. 2018 Oct 8;4(10):3610–6.
22. Lee JM, Suen SKQ, Ng WL, Ma WC, Yeong WY. "Bioprinting of Collagen: Considerations, Potentials, and Applications". Macromol Biosci. 2021 Jan 1;21(1):2000280.
23. Sarker B, Rompf J, Silva R, Lang N, Detsch R, Kaschta J, Fabry B, Boccaccini AR. "Alginate-based hydrogels with improved adhesive properties for cell encapsulation". Int J Biol Macromol. 2015;78:72–8.
24. Cambria E, Brunner S, Heusser S, Fisch P, Hitzl W, Ferguson SJ, Wuertz-Kozak K. "Cell-Laden Agarose-Collagen Composite Hydrogels for Mechanotransduction Studies " [Internet]. Vol. 8, Frontiers in Bioengineering and Biotechnology . 2020.
25. Antoine EE, Vlachos PP, Rylander MN. "Review of collagen I hydrogels for bioengineered tissue microenvironments: characterization of mechanics, structure, and transport.". Tissue Eng Part B Rev. 2014 Dec;20(6):683–96.
26. Atoufi Z, Kamrava SK, Davachi SM, Hassanabadi M, Saeedi Garakani S, Alizadeh R, Farhadi M, Tavakol S, Bagher Z, Hashemi Motlagh G. "Injectable PNIPAM/Hyaluronic acid hydrogels containing multipurpose modified particles for cartilage tissue engineering: Synthesis, characterization, drug release and cell culture study". Int J Biol Macromol. 2019;139:1168–81.
27. Cao M, Wang Y, Hu X, Gong H, Li R, Cox H, Zhang J, Waigh TA, Xu H, Lu JR. "Reversible Thermoresponsive Peptide–PNIPAM Hydrogels for Controlled Drug Delivery". Biomacromolecules. 2019 Sep 9;20(9):3601–10.
28. Kim H, Witt H, Oswald TA, Tarantola M. "Adhesion of Epithelial Cells to PNIPAm Treated Surfaces for Temperature-Controlled Cell-Sheet Harvesting". ACS Appl Mater Interfaces. 2020 Jul 29;12(30):33516–29.
29. Jain K, Vedarajan R, Watanabe M, Ishikiriyama M, Matsumi N. "Tunable LCST behavior of poly(N-isopropylacrylamide/ionic liquid) copolymers". Polym Chem. 2015;6(38):6819–25.
30. Tavagnacco L, Zaccarelli E, Chiessi E. "Molecular description of the coil-to-globule transition of Poly(N-isopropylacrylamide) in water/ethanol mixture at low alcohol concentration". J Mol Liq. 2020;297:111928.
31. Podewitz M, Wang Y, Quoika PK, Loeffler JR, Schauperl M, Liedl KR. "Coil–Globule Transition Thermodynamics of Poly(N-isopropylacrylamide)". J Phys Chem B. 2019 Oct 17;123(41):8838–47.
32. Ribeiro CA, Martins MVS, Bressiani AH, Bressiani JC, Leyva ME, de Queiroz AAA. "Electrochemical preparation and characterization of PNIPAM-Hap scaffolds for bone tissue engineering". Mater Sci Eng C. 2017;81:156–66.
33. Dosh RH, Jordan-Mahy N, Sammon C, Le Maitre CL. "Use of l-pNIPAM hydrogel as a 3D-scaffold for intestinal crypts and stem cell tissue engineering.". Biomater Sci. 2019 Sep;7(10):4310–24.
34. Ohya S, Nakayama Y, Matsuda T. "Thermoresponsive Artificial Extracellular Matrix for Tissue Engineering: Hyaluronic Acid Bioconjugated with Poly(N-isopropylacrylamide) Grafts". Biomacromolecules. 2001 Sep 1;2(3):856–63.
35. Naito H, Takewa Y, Mizuno T, Ohya S, Nakayama Y, Tatsumi E, Kitamura S, Takano H, Taniguchi S, Taenaka Y. "Three-Dimensional Cardiac Tissue

Engineering Using a Thermoresponsive Artificial Extracellular Matrix". ASAIO J. 2004;50(4).
36. Navara AM, Kim YS, Xu Y, Crafton CL, Diba M, Guo JL, Mikos AG. "A dual-gelling poly(N-isopropylacrylamide)-based ink and thermoreversible poloxamer support bath for high-resolution bioprinting". Bioact Mater. 2022;14:302–12.
37. Montero FE, Rezende RA, da Silva JVL, Sabino MA. "Development of a Smart Bioink for Bioprinting Applications " [Internet]. Vol. 5, Frontiers in Mechanical Engineering . 2019.
38. Kesti M, Müller M, Becher J, Schnabelrauch M, D'Este M, Eglin D, Zenobi-Wong M. "A versatile bioink for three-dimensional printing of cellular scaffolds based on thermally and photo-triggered tandem gelation". Acta Biomater. 2015;11:162–72.
39. Strachota B, Strachota A, Šlouf M, Brus J, Cimrová V. "Monolithic intercalated PNIPAm/starch hydrogels with very fast and extensive one-way volume and swelling responses to temperature and pH: prospective actuators and drug release systems". Soft Matter. 2019;15(4):752–69.
40. Patenaude M, Hoare T. "Injectable, Degradable Thermoresponsive Poly(N-isopropylacrylamide) Hydrogels". ACS Macro Lett. 2012 Mar 20;1(3):409–13.
41. Lima LH, Morales Y, Cabral T. "Poly-N-isopropylacrylamide (pNIPAM): a reversible bioadhesive for sclerotomy closure". Int J Retin Vitr. 2016;2(1):23.
42. Ohya S, Kidoaki S, Matsuda T. "Poly(N-isopropylacrylamide) (PNIPAM)-grafted gelatin hydrogel surfaces: interrelationship between microscopic structure and mechanical property of surface regions and cell adhesiveness". Biomaterials. 2005;26(16):3105–11.
43. Teodorescu M, Andrei M, Turturică G, Stănescu PO, Zaharia A, Sârbu A. "Novel Thermoreversible Injectable Hydrogel Formulations Based on Sodium Alginate and Poly(N-Isopropylacrylamide)". Int J Polym Mater Polym Biomater. 2015 Nov 22;64(15):763–71.
44. Zeng K, Doberenz F, Lu YT, Nong JP, Fischer S, Groth T, Zhang K. "Synthesis of Thermoresponsive PNIPAM-Grafted Cellulose Sulfates for Bioactive Multilayers via Layer-by-Layer Technique". ACS Appl Mater Interfaces. 2022 Oct 20;
45. Liu W, Zhang B, Lu WW, Li X, Zhu D, De Yao K, Wang Q, Zhao C, Wang C. "A rapid temperature-responsive sol–gel reversible poly(N-isopropylacrylamide)-g-methylcellulose copolymer hydrogel". Biomaterials. 2004;25(15):3005–12.
46. Stalling SS, Akintoye SO, Nicoll SB. "Development of photocrosslinked methylcellulose hydrogels for soft tissue reconstruction.". Acta Biomater. 2009 Jul;5(6):1911–8.
47. Ouyang L, Yao R, Zhao Y, Sun W. "Effect of bioink properties on printability and cell viability for 3D bioplotting of embryonic stem cells". Biofabrication. 2016 Sep;8(3):035020.
48. Hilkens P, Gervois P, Fanton Y, Vanormelingen J, Martens W, Struys T, Politis C, Lambrichts I, Bronckaers A. "Effect of isolation methodology on stem cell properties and multilineage differentiation potential of human dental pulp stem cells.". Cell Tissue Res. 2013 Jul;353(1):65–78.
49. Mitchell HT, Schultz SA, Costanzo PJ, Martinez AW. "Poly(N-isopropylacrylamide) Hydrogels for Storage and Delivery of Reagents to Paper-Based Analytical Devices". Vol. 2, Chromatography. 2015. P. 436–51.

50. Shirangi M, Sastre Toraño J, Sellergren B, Hennink WE, Somsen GW, van Nostrum CF. “Methyleneation of Peptides by N,N,N,N-Tetramethylethylenediamine (TEMED) under Conditions Used for Free Radical Polymerization: A Mechanistic Study”. Bioconjug Chem. 2015 Jan 21;26(1):90–100.
51. Zubik K, Singhsa P, Wang Y, Manuspiya H, Narain R. “Thermo-Responsive Poly(N-Isopropylacrylamide)-Cellulose Nanocrystals Hybrid Hydrogels for Wound Dressing”. Vol. 9, Polymers . 2017.
52. Gold GT, Varma DM, Taub PJ, Nicoll SB. “Development of crosslinked methylcellulose hydrogels for soft tissue augmentation using an ammonium persulfate-ascorbic acid redox system”. Carbohydr Polym. 2015;134:497–507.
53. Nasatto PL, Pignon F, Silveira JLM, Duarte MER, Noseda MD, Rinaudo M. “Methylcellulose, a Cellulose Derivative with Original Physical Properties and Extended Applications”. Vol. 7, Polymers. 2015. P. 777–803.
54. Sekiguchi Y, Sawatari C, Kondo T. “A facile method of determination for distribution of the substituent in O-methylcelluloses using 1H-NMR spectroscopy”. Polym Bull. 2002;47(6):547–54.
55. Burdukova E, Li H, Bradshaw DJ, Franks G V. “Poly (N-isopropylacrylamide) (PNIPAM) as a flotation collector: Effect of temperature and molecular weight”. Miner Eng. 2010;23(11):921–7.
56. de Oliveira TE, Mukherji D, Kremer K, Netz PA. “Effects of stereochemistry and copolymerization on the LCST of PNIPAm”. J Chem Phys. 2017 Jan 20;146(3):34904.
57. Lü S, Liu M, Ni B. “Degradable, injectable poly(N-isopropylacrylamide)-based hydrogels with low gelation concentrations for protein delivery application”. Chem Eng J. 2011;173(1):241–50.
58. Pollock JF, Healy KE. “Mechanical and swelling characterization of poly(N-isopropyl acrylamide -co- methoxy poly(ethylene glycol) methacrylate) sol–gels”. Acta Biomater. 2010;6(4):1307–18.
59. Aday AN, Matar MG, Osio-Norgaard J, Srubar W V. “Thermo-Responsive Poly(N-isopropylacrylamide) (PNIPAM) Hydrogel Particles Improve Workability Loss and Autogenous Shrinkage in Cement Paste”. CEMENT. 2022;100049.
60. Cui Z, Lee BH, Pauken C, Vernon BL. “Degradation, cytotoxicity, and biocompatibility of NIPAAm-based thermosensitive, injectable, and bioresorbable polymer hydrogels.”. J Biomed Mater Res A. 2011 Aug;98(2):159–66.
61. Rimdusit S, Jingjid S, Damrongsakkul S, Tiptipakorn S, Takeichi T. “Biodegradability and property characterizations of Methyl Cellulose: Effect of nanocompositing and chemical crosslinking”. Carbohydr Polym. 2008;72(3):444–55.
62. Xue C, Choi BC, Choi S, Braun P V, Leckband DE. “Protein Adsorption Modes Determine Reversible Cell Attachment on Poly(N-isopropyl acrylamide) Brushes”. Adv Funct Mater. 2012 Jun 6;22(11):2394–401.

Chapter 6. Development and characterization of colloidal pNIPAM-based microgels for drug delivery in dentoalveolar tissue engineering strategies

Mehdi Salar Amoli [a,b,c], Huimin Yang [a], Resmi Anand [a,d], Mostafa EzEldeen [b,e], Merve Kubra Aktan [c], Annabel Braem [c], Reinhilde Jacobs [b,f] , Veerle Bloemen [a,c,d]

[a] Surface and Interface Engineered Materials (SIEM), Campus Group T, KU Leuven, Andreas Vesaliusstraat 13, 3000 Leuven, Belgium;

[b] OMFS IMPATH Research Group, Department of Imaging and Pathology, Faculty of Medicine, KU Leuven and Oral and Maxillofacial Surgery, University Hospitals Leuven, Kapucijnenvoer 33, 3000 Leuven, Belgium;

[c] Biomaterials and Tissue Engineering Research Group, Department of Materials Engineering (MTM), KU Leuven, Kasteelpark Arenberg 44 – box 2450, B-3001, Leuven, Belgium

[d] Prometheus, Division of Skeletal Tissue Engineering Leuven, KU Leuven , Leuven, Belgium

[e] Department of Oral Health Sciences, KU Leuven and Paediatric Dentistry and Special Dental Care, University Hospitals Leuven, Kapucijnenvoer 33, 3000 Leuven, Belgium

[f] Department of Dental Medicine, Karolinska Institutet, SE-171 77 Stockholm, Sweden

Manuscript in preparation

Chapter summary

Incorporation of growth factors, signalling molecules and drugs can be vital for the success of tissue engineering strategies, such as bioprinting. This has resulted in the development of a variety of drug release systems for use in such strategies. Hence, this chapter aims to develop pNIPAM-methylcellulose microgels with different synthesis parameters based on a 2^3 full factorial design of experiments, for delivery of drugs and factors in tissue engineering strategies. Microgel properties, including volume phase transition temperature (VPTT), hydrodynamic size, drug loading and release, and their cytocompatibility on dental pulp stromal/stem cells (DPSCs) were systematically evaluated. The results demonstrated successful copolymerization and development of the microgels, a hydrodynamic size ranging from 200 to 400 μm, and VPTT in the range of 34-39 °C. Furthermore, loading of genipin, capable of inducing odontoblastic differentiation of DPCs, and its sustained release over a week was shown in all formulations. These results can serve as a solid basis for development of drug-delivering pNIPAM-methylcellulose microgels for tissue engineering applications in the dentoalveolar region.

6.1 Introduction

Success of tissue engineering strategies relies on control over the behavior of stem cells used within such approaches, along with acceleration of tissue regeneration in the implant area, and control of undesirable biological processes such as the inflammatory response of the body [1]. These requirements are much more pronounced in tissue engineering of complex regions such as the dentoalveolar region [2], where a range of different tissues including enamel, dentin, pulp, vascular tissue, nervous tissue, gingiva, periodontal ligament, and alveolar bone [3,4], each impose specific biological requirements [4,5]. Growth factors, signalling molecules, and a variety of drugs have been known to impact the behavior of stem cells, such as proliferation or differentiation, hence making them an integral part of tissue engineering strategies [6,7]. However, such molecules often suffer from a short half-life in the physiological environment, introducing a challenge in maintaining the required dosage of these factors without facing negative side effects of over-dosage, such as uncontrolled tissue formation, inflammation, or carcinogenicity [8–10]. To address this, a range of drug delivery approaches have been developed to be incorporated in tissue engineering strategies [11].

A considerable effort in these drug delivery approaches has focused on prolonging the timespan of the drug release, to increase the availability of the drug or biological factor over the tissue regeneration process. Some of these methods include the incorporation of drugs within porous scaffold architectures [12–14], or the use of polymeric networks, such as hydrogels, as delivery vehicles due to their superior ability to encapsulate drugs and to release them based on network degradation or diffusion [15]. Furthermore, microspheres based on these polymeric networks, originated from natural polymers such as alginate [16], chitosan [17], etc, or synthetic polymers, such as PLGA [18] , have been developed as drug delivery systems and used within tissue engineering approaches [18]. However, these approaches are faced with specific challenges affecting their usefulness in tissue engineering strategies. Physical incorporation of drugs in scaffolds and hydrogels suffers from the need for specific design of biomaterials potentially affecting other properties, in addition to an inability to

incorporate multiple growth factors/drugs in the same tissue engineering scaffold. Furthermore, covalent bonding of such molecules to the scaffolds might potentially affect their potency [1,19]. Additionally, the microparticles currently used for drug delivery in the tissue engineering strategies also have disadvantages. PLGA based microparticles release acidic biproducts upon degradation, which might affect the tissue regeneration process, and with natural polymers such as alginate or chitosan there is a lack of control over macromolecular properties which could translate to undesired release rates [20]. As a result, development of a suitable system for drug delivery in tissue engineering is still an active area of research.

Among the drug delivery approaches not yet applied extensively to tissue engineering, the use of poly N-isopropylacrylamide (pNIPAM) based microgels is one of the most widely investigated strategies [21–23]. This is firstly due to the thermosensitive behavior of pNIPAM, demonstrating a volume phase transition temperature (VPTT), above which the microgels de-swell and release a portion of the solvent in their network, making them suitable for a stimuli responsive drug release [24,25]. Additionally, the presence of a polymeric network enables the encapsulation of drugs and their release based on diffusion, suggesting the possibility of a sustained release from them [26].

However, the large water release above the VPTT, a VPTT of around 32 °C, and non-degradability of pNIPAM microgels present challenges against their use in tissue engineering. Consequently, while a range of approaches have been suggested for adjustment of the properties of pNIPAM based microgels, development of pNIPAM based materials designed specifically for sustained release of the drugs within tissue engineering is still a challenge. Among such approaches to control the properties of pNIPAM based microparticles, one of the main strategies is copolymerization with other polymers [27–29]. The range of the effects observed through copolymerization, demonstrate the ability of this approach to induce properties required in tissue engineering, such as degradability of the polymer network, or a sustained release of drugs from the microgels.

To obtain these properties, a range of different materials could be used to be copolymerized with pNIPAM. Among them, natural polymers seem to be more suitable for incorporation in tissue engineering

strategies, as the combination of synthetic and natural polymers will allow the control over properties granted by the synthetic component, as well as degradability and cell friendliness through the presence of the natural component. Copolymerizing pNIPAM with polyaminoacids, has been among such approaches [30]. However, copolymerizing with materials based on methyl cellulose, such as carboxymethylcellulose, has been one of the most effective ways of modifying pNIPAM properties, leading to an increased VPTT, degradability of the material, and biocompatibility of the material [31]. Still, this approach has only been applied to macroscopic gels and not microgels. One reason for this lack of investigation could be the difficulty in microgel synthesis, resulting from the LCST behavior of methyl cellulose, hindering synthesis at temperatures of above 40- 45 °C.

In addition, pNIPAM based microgels have been known to be capable of loading and release of a range of drugs and biomolecules, such as, insulin-like growth factor (IGF-1) [32], vascular endothelial growth factor (VEGF) [33], etc. Similar molecules and growth factors have been suggested for use in the tissue engineering of dentoalveolar region, including dexamethasone [34], simvastatin [35] or bone morphogenetic proteins [36]. Among these, genipin, a natural based molecule believed to induce differentiation of dental pulp cells (DPCs) to odontoblasts [37] seems an interesting choice due to its resemblance of a wide range of small molecules and its effect on DPSCs.

Consequently, it was hypothesized in this study that copolymerization of pNIPAM and methylcellulose could potentially result in development of novel microgels, suitable for delivery of drugs and growth factors in dentoalveolar tissue engineering strategies, which could be capable of sustained drug release over several days. Following this, this study determines the effect of different synthesis parameters on properties of the pNIPAM based microgels, by using a factorial design of experiments, analyzing the effect of key parameters including co-monomer ratio, crosslinking degree and the presence of surfactants on final properties.

6.2 Materials and Methods

6.2.1 Materials

N-isopropylacrylamide (NIPAM) (97 % purity), methylcellulose, methylene-bis-acrylamide, sodium Dodecyl Sulfate (SDS), and glycine were obtained from Sigma-Aldrich (Belgium). Genipin was obtained from Challenge Bioproducts Co., Ltd (Taiwan). Sodium chloride and phosphate buffered saline (PBS) tablets were obtained from VWR (Belgium). Calcein AM, ethidium homodimer, sterile PBS, Gibco minimum essential alpha medium, Gibco antibiotic-antimycotic, and Biowest fetal bovine serum (FBS) were obtained from ThermoFisher Scientific (Belgium).

6.2.2 Methods

6.2.2.1 Synthesis of microgels

Methylcellulose was dissolved in deionized water in a round bottom flask overnight, with a concentration of 2.5 mg/mL and a volume of 100 mL. The solution was then purged with Argon and the temperature was increased to 45 °C under Argon atmosphere. According to table 6.1, different amounts of NIPAM were dissolved in 3 mL deionized water and added to methylcellulose dropwise. Different concentrations of methylene bis acrylamide (MBA) following table 6.1, were dissolved in 1 mL deionized water and added to the round bottom flask dropwise. Next, 100 mg ammonium persulfate (APS) was added to the reaction chamber as the radical initiator. To activate the initiator and start the reaction, 50 µL tetramethylethylenediamine (TEMED) was added to the mixture. Depending on the microgel formulation, appropriate amount of sodium dodecyl sulfate (SDS) according to table 6.1 was added to the reaction as the emulsifier. The reaction was allowed to continue for 3h under Argon atmosphere before being exposed to air to stop the reaction. Samples were then dialyzed against DI water using dialysis tubing with a 14 kDa molecular cutoff for 5 days at room temperature, and lyophilized (Alpha 1-2 LD plus, Martin Christ Freeze Dryers, Osterode, Germany) to obtain the microgels. To evaluate the effect of different synthesis parameters on the properties of the microgels, a full factorial design of experiments, consisting of 3

factors and 2 levels for each, was used to synthesize the microgels. The evaluated factors include ratio of monomers, concentration of crosslinker and the presence of surfactant in the synthesis. Details of the full factorial design are presented in Table 6.1.

Table 6.1. Composition of different microgel formulations.

Label	Ratio of NIPAM : methylcellulose	MBA (mol%)	SDS (mM)
L-2.5	2:1	2.5	0
H-2.5	5:1	2.5	0
L-10	2:1	10.0	0
H-10	5:1	10.0	0
L-2.5-S	2:1	2.5	2
H-2.5-S	5:1	2.5	2
L-10-S	2:1	10.0	2
H-10-S	5:1	10.0	2

6.2.2.2 Structural characterization

The fourier transform infrared spectroscopy (FTIR) spectra of the freeze dried microgels were recorded using an spectrometer (Vertex 70, Bruker, Massachusetts, USA) with the attenuated total reflection (ATR) accessory, in the wavelength range of 600-4000 cm^{-1}. The analysis was performed with a resolution of 2 cm^{-1} and an average of 32 scans for each condition.

The structure of the synthesized microgels was further analyzed by obtaining proton nuclear magnetic resonance (^{1}H NMR) spectra (Avance III HD-400 MHz, Bruker, Massachusetts, USA) using D_2O as the solvent, a 30° flip angle, a spectrometer frequency of 400 MHz and a spectral resolution of 0.15 Hz.

6.2.2.3 Evaluation of volume phase transition temperature (VPTT)

To measure the VPTT of the microgels, a concentration of 10 mg/mL lyophilized microgel was re-suspended in either DI water or PBS. The

turbidity of the microgel suspensions was evaluated by measuring the absorbance at 1000 nm wavelength (Infinite 200 pro microplate reader, Tecan, Männedorf, Switzerland). The temperature of the suspensions was increased from 30 °C to 40 °C in 1 °C increments, and a 30 min wait time to allow for temperature stabilization. The temperature at which an increase in turbidity could be observed, was considered as the range of the VPTT.

6.2.2.4 Evaluation of microgel size in PBS

The hydrodynamic size distribution of various microgel particles in PBS was analyzed by dynamic light scattering (DLS) (Litesizer™ 500, Anton Paar GmbH, Austria) using a semiconductor laser at a wavelength of 658 nm and a maximum power of 40 mW. Immediately prior to the measurements, microgel suspensions were prepared at a concentration of 1 mg/mL in PBS and a sample volume of 1 ml was placed in a polystyrene cuvette and measured at 37 °C. The preferred measurement angle was automatically selected by the instrument and the refractive index PBS was set same as water, at 1.33.

6.2.2.5 Evaluation of drug loading in the microgels

To evaluate the efficiency of drug loading onto the developed microgels, genipin was used as a model drug and a “breathing-in” method was used to load the drugs onto the microgels [38]. For this purpose, a stock solution of 44 mM genipin in PBS was prepared. Freeze dried microgels were suspended in drug stock solution at a concentration of 30 mg/mL and were stirred mildly for 24 h at 37 °C to be fully swollen with the drug solution. Next, the drug loaded microgels were centrifuged at 356160 g (Optima TL ultracentrifuge and rotor TLA-120.2, Beckman Coulter life sciences, California, USA) at 37 °C. The supernatant was removed and reacted with glycine producing the hallmark blue color of genipin. Using a calibration curve of the glycine-genipin reaction, the absorbance was measured by spectrophotometry (Infinite 200 pro microplate reader, Tecan, Männedorf, Switzerland) at 578 nm to calculate the amount of genipin in the supernatant of the microgel solution. By measuring the remaining genipin in the supernatant, the amount encapsulated in the microgels was calculated. Control samples consisted of genipin

solution without microgels, and loading experiments for all formulations were performed in three independent replicates.

6.2.2.6 Evaluation of drug release from the microgels

To evaluate the rate of drug release from the microgels, first, loading of genipin onto the microgels was performed as described. Next, drug loaded microgels were suspended in PBS, and kept on a shaker at 37 °C in a closed tube. At each timepoint, the microgel suspensions were centrifuged at 356160 g (Optima TL ultracentrifuge and rotor TLA-120.2, Beckman Coulter life sciences, California, USA) at 37 °C. 20 µL of the supernatant was taken for reaction with glycine, where the concentration of genipin in supernatant was determined by measuring absorbance at 578 nm and correlated with a calibration curve of genipin/glycine reaction. The remaining microgels were re-suspended in the supernatant and left on the shaker until the next timepoint.

6.2.2.7 Evaluation of microgel toxicity

Subculturing of dental pulp stem cells (DPSCs) was performed using the protocol described by Hilkens et al. [39]. A cell monolayer of $5x10^3$ cells/cm^2 hDPSCs (passage 9) was seeded in each well of a 48 well plate (Corning costar). Different lyophilized microgel formulations were prepared, and suspended in α-MEM, supplemented with 10 %(w/v) FBS and 1 %(w/v) antibiotics with a concentration of 5 mg/mL. The microgel suspensions were added on the cell monolayer, and cells were cultured for one week with medium change on every two days using medium containing microgels, and medium alone for control groups. Possible cytotoxicity of the microgels was evaluated at day 1, 3 and 7 by live/dead staining (Live/Dead viability cytotoxicity kit, Invitrogen, Thermofisher Scientific, Brussels, Belgium) according to the manufacturer's protocol, and fluorescent microscopy was performed (IX83 inverted microscope, Olympus scientific solutions, Tokyo, Japan). Control samples consisted of cell monolayers cultured in α-MEM, supplemented with 10 %(v/v) FBS and 1 %(v/v) antibiotics and without the addition of microgels in the culture. At least 3 separate wells were exposed to each microgel formulation for this test, and microscopy images were subjected to non-linear adjustments to remove background signal.

6.2.2.8 DNA quantification

Monolayers of DPSCs were cultured in 48 well plates similar to the samples for the live/dead assay and were cultured in the presence of microgels similarly. To evaluate the possible cytotoxicity quantitatively, DNA quantification was performed on cultured DPSCs. At 1, 3, and 7 days, the microgel suspension was removed, and 350 µL commercial RLT lysis buffer (Qiagen, Hilden, Germany) plus 1 %(v/v) B-mercapto-ethanol was added to the cell monolayer to prepare the lysate. Quant-iTTM dsDNA HS reagent was diluted in Quant-iTTM dsDNA HS buffer (Quant-iT dsDNA Assay Kit, Thermofisher Scientific, Belgium) with a 1:200 ratio. 5 µL of the lysate was mixed with 195 µL of the working solution. Standards were prepared following the manufacturers protocol. Next, samples were transferred to Qubit tubes and readings were performed using Qubit fluorometer. Three separate samples were prepared for each microgel formulation and three readings were performed for each sample.

6.2.2.9 Statistical analysis

All experiments were performed in three independent replicates (n=3), ANOVA followed by amultiple comparisons test were performed using GraphPad Prism (version 8.0.0 for Windows, GraphPad Software, San Diego, California USA, www.graphpad.com) to compare differences in different sections. Corrections on multiple comparisons were performed using Tukey's correction method and false discovery rate through the method of Benjamini, Krieger and Yekutieli. Factorial analysis and calculation of effect estimates was performed using JMP software (JMP®, Version <16>. SAS Institute Inc., Cary, NC, 1989–2021).

6.3 Results

To synthesize the crosslinked pNIPAM-methylcellulose microgels, with all different constituents being soluble in water, they were dissolved in DI water and mixed, resulting in a homogeneous solution. After combining the monomers, crosslinker, initiator and surfactant in DI water, the temperature was increased to 45 °C, which is higher than the LCST of pNIPAM, (~ 32 – 33 °C) [40]. Next, TEMED was added

to the reaction chamber which resulted in a redox initiator system, providing the radicals required for initiation of the polymerization reaction. This was shown by the fact that after 30 minutes following the addition of TEMED, the transparent solution turned into a milky opaque color, signalling chain growth and formation of the microgels. The synthesis procedure is represented in scheme 6.1.

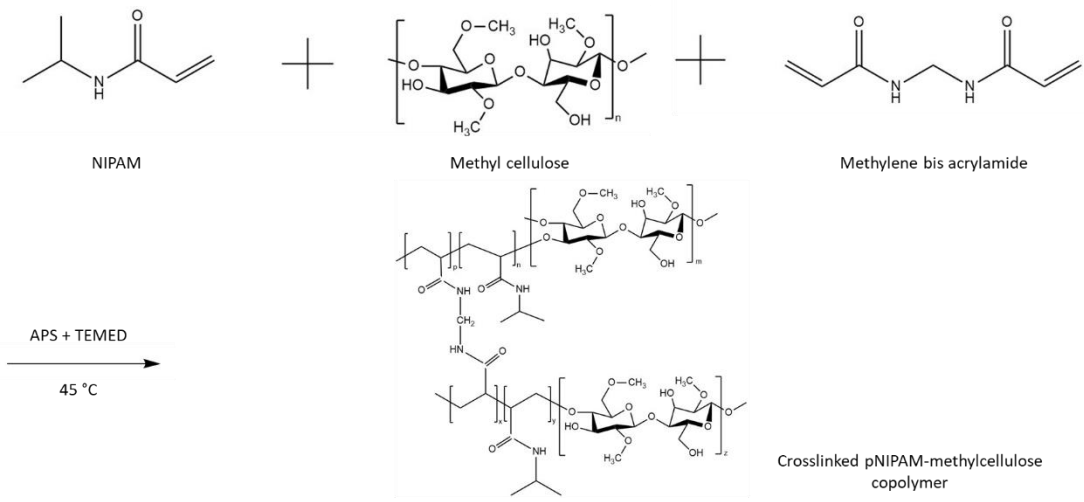

Scheme 6.1. Schematic representation of the reaction of NIPAM and methylcellulose, and synthesis of pNIPAM-methylcellulose copolymer *(scheme made using chemdraw software)*

6.3.1 Structural characterization

To characterize the synthesized copolymer, FTIR spectra of the samples were recorded, along with those of pNIPAM and methylcellulose alone, as demonstrated in figure 6.1.A. The FTIR spectrum of methylcellulose represents peaks at 941, 1046, and 3445 cm^{-1} corresponding to methyl groups, C-O stretching, and the vibration of hydroxyl group, respectively [41]. On the pNIPAM spectra, the peaks appearing at 1543 and 1646 cm^{-1} are attributed to the N-H bending and C=O stretching of pNIPAM. Taken together, the presence of the characteristic peaks of both pNIPAM and methylcellulose on the

spectra recorded from the microgels confirms success of the copolymerization [42,43].

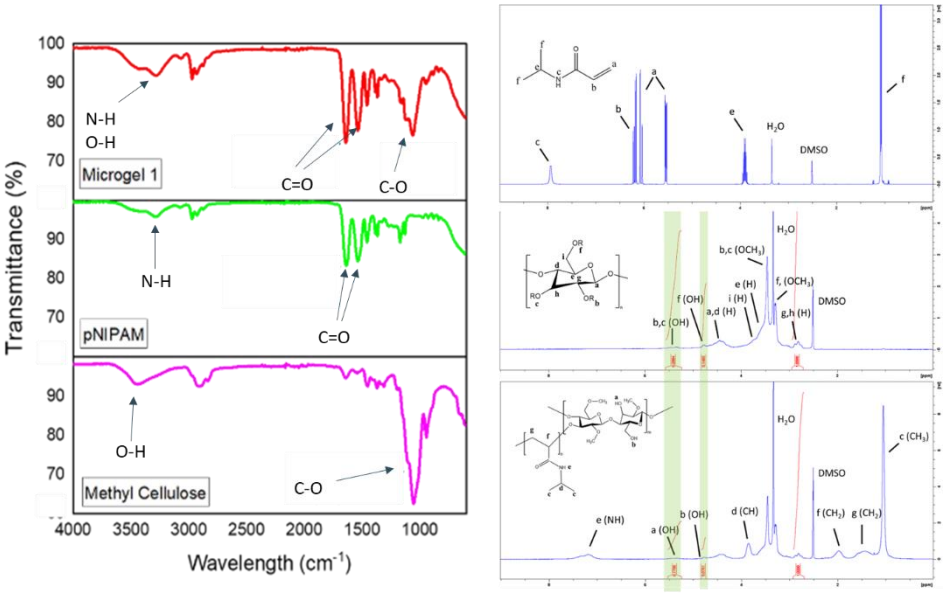

Figure 6.1. Structural characterization A. FTIR spectra and B. 1H NMR spectra of methylcellulose, pNIPAM and the microgels

To further confirm the grafting, ^{1}H NMR spectra of the samples was recorded, as shown in figure 6.1.B. The peaks appearing at 3.27 and 3.47 ppm correspond to methyl peaks of the methylcellulose, and the peaks at 4.78 and 5.48 correspond to the hydroxyl groups of methylcellulose. On the pNIPAM spectrum the peaks appearing at 1.07 ppm, 3.90 ppm and 7.93 ppm correspond to methyl groups of NIPAM, isopropyl groups of NIPAM, and the amide group, respectively [44,45]. These peaks were present both in the microgel spectrum and the pNIPAM spectrum. The reduction in the area under the peaks corresponding to methylcellulose hydroxyl, demonstrates successful grafting and a substitution degree of approximately 50.6 %. The presence of these peaks confirms copolymerization of pNIPAM and methylcellulose in microgel formulations [43]. Furthermore, the spectra do not show the peaks corresponding to the double bonds of monomer NIPAM, present at 5.55 ppm and 6.14 ppm, further ensuring the polymerization [46].

6.3.2 Evaluation of volume phase transition temperature (VPTT)

As described in table 6.1. The VPTT of the microgels was evaluated in DI water and PBS to analyze their thermosensitive behavior in each medium. As demonstrated in figure 6.2.A , the VPTT in water is higher than 39 °C for different microgel samples, while suspension of the microgels in PBS reduces this temperature to a range of 35 to 41°C, as can be seen in figure 6.2.B. This shift in VPTT resulting from the change in ionic strength of the medium is widely reported in studies on pNIPAM thermal behavior [47].

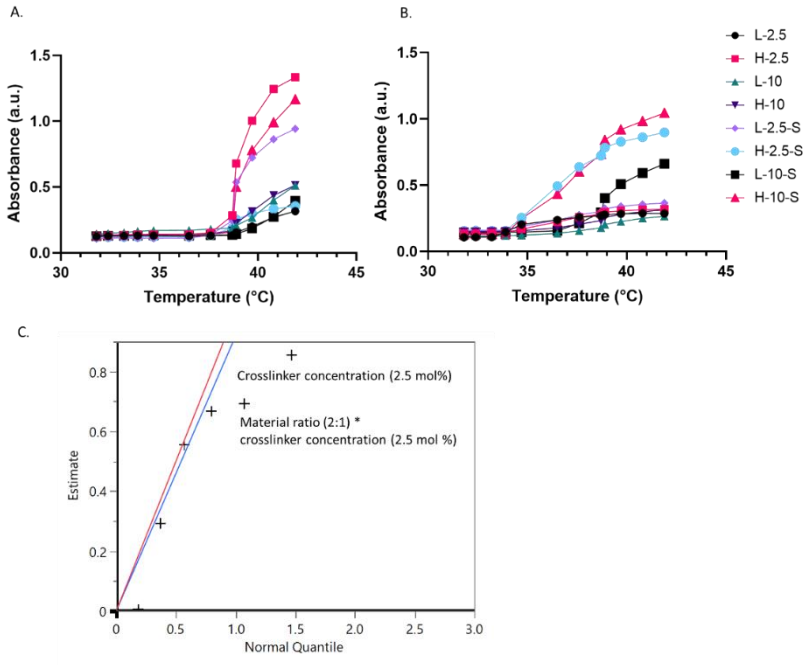

Figure 6.2. A. VPTT of the microgels in DI water, B. VPTT of the microgels in PBS, and C. Half normal probability plot of the magnitude of different effects on VPTT, the red line has a slope of 1 and the blue light has a slope equal to Lenth's PSE

As presented in figure 6.2.A and figure 6.2.B, the temperature-based phase transition takes place over a range of temperatures. In this study, it was determined that the VPTT for the entire range of the synthesized

microgels was close to the physiological temperature, which is higher than the pure pNIPAM VPTT of ~32 °C [48]. Furthermore, as presented in figure 6.2.C. among the different parameters evaluated through the factorial design of experiments, it was determined that an increased amount of crosslinker had the largest effect on increasing VPTT, followed by an interaction of the material ratio and the crosslinker concentration. While this shows the general trend of the VPTT with regards to different parameters, among the range of parameters chosen in this study, no effect had a p-value lower than 0.05.

6.3.3 Evaluation of microgel size

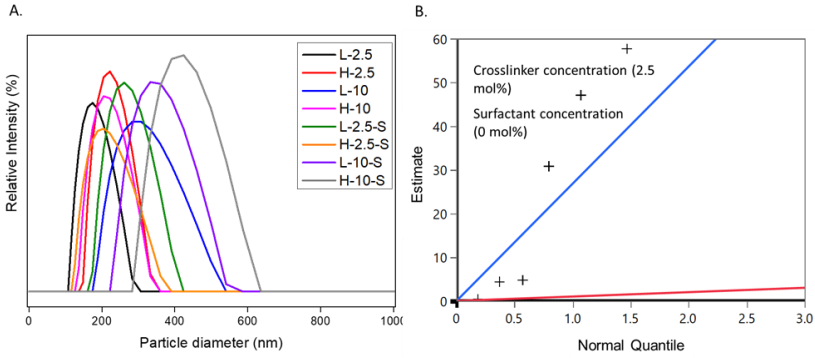

Figure 6.3. A. Size distribution of various microgel formulations suspended in PBS at 37 °C and B. Half normal probability plot of the effect estimates determining parameters with highest impact on microgel size, the red line has a slope of 1 and the blue light has a slope equal to Lenth's PSE

The hydrodynamic size of the microgels in PBS at 37 °C was evaluated through DLS, and the size distribution for various microgel formulations is demonstrated in figure 6.3.A. As can be observed, the Z-average hydrodynamic diameter of the microgels ranges from 187 nm to 479 nm, depending on the synthesis parameters mentioned in table 6.1. Furthermore, all microgel formulations except for H-2.5-S, synthesized with 5:1 NIPAM to methylcellulose ratio, 2.5 mol % crosslinker and in presence of SDS, had a polydispersity index (PDI) of less than 7 %, defined as the typical value for monodisperse samples

[49], and the H-2.5-S had a PDI of ~13 %, which is generally accepted for practical applications [50].

6.3.4 Evaluation of drug loading in the microgels

Genipin, a compound obtained from natural sources and known for its potential to induce odontoblastic differentiation in DPCs [37] was used as a model drug to evaluate the capacity of the synthesized microgels with different formulations to encapsulate drugs. The loading of genipin onto different formulations of the microgels is presented in figure 6.4.A.

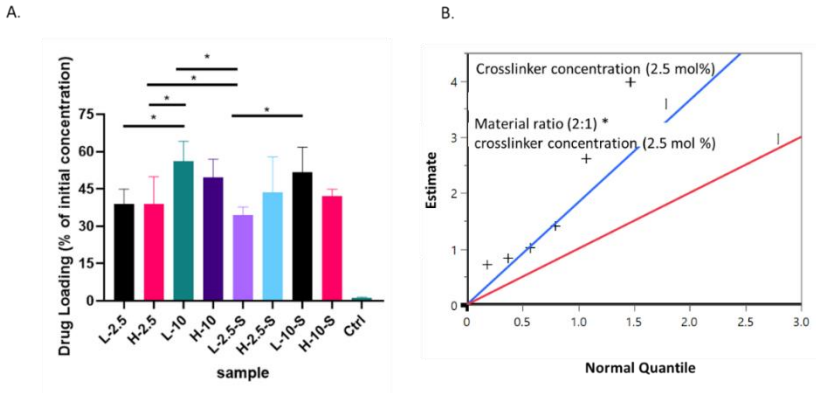

Figure 6.4. A. Loading of genipin onto different microgel formulations, n=3 B. Half-normal probability plot of the effect of different parameters on drug loading, the red line has a slope of 1 and the blue light has a slope equal to Lenth's PSE

It is demonstrated in figure 6.4.A, that the main significant differences in drug loading among different microgel formulations are between the microgels synthesized with a high amount of crosslinker and those synthesized with low amount of crosslinker, suggesting the increased crosslinker as contributing to a higher loading degree. However, other parameters, including the presence of surfactant in the synthesis and the ratio of the monomers did not have a meaningful impact on the loading capacity of the microgels, as there are no significant differences among the loading data for these microgels. These conclusions were confirmed by a factorial analysis shown in figure 6.4.B and table 6.2, demonstrating the low crosslinker concentration to

have a significantly negative impact on loading of genipin in the microgel networks.

*Table 6.2. Analysis of the effect of different parameters on the loading capacity of the studied microgels. The most significant effect estimate is marked by *.*

Parameter	Effect estimate	p-value
Material ratio (2.1)	1.67	0.6464
Crosslinker concentration (2.5 mol%)	-7.97*	0.0396
Surfactant concentration (0 mM)	2.83	0.4403
Material ratio (2:1) * crosslinker concentration (2.5 mol%)	-5.24	0.1615
Material ratio (2:1) * surfactant concentration (0 mM)	1.44	0.6915
Crosslinker concentration (2.5 mol%) * surfactant concentration (0 mM)	-2.04	0.5749

6.3.5 Evaluation of drug release from the microgels

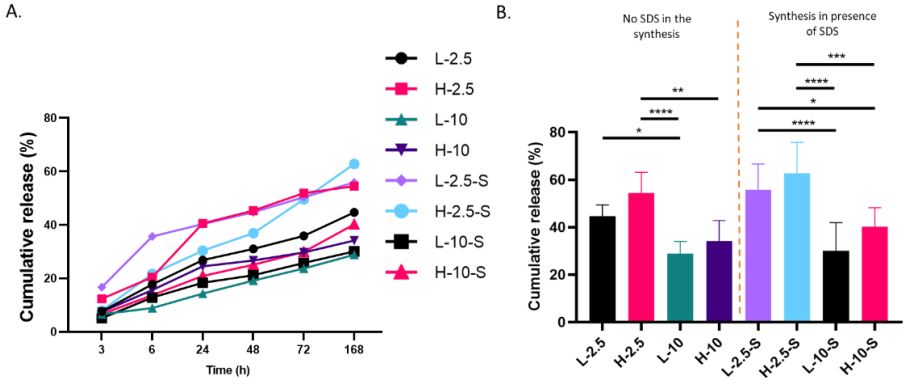

Figure 6.5. Release of genipin from different microgel formulations into PBS at 37 °C A) cumulative release over time and B) comparison of release from different microgel formulations after 7 days

Drug release from the microgels was evaluated in PBS at 37 °C. As demonstrated in figure 6.5.A, the rate of genipin release from the microgels is higher in the first 24 h, with the rate decreasing over time for all microgel samples. However, the rate of release from different

microgel formulations is vastly different. As shown in figure 6.5.B, the microgels with higher crosslinker content generally have a slower rate of drug release, with microgels L-10-S and H-10-S having a much lower release after 7 days compared to microgels L-2.5-S and H-2.5-S (p-value < 0.01), and microgels L-10 and H-10 having a significantly lower release after 7 days compared to formulations L-2.5 and H-2.5 (p-value < 0.05).

6.3.6 Evaluation of microgel toxicity

As different microgel formulations in this study are designed to be used in tissue engineering strategies, evaluation of their cytotoxicity is of paramount importance. For this purpose, a qualitative evaluation of microgel toxicity was performed using a live/dead assay after exposing dental pulp stromal/stem cells (DPSCs) to the microgels. Figure 6.6 demonstrates the live/dead staining of microgels after 7 days of culture. Living cells are visualized in green, whereas dying cells are visualized in red. In general, it can be observed that after 7 days of culture, the majority of the cells were viable in all conditions. However, the amount of cells present in the cultures with microgels is smaller compared to the amount observed in the control samples where no microgels were present.

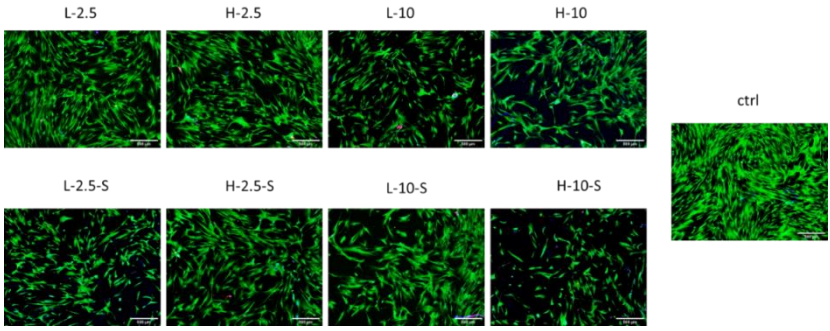

Figure 6.6. Viability of cells cultured for 7 days in presence of different microgel formulations, green color represent live cells, red color represent dead cells. Scale bar 500 μm.

6.3.7 DNA quantification

To further investigate the effect of exposure to microgels in DPSCs in a quantitative manner, a DNA quantification was performed on cells cultured in the presence of different microgel formulations. The results, presented in figure 6.7, confirm the qualitative analysis of live dead staining. While there is no difference among the control sample and the microgels in days 1 and 3 following the culture, after 7 days, the control represents higher values, with the most significant difference being with the microgel formulations synthesized in presence of SDS (p-value < 0.0001).

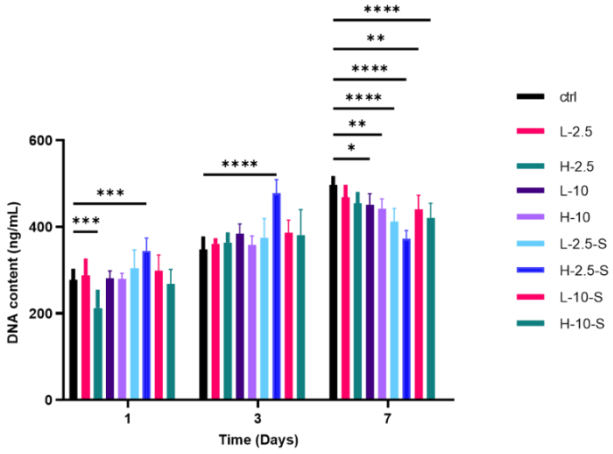

Figure 6.7. DNA content of cells cultured for 7 days in presence of different microgel formulations (n=3)

6.4 Discussion

In this chapter, microgels of pNIPAM-methylcellulose copolymer were synthesized for the first time using a free radical precipitation polymerization of pNIPAM, in the presence of methylcellulose, methylene bis acrylamide (MBA), and ammonium persulfate (APS) as initiator. Usually, the temperature required for the synthesis of pNIPAM based microgels is above 60 °C to decompose the persulfate initiating the reaction [51]. However, this is not possible for a pNIPAM methylcellulose microgel, because methylcellulose demonstrates phase separation at higher temperatures (with a lower critical solution

temperature (LCST) in the range of 50 to 60 °C [52]). Consequently, an APS/TEMED system was used to enhance radical availability for initiation of the polymerization reaction. Reaction of TEMED and APS results in formation of bisulfate radicals [53], which will then attack the hydroxyl groups on methylcellulose, resulting In formation of alkoxy radicals, which will react with NIPAM resulting in copolymerization [54], as demonstrated in scheme 6.1. In addition to being effective, the strategy to use TEMED/APS initiation system has been proposed as a method of developing uniform pNIPAM microgels [55]. Furthermore, the synthesis temperature close to the VPTT of the microgels is known to prevent entanglements of the pNIPAM chains, which enhances degradability of the designed microgels.

To evaluate the effect of different synthesis formulations on the final properties of the microgels, a factorial design of experiments was used resulting in 8 microgel formulations. First, the VPTT of the microgels was analyzed. It is well known that the thermal behavior of pNIPAM is due to the transition of random coil to globule conformation [56], where below the VPTT, the amide groups on the side chain are exposed to water, and the surrounding water preserves the structure by creating hydrogen bonds. However, with increasing temperature and rise of entropy of water molecules surrounding isopropyl groups, the molecule collapses to reduce the exposed surface, breaking hydrogen bonds, and leading to water release [57,58]. This phenomenon is measured by turbidimetry, as the release of water molecules leads to formation of a colloidal turbid state. It is known that copolymerization of pNIPAM with other polymers can affect the VPTT to a large extent as the presence of a copolymer can alter the hydrogen bonds surrounding the polymer chains. For instance, incorporation of cellulose nanocrystals in pNIPAM has resulted in a VPTT in the range of 36 – 39 °C [54].

As shown in figure 6.2, It was determined that the VPTT of the microgels synthesized in this study is in the same range as the physiological temperature. This would make these microgels suitable for tissue engineering applications, as they only partially release their water content, while they would maintain a tightly held network structure at physiological temperatures, capable of encapsulating drugs. Additionally, this means there is a balance in the exposure of the hydrophobic and hydrophilic groups on the polymer, resulting in

suitability of these microgels for both hydrophobic and hydrophilic types of drugs [59].

Furthermore, hydrodynamic size of the synthesized microgels was analyzed. In general, the size range of the particles is similar to the size of other pNIPAM based copolymers in PBS, which is lower than their size in water due to a reduction in electrostatic repulsion among polymer chains [60]. However, the general trend of reduction in polymer size upon incorporation of surfactants in the synthesis, usually observed in pNIPAM based microgels [61], was not observed. It is known that increased hydrophobicity leads to stabilization of precursor particles at lower chain lengths in early stages of the synthesis, resulting in an increase in number of such precursors and therefore, smaller size of the resulting microgels [62]. One explanation for the observed behavior could be that the incorporation of comparatively hydrophilic methylcellulose disrupts this stabilization, resulting in more similarity among the samples synthesized with or without SDS. Furthermore, the VPTT results demonstrate that at 37 °C, microgels synthesized in the presence of SDS still contain a large portion of their water content, where the most significant syneresis takes place above this temperature. For microgels synthesized without SDS, this is not the case. As presented in figure 6.3.B, a higher degree of crosslinking increases the microgel size at 37 °C, while the effect of SDS is not as pronounced as in the literature [61,62].

Following physiochemical characterization of the microgels, drug loading onto the microgels, and its release was analyzed through incorporation of genipin as a model drug in the microgels. As demonstrated, a higher crosslinking degree resulted in a higher drug loading. The behavior of higher loading in highly crosslinked samples has been reported before [63,64]. This phenomenon could be attributed to the tight network present in highly crosslinked hydrogels, which enhances the ability of the microgel network to entrap drug molecules [64]. The initial high rate of drug release from the microgels could be attributed to a high initial difference in the concentration of genipin within the microgels and the surrounding environment, leading to a higher rate of diffusion, while this difference is reduced as genipin is released over time. The effect of crosslinking degree could be observed in the release rate as well. This phenomenon can again be attributed to

the tight microgel network in highly crosslinked samples [64,65]. The release rate can be compared with the release observed at 25 °C from pNIPAM based microgels [66,67], which can be attributed to the increased VPTT of the microgels synthesized in this study.
Considering the desired application of the developed microgels, being their use in tissue engineering applications, the possible cytotoxicity of the microgels on cell monolayers was also analyzed. The live dead analysis demonstrated a lower number of DPSCs after 7 days of the cells being cultured in presence of microgels. This could possibly be attributed to the possible uptake of the microgels by the cells, which could affect their ability for proliferation [68,69]. Although the pNIPAM based microgels have been demonstrated to be non-toxic in microgel concentrations lower than 1 mg/mL [70], it might be that the higher concentration used in this study (5 mg/mL), representing the theoretically maximum possible amount of microgels for efficient delivery of genipin to DPSCs [37], might affect capability of the cells to proliferate. The DNA quantification also confirms the hypothesis that this concentration of microgels in suspension form (5 mg/mL) does not cause cell death, while it can affect the proliferative capacity of DPSCs, which could possibly be caused by uptake of the microgels by the cells [68,69]. This demonstrates that for applications involving the proposed microgels in a suspension, a lower concentration might be favorable. However, for tissue engineering applications where the microgels will be embedded within tissue engineering strategies such as scaffolds, they will be suitable, as the day 1 and 3 results show absence of any direct toxicity, and the possibility of uptake in such applications would be negligible [70]. Hence, it can be concluded that these microgels could be suitable for a range of dentoalveolar tissue engineering applications.

6.5 Conclusion

In this study, microgels of pNIPAM-methylcellulose copolymer were synthesized to be used in dentoalveolar tissue engineering strategies. A factorial design of experiments was applied to evaluate the effect of different synthesis parameters on microgel properties. Characterizations including measurement of size, VPTT, drug loading, drug release and cytotoxicity on DPSCs were performed to evaluate the

suitability of the microgels for drug delivery in tissue engineering strategies, and to determine the most important parameters to optimize according to the application. Among these, crosslinker concentration was demonstrated as the most important parameter affecting drug loading and release. These results, along with the shown cytocompatiblity of the microgels, manifest their potential application in tissue engineering, as well as the most important parameters affecting different properties, hence, acting as a sound basis for further research in this area.

6.6 References

1. Rambhia KJ, Ma PX.“”Controlled drug release for tissue engineerin””. J Control Release. 2015/08/29. 2015 Dec 10;219:119–28.
2. Mangione F, Salmon B, EzEldeen M, Jacobs R, Chaussain C, Vital S.“”Characteristics of Large Animal Models for Current Cell-Based Oral Tissue Regeneratio””. Tissue Eng Part B Rev. 2021 Apr 21;28(3):489–505.
3. Amoli M, EzEldeen M, Jacobs R, Bloemen V, Salar Amoli M, EzEldeen M, Jacobs R, Bloemen V.“”Materials for Dentoalveolar Bioprinting: Current State of the Ar””. Biomed . 2022 Dec 30;10(1):71.
4. Grawish ME, Grawish LM, Grawish HM, Grawish MM, El-Negoly SA.“”Challenges of Engineering Biomimetic Dental and Paradental Tissue””. Tissue Eng Regen Med. 2020;17(4):403–21.
5. Abou Neel EA, Chrzanowski W, Salih VM, Kim HW, Knowles JC.“”Tissue engineering in dentistr””. J Dent. 2014 Aug 1 [cited 2020 Feb 18];42(8):915–28.
6. Thant AA, Ruangpornvisuti V, Sangvanich P, Banlunara W, Limcharoen B, Thunyakitpisal P.“”Characterization of a bioscaffold containing polysaccharide acemannan and native collagen for pulp tissue regeneratio””. Int J Biol Macromol. 2022;
7. Guan N, Liu Z, Zhao Y, Li Q, Wang Y.“”Engineered biomaterial strategies for controlling growth factors in tissue engineerin””. Drug Deliv. 2020 Dec;27(1):1438–51.
8. Lin MJ, Lu MC, Chan YC, Huang YF, Chang HY.“”An Insulin-like Growth Factor-1 Conjugated Bombyx mori Silk Fibroin Film for Diabetic Wound Healing: Fabrication, Physicochemical Property Characterization, and Dosage Optimization In Vitro and In Viv””. Pharmaceutics. 2021 Sep 13;13(9):1459.
9. Qu M, Jiang X, Zhou X, Wang C, Wu Q, Ren L, Zhu J, Zhu S, Tebon P, Sun W, Khademhosseini A.“”Stimuli-Responsive Delivery of Growth Factors for Tissue Engineerin””. Adv Healthc Mater. 2020 Apr 1;9(7):1901714.
10. Tian H, Zhao J, Brochmann EJ, Wang JC, Murray SS.“”Bone morphogenetic protein-2 and tumor growth: Diverse effects and possibilities for therapy””. Cytokine Growth Factor Rev. 2017 Apr;34:73–91.
11. Ekenseair AK, Kasper FK, Mikos AG.“”Perspectives on the interface of drug delivery and tissue engineerin””. Adv Drug Deliv Rev. 2012/09/20. 2013 Jan;65(1):89–92.
12. Bharathi R, Ganesh SS, Harini G, Vatsala K, Anushikaa R, Aravind S,

Abinaya S, Selvamurugan N.“”Chitosan-based scaffolds as drug delivery systems in bone tissue engineerin””. Int J Biol Macromol. 2022;222:132–53.
13. Quinlan E, Thompson EM, Matsiko A, O'Brien FJ, López-Noriega A.“”Long-term controlled delivery of rhBMP-2 from collagen–hydroxyapatite scaffolds for superior bone tissue regeneratio””. J Control Release. 2015;207:112–9.
14. Sadeghi A, Fatemi MJ, Zandi M, Bagheri T, Ghadimi T, Tamimi M, Pezeshki-Modaress M.“”Multilayered 3-D nanofibrous scaffold with chondroitin sulfate sustained release as dermal substitut””. Int J Biol Macromol. 2022;206:718–29.
15. Zhao J, Zhao X, Guo B, Ma PX.“”Multifunctional Interpenetrating Polymer Network Hydrogels Based on Methacrylated Alginate for the Delivery of Small Molecule Drugs and Sustained Release of Protei””. Biomacromolecules. 2014 Sep 8;15(9):3246–52.
16. Suhail M, Li XR, Liu JY, Hsieh WC, Lin YW, Wu PC.“”Fabrication of alginate based microgels for drug-sustained release: In-vitro and in-vivo evaluation””. Int J Biol Macromol. 2021 Dec;192:958–66.
17. Montiel-Herrera M, Gandini A, Goycoolea FM, Jacobsen NE, Lizardi-Mendoza J, Recillas-Mota M, Argüelles-Monal WM.“”N-(furfural) chitosan hydrogels based on Diels–Alder cycloadditions and application as microspheres for controlled drug releas””. Carbohydr Polym. 2015;128:220–7.
18. Elisseeff J, McIntosh W, Fu K, Blunk T, Langer R.“”Controlled-release of IGF-I and TGF-β1 in a photopolymerizing hydrogel for cartilage tissue engineerin””. J Orthop Res. 2001 Nov 1;19(6):1098–104.
19. Atienza-Roca P, Cui X, Hooper GJ, Woodfield TBF, Lim KS.“”Growth Factor Delivery Systems for Tissue Engineering and Regenerative Medicine BT - Cutting-Edge Enabling Technologies for Regenerative Medicin””. In: Chun HJ, Park CH, Kwon IK, Khang G, editors. Singapore: Springer Singapore; 2018. P. 245–69.
20. Sherstneva AA, Demina TS, Monteiro APF, Akopova TA, Grandfils C, Ilangala AB.“”Biodegradable Microparticles for Regenerative Medicine: A State of the Art and Trends to Clinical Application””. Polymers (Basel). 2022 Mar;14(7).
21. Vikulina AS, Feoktistova NA, Balabushevich NG, von Klitzing R, Volodkin D.“”Cooling-Triggered Release from Mesoporous Poly(N-isopropylacrylamide) Microgels at Physiological Condition””. ACS Appl Mater Interfaces. 2020 Dec 23;12(51):57401–9.
22. Liu L, Zeng J, Zhao X, Tian K, Liu P.“”Independent temperature and pH dual-responsive PMAA/PNIPAM microgels as drug delivery system: Effect of swelling behavior of the core and shell materials in fabrication proces””. Colloids Surfaces A Physicochem Eng Asp. 2017;526:48–55.
23. Pilipenko I, Korzhikov-Vlakh V, Valtari A, Anufrikov Y, Kalinin S, Ruponen M, Krasavin M, Urtti A, Tennikova T.“”Mucoadhesive properties of nanogels based on stimuli-sensitive glycosaminoglycan-graft-pNIPAAm copolymer””. Int J Biol Macromol. 2021;186:864–72.
24. Kwon Y, Choi Y, Jang J, Yoon S, Choi J.“”NIR Laser-Responsive PNIPAM and Gold Nanorod Composites for the Engineering of Thermally Reactive Drug Delivery Nanomedicin””. Pharmaceutics. 2020 Feb 27;12(3):204.
25. Carneiro MJM, Paula CBA, Ribeiro IS, de Lima LRM, Ribeiro FOS, Silva DA, Araújo GS, Marinho Filho JDB, Araújo AJ, Freire RS, Feitosa JPA, de

Paula RCM.“”Dual responsive dextran-graft-poly (N-isopropylacrylamide)/doxorubicin prodrug via Schiff base reactio””. Int J Biol Macromol. 2021;185:390–402.
26. Kjøniksen A, Calejo MT, Zhu K, Cardoso AMS, de Lima MCP, Jurado AS, Nyström B, Sande SA.“”Sustained Release of Naltrexone from Poly(N-Isopropylacrylamide) Microgel””. J Pharm Sci. 2014;103(1):227–34.
27. Bradley M, Ramos J, Vincent B.“”Equilibrium and Kinetic Aspects of the Uptake of Poly(ethylene oxide) by Copolymer Microgel Particles of N-Isopropylacrylamide and Acrylic Aci””. Langmuir. 2005 Feb 1;21(4):1209–15.
28. Wang Y, Zhu L, Zhang H, Huang H, Jiang L.“”Formulation of pH and temperature dual-responsive Pickering emulsion stabilized by chitosan-based microgel for recyclable biocatalysi””. Carbohydr Polym. 2020;241:116373.
29. Su C, Liu J, Yang Z, Jiang L, Liu X, Shao W.“”UV-mediated synthesis of carboxymethyl cellulose/poly-N-isopropylacrylamide composite hydrogels with triple stimuli-responsive swelling performance””. Int J Biol Macromol. 2020;161:1140–8.
30. Yoshida T, Aoyagi T, Kokufuta E, Okano T.“”Newly designed hydrogel with both sensitive thermoresponse and biodegradabilit””. J Polym Sci Part A Polym Chem. 2003 Mar 15;41(6):779–87.
31. Vasile C, Marinescu C, Vornicu R, Staikos G.“”Enzymatic degradation of thermoresponsive poly(N-isopropylacrylamide) grafted to carboxymethylcellulose copolymer””. J Appl Polym Sci. 2003 Feb 28;87(9):1383–6.
32. Cui X, Tang J, Hartanto Y, Zhang J, Bi J, Dai S, Qiao SZ, Cheng K, Zhang H.“”NIPAM-based Microgel Microenvironment Regulates the Therapeutic Function of Cardiac Stromal Cell””. ACS Appl Mater Interfaces. 2018 Nov 7;10(44):37783–96.
33. Adibfar A, Amoabediny G, Baghaban Eslaminejad M, Mohamadi J, Bagheri F, Zandieh Doulabi B.“”VEGF delivery by smart polymeric PNIPAM nanoparticles affects both osteogenic and angiogenic capacities of human bone marrow stem cells””. Mater Sci Eng C Mater Biol Appl. 2018 Dec;93:790–9.
34. Jäger M, Fischer J, Dohrn W, Li X, Ayers DC, Czibere A, Prall WC, Lensing-Höhn S, Krauspe R.“”Dexamethasone modulates BMP-2 effects on mesenchymal stem cells in vitro””. J Orthop Res Off Publ Orthop Res Soc. 2008 Nov;26(11):1440–8.
35. Okamoto Y, Sonoyama W, Ono M, Akiyama K, Fujisawa T, Oshima M, Tsuchimoto Y, Matsuka Y, Yasuda T, Shi S, Kuboki T.“”Simvastatin induces the odontogenic differentiation of human dental pulp stem cells in vitro and in vivo””. J Endod. 2009 Mar;35(3):367–72.
36. Nakashima M.“”Bone morphogenetic proteins in dentin regeneration for potential use in endodontic therap””. Cytokine Growth Factor Rev. 2005;16(3):369–76.
37. Kwon YS, Lim ES, Kim HM, Hwang YC, Lee KW, Min KS.“”Genipin, a cross-linking agent, promotes odontogenic differentiation of human dental pulp cells””. J Endod. 2015 Apr;41(4):501–7.
38. Blackburn WH, Dickerson EB, Smith MH, McDonald JF, Lyon LA.“”Peptide-Functionalized Nanogels for Targeted siRNA Deliver””. Bioconjug Chem. 2009 May 20;20(5):960–8.
39. Hilkens P, Gervois P, Fanton Y, Vanormelingen J, Martens W, Struys T,

Politis C, Lambrichts I, Bronckaers A.“”Effect of isolation methodology on stem cell properties and multilineage differentiation potential of human dental pulp stem cells””. Cell Tissue Res. 2013 Jul;353(1):65–78.
40. Jain K, Vedarajan R, Watanabe M, Ishikiriyama M, Matsumi N.“”Tunable LCST behavior of poly(N-isopropylacrylamide/ionic liquid) copolymer””. Polym Chem. 2015;6(38):6819–25.
41. Nadour M, Daoud F, Ouradi A, Benaboura A.“”Effects of Methylcellulose on the Properties and Morphology of Polysulfone Membranes Prepared by Phase Inversio””. Mater Res. 2017 Apr 1;20.
42. Liu W, Zhang B, Lu WW, Li X, Zhu D, De Yao K, Wang Q, Zhao C, Wang C.“”A rapid temperature-responsive sol–gel reversible poly(N-isopropylacrylamide)-g-methylcellulose copolymer hydroge””. Biomaterials. 2004;25(15):3005–12.
43. Sá-Lima H, Tuzlakoglu K, Mano JF, Reis RL.“”Thermoresponsive poly(N-isopropylacrylamide)-g-methylcellulose hydrogel as a three-dimensional extracellular matrix for cartilage-engineered application””. J Biomed Mater Res Part A. 2011 Sep 15;98A(4):596–603.
44. Mukherji D, Wagner M, Watson MD, Winzen S, de Oliveira TE, Marques CM, Kremer K.“”Relating side chain organization of PNIPAm with its conformation in aqueous methano””. Soft Matter. 2016;12(38):7995–8003.
45. Martinez-Moro M, Jenczyk J, Giussi JM, Jurga S, Moya SE.“”Kinetics of the thermal response of poly(N-isopropylacrylamide co methacrylic acid) hydrogel microparticles under different environmental stimuli: A time-lapse NMR stud””. J Colloid Interface Sci. 2020;580:439–48.
46. Cooperstein MA, Canavan HE.“”Assessment of cytotoxicity of (N-isopropyl acrylamide) and poly(N-isopropyl acrylamide)-coated surface””. Biointerphases. 2013/08/07. 2013 Dec;8(1):19.
47. Dutta S, Dhara D.“”Effect of preparation temperature on salt-induced deswelling and pattern formation in poly(N-isopropylacrylamide) hydrogel””. Polymer (Guildf). 2015;76:62–9.
48. Jelken J, Jung SH, Lomadze N, Gordievskaya YD, Kramarenko EY, Pich A, Santer S.“”Tuning the Volume Phase Transition Temperature of Microgels by Ligh””. Adv Funct Mater. 2022 Jan 1;32(2):2107946.
49.“”Particle size analysis — Dynamic light scattering (DLS), ISO 22412:2017(en””. 2017;
50. Danaei M, Dehghankhold M, Ataei S, Hasanzadeh Davarani F, Javanmard R, Dokhani A, Khorasani S, Mozafari MR.“”Impact of Particle Size and Polydispersity Index on the Clinical Applications of Lipidic Nanocarrier Systems””. Pharmaceutics. 2018 May;10(2).
51. Tourrette A, De Geyter N, Jocic D, Morent R, Warmoeskerken MMCG, Leys C.“”Incorporation of poly(N-isopropylacrylamide)/chitosan microgel onto plasma functionalized cotton fibre surfac””. Colloids Surfaces A Physicochem Eng Asp. 2009;352(1):126–35.
52. Contessi N, Altomare L, Filipponi A, Farè S.“”Thermo-responsive properties of methylcellulose hydrogels for cell sheet engineerin””. Mater Lett. 2017;207:157–60.
53. Shirangi M, Sastre Toraño J, Sellergren B, Hennink WE, Somsen GW, van Nostrum CF.“”Methyleneation of Peptides by N,N,N,N-Tetramethylethylenediamine (TEMED) under Conditions Used for Free Radical Polymerization: A Mechanistic Stud””. Bioconjug Chem. 2015 Jan 21;26(1):90–100.

54. Zubik K, Singhsa P, Wang Y, Manuspiya H, Narain R.“”Thermo-Responsive Poly(N-Isopropylacrylamide)-Cellulose Nanocrystals Hybrid Hydrogels for Wound Dressin””. Vol. 9, Polymers . 2017.
55. Hu X, Tong Z, Lyon LA.“”Control of poly(N-isopropylacrylamide) microgel network structure by precipitation polymerization near the lower critical solution temperatur””. Langmuir. 2011/03/14. 2011 Apr 5;27(7):4142–8.
56. Werner P, Münzberg M, Hass R, Reich O.“”Process analytical approaches for the coil-to-globule transition of poly(N-isopropylacrylamide) in a concentrated aqueous suspensio””. Anal Bioanal Chem. 2017;409(3):807–19.
57. Tavagnacco L, Zaccarelli E, Chiessi E.“”On the molecular origin of the cooperative coil-to-globule transition of poly(N-isopropylacrylamide) in wate””. Phys Chem Chem Phys. 2018;20(15):9997–10010.
58. Podewitz M, Wang Y, Quoika PK, Loeffler JR, Schauperl M, Liedl KR.“”Coil–Globule Transition Thermodynamics of Poly(N-isopropylacrylamide””. J Phys Chem B. 2019 Oct 17;123(41):8838–47.
59. Kawaguchi H.“”On Going to a New Era of Microgel Exhibiting Volume Phase Transitio””. Gels (Basel, Switzerland). 2020 Aug 17;6(3):26.
60. Farooqi ZH, Khan HU, Shah SM, Siddiq M.“”Stability of poly(N-isopropylacrylamide-co-acrylic acid) polymer microgels under various conditions of temperature, pH and salt concentratio””. Arab J Chem. 2017;10(3):329–35.
61. Andersson M, Maunu SL.“”Structural studies of poly(N-isopropylacrylamide) microgels: Effect of SDS surfactant concentration in the microgel synthesi””. J Polym Sci Part B Polym Phys. 2006 Dec 1;44(23):3305–14.
62. Wedel B, Brändel T, Bookhold J, Hellweg T.“”Role of Anionic Surfactants in the Synthesis of Smart Microgels Based on Different Acrylamide””. ACS Omega. 2017 Jan 31;2(1):84–90.
63. Qasim SSB, Nogueria LP, Fawzy AS, Daood U.“”The Effect of Cross-linking Efficiency of Drug-Loaded Novel Freeze Gelated Chitosan Templates for Periodontal Tissue Regeneratio””. AAPS PharmSciTech. 2020;21(5):173.
64. Hoang HT, Jo SH, Phan QT, Park H, Park SH, Oh CW, Lim KT.“”Dual pH-/thermo-responsive chitosan-based hydrogels prepared using “click” chemistry for colon-targeted drug delivery application””. Carbohydr Polym. 2021;260:117812.
65. Zhu G, Wang K, Qin H, Zhao X, Chen W, Xu L, Cao W, Guo H.“”Internal cross-linked polymeric nanoparticles with dual sensitivity for combination therapy of muscle-invasive bladder cance””. J Nanobiotechnology. 2020;18(1):124.
66. Jin X, Wang Q, Sun J, Panezail H, Wu X, Bai S.“”Dual temperature- and pH-responsive ibuprofen delivery from poly(N-isopropylacrylamide-co-acrylic acid) nanoparticles and their fractal feature””. Polym Bull. 2017;74(9):3619–38.
67. Lin YK, Yu YC, Wang SW, Lee RS.“”Temperature, ultrasound and redox triple-responsive poly(N-isopropylacrylamide) block copolymer: synthesis, characterization and controlled releas””. RSC Adv. 2017;7(68):43212–26.
68. Gan T, Guan Y, Zhang Y.“”Thermogelable PNIPAM microgel dispersion as 3D cell scaffold: effect of syneresi””. J Mater Chem. 2010;20:5937–44.
69. Zhang W, Mao Z, Gao C.“”Preparation of TAT peptide-modified poly(N-isopropylacrylamide) microgel particles and their cellular uptake, intracellular distribution, and influence on cytoviability in response to temperature

chang””. J Colloid Interface Sci. 2014;434:122–9.
70. Switacz VK, Wypysek SK, Degen R, Crassous JJ, Spehr M, Richtering W.“”Influence of Size and Cross-Linking Density of Microgels on Cellular Uptake and Uptake Kinetic””. Biomacromolecules. 2020 Nov 9;21(11):4532–44.

Chapter 7. Encapsulation of pNIPAM-methylcellulose microgels in gelMA aimed at bioprinting dentoalveolar tissues: preliminary validations

Chapter summary

This chapter performs preliminary analysis required towards incorporation of genipin loaded microgels in bioinks aimed at dentoalveolar bioprinting. For this purpose, the capability of encapsulating the microgels developed in chapter 6 in bioprinting strategies was evaluated. To do this, a fully functionalized gelMA hydrogel was synthesized through methacrylation of gelatin at basic pH. Success of the synthesis was evaluated and confirmed through nuclear magnetic resonance spectroscopy. Furthermore, it was demonstrated that the developed microgels could be successfully incorporated within the bioinks. Not only do they not have any negative effect on the printability of gelMA, they enhance the quality of printing. Furthermore, as genipin was aimed to be loaded onto the microgels, preliminary analysis was performed to evaluate the effect of genipin on odontoblastic differentiation of dental pulp stem cells. While the results of the alizarin red staining demonstrate an effect on the differentiation, further research and optimizations are required to achieve differentiation similar to the positive control. Following this, a next step could be the encapsulation of genipin loaded microgels in gelMA bioink, and the evaluation of the effects on differentiation of encapsulated cells.

7.1 Introduction

While tissue engineering has opened up some hope towards addressing certain shortcomings of current treatments in the dentoalveolar region, tissue engineering of the dentoalveolar region is a challenging area of research [1,2]. One of the reasons for the difficulty in tissue engineering in this area is the inherent complexity of the tissue structures in the region [3]. Firstly, the dentoalveolar region is composed of several tissues with a wide range or properties. These include soft tissues such as dental pulp, periodontal ligament, and gingiva, along with hard tissues such as dentin, enamel and dentoalveolar bone. Second, there is heterogeneity in physical, mechanical and biological properties within each of these structures [3,4]. For example, dental pulp is consisted of a viscoelastic gel like structure incorporating fibroblasts in its core, dental pulp stem cells surrounding the core, and odontoblasts producing dentin at the outer layer. Furthermore, it includes a cell free layer housing capillary networks and nerves [5,6]. This significant degree of complexity can also be observed in other dentoalveolar tissues, such as the tubular structure of the dentin resulting in a range of physicomechanical properties depending on the distance from dental pulp [7]. Similarly, the alveolar bone has a layered structure consisting of periosteum, compact bone, cancellous bone and the cribriform with varying degrees of porosity, mechanical strength and mineralization [8,9]. Furthermore, trapped between alveolar bone and cementum is the periodontal ligament. The narrow width of the periodontal ligament, coupled with being surrounded and anchored to hard tissues [10], self-repair capability [11] and functional fibre alignments [12] are some of the challenges in its tissue engineering.

A range of approaches have been utilized to address this heterogeneity within tissue engineering strategies of this region with varying degrees of success. This is represented in pulp-dentin tissue engineering, where the first challenge is to recapitulate the structure of pulp with dentin surrounding it. For this purpose, scaffolds consisting of a gradient of stiffness have been developed, where this stiffness gradient resulted in formation of a tissue with high degree of similarity to pulp-dentin following implantation *in vivo* [13], or *in vitro* combined with

bioprinting strategies [14]. A similar strategy was used to induce dentin formation around the pulp using a spatial gradient of growth factors encapsulated within the scaffold [15]. Also, use of different cell types for regeneration of different compartments has been another suggested approach [16]. While these approaches have been successful to a certain degree in mimicking the general structure of pulp-dentin, there are still a range of challenges associated with tissue engineering in this area. For example, dental pulp houses both sensory and sympathetic nerves with a range of functionalities such as regulation of blood flow, pressure and inflammation, in addition to maintaining the homeostasis [17]. Furthermore, the vascularization in the dental pulp is critical for supply of oxygen and nutrients and removal of metabolic waste from the tissue, and regeneration of these blood vessels imposes additional requirements in the use of biomaterials, cell types and growth factors [18]. Such challenges are suggested to be addressed through delivery of growth factors such as vascular endothelial growth factor (VEGF), along with delivery of genes and gene transfer [19].

Similar challenges have also been faced and addressed through different strategies in tissue engineering of other dentoalveolar tissues. Development of biphasic scaffolds aimed at regeneration of alveolar bone and the periodontal ligament layer simultaneously, by incorporating a sheet of periodontal ligament stem cells on the bone scaffold layer [20], or in another approach, 3D printing of bone scaffolds with a gradient of different materials and physical properties aimed to address the layered structure of bone [21].

As demonstrated in some of the examples, one of the most efficient methods to address such challenges caused by heterogeneity in the tissues is to administer drugs, growth factors and signalling molecules within the tissue engineering strategies [22]. However, there are challenges associated with use of such molecules, as their potency in enhancing tissue regeneration depends significantly on temporal and spatial accuracy of their presence [23]. The efforts to address this demand encompass a range of strategies. One of the widely investigated strategies involve covalent bonding of the biomolecule to the tissue engineering scaffold. This has been shown through covalent immobilization of vascular endothelial growth factor (VEGF) onto collagen-based scaffolds to enhance angiogenesis [24], or through

binding of bone morphogenetic protein 2 (BMP-2) to poly ethyleneglycol based scaffolds for osteochondral tissue engineering [25]. However, this strategy suffers from limitations including blocking a functional group limiting the molecules bioactivity, dependence on the efficacy of modification, and required optimizations for controlling the steric hinderance of the conjugated proteins [26]. In a different strategy, incorporation of drugs and growth factors within the structure of porous scaffolds has been evaluated, such as incorporation of BMP in collagen scaffolds [27,28]. However, this strategy suffers from limitations such as poor release kinetics [28], and difficulty in administration of various drugs or various concentration of drugs within a single tissue engineering scaffold [29]. Consequently, incorporation of microparticles in tissue engineering matrices has been suggested as a method to circumvent these challenges, such as incorporating PLGA microparticles in chitosan scaffolds [30], or BMP loaded silk microparticles in a silk scaffold for osteochondral regeneration [31].

Aside from these strategies to address the biological heterogeneity, the structural complexity needs to be addressed through fabrication of accurate tissue engineering constructs. While traditional techniques, such as development of gradient scaffolds [32] have been suggested for tissue engineering of the dentoalveolar tissues, the emerging bioprinting technique has opened up new horizons for tissue engineering of dental tissues through precise placement of cells, biomaterials and incorporated biomolecules, in addition to the possibility of using multiple materials and cell types within the engineering process [33]. This technique has the capability to be combined with drug delivery approaches to enhance the tissue regeneration process. Encapsulation of microparticles within bioinks used for bioprinting has been reported to be beneficial for bioprinting of gelMA, through increasing its printing resolution by modification of material properties such as viscosity [34]. In addition, due to versatility, drug loaded microparticles have been used for delivery of drugs and growth factors within bioprinting strategies [35].

Aside from the technique, a range of drugs and biomolecules have been used for tissue engineering in the dentoalveolar region. As a first step, several molecules such as simvastatin [36], transforming growth factor

beta 1 (TGF-β1) [37], and dentin matrix protein 1 (DMP-1) [38] have been used to enhance regeneration of dentin pulp complex. Also, genipin, a natural molecule obtained from fruit extracts, is reported to stimulate odontoblastic differentiation of dental pulp cells [39]. Considering that genipin is a widely available small molecule compared to proteins, it appears to be a suitable choice for encapsulation in microparticles capable of being used in the tissue engineering process.

Consequently, this chapter aims to perform preliminary analysis required for incorporation of pNIPAM based microgels developed in previous chapter, inside gelatin methacrylate (gelMA), as it is one of the most widely used biomaterials for bioprinting applications, and evaluate the possibility of inducing differentiation through incorporation of genipin loaded microgels within the tissue engineering strategies. Indeed, further research following this preliminary validation will be required to achieve this goal.

7.2 Materials and methods

7.2.1 Materials

Gelatin (from porcine skin, 240-270 g bloom), methacrylic anhydride, lithium phenyl-2,4,6-trimethylbenzoylphosphintae (LAP), deuterated dimethyl sulfoxide (DMSO-d_6), Sodium bicarbonate ($NaHCO_3$), sodium carbonate (Na_2CO_3), n-isopropylacrylamide (NIPAM), methylcellulose, methylene-bis-acrylamide, sulforhodamine b, and alizarin red S were obtained from Sigma Aldrich (Overijse, Belgium). Genipin was obtained from Challenge Bioproducts Co., Ltd (Taiwan).

7.2.2 Methods

7.2.2.1 Synthesis of gelMA

GelMA was prepared according to a previously reported protocol [40]. Briefly, a carbonate bicarbonate buffer was prepared by dissolving 20 g $NaHCO_3$ and 1.1 g Na_2CO_3 in 1L Deionized water, and the pH was adjusted to 9 by adding 5N NaOH. Gelatin was dissolved in the buffer in a round bottom flask with a concentration of 100 g/L. The mixture was stirred for 12 h at 40 °C to ensure dissolution. Next, methacrylic anhydride was added with a concentration of 15 mL in 1 L of the

solution, and the pH was periodically adjusted to 9 over a reaction time of 12 h. the sample was then dialyzed against DI water for 5 days, using a 14 kDa dialysis membrane before being freeze dried (Alpha 1-2 LD plus, Martin Christ Freeze Dryers, Osterode, Germany) to obtain the gelMA.

7.2.2.2 Synthesis of microgels

The pNIPAM-methylcellulose microgels were prepared according to the protocol described in chapter 4 of this thesis. Briefly, methylcellulose was dissolved in deionized water in a round bottom flask overnight, with a concentration of 2.5 mg/mL and a volume of 100 mL. The solution was then purged with Argon and the temperature was increased to 45 °C under Argon atmosphere. NIPAM was dissolved in 4 mL deionized water with a concentration of 125 mg/mL and added to methylcellulose dropwise. Methylene bis acrylamide was dissolved in 1 mL deionized water (10 mol %) and added to the round bottom flask dropwise. Next, 100 mg ammonium persulfate (APS) was added to the reaction chamber as the radical initiator. To activate the initiator and start the reaction, 50 µL tetramethylethylenediamine (TEMED) was added to the mixture. . The reaction was allowed to continue for 3h under Argon atmosphere before being exposed to air to stop the reaction. Samples were then dialyzed against DI water using dialysis tubing with a 14 kDa molecular cutoff for 5 days at room temperature, and lyophilized (Alpha 1-2 LD plus, Martin Christ Freeze Dryers, Osterode, Germany) to obtain the microgels.

7.2.2.3 Proton nuclear magnetic resonance

The structure of the synthesized gelMA was further analyzed by obtaining proton nuclear magnetic resonance (1H NMR) spectra (Avance III HD-400 MHz, Bruker, Massachusetts, USA) using DMSO-d_6 as the solvent, a 30° flip angle, a spectrometer frequency of 400 MHz and a spectral resolution of 0.15 Hz.

7.2.2.4 Evaluation of printability

To evaluate the possibility of printing gelMA along with incorporated microgels, a printability analysis was conducted. For this purpose, solutions of 7.5 %(w/v) gelMA and 0.05 %(w/v) in phosphate buffer

saline (PBS) were prepared. The solutions were then mixed with microgels with concentrations of 1, 5 and 10 mg/mL. The samples were then transferred to cartridges with a diameter of 7.29 mm, and several shapes for different analysis were printed using a 250 μm (25 G) nozzle through a piston driven extrusion printing (3dDiscovery, RegenHu, Villaz-Saint-Pierre, Switzerland). To analyze one-dimensional shape fidelity, lines of 3 cm in length were printed, the perimeter of the lines was then measured using an online software (www.sketchandcalc.com) and compared to the theoretical value. Additionally, to evaluate the two-dimensional accuracy of the print, squares were printed, and a circularity factor was calculated as previously reported [41], where a value closer to 1 represents a more accurate print. Furthermore, to assess distribution of microgels in printed constructs, microgels loaded with fluorescent sulforhodamine B were encapsulated in gelMA. For this purpose, freeze dried microgels were re-suspended in a 30 mg/mL solution of sulforhodamine B with a concentration of 50 mg/mL, and stirred for 24h. Next, the microgels were centrifuged at 356160 g (Optima TL ultracentrifuge and rotor TLA-120.2, Beckman Coulter life sciences, California, USA). The centrifuged microgels were then re-suspended in a solution of 7.5 %(w/v) gelMA, printed in shape of lines and grids, and imaged using fluorescent microscopy (IX83 inverted microscope, Olympus scientific solutions, Tokyo, Japan). Images where then subjected to non-linear background removal to eliminate background signal.

7.2.2.5 Evaluation of microgel cytotoxicity

Subculturing of dental pulp stem cells (DPSCs) was performed using the protocol described by Hilkens et al. [39]. A cell monolayer of $5x10^3$ cells/cm^2 hDPSCs (passage 7) was seeded in each well of a 48 well plate (Corning costar). Lyophilized microgels were prepared, and suspended in α-MEM, supplemented with 10 %(w/v) FBS and 1 %(w/v) antibiotics with a concentration of 5 mg/mL. The microgel suspensions were added on the cell monolayer, and cells were cultured for one week with medium change on every two days using medium containing microgels, and medium alone for control groups. Possible cytotoxicity of the microgels was evaluated at day 1, 7, and 14 by live/dead staining (Live/Dead viability cytotoxicity kit, Invitrogen,

Thermofisher Scientific, Brussels, Belgium) according to the manufacturer's protocol, and fluorescent microscopy was performed (IX83 inverted microscope, Olympus scientific solutions, Tokyo, Japan). Control samples consisted of cell monolayers cultured in α-MEM, supplemented with 10 %(v/v) FBS and 1 %(v/v) antibiotics and without the addition of microgels in the culture. Microscopy images were subjected to non-linear adjustments to remove background signal. For DNA quantification, monolayers of DPSCs were cultured in 48 well plates similar to the samples for the live/dead assay and were cultured in the presence of microgels similarly. At 1, 7, and 14 days, the microgel suspension was removed, and 350 µL commercial RLT lysis buffer (Qiagen, Hilden, Germany) plus 1 %(v/v) β-mercapto-ethanol was added to the cell monolayer to prepare the lysate. Quant-iTTM dsDNA HS reagent was diluted in Quant-iTTM dsDNA HS buffer (Quant-iT dsDNA Assay Kit, Thermofisher Scientific, Belgium) with a 1:200 ratio. 5 µL of the lysate was mixed with 195 µL of the working solution. Standards were prepared following the manufacturers protocol. Next, samples were transferred to Qubit tubes and readings were performed using Qubit fluorometer. Three separate samples were prepared for each microgel formulation and three readings were performed for each sample.

7.2.2.6 Differentiation study

Subculturing of dental pulp stem cells (DPSCs) was performed using the protocol described by Hilkens et al. [42]. To assess differentiation of dental pulp stem cells. DPSCs at passage 5 were cultured in 6 well plates with a concentration of 2×10^4 cells/cm^2. To assess differentiation, three sets of samples were prepared. One set was cultured in α-MEM supplemented with 10 % FBS and 1 % antibiotics, as the negative control. The positive control consisted of samples cultured in α-MEM supplemented with 10 % FBS, 1 % antibiotics, 0.1 µM dexamethasone, 50 µg/mL ascorbic acid, and 5 mM β-glycerophosphate. The third set of samples were cultured in α-MEM supplemented with 10 % FBS, 1 % antibiotics, in addition to 0.1 mM genipin.

7.2.2.7 Alizarin red staining

To assess mineralization in the cultured samples, an alizarin red assay was performed. For this purpose, culture medium was removed after 21 days of culture and cells were washed with PBS twice. Next, the cells were fixed in 2 mL ice cold methanol for 1 h at 4 ℃. Samples were washed again with PBS and 2 mL alizarin solution, consisting of 2 %(w/v) alizarin red S in DI water at pH 4.1-4.2, was added to the cells. The cells were incubated for 1h at room temperature on a tilting plate. Samples were then washed until no stain came off, and imaging was performed using brightfield microscopy (IX83 inverted microscope, Olympus scientific solutions, Tokyo, Japan). Following imaging, to quantify the assay, 1 mL solution of cetylpyridinium chloride (CPC) in water (10 %(w/v)) was added to the cells and incubated at room temperature on a tilting plate overnight. The solution was then transferred to a 48 wellplate along with blank samples, and absorbance was measured at 570 nm.

7.2.2.8 Quantitative real time polymerase chain reaction

To further analyze the differentiation, qPCR was used. For this purpose, cells were cultured similar to the samples for alizarin red. After culturing the cells for 21 days, total RNA was extracted using a total RNA extraction kit (rNeasy mini kit, Qiagen, Hilden, Germany) according to manufacturers' protocol. Next, cDNA was synthesized using a cDNA synthesis kit (PrimeScript RT reagent kit, Takara Bio, Shiga, Japan). Consequently, qPCR was performed through preparation of samples using a labeling kit (Fast Sybr Green mastermix, thermofisher scientific, Massachusetts, United States) on a real time PCR cycler (Rotor-Gene Q, Qiagen, Hilden, Germany). For the qPCR, the housekeeping gene used was β-Actin, and the genes analyzed included dentin sialophosphoprotein (DSPP), dentin matrix protein 1 (DMP-1), and osteopontin (OPN). The sequences for the primers used are presented in table 7.1, and the heating cycle included 2 min hold at 95 ℃, followed by 40 cycles of 10 sec at 95 ℃, 15 sec at 60 ℃, and 20 sec at 72 ℃.

Table 7.1. Primer sequences

Gene	Forward primer	Reverse primer
B-ACT	ATTGCCGACAGGATGCAGA	GAGTACTTGCGCTCAGGAGGA
DSPP	ATATTGAGGGCTGGAATGGGGA	TTTGTGGCTCCAGCATTGTCA
DMP-1	TGGGGATTATCCTGTGCTCT	GCTGTCACTGGGGTCTTCAT
OPN	TGAAACGAGTCAGCTGGATGACCA	TGGCTGTGAAATTCATGGCTGTGG

7.2.2.9 Statistical analysis

All experiments in all sections were performed in three independent replicates (n=3). Two-way ANOVA and Tukey's multiple comparisons test were performed using GraphPad Prism (version 8.0.0 for Windows, GraphPad Software, San Diego, California USA, www.graphpad.com) to analyze differences.

7.3 Results

7.3.1 GelMA synthesis

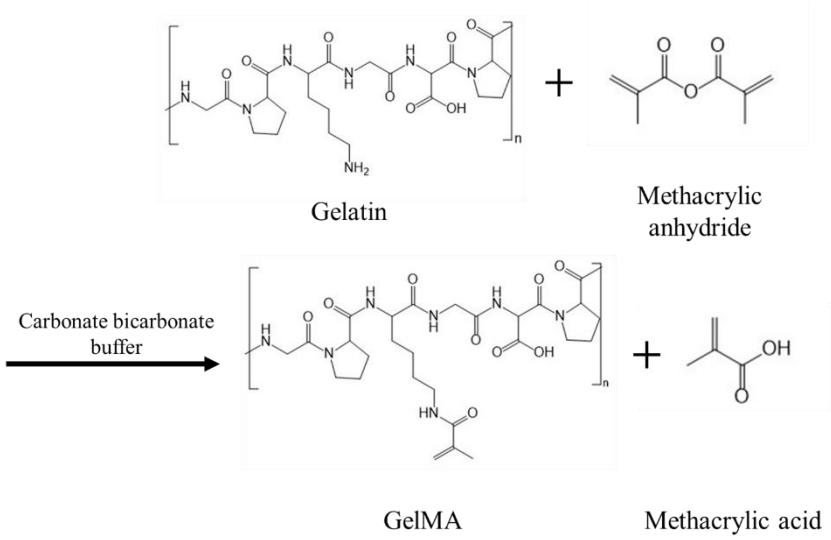

Scheme 7.1. Synthesis of gelatin methacrylate through reaction with methacrylic anhydride (scheme made using chemdraw software)

GelMA was synthesized through modification of the amine groups on the backbone of gelatin type A with methacrylic groups at pH 9. The synthesis procedure is presented schematically in scheme 7.1.
Following synthesis, the resulting material was characterized through ^{1}H NMR to confirm formation of gelMA. As demonstrated in figure 7.1, acrylic protons of the methacrylamide group grafted to gelatin can be observed at 5.2 and 5.6 ppm, confirming presence of methacylamide groups on the polymer backbone [43,44]. Furthermore, the methyl protons of the methacrylamide have resulted in a sharp peak observable at 1.85 ppm. In addition, the methylene proton on lysine moieties of gelatin, appearing at 2.76 ppm, has disappeared on the gelMA spectrum.

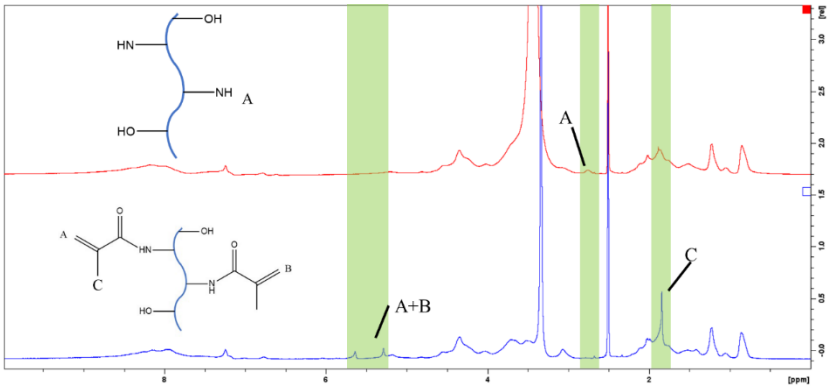

Figure 7.1. 1H NMR spectra of top: gelatin and bottom: gelMA

7.3.2 Evaluation of printability following microgel encapsulation

Following synthesis of gelMA, the incorporation of pNIPAM-methylcellulose microgels in the gel was evaluated, and the possibility of bioprinting using the microgel encapsulated hydrogels was examined. With the perimeter ratio being a measure of accuracy of the printed constructs compared to the initial design, it is shown in figure 7.2.A that there is no significant difference in the perimeter ratio of the printed gelMA, with samples encapsulating 1 mg/mL and 5 mg/mL microgels. However, increasing the concentration of encapsulated microgels to 10 mg/mL results in a perimeter ratio closer to 1, demonstrating a more accurate print than pure gelMA. Similar results

are obtained in analysis of circularity factor. As demonstrated in figure 7.2.B, the values obtained from gelMA encapsulating 10 mg/mL of microgels are significantly closer to 0 compared to pure gelMA. Furthermore, loading of fluorescent sulforhodamine B in microgels, followed by encapsulation of the microgels in gelMA was used to demonstrate distribution of microgels in gelMA following the printing process. As shown in figure 7.2.C, the microgels are distributed in the gelMA following the printing, while the control without the microgels did not show any fluorescence.

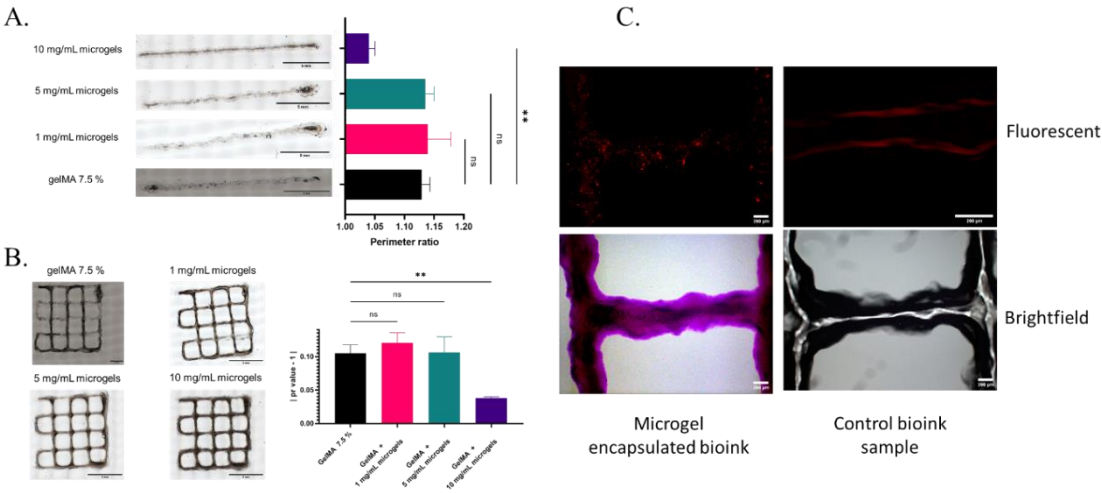

Figure 7.2. Printability of microgel encapsulated gelMA. A) analysis of the perimeter ratio B) analysis of the circularity factor and C) printing of gelMA encapsulating microgels loaded with fluorescent sulforhodamine B

7.3.3 Evaluation of microgel cytotoxicity

Considering the targeted application of the microgels for bioprinting strategies, the possible cytotoxic effects of microgels on monolayer of cells was evaluated. As demonstrated in figure 7.3, both live/dead imaging and DNA quantification demonstrated no differences in viability of the cells cultured in presence of microgels, and the control group up to day 7, showing absence of any toxicity. However, at day 14, a difference in the DNA content of the two groups was observed,

suggesting the possibility of some effect on proliferative ability of the cells.

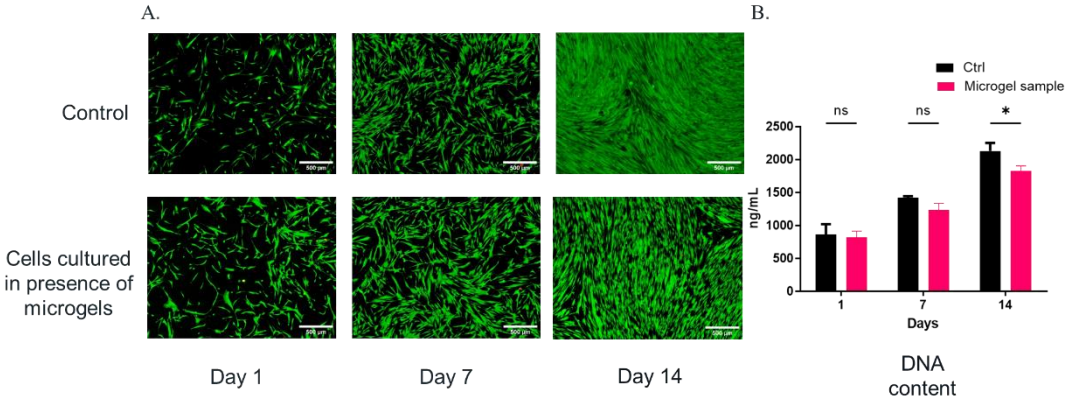

Figure 7.3. Evaluation of the possible cytotoxicity of microgels through A) Live/dead assay, and B) DNA quantification (n=3)

7.3.4 Evaluation of DPSCs differentiation through alizarin red assay

As this chapter aims to perform preliminary validations aimed at loading of genipin into the microgels to induce odontoblastic differentiation of DPSCs, the effect of genipin on differentiation of the DPSCs, which is previously reported on DPCs [39], was evaluated. For this purpose, alizarin red assay was performed to assess mineralization in samples cultured in presence of genipin. As shown in figure 7.4.A, the bright red colour characteristic of alizarin red staining the calcium deposits can be observed in DPSCs cultured in differentiation medium. While the negative control samples show no signs of mineralization, samples cultured in presence of 0.1 mM genipin demonstrate difference from the control samples, as some mineral deposition appears on the stained samples. However, the amount of this deposition is significantly smaller than the samples cultured in differentiation medium. This difference is represented in quantification of the alizarin red assay following de-staining, as shown in figure 7.4.B.

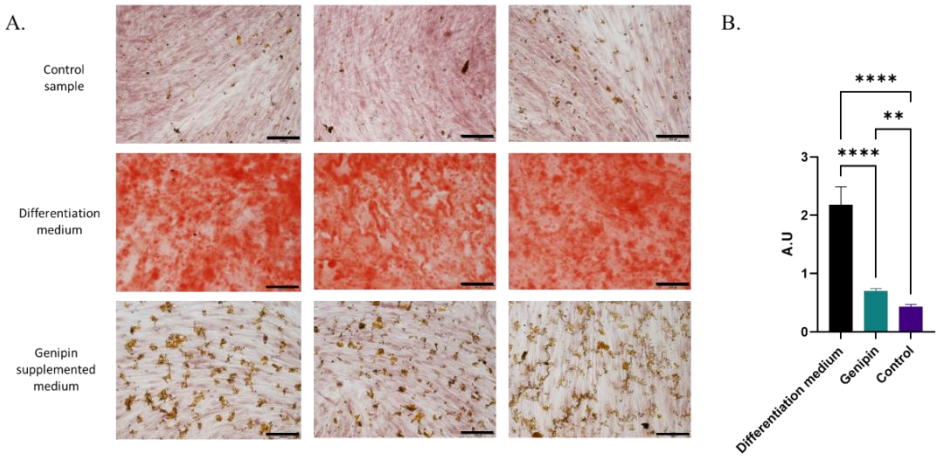

Figure 7.5. A) Alizarin red staining of cells cultured in differentiation medium, control samples cultured in base medium, and samples cultured in genipin supplemented medium for 21 days, and B) quantification of the alizarin red results. Scale bar 200 µm

7.3.5 Evaluation of DPSCs differentiation through qPCR

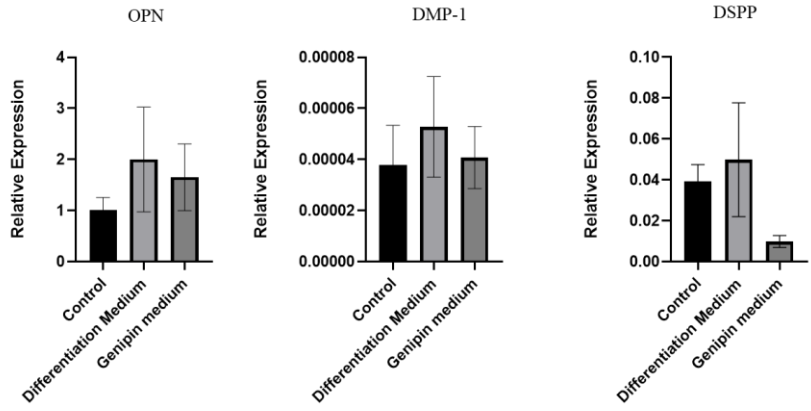

Figure 7.4. Expression of OPN, DMP-1 and DSPP analyzed through qPCR after 21 days of culture

Figure 7.5 demonstrates the results of qPCR analysis performed to assess further assess the differentiation after 21 days of culture. For this purpose, the expression of 3 differentiation genes, OPN, DSPP and DMP-1 were analyzed. As demonstrated in the figure, expression of OPN and DMP-1 seems to be higher in differentiation medium and

genipin supplemented medium. While this difference is not observed in the DSPP analysis, the differences in expression of neither genes were found to be statistically significant. This is caused by the relatively large variability observed in the samples, as shown in the error bars on the figure.

7.4 Discussion

In this chapter, methacrylated gelatin (gelMA) was synthesized, to be combined with microgels developed in chapter 6 of this thesis and printed, aiming to perform preliminary validations required for use of these microgels to induce odontoblastic differentiation in DPSCs. Synthesis of gelMA was performed following a previously reported protocol [40] aimed at synthesis of 100 % substituted gelMA. Considering the eventual aim of this preliminary analysis to encapsulate genipin loaded microgels inside gelMA, this high degree of substitution is necessary, as genipin is known to react with primary amines, and hence, could react with amine groups available on gelatin backbone [45]. For this purpose, a methacrylation reaction was performed at pH 9. Considering the isoelectric point of the gelatin being between 8 to 9, this synthesis pH ensures neutrality of the lysine groups and hence, availability of the amine groups for reaction with methacrylic anhydride. Considering the pH did not drop to lower than 7, required for modification of hydroxyl groups, during the synthesis, it was expected that the modification takes place on the amine groups rather than the hydroxyl groups. The synthesis of fully functionalized gelMA was confirmed by elimination of the lysine methylene proton in the ^{1}H NMR spectra.

Following the synthesis, as printability of gelMA is previously shown in a wide range of studies [46–48], possibility of incorporating the pNIPAM-methylcellulose microgels developed in previous chapters inside the gelMA bioprinting strategies was evaluated. As demonstrated in figure 7.2, incorporation of microgels doesn't negatively affect the accuracy of bioprinting using gelMA, and the higher concentration of the encapsulated microgels enhances the printing quality. A similar phenomenon has been reported by incorporation of extracellular matrix microparticles in gelMA, and this behavior has been attributed to an increased viscosity, in addition to

reduction of the yield stress, resulting in better printability for gelMA [34].

As it was shown in chapter 6 of this thesis, that the developed pNIPAM-methylcellulose microgels are capable of loading and sustained release of genipin. As a result, the next step for this preliminary analysis was to evaluate the effect of genipin on the differentiation of DPSCs. As demonstrated in the alizarin red assay, it was shown that genipin does have some impact on mineral deposition by these cells, but this impact was found to be significantly less than the effect of differentiation medium. Considering the previous studies demonstrating a significant increase in calcium deposition by the DPCs cultured in presence of genipin [39], further research on concentration of genipin is necessary to achieve a suitable concentration for maximum effect on odontoblastic differentiation of DPSCs. Furthermore, expression of three genes, OPN, DSPP and DMP-1 were analyzed to further assess the differentiation. Osteopontin is a gene expressed in bone cells including osteoblasts and osteocytes [49] and hence, it was used to evaluate possibility of osteogenic differentiation of the DPSCs [50]. Dentin sialophosphoprotein is a protein giving rise to majority of non-collagenous proteins in dentin [51], consequently, it has been used widely to evaluate differentiation of dental pulp stem cells to odontoblasts capable of producing dentin [52]. Finally, dentin matrix protein 1 (DMP-1), which has an important role in mineralizationo of dentin is also used extensively to assess differentiation of DPSCs [53]. Consequently, analysis of the expression of genes giving rise to these proteins could shed light on differentiation of the DPSCs. However, the amount of gene expression was not found in this study to be statistically significant. Considering a similar study using genipin reported significantly higher expression of DSPP and DMP-1 in cells cultured in presence of genipin [39], the observed expressions could be attributed to large variety within the readings, as demonstrated with the large standard deviation, signalling the need for further optimization of the measurement process.

7.5 Conclusion

In this chapter, fully functionalized gelMA was synthesized as a versatile bioink capable of encapsulating drug loaded microgels for

bioprinting applications in the dentoalveolar region. It was demonstrated that incorporation of previously developed pNIPAM-methylcellulose microgels does not impact the prinability of gelMA in low concentrations and enhances it in high concentrations. Additionally, microgels were distributed inside gelMA, as observed through incorporation of sulforhodamine loaded microgels. As this research aims to perform preliminary validations for loading of genipin in the microgels, aimed at inducing odontoblastic differentiation of DPSCs, the effect of this molecule on DPSC differentiation, also reported in the literature, was analyzed. While the results suggest genipin may have a positive effect on differentiation of DPSCs, further research and optimizations are required to achieve the optimum conditions for inducing differentiation in DPSCs. Following this, evaluation of the potential of the microgels to differentiate cells towards odontoblasts when encapsulated in the bioink, is required. This will aim to assess the capability for inducing localized differentiation and addressing the biological heterogeneity in tissue engineering of dental pulp.

7.6 References

1. Na S, Zhang H, Huang F, Wang W, Ding Y, Li D, J“n Y. "Regeneration of dental pulp/dentine complex with a three-dimensional and scaffold-free stem-cell sheet-derived p”llet.". J Tissue Eng Regen Med. 2016 Mar;10(3):261–70.
2. Khodakaram-Tafti A, Mehrabani D, Shaterzadeh-Yazdi H, Zamiri B, Omi“i M. "Tissue Engineering in Maxillary Bone D”fects". World J Plast Surg. 2018 Jan;7(1):3–11.
3. Grawish ME, Grawish LM, Grawish HM, Grawish MM, El-Negol“ SA. "Challenges of Engineering Biomimetic Dental and Paradental T”ssues". Tissue Eng Regen Med. 2020;17(4):403–21.
4. Abou Neel EA, Chrzanowski W, Salih VM, Kim HW, Knowle“ JC. "Tissue engineering in den”istry". J Dent. 2014 Aug 1 [cited 2020 Feb 18];42(8):915–28.
5. Sloa“ AJ. "Chapt–r 29 - Biology of the Dentin-Pulp C”mplex". In: Vishwakarma A, Sharpe P, Shi S, Ramalingam MBTSCB and TE in DS, editors. Boston: Academic Press; 2015. p. 371–8.
6. Abbass MMS, El-Rashidy AA, Sadek KM, Moshy S El, Radwan IA, Rady D, Dörfer CE, Fawzy El-Saye“ KM. "Hydrogels and Dentin-Pulp Complex Regeneration: From the Benchtop to Clinical Trans”ation". Polymers (Basel). 2020 Dec 9;12(12):2935.
7. Zhang YR, Du W, Zhou XD, Y“ HY. "Review of research on the mechanical properties of the human”tooth". Int J Oral Sci. 2014 Jun;6(2):61–9.
8. Gorrel C, Andersson S, Verhae“t L. "Chap–er 4 - Anatomy of the teeth and period”ntium". In: Gorrel C, Andersson S, Verhaert LBTVD for the GP

(Second E, editors. W.B. Saunders; 2013. p. 37–41.
9. Scaglione S, Giannoni P, Bianchini P, Sandri M, Marotta R, Firpo G, Valbusa U, Tampieri A, Diaspro A, Bianco P, Quar“o R. "Order versus Disorder: in vivo bone formation within osteoconductive scaf”olds.". Sci Rep. 2012;2:274.
10. O’Brien EJO, Frank CB, Shrive NG, Hallgrímsson B, Har“ DA. "Heterotopic mineralization (ossification or calcification) in tendinopathy or following surgical tendon t”auma.". Int J Exp Pathol. 2012 Oct;93(5):319–31.
11. Lekic P, McCulloc“ CA. "Periodontal ligament cell population: the central role of fibroblasts in creating a unique t”ssue.". Anat Rec. 1996 Jun;245(2):327–41.
12. Berendsen AD, Smit TH, Walboomers XF, Everts V, Jansen JA, Bronckers “LJJ. "Three-Dimensional Loading Model for Periodontal Ligament Regeneration In”Vitro". Tissue Eng Part C Methods. 2009 Feb 13;15(4):561–70.
13. Qu T, Jing J, Ren Y, Ma C, Feng JQ, Yu Q, L“u X. "Complete pulpodentin complex regeneration by modulating the stiffness of biomimetic ”atrix". Acta Biomater. 2015;16:60–70.
14. Han J, Kim DS, Jang H, Kim HRHW, Kang HW, Shaddox LM, Walker CB, Schiffman EL, Velly AM, Look JO, Hodges JS, Swift JQ, Decker KL, Anderson QN, Templeton RB, Lenton PA, Kang W, Fricton JR, Amrollahi P, e“ al. "Bioprinting of three-dimensional dentin-pulp complex with local differentiation of human dental pulp stem ”ells.". Kahveci MU, editor. J Tissue Eng. 2017/10/03. 2019 Mar 10;10(3):2041731419845849.
15. Chen J, Liao L, Lan T, Zhang Z, Gai K, Huang Y, Chen J, Tian W, G“o W. "Treated dentin matrix-based scaffolds carrying TGF-β1/BMP4 for functional bio-root regene”ation". Appl Mater Today. 2020;20:100742.
16. Hadjichristou C, Papachristou E, Bonovolias I, Bakopoul“u A. "Three-dimensional tissue engineering-based Dentin/Pulp tissue analogue as advanced biocompatibility evaluation tool of dental restorative mat”rials". Dent Mater. 2020;36(2):229–48.
17. Nakashima M, Akami“e A. "The Application of Tissue Engineering to Regeneration of Pulp and Dentin in Endod”ntics". J Endod. 2005;31(10):711–8.
18. Iijima T, Zhan“ JQ. "Three-dimensional wall structure and the innervation of dental pulp blood v”ssels". Microsc Res Tech. 2002 Jan 1;56(1):32–41.
19. Hashemi-Beni B, Khoroushi M, Foroughi MR, Karbasi S, Khadem“ AA. "Tissue engineering: Dentin – pulp complex regeneration approaches (A r”view)". Tissue Cell. 2017;49(5):552–64.
20. Vaquette C, Fan W, Xiao Y, Hamlet S, Hutmacher DW, Ivanovs“i S. "A biphasic scaffold design combined with cell sheet technology for simultaneous regeneration of alveolar bone/periodontal ligament c”mplex". Biomaterials. 2012;33(22):5560–73.
21. Bittner SM, Smith BT, Diaz-Gomez L, Hudgins CD, Melchiorri AJ, Scott DW, Fisher JP, Miko“ AG. "Fabrication and mechanical characterization of 3D printed vertical uniform and gradient scaffolds for bone and osteochondral tissue engin”ering". Acta Biomater. 2019;90:37–48.
22. Tessmar JK, Göpferic“ AM. "Matrices and scaffolds for protein delivery in tissue engin”ering". Adv Drug Deliv Rev. 2007;59(4):274–91.
23. Biondi M, Ungaro F, Quaglia F, Nett“ PA. "Controlled drug delivery in tissue engin”ering". Adv Drug Deliv Rev. 2008;60(2):229–42.
24. Chiu LLY, Weisel RD, Li RK, Radis“c M. "Defining conditions for covalent

immobilization of angiogenic growth factors onto scaffolds for tissue engin”ering". J Tissue Eng Regen Med. 2011 Jan 1;5(1):69–84.
25. Di Luca A, Klein-Gunnewiek M, Vancso JG, van Blitterswijk CA, Benetti EM, Moro“i L. "Covalent Binding of Bone Morphogenetic Protein-2 and Transforming Growth Factor-β3 to 3D Plotted Scaffolds for Osteochondral Tissue Regene”ation". Biotechnol J. 2017 Dec 1;12(12):1700072.
26. Reed S, “u B. "Sustained Growth Factor Delivery in Tissue Engineering Applic”tions". Ann Biomed Eng. 2014;42(7):1528–36.
27. Boerckel JD, Kolambkar YM, Dupont KM, Uhrig BA, Phelps EA, Stevens HY, García AJ, Guldber“ RE. "Effects of protein dose and delivery system on BMP-mediated bone regene”ation". Biomaterials. 2011;32(22):5241–51.
28. Geiger M, Li RH, Frie“s W. "Collagen sponges for bone regeneration with r”BMP-2". Adv Drug Deliv Rev. 2003;55(12):1613–29.
29. Blackwood KA, Bock N, Dargaville TR, Ann Woodru“f M. "Scaffolds for Growth Factor Delivery as Applied to Bone Tissue Engin”ering". Batich C, editor. Int J Polym Sci. 2012;2012:174942.
30. Hu X, Zhou J, Zhang N, Tan H, G“o C. "Preparation and properties of an injectable scaffold of poly(lactic-co-glycolic acid) microparticles/chitosan hy”rogel". J Mech Behav Biomed Mater. 2008;1(4):352–9.
31. Rockwood DN, Gil ES, Park SH, Kluge JA, Grayson W, Bhumiratana S, Rajkhowa R, Wang X, Kim SJ, Vunjak-Novakovic G, Kapla“ DL. "Ingrowth of human mesenchymal stem cells into porous silk particle reinforced silk composite scaffolds: An in vitro”study". Acta Biomater. 2011;7(1):144–51.
32. Porta M, Tonda-Turo C, Pierantozzi D, Ciardelli G, Mancu“o E. "Towards 3D Multi-Layer Scaffolds for Periodontal Tissue Engineering Applications: Addressing Manufacturing and Architectural Chal”enges". Vol. 12, Polymers. 2020.
33. Morrison DG, Tomlinso“ RE. "Leveraging advancements in tissue engineering for bioprinting dental t”ssues". Bioprinting. 2021;23:e00153.
34. Galliger Z, Vogt CD, Helms HR, Panoskaltsis-Morta“i A. "Extracellular Matrix Microparticles Improve GelMA Bioink Resolution for 3D Bioprinting at Ambient Tempe”ature". Macromol Mater Eng. 2022 Oct 1;307(10):2200196.
35. Sharma R, Smits IPM, De La Vega L, Lee C, Willert“ SM. "3D Bioprinting Pluripotent Stem Cell Derived Neural Tissues Using a Novel Fibrin Bioink Containing Drug Releasing Microsphe“es " [Internet]. Vol. 8, Frontiers in Bioengineering and Biotechnology . 2020.
36. Okamoto Y, Sonoyama W, Ono M, Akiyama K, Fujisawa T, Oshima M, Tsuchimoto Y, Matsuka Y, Yasuda T, Shi S, Kubo“i T. "Simvastatin induces the odontogenic differentiation of human dental pulp stem cells in vitro and in”vivo.". J Endod. 2009 Mar;35(3):367–72.
37. Tsutsu“ TW. "Dental Pulp Stem Cells: Advances to Applica”ions.". Stem Cells Cloning. 2020;13:33–42.
38. Paduano F, Marrelli M, White LJ, Shakesheff KM, Tatul“o M. "Odontogenic Differentiation of Human Dental Pulp Stem Cells on Hydrogel Scaffolds Derived from Decellularized Bone Extracellular Matrix and Collagen T”pe i.". PLoS One. 2016;11(2):e0148225.
39. Kwon YS, Lim ES, Kim HM, Hwang YC, Lee KW, Mi“ KS. "Genipin, a cross-linking agent, promotes odontogenic differentiation of human dental pulp ”ells.". J Endod. 2015 Apr;41(4):501–7.
40. Anand R, Salar Amoli M, Huysecom AS, Amorim PA, Agten H, Geris L,

Bloem“n V. "A tunable gelatin-hyaluronan dialdehyde/methacryloyl gelatin interpenetrating polymer network hydrogel for additive tissue manufact”ring.". Biomed Mater. 2022 Jun;17(4).
41. Ouyang L, Yao R, Zhao Y, S“n W. "Effect of bioink properties on printability and cell viability for 3D bioplotting of embryonic stem”cells". Biofabrication. 2016 Sep;8(3):035020.
42. Hilkens P, Gervois P, Fanton Y, Vanormelingen J, Martens W, Struys T, Politis C, Lambrichts I, Bronckae“s A. "Effect of isolation methodology on stem cell properties and multilineage differentiation potential of human dental pulp stem ”ells.". Cell Tissue Res. 2013 Jul;353(1):65–78.
43. Krishnamoorthy S, Noorani B, “u C. "Effects of Encapsulated Cells on the Physical-Mechanical Properties and Microstructure of Gelatin Methacrylate Hydr”gels.". Int J Mol Sci. 2019 Oct;20(20).
44. Thattaruparambil Raveendran N, Vaquette C, Meinert C, Samuel Ipe D, Ivanovs“i S. "Optimization of 3D bioprinting of periodontal ligament”cells". Dent Mater. 2019 Dec 1 [cited 2020 Feb 11];35(12):1683–94.
45. Zhao Y, S“n Z. "Effects of gelatin-polyphenol and gelatin–genipin cross-linking on the structure of gelatin hyd”ogels". Int J Food Prop. 2017 Dec 31;20(sup3):S2822–32.
46. Schuurman W, Levett PA, Pot MW, van Weeren PR, Dhert WJA, Hutmacher DW, Melchels FPW, Klein TJ, Mal“a J. "Gelatin-methacrylamide hydrogels as potential biomaterials for fabrication of tissue-engineered cartilage const”ucts.". Macromol Biosci. 2013 May;13(5):551–61.
47. Shi Y, Xing TL, Zhang HB, Yin RX, Yang SM, Wei J, Zhan“ WJ. "Tyrosinase-doped bioink for 3D bioprinting of living skin const”ucts.". Biomed Mater. 2018 Mar;13(3):35008.
48. Xu L, Varkey M, Jorgensen A, Ju J, Jin Q, Park JH, Fu Y, Zhang G, Ke D, Zhao W, Hou R, Ata“a A. "Bioprinting small diameter blood vessel constructs with an endothelial and smooth muscle cell bilayer in a single”step.". Biofabrication. 2020 Jul;12(4):45012.
49. Noda M, Denhard“ DT. "Chapt–r 18 - Osteo”ontin". In: Bilezikian JP, Raisz LG, Martin TJBTP of BB (Third E, editors. San Diego: Academic Press; 2008. p. 351–66.
50. Mori G, Brunetti G, Oranger A, Carbone C, Ballini A, Muzio L Lo, Colucci S, Mori C, Grassi FR, Gra“o M. "Dental pulp stem cells: osteogenic differentiation and gene expr”ssion". Ann N Y Acad Sci. 2011 Nov 1;1237(1):47–52.
51. Yamakos“i Y. "Dentinogenesis and Dentin Sialophosphoprotein (”SPP).". J oral Biosci. 2009 Sep;51(3):134.
52. Baldión PA, Velandia-Romero ML, Castellano“ JE. "Odontoblast-Like Cells Differentiated from Dental Pulp Stem Cells Retain Their Phenotype after Subculti”ation". Roubelakis M, editor. Int J Cell Biol. 2018;2018:6853189.
53. He W, Wang Z, Luo Z, Yu Q, Jiang Y, Zhang Y, Zhou Z, Smith AJ, Coope“ PR. "LPS Promote the Odontoblastic Differentiation of Human Dental Pulp Stem Cells via MAPK Signaling P”thway". J Cell Physiol. 2015 Mar 1;230(3):554–61.

Chapter 8. General Discussion

8.1 General discussion

Complications in the dentoalveolar region such as alveolar bone loss, periodontitis, missing teeth, and congenital abnormalities affect millions of people around the world, undermining their quality of life significantly [1–3]. As a consequence, a range of treatments have been developed to address such afflictions, such as implant placement, autotransplantation, and bone grafting [4–6]. However, these treatments are often faced with challenges including the inability of implant placement in paediatric patients, the limited success in periodontal treatment, and limitations of transplantation techniques [2,4,7]. Due to these challenges, regenerative medicine and tissue engineering approaches have been suggested as an alternative to the current dentoalveolar treatments. These efforts include injection of cells in the pulp cavity as pellets aiming to regenerate dental pulp tissue [8] or encouraging tissue regeneration by inducing migration of resident stem/stromal cells to the defect site, upon injection of growth factors and cytokines into the defect site [9]. Such strategies led to limited success due to challenges such as inaccurate localization of cells or challenges in delivering the required growth factors [10,11]. In addition, tissue engineering strategies involving biomaterials have been developed, through incorporation of cells in hydrogels [12], or incorporation of scaffolds made of natural or synthetic polymers [13,14]. These approaches have been beneficial in terms of replicating the environment of the extracellular matrix and maintaining cell viability. Still, challenges remain in complex regions due to limited of control over scaffold properties such as degradability or porosity, lack of vasculature formation, or immunological rejection [11,15–19]. Indeed, the inherent complexity of the dentoalveolar tissues in terms of physical, mechanical and biological heterogeneity complicates the recapitulation of such tissue properties via tissue engineering strategies [20,21].

Therefore, bioprinting strategies have been adopted to address some of the difficulties faced in tissue engineering of these tissue structures. Bioprinting enables the fabrication of geometrically accurate tissue engineering constructs through a 3D manufacturing process, and allows the incorporation of several biomaterials, cell types and

biological molecules within the fabrication process [22]. However, applying bioprinting strategies in the dentoalveolar region is a relatively novel area of research, and it faces specific obstacles. As demonstrated in chapter one of this thesis, some of these challenges include the development of tunable biomaterials with controllable properties capable of being used in the bioprinting process, in addition to methods for efficient incorporation of growth factors and signalling molecules within these strategies [23,24]. Consequently, this thesis focused on addressing these two challenges through the development of biomaterials which can be used as bioinks and biomaterial inks, and of delivery systems capable of efficiently delivering biomolecules within these systems.

Chapter 3 of this thesis includes the development of a water-soluble chitosan derivative to be used as a biomaterial ink for printing tissue engineering constructs aimed at the regeneration of the dentoalveolar region. Chitosan and its derivatives have been used widely for a range of tissue engineering applications [25], including in tissue engineering of the dentoalveolar region [26] due to favourable properties such as antimicrobial activity, biocompatibility and biodegradability [27]. However, chitosan is only soluble in weak acidic solvents, presenting a hurdle in its application where direct contact of a chitosan-based hydrogel with cells is required [28]. Consequently, a water-soluble chitosan derivative, maleic grafted chitosan, was synthesized and its applicability in fabrication of tissue engineering scaffolds through 3D printing was demonstrated [29]. This demonstration could lead to further research on tissue engineering using this material, as the procedure for synthesis of this chitosan derivative involves fewer steps than other derivatives such as catechol modified chitosan [30] or carboxymethyl chitosan [31]. This ease of development, along with demonstrated lack of toxicity and its support of cell viability and proliferation, can enhance the utilization of chitosan-based materials in bioprinting strategies. Furthermore, it was shown that crosslinking with genipin could be used as a tool to modify the properties such as degradation rate or swelling, without having any negative impact on cell response. This tunable design, along with the ability to be used in 3D printing of scaffolds could enable further research in which scaffolds of gradient properties can be developed addressing variability

in mechanical properties of the target tissues. While proven biocompatible to seeded cells, in this chapter, the maleic grafted chitosan and gelatin were crosslinked using genipin. This crosslinking method takes place over 24 hours, meaning the initial genipin concentrations would be toxic for the cells [32] and hence, encapsulation of the cells in the hydrogel would not be feasible.

Consequently, the development of a bioink capable of rapid gelation to allow cell encapsulation became the focus of fourth and fifth chapters. For this purpose, poly n-isopropylacrylamide (pNIPAM) was selected as a candidate due to several reasons. The first reason is the thermo-sensitive behaviour of pNIPAM. Above a certain critical temperature, called the lower critical solution temperature (LCST), pNIPAM chains transform from a random coil phase to a globular phase, resulting in expulsion of entrapped solvent and precipitation or gelation of the material [33,34]. In addition to this, being a synthetic polymer, physical and mechanical properties of pNIPAM are easily tunable depending on the chain length, side groups, and concentration [35,36]. These properties have resulted in the widespread use of pNIPAM-based polymers in biomedical applications. This use has expanded from applications in drug delivery [37], to cell sheet engineering [38], and tissue engineering [39]. However, application of pNIPAM for scaffold fabrication through different methods, including bioprinting, faces specific difficulties. One of the challenges in this regard is the relatively large syneresis above the LCST, resulting in a rapid loss of water at physiological temperatures and precipitation of the polymer [40]. In addition to having a detrimental effect on the printing process, this rapid water loss has a significantly negative impact on cell viability and scaffold stability. Furthermore, pure pNIPAM is largely known to be non-degradable, preventing its application in tissue engineering strategies [41]. To address these issues, chapter four focused on the development of a chitosan-pNIPAM copolymer through a one-step polymerization reaction in the presence of methylene bis acrylamide, which acts as a crosslinking agent for pNIPAM. Presence of the crosslinker resulted in a sol-gel synthesis, forming a copolymer capable of being processed through printing. The designed copolymer demonstrated biocompatibility and biodegradability, essential requirements for tissue engineering strategies through bioprinting, over

a 7-day period. However, in this study the main method to control syneresis at 37 ℃ involved utilization of the chemical crosslinker, in addition to incorporation of chitosan, which inhibits the encapsulation of cells. Consequently, chapter 5 included substitution of chitosan with methylcellulose. While the structure of chitosan and methylcellulose are largely similar, the larger number of hydroxyl groups in methylcellulose results in stronger hydrogen bonding [42] and thus, greater capability at retaining the water content upon increasing the temperature. In this chapter, the chemical crosslinker was removed as it prevents the capability of the material to encapsulate cells, caused by concerns over cytotoxicity. As a result, to enable permanent stabilization of the products, developed copolymers of pNIPAM-methylcellulose were further modified with methacrylate groups to enable photocrosslinking. This developed product demonstrated no statistically significant syneresis in specific copolymer ratios, as demonstrated in the measurement of water content at room temperature and 37 ℃. Furthermore, it demonstrated effective gelation of the material at physiological temperature, enabling combination with cells at room temperature and printing at 37 ℃, as shown by the printability of the material at this temperature. Currently, the majority of bioprinting research takes place using materials that form a gel at temperatures lower than 25 ℃ [43,44], this would require the incubation of cells at temperatures lower than the physiological temperature. This low temperature might have a negative impact on the cells, as it has been shown that a temperature closer to the physiological temperature results in a higher cell viability, and temperatures below 20 ℃ can negatively affect the cell membrane [45,46]. Consequently, some studies have focused on the development of bioinks capable of printing at 37 ℃. However, they often suffer from shortcomings such as a high cost of required materials, variability of properties in natural polymers, long crosslinking times, and challenges with cell encapsulation [47–49]. Having demonstrated the suitability of the designed copolymer for bioprinting applications, this study can act as a basis for the development of a range of bioinks with a variety of physical and mechanical properties such as stiffness, compressive and tensile strength, and degradability through tuning of the pNIPAM structure, which could be used through different printing modalities

such as inkjet or extrusion and be used for bioprinting at 37 °C. Having used a synthetic polymer, tuning the properties could be simply achieved through adjusting synthesis parameters such as time of synthesis, temperature, ratio of monomers, and degree of methacrylate substitution depending on the application, enabling fabrication of bioprinted constructs with a gradient of properties in applications such as pulp-dentin tissue engineering where e.g. the range of stiffness could affect the differentiation behaviour of dental pulp stem cells [50].

Following development of the inks for bioprinting, another major challenge in bioprinting aimed at the regeneration of dentoalveolar region is to address the biological heterogeneity. While different biomaterial properties are known to affect the behaviour of stem cells, such as the impact of stiffness on the differentiation behaviour of dental pulp stem cells [51,52], addressing the very complex heterogeneity of the dentoalveolar tissues could be achieved through the incorporation of specific sustained release drug delivery systems [53]. A range of such systems have been designed to be integrated in tissue engineering strategies [54,55], including solutions such as the development of porous scaffolds with controlled pore size and structure [56]. However, the most versatile option appears to be incorporation of the micro and nano particles within tissue engineering strategies. The reason for this is the capability to incorporate different biomolecules and drugs within the same tissue engineering scaffold [57], in addition to specific control over the release profile for each of these molecules [54]. However, to be useful for tissue engineering strategies, such systems require properties such as degradability, biocompatibility, and a sustained release profile [58]. Current systems used for delivery in tissue engineering strategies suffer from shortcomings such as a lack of degradability or toxic byproducts, lack of control over release properties, and absence of a uniform molecular structure caused by simple blending of different constituents [58,59]. PNIPAM-based microgels are widely known to be useful in a range of drug delivery approaches [60,61]. While pNIPAM-based microgels consist of a polymeric network capable of encapsulating drugs and biological molecules, most of these strategies utilize the temperature sensitivity of pNIPAM to induce localized release based on the temperature [62]. In these strategies, the majority of the drug is released upon application

of temperature, and hence, might not be suitable for sustained release profiles required in tissue engineering strategies [63,64]. Still, it was demonstrated in chapter 5 of this thesis, that the water release from pNIPAM could be controlled through copolymerization with methylcellulose. Consequently, it was hypothesized that synthesis of this material in the form of microgels, could potentially form drug carrier microgels capable of releasing the drugs over prolonged periods of time. As a result, chapter 6 focused on the development of pNIPAM-methylcellulose microgels, crosslinked through the incorporation of methylene bis acrylamide, aimed at delivery of drugs within tissue engineering strategies. A factorial design of experiments was used to evaluate the effect of different synthesis parameters on the final properties of these microgels such as drug loading and drug release. It was successfully demonstrated in this study, that pNIPAM based microgels could be used for efficient sustained delivery of drugs and signalling molecules over a week, while the majority of research before this was focused on burst release from these microgels [63–65]. Additionally, it was shown that properties (such as its release profile) could be effectively controlled through the adjustment of synthesis parameters, since for example the crosslinking degree was shown to be significantly influential on drug loading and drug release. Following this, the microgels developed in this study were evaluated for their ability to be incorporated within bioprinting strategies. As demonstrated in chapter 7, these microgels could be effectively encapsulated in gelMA, which was chosen as one of the most widely used bioinks [66,67], without having any negative impact on printability of gelMA. In fact, incorporation of these microgels enhanced the printability of gelMA resulting in an increased accuracy within the printed constructs and hence, confirming the applicability of the microgels within tissue engineering strategies including bioprinting.

8.2 Conclusions and future perspectives

Considering the recent application of bioprinting in tissue engineering strategies aimed at the regeneration of dentoalveolar region, this thesis focused on the development of biomaterials capable of being used as bioinks and biomaterial inks for bioprinting strategies in this region.

Maleic modified chitosan was the first biomaterial developed for this purpose. While this material proved suitable for tissue engineering research, including fabrication of scaffolds through 3D printing, encapsulation of cells in the proposed strategy was not possible due to the prolonged crosslinking times. Further research on this material could include the development of strategies to encapsulate cells and move from a biomaterial ink towards a bioink. This could be performed through reducing the crosslinking time, and hence, exposure of the cells to toxic concentrations of the crosslinkers. For example, this could be performed through analysis and optimization of photocrosslinking of maleic side groups. Other than that, this material could be used for analysis of tissue formation through cell seeding on hydrogel-based scaffolds including the chitosan derivative. In addition to this material, a copolymer of chitosan and pNIPAM was developed and its suitability for 3D printing of scaffolds, along with its biocompatibility were demonstrated. Control of syneresis without the use of chemical crosslinker is an area of research which could result in further use of this material in bioprinting strategies. In this thesis, this was achieved through the use of methylcellulose, and development of methacrylated methylcellulose pNIPAM copolymer. This developed copolymer proved suitable for bioprinting applications, as rapid gelation upon application of temperature was observed, along with the suitability of the gel for encapsulation of cells and bioprinting at 37 °C. Considering the heterogeneity of the dentoalveolar complex, this material, based on a synthetic polymer, could be used in further research, controlling its physical and mechanical properties such as stiffness to address tissue engineering of different tissues in the region. This could be achieved via modification of the synthesis procedure to achieve specific polymer chain lengths, enhancing the capability to tune material properties based on requirements of each specific tissue. Thus, this biomaterial enables research on tissue engineering of complex structures such as pulp-dentin or periodontal ligament. Furthermore, such control enables the use of this polymer for different bioprinting modalities, as the material properties vary significantly depending on temperature and hence, it can be optimized for use in inkjet bioprinting in addition to extrusion. For example, this could be achieved through inkjet printing of the material at room temperature coupled with a heated printbed,

enabling inkjet printing aimed at tissues requiring a higher resolution, such as the periodontal ligament. Furthermore, protein adsorption on pNIPAM, which enhances the cell response, is temperature-dependent and takes place at temperatures above the LCST. As a result, further modification of the material through covalent linking of the proteins could be used to enhance the cell response of the cells encapsulated in the proposed material. Consequently, further research using this material will be focused on modification of the material to address requirements of different tissue structures in the region.

In addition to these, the methylcellulose-pNIPAM based microgels developed demonstrated a capability of loading and sustained release of a model for small molecule drugs, and capability of being used in tissue engineering strategies. In this thesis, the focus has been on the development and characterization of these delivery vehicles, and demonstration of their applicability in tissue engineering strategies. Consequently, further research would encompass first, analysing the use of these microgels for delivery of proteins and growth factors, and second, use of these products in tissue engineering strategies, including entrapment of growth factors, and demonstrating their impact on cells utilized in the tissue engineering strategies.

Overall, this thesis developed solutions which could be applied in bioprinting strategies, and enable addressing of the biological, physical and mechanical heterogeneity of the dentoalveolar tissues. This was performed through the development of biomaterials for biomaterial ink and bioink formulations based on highly tunable chemistry, and through the development of drug delivery approaches capable of being integrated with those bioinks. Further research would require a focus on utilizing these developed solutions in the development of tissue engineering scaffolds with gradients of properties aimed at regeneration of specific tissues within the dentoalveolar region. Some possible strategies for this research are presented in figure 8.1, where these solutions could be applied to tissue engineering of pulp-dentin, alveolar bone and the periodontal ligament through bioprinting.

As suggested in figure 8.1, different ratios of NIPAM to methylcellulose could be used in the synthesis of the pNIPAM-methylcellulose bioink to achieve varying degrees of stiffness for the core and the outer layer, guiding differentiation of DPSCs to

odontoblasts at the interface with dentin [50]. This is feasible through the developed synthesis method as the collapse of pNIPAM chains is known to significantly affect hydrogel stiffness [68] and thus, a higher ratio of pNIPAM could be used to enhance the stiffness of the bioink. Furthermore, to enhance the dentin regeneration in layers surrounding the pulp core, sustained release of TGF-β can be used to induce odontoblastic differentiation of DPSCs [69]. In addition to this localized differentiation, the pulp core is a vascularized tissue. To address this demand, a coculture of DPSCs and HUVECs can be suggested, along with sustained release of VEGF through encapsulation in microgels aimed at promoting angiogenesis in the hydrogels, as each of these strategies have been used to engineer vascular tissue [9,70]. The same bioink useful for dentin, could be applied to regeneration of alveolar bone with different cell types and growth factors. For this purpose, stem cells from apical papilla (SCAPs), which have been used for bone regeneration through bioprinting [71], could be coupled with microgels releasing PDGF to further enhance bone regeneration, along with a thermoplastic support to assure construct integrity upon implantation. Similarly, the developed bioink and microgels could be applied for regeneration of periodontal ligament. For this purpose, the pNIPAM-methylcellulose bioink could be modified for inkjet printing at room temperature to enhance the printing resolution, as the polymer is in a highly viscose solution state at room temperature. Microgels loaded with IGF, encapsulated along with periodontal ligament stem cells (PDLSCs), could be used to enhance bone regeneration at the interface with bone, and the interface with the tooth could be printed using the genipin crosslinked copolymer of gelatin and maleic grafted chitosan developed in chapter 3, due to the antimicrobial properties offered by chitosan. The middle section would include PDLSCs in the bioink with a lower pNIPAM ratio to allow for a closer resemblance to the natural soft tissue.

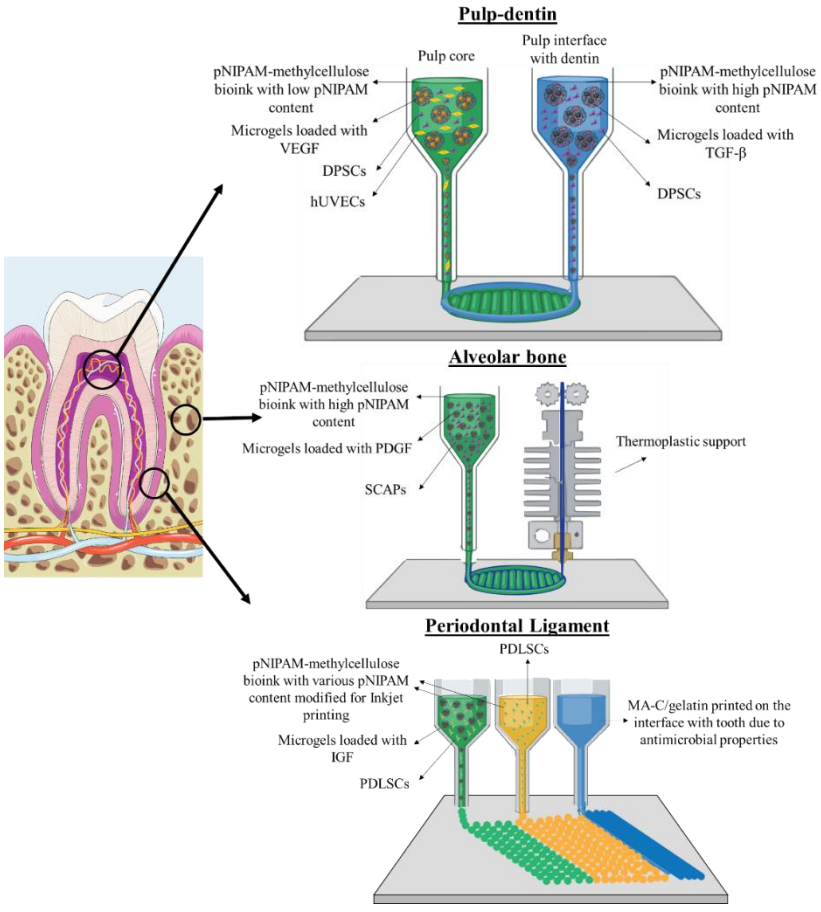

Figure 8.1. Schematic representation of suggestive approaches for further utilization of the strategies developed in this thesis towards addressing the complexities in tissue engineering of the dentoalveolar region, the top picture represents a suggestive strategy for pulp-dentin regeneration, followed by alveolar bone and periodontal ligament. Abbreviations: pNIPAM: poly n-isopropylacrylamide, VEGF: vascular endothelial growth factor, DPSC: dental pulp stem cell, hUVEC: human umbilical vein endothelial cell, TGF: transforming growth factor, PDGF: platelet derived growth factor, SCAP: stem cells from apical papilla, IGF: insulin like growth factor, PDLSC: periodontal ligament stem cell, MA-C: maleic grafted chitosan (figure elements obtained from smart.servier.com, and biorender.com)

8.3 References

1. Khodakaram-Tafti A, Mehrabani D, Shaterzadeh-Yazdi H, Zamiri B, Omidi M. "Tissue Engineering in Maxillary Bone Defects". World J Plast Surg. 2018 Jan;7(1):3–11.
2. Shaddox LM, Walker CB. "Treating chronic periodontitis: current status, challenges, and future directions.". Clin Cosmet Investig Dent. 2010;2:79–91.
3. "Oral health". 2020 Jul 28 [cited 2020 Jul 28];
4. Hanif A, Qureshi S, Sheikh Z, Rashid H. "Complications in implant dentistry". Eur J Dent. 2017;11(1):135–40.
5. EzEldeen M, Wyatt J, Al-Rimawi A, Coucke W, Shaheen E, Lambrichts I, Willems G, Politis C, Jacobs R. "Use of CBCT Guidance for Tooth Autotransplantation in Children.". J Dent Res. 2019 Apr;98(4):406–13.
6. Mahardawi B, Boonsiriseth K, Pairuchvej V, Wongsirichat N. "Alveolar cleft bone grafting: factors affecting case prognosis.". J Korean Assoc Oral Maxillofac Surg. 2020 Dec;46(6):409–16.
7. Martin K, Nathwani S, Bunyan R. "Autotransplantation of teeth: an evidence-based approach.". Br Dent J. 2018 Jun;224(11):861–4.
8. Na S, Zhang H, Huang F, Wang W, Ding Y, Li D, Jin Y. "Regeneration of dental pulp/dentine complex with a three-dimensional and scaffold-free stem-cell sheet-derived pellet.". J Tissue Eng Regen Med. 2016 Mar;10(3):261–70.
9. Kim JY, Xin X, Moioli EK, Chung J, Lee CH, Chen M, Fu SY, Koch PD, Mao JJ. "Regeneration of dental-pulp-like tissue by chemotaxis-induced cell homing.". Tissue Eng Part A. 2010 Oct;16(10):3023–31.
10. Chen FM, Zhang J, Zhang M, An Y, Chen F, Wu ZF. "A review on endogenous regenerative technology in periodontal regenerative medicine". Biomaterials. 2010;31(31):7892–927.
11. Abou Neel EA, Chrzanowski W, Salih VM, Kim HW, Knowles JC. "Tissue engineering in dentistry". J Dent. 2014 Aug 1 [cited 2020 Feb 18];42(8):915–28.
12. Galler KM, Hartgerink JD, Cavender AC, Schmalz G, D'Souza RN. "A customized self-assembling peptide hydrogel for dental pulp tissue engineering.". Tissue Eng Part A. 2012 Jan;18(1–2):176–84.
13. Kim NR, Lee DH, Chung PH, Yang HC. "Distinct differentiation properties of human dental pulp cells on collagen, gelatin, and chitosan scaffolds.". Oral Surg Oral Med Oral Pathol Oral Radiol Endod. 2009 Nov;108(5):e94-100.
14. Cordeiro MM, Dong Z, Kaneko T, Zhang Z, Miyazawa M, Shi S, Smith AJ, Nör JE. "Dental pulp tissue engineering with stem cells from exfoliated deciduous teeth.". J Endod. 2008 Aug;34(8):962–9.
15. Kim SG, Zheng Y, Zhou J, Chen M, Embree MC, Song K, Jiang N, Mao JJ. "Dentin and dental pulp regeneration by the patient's endogenous cells". Endod Top. 2013 Mar;28(1):106–17.
16. Galler KM, Eidt A, Schmalz G. "Cell-free Approaches for Dental Pulp Tissue Engineering". J Endod. 2014 Apr 1;40(4):S41–5.
17. EzEldeen M, Van Gorp G, Van Dessel J, Vandermeulen D, Jacobs R. "3-dimensional analysis of regenerative endodontic treatment outcome.". J Endod. 2015 Mar;41(3):317–24.
18. Scantlebury T, Ambruster J. "The Development of Guided Regeneration: Making the Impossible Possible and the Unpredictable Predictable". J Evid Based Dent Pract. 2012;12(3, Supplement):101–17.
19. Smith BT, Shum J, Wong M, Mikos AG, Young S. "Bone Tissue Engineering

Challenges in Oral & Maxillofacial Surgery.". Adv Exp Med Biol. 2015;881:57–78.
20. Porta M, Tonda-Turo C, Pierantozzi D, Ciardelli G, Mancuso E. "Towards 3D Multi-Layer Scaffolds for Periodontal Tissue Engineering Applications: Addressing Manufacturing and Architectural Challenges". Vol. 12, Polymers. 2020.
21. Sloan AJ. "Chapter 29 - Biology of the Dentin-Pulp Complex". In: Vishwakarma A, Sharpe P, Shi S, Ramalingam MBTSCB and TE in DS, editors. Boston: Academic Press; 2015. p. 371–8.
22. Moroni L, Boland T, Burdick JA, De Maria C, Derby B, Forgacs G, Groll J, Li Q, Malda J, Mironov VA, Mota C, Nakamura M, Shu W, Takeuchi S, Woodfield TBF, Xu T, Yoo JJ, Vozzi G. "Biofabrication: A Guide to Technology and Terminology". Trends Biotechnol. 2018 Apr 1;36(4):384–402.
23. Jammalamadaka U, Tappa K. "Recent Advances in Biomaterials for 3D Printing and Tissue Engineering.". J Funct Biomater. 2018 Mar;9(1).
24. Amoli M, EzEldeen M, Jacobs R, Bloemen V, Salar Amoli M, EzEldeen M, Jacobs R, Bloemen V. "Materials for Dentoalveolar Bioprinting: Current State of the Art". Biomed . 2022 Dec 30;10(1):71.
25. Ahsan SM, Thomas M, Reddy KK, Sooraparaju SG, Asthana A, Bhatnagar I. "Chitosan as biomaterial in drug delivery and tissue engineering". Int J Biol Macromol. 2018;110:97–109.
26. Fakhri E, Eslami H, Maroufi P, Pakdel F, Taghizadeh S, Ganbarov K, Yousefi M, Tanomand A, Yousefi B, Mahmoudi S, Kafil HS. "Chitosan biomaterials application in dentistry". Int J Biol Macromol. 2020;162:956–74.
27. LogithKumar R, KeshavNarayan A, Dhivya S, Chawla A, Saravanan S, Selvamurugan N. "A review of chitosan and its derivatives in bone tissue engineering". Carbohydr Polym. 2016;151:172–88.
28. Qin C, Li H, Xiao Q, Liu Y, Zhu J, Du Y. "Water-solubility of chitosan and its antimicrobial activity". Carbohydr Polym. 2006;63(3):367–74.
29. Salar Amoli M, Anand R, EzEldeen M, Amorim PA, Geris L, Jacobs R, Bloemen V. "The development of a 3D printable chitosan-based copolymer with tunable properties for dentoalveolar regeneration". Carbohydr Polym. 2022;289:119441.
30. Lee D, Park JP, Koh MY, Kim P, Lee J, Shin M, Lee H. "Chitosan-catechol: a writable bioink under serum culture media". Biomater Sci. 2018;6(5):1040–7.
31. Huang J, Fu H, Wang Z, Meng Q, Liu S, Wang H, Zheng X, Dai J, Zhang Z. "BMSCs-laden gelatin/sodium alginate/carboxymethyl chitosan hydrogel for 3D bioprinting". RSC Adv. 2016;6(110):108423–30.
32. Wang C, Lau TT, Loh WL, Su K, Wang DA. "Cytocompatibility study of a natural biomaterial crosslinker--Genipin with therapeutic model cells.". J Biomed Mater Res B Appl Biomater. 2011 Apr;97(1):58–65.
33. Jain K, Vedarajan R, Watanabe M, Ishikiriyama M, Matsumi N. "Tunable LCST behavior of poly(N-isopropylacrylamide/ionic liquid) copolymers". Polym Chem. 2015;6(38):6819–25.
34. Lemanowicz M, Gierczycki A, Kuźnik W, Sancewicz R, Imiela P. "Determination of Lower Critical Solution Temperature of thermosensitive flocculants". Miner Eng. 2014;69:170–6.
35. Strachota B, Strachota A, Šlouf M, Brus J, Cimrová V. "Monolithic intercalated PNIPAm/starch hydrogels with very fast and extensive one-way

volume and swelling responses to temperature and pH: prospective actuators and drug release systems". Soft Matter. 2019;15(4):752–69.
36. Contreras-Cáceres R, Pacifico J, Pastoriza-Santos I, Pérez-Juste J, Fernández-Barbero A, Liz-Marzán LM. "Au@pNIPAM Thermosensitive Nanostructures: Control over Shell Cross-linking, Overall Dimensions, and Core Growth". Adv Funct Mater. 2009 Oct 9;19(19):3070–6.
37. Duan C, Zhang D, Wang F, Zheng D, Jia L, Feng F, Liu Y, Wang Y, Tian K, Wang F, Zhang Q. "Chitosan-g-poly(N-isopropylacrylamide) based nanogels for tumor extracellular targeting". Int J Pharm. 2011;409(1):252–9.
38. Sanzari I, Buratti E, Huang R, Tusan CG, Dinelli F, Evans ND, Prodromakis T, Bertoldo M. "Poly(N-isopropylacrylamide) based thin microgel films for use in cell culture applications". Sci Rep. 2020;10(1):6126.
39. Ribeiro CA, Martins MVS, Bressiani AH, Bressiani JC, Leyva ME, de Queiroz AAA. "Electrochemical preparation and characterization of PNIPAM-HAp scaffolds for bone tissue engineering". Mater Sci Eng C. 2017;81:156–66.
40. Tavagnacco L, Zaccarelli E, Chiessi E. "On the molecular origin of the cooperative coil-to-globule transition of poly(N-isopropylacrylamide) in water". Phys Chem Chem Phys. 2018;20(15):9997–10010.
41. Zhang L, Wang L, Guo B, Ma PX. "Cytocompatible injectable carboxymethyl chitosan/N-isopropylacrylamide hydrogels for localized drug delivery.". Carbohydr Polym. 2014 Mar;103:110–8.
42. Spencer JN, Wolbach WS, Hovick JW, Ansel L, Modarress KJ. "Hydrogen bonding by alcohols and amines". J Solution Chem. 1985;14(11):805–14.
43. Monteiro N, Thrivikraman G, Athirasala A, Tahayeri A, França CM, Ferracane JL, Bertassoni LE. "Photopolymerization of cell-laden gelatin methacryloyl hydrogels using a dental curing light for regenerative dentistry.". Dent Mater. 2018 Mar;34(3):389–99.
44. Lin YT, Hsu TT, Liu YW, Kao CT, Huang TH. "Bidirectional Differentiation of Human-Derived Stem Cells Induced by Biomimetic Calcium Silicate-Reinforced Gelatin Methacrylate Bioink for Odontogenic Regeneration". Vol. 9, Biomedicines . 2021.
45. Willing RP, Leopold AC. "Cellular expansion at low temperature as a cause of membrane lesions.". Plant Physiol. 1983 Jan;71(1):118–21.
46. Ouyang L, Yao R, Zhao Y, Sun W. "Effect of bioink properties on printability and cell viability for 3D bioplotting of embryonic stem cells". Biofabrication. 2016 Sep;8(3):035020.
47. Schuurman W, Levett PA, Pot MW, van Weeren PR, Dhert WJA, Hutmacher DW, Melchels FPW, Klein TJ, Malda J. "Gelatin-methacrylamide hydrogels as potential biomaterials for fabrication of tissue-engineered cartilage constructs.". Macromol Biosci. 2013 May;13(5):551–61.
48. Narayanan LK, Huebner P, Fisher MB, Spang JT, Starly B, Shirwaiker RA. "3D-Bioprinting of Polylactic Acid (PLA) Nanofiber–Alginate Hydrogel Bioink Containing Human Adipose-Derived Stem Cells". ACS Biomater Sci Eng. 2016 Oct 10;2(10):1732–42.
49. Du M, Chen B, Meng Q, Liu S, Zheng X, Zhang C, Wang H, Li H, Wang N, Dai J. "3D bioprinting of BMSC-laden methacrylamide gelatin scaffolds with CBD-BMP2-collagen microfibers.". Biofabrication. 2015 Dec;7(4):44104.
50. Liu N, Zhou M, Zhang Q, Zhang T, Tian T, Ma Q, Xue C, Lin S, Cai X. "Stiffness regulates the proliferation and osteogenic/odontogenic differentiation of human dental pulp stem cells via the WNT signalling

pathway". Cell Prolif. 2018 Apr 1;51(2):e12435.
51. Ansari S, Chen C, Hasani-Sadrabadi MM, Yu B, Zadeh HH, Wu BM, Moshaverinia A. "Hydrogel elasticity and microarchitecture regulate dental-derived mesenchymal stem cell-host immune system cross-talk.". Acta Biomater. 2017 Sep;60:181–9.
52. Han J, Kim DS, Jang H, Kim HRHW, Kang HW, Shaddox LM, Walker CB, Schiffman EL, Velly AM, Look JO, Hodges JS, Swift JQ, Decker KL, Anderson QN, Templeton RB, Lenton PA, Kang W, Fricton JR, Amrollahi P, et al. "Bioprinting of three-dimensional dentin-pulp complex with local differentiation of human dental pulp stem cells.". Kahveci MU, editor. J Tissue Eng. 2017/10/03. 2019 Mar 10;10(3):2041731419845849.
53. Moioli EK, Clark PA, Xin X, Lal S, Mao JJ. "Matrices and scaffolds for drug delivery in dental, oral and craniofacial tissue engineering.". Adv Drug Deliv Rev. 2007 May;59(4–5):308–24.
54. Reed S, Wu B. "Sustained Growth Factor Delivery in Tissue Engineering Applications". Ann Biomed Eng. 2014;42(7):1528–36.
55. Biondi M, Ungaro F, Quaglia F, Netti PA. "Controlled drug delivery in tissue engineering". Adv Drug Deliv Rev. 2008;60(2):229–42.
56. Calori IR, Braga G, de Jesus P da CC, Bi H, Tedesco AC. "Polymer scaffolds as drug delivery systems". Eur Polym J. 2020;129:109621.
57. Santoro M, Tatara AM, Mikos AG. "Gelatin carriers for drug and cell delivery in tissue engineering". J Control Release. 2014;190:210–8.
58. Balmayor ER, Tuzlakoglu K, Azevedo HS, Reis RL. "Preparation and characterization of starch-poly-ε-caprolactone microparticles incorporating bioactive agents for drug delivery and tissue engineering applications". Acta Biomater. 2009;5(4):1035–45.
59. Sherstneva AA, Demina TS, Monteiro APF, Akopova TA, Grandfils C, Ilangala AB. "Biodegradable Microparticles for Regenerative Medicine: A State of the Art and Trends to Clinical Application.". Polymers (Basel). 2022 Mar;14(7).
60. Liu L, Zeng J, Zhao X, Tian K, Liu P. "Independent temperature and pH dual-responsive PMAA/PNIPAM microgels as drug delivery system: Effect of swelling behavior of the core and shell materials in fabrication process". Colloids Surfaces A Physicochem Eng Asp. 2017;526:48–55.
61. Chen Y, Chen Y, Nan J, Wang C, Chu F. "Hollow poly(N-isopropylacrylamide)-co-poly(acrylic acid) microgels with high loading capacity for drugs". J Appl Polym Sci. 2012 Jun 15;124(6):4678–85.
62. Martinez-Moro M, Jenczyk J, Giussi JM, Jurga S, Moya SE. "Kinetics of the thermal response of poly(N-isopropylacrylamide co methacrylic acid) hydrogel microparticles under different environmental stimuli: A time-lapse NMR study". J Colloid Interface Sci. 2020;580:439–48.
63. Kim YK, Kim EJ, Lim JH, Cho HK, Hong WJ, Jeon HH, Chung BG. "Dual Stimuli-Triggered Nanogels in Response to Temperature and pH Changes for Controlled Drug Release.". Nanoscale Res Lett. 2019 Mar;14(1):77.
64. Xu F, Yan TT, Luo YL. "Thermosensitive poly(N-isopropyl acrylamide-co-N,N-dimethyl acryl amide)-block-poly(D,L-lactide) amphiphilic block copolymer micelles for prednisone drug release". J Bioact Compat Polym. 2013 Jan 15;28:66–85.
65. Feng Q, Zhao Y, Li H, Zhang Y, Xia X, Yan Q. "Frontal polymerization and characterization of interpenetrating polymer networks composed of poly(N-isopropylacrylamide) and polyvinylpyrrolidone". Colloid Polym Sci.

2018;296(1):165–72.
66. Shi Y, Xing TL, Zhang HB, Yin RX, Yang SM, Wei J, Zhang WJ. "Tyrosinase-doped bioink for 3D bioprinting of living skin constructs.". Biomed Mater. 2018 Mar;13(3):35008.
67. Xu L, Varkey M, Jorgensen A, Ju J, Jin Q, Park JH, Fu Y, Zhang G, Ke D, Zhao W, Hou R, Atala A. "Bioprinting small diameter blood vessel constructs with an endothelial and smooth muscle cell bilayer in a single step.". Biofabrication. 2020 Jul;12(4):45012.
68. de Almeida P, Jaspers M, Vaessen S, Tagit O, Portale G, Rowan AE, Kouwer PHJ. "Cytoskeletal stiffening in synthetic hydrogels.". Nat Commun. 2019 Feb;10(1):609.
69. Tsutsui TW. "Dental Pulp Stem Cells: Advances to Applications.". Stem Cells Cloning. 2020;13:33–42.
70. Dissanayaka WL, Hargreaves KM, Jin L, Samaranayake LP, Zhang C. "The Interplay of Dental Pulp Stem Cells and Endothelial Cells in an Injectable Peptide Hydrogel on Angiogenesis and Pulp Regeneration In Vivo". Tissue Eng Part A. 2014 Sep 9;21(3–4):550–63.
71. Touya N, Devun M, Handschin C, Casenave S, Ahmed Omar N, Gaubert A, Dusserre N, De Oliveira H, Kérourédan O, Devillard R. "In vitroandin vivocharacterization of a novel tricalcium silicate-based ink for bone regeneration using laser-assisted bioprinting.". Biofabrication. 2022 Mar;14(2).

Chapter 9. Valorization potential of the research

Chapter summary

Within this PhD thesis, a range of solutions have been proposed to address some challenges associated with the tissue engineering of the complex tissue architecture, present in the dentoalveolar region. Developed solutions are mainly within two categories, the first one being the materials with potential to be used in advanced manufacturing techniques, such as bioprinting, and the second one being delivery vehicles beneficial to address biological heterogeneity within such tissues and organs. However, while the field of tissue engineering and more specifically, bioprinting, has aimed to address the challenge of mimicking natural tissue architecture through a wide range of studies and research, a long road still exists before such technologies could be used in clinics benefiting patients. Consequently, to achieve this invaluable goal, collective effort of all researchers in the field including biomaterial scientists, biologists and clinical experts, is necessary, enhancing the progress of research towards clinically relevant developments. Being one of the first steps in the tissue engineering process, certain innovative solutions such as the biomaterials for tissue engineering, have been commercialized by some companies and businesses with varying degrees of success. This will enable further researchers to take a leap from development of such solutions to clinically relevant studies. As a result, this chapter will provide a roadmap for the solutions developed in this thesis, including the biomaterials aimed at bioprinting of the dentoalveolar tissues, and the microgels developed for drug delivery in these strategies, to be valorised within the academic community. This could enable the access of researchers to developed solutions for further studies.

9.1 Introduction

The field of tissue engineering has presented a promising opportunity to address shortcomings of traditional clinical interventions by combination of cells, materials and signalling molecules aimed at the regeneration of damaged tissues [1]. However, for the tissue engineering effort to be successful, developing tissue analogues need to reflect the native tissue, in terms of both its structure, and its biological properties [2]. Recent advances in scaffold fabrication, and emergence of techniques such as 3D bioprinting has enhanced precision of replicating tissue architectures significantly through a robust and replicable manufacturing process [3]. Still, while these techniques enable mimicking the natural structure in terms of its architecture, replicating the mechanical, physical and biological heterogeneities demands further research regarding control over material properties and behavior of cells incorporated within these tissue engineering strategies [4, 5].

The development of biomaterials for use within bioprinting strategies, and the development of delivery systems capable of being incorporated within these efforts, are wide areas of research requiring significant cost, time and effort. Consequently, commercialization of products useful for these studies can significantly accelerate the research and enable leaps towards fruition of the tissue engineering research in a clinical setting. Among the developed strategies, a range of such biomaterials, capable of being used along with the cells for the bioprinting process, have already been commercialized. Some of these materials include methacrylated gelatin (gelMA) [6], methacrylated hyaluronic acid [7], methacrylated collagen, and polyethylene glycol diacrylate [8]. While such commercialized products are valuable in promoting further research in the field and in enabling use of such technologies for biologists and clinical scientists, their variety is limited, and they offer a very narrow range of properties which might not be suitable for a large part of the demand. Furthermore, while addressing biological heterogeneity has been a concern in many of the commercialized products, such as products combining mentioned hydrogels with calcium phosphates for bone regeneration [9], controlling the behavior of stem cells through development of delivery

vehicles capable of efficient delivery of drugs and growth factors within the tissue engineering scaffolds and bioprinted constructs remains unexplored in the commercial space, despite being of major interest in the academic space.
Considering this demand, this chapter aims to demonstrate how the results presented within this PhD thesis could potentially be used in the development of a spin-off company offering viable solutions for academic researchers focusing on tissue engineering and bioprinting research.

9.2 Products and solutions

As mentioned in the introduction, a range of products already exist which are aimed at the bioprinting research market, and most of them are hydrogels and materials suitable for bioprinting. Still, they face shortcomings and only cover a small portion of the demands. Some of these demands include incorporation of other biomaterials with different properties, and the need for delivery systems within these approaches.
In this thesis, a variety of solutions have been developed addressing different demands within the tissue engineering research. Chapters 3, 4, and 5 are focused on development of biomaterials that could be used as inks for 3D printing and bioprinting research, along with other tissue engineering strategies. The water soluble chitosan derivative developed in chapter 3 enables the use of chitosan-based materials in the hydrogel form for tissue engineering and could have a wide range of applications in the biomedical research, and the thermo-sensitive pNIPAM biomaterials developed in chapters 4 and 5 could address a range of applications where instant temperature-based gelation of the material is required, such as *in situ* tissue engineering, in addition to bioprinting applications where incubation of cells at lower temperatures is not desired due to potential harmful effects on the cells [10,11]. This presents an advantage over commercially available temperature sensitive materials, where most of them, such as gelatin based materials, form a gel at temperatures lower than physiological temperature.
Aside from the developed biomaterials, microgels capable of loading and sustained release of small molecule drugs within the tissue

engineering strategies were developed as described in chapter 6. While further optimization is required to evaluate loading and release of macromolecules such as proteins, these microgels could be used to address biological heterogeneity within tissue structures through delivery of required signalling molecules. Taking into account lack of commercially available delivery vehicles with tuenable properties for different demands, these microgels could address a wide variety of requirements within the research community looking for efficient delivery of biomolecules within their strategies.

The solutions described in chapters 3 to 6, each address specific demands within the field of tissue engineering. Providing access to these solutions through commercialization targeting the academic research community could provide a basis for further research using each of the described solutions, and in turn, assist in taking necessary steps towards clinical use of these products.

9.3 Market

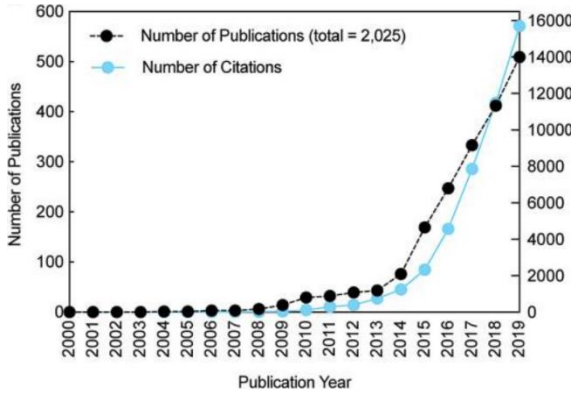

Figure 9.1. Number of studies involving bioprinting from year 2000 to 2019, obtained from [12]

Bioprinting and 3D printing is an emerging area of research within the larger horizon of tissue engineering. Yet, the number of studies focused on these technologies has grown exponentially within the last few years, due to the advantages and potentials offered by these solutions. This significant growth in research using bioprinting is represented in figure 9.1, demonstrating the number of studies performed using bioprinting from 2000 to 2019, obtained from [12].

This significant rise in research on bioprinting represents a vast interest and focus on research and development within this field. The global market value of the 3D bioprinting was estimated to be 1.7 billion USD in 2021, and it is estimated to have a compound annual growth rate (CAGR) of 15.8 % up to year 2030, reaching a value of 5.3 billion USD [13]. Given the fact that the application of bioprinting in a clinical setting is very limited, this market consists entirely of research and development. Consequently, the target market for the products described in section 3 of this chapter would be the tissue engineering research market focused on 3D printing and bioprinting, along with the more general tissue engineering market that can benefit from premade scaffolds and sustained release strategies within their approaches.

9.4 Exploitation strategy

The significant interest in the field of bioprinting, and the large market for its products resulted from that, has led to a significant amount of investment in small companies and start-ups producing bioprinters, bioinks, and other relating products. For example, Readily3D, a Switzerland based company specializing in development of volumetric bioprinting strategies received a €600,000 funding from European Union in 2021, or Aspect Biosystems, a Canadian start-up focused on development of tissue models through 3D bioprinting, received $20 million investment from a venture capital firm since 2013 when it was founded [14]. Furthermore, BIO INX, a Belgian company focused on development of bioinks, received an investment of €700,000 in 2022, demonstrating the interest in this market [15].

Consequently, the general aim of this valorisation plan is to demonstrate how the four presented products could be used as starting products for a start-up, focused on the development of materials and solutions for use in 3D bioprinting strategies. It should be noted that the described products are already published and consequently, are considered public domain. As a result, the major advantage in terms of entering the market would be the technical know-how for the process of production and analysis of the materials. However, for further products being derived from these, or modifications of these products, the general strategy would be to protect the products using patents

within the major markets, including Europe, USA, and China, before publishing the results in peer reviewed journals.
Following formation of the start-up, a multi angle dissemination strategy would be required to create awareness regarding these products within the scientific community and generate sales. In terms of creating awareness, this includes publication of the research and development results in peer-reviewed journals, creating an online presence and advertisement campaigns targeting researchers, including advertisement in online scientific forums such as LinkedIn, attending regional and international conferences and seminars in relevant fields, and direct contact with researchers in this area of study along with providing test samples. With regards to sales, the strategy needs to consider both direct sales through a website, and indirect sales through collaboration with industrial commercial partners such as Merck, ThermoFisher Scientifc or Abcam.

9.5 Challenges and competitors

Considering the widespread research on bioprinting, a large number of companies and start-ups have started focusing on this area of research, providing for different demands including bioprinters with multiple technologies, materials, along with cells and growth factors. Some of the most prominent businesses in this area include BICO group, Collplant biotechnologies, Jellagen, Rousselot, 4D Biomaterials, UPM biomedicals, Innoregen, Akira science, Axolotl Biosciences, Biofabics, Viscofan bioengineering, Foldink, Organovo Holdings, Inventia Life Science PTY, Vivax Bio, BIO INX, Allevi, Aspect Biosystems, Advanced Solutions Life Sciences, Rokit Healthcare, Pandorum Technologies, and Revotek co.
The range of companies mentioned focus on different aspects of the bioprinting process, such as development of materials for bioprinting, in companies such as Allevi or Bico group, or bioprinted implants such as Collplant Biotechnologies or Rokit Healthcare. This large number of competitors can be considered as a potential challenge against commercialization of the products through the spin-off strategy. However, this could be alleviated considering novelty of the products offered in this chapter compared to the currently available materials and solutions, and the widespread demand for them both in terms of

different materials, and in terms of the type of products offered, such as delivery vehicles capable of being used within tissue engineering strategies. Furthermore, this demand also presents an opportunity, as it demonstrates the interest of investors and funding agencies towards the aims of such companies, along with the demand in the market.
In addition to this, another challenge would be the translation of the work which has been performed in a laboratory setup to an industrial scale production. The larger industrial scale would require a different set of equipment capable of handling the required volume, and the production protocols would need to be optimized for this different setup. To address this, the equipment required for the sensitive, knowledge-based part of the production must be acquired, and this needs to be taken into account in the initial investment demands. However, some important parts of the production could be outsourced through collaboration with production companies. For example, steps in the production protocol such as lyophilization or sterilization, could be outsourced to businesses with specialized equipment for this type of procedures, such as Medistri or SGS belgium.

9.6 Economic/social value

Considering the significant rise in bioprinting research, and the advantages offered by the developed solutions for these studies, development of a spin-off company producing these products, and developing further products based on them can be of significant value for the community, both in terms of its economic output, and its effect on healthcare research.
In terms of the economic value, a startup producing solutions for bioprinting research could be compared with similar startups in Europe and United States. For example, Allevi, a US based company founded in 2014 specializing in bioprinters and bioinks, started with a 50 K USD initial investment and was valued at 3.5 million USD in 2021, employing 19 people [16]. Furthermore, Advanced BioMatrix, a similar company focused on development of materials for cell culture applications, was founded in 2006 and grew to a 15 million USD by 2021 when it was acquired by the BICO group [17]. These examples demonstrate significant room for growth for start-ups offering viable

solutions for different demands within the bioprinting/biomaterial research area.
However, while such companies offer valuable economic benefits to the society, in terms of the added value and employment of highly educated people, their impact is not limited to this direct economic value. As described extensively during the introduction of this thesis, medical interventions could benefit significantly from the development of tissue analogues capable of replicating the structure of complex heterogeneous tissue structures. However, development of such products requires extensive research on biomaterials capable of supporting functionality of cells, and on advanced manufacturing techniques such as bioprinting, along with further research on biology of tissue development, plus clinical trials and evaluations. Making developed solutions and biomaterials commercially available helps significantly in taking this research one step forward, through reducing the need for further research on biomaterials, and enhancing the capability of performing research on biological and clinical demands, potentially paving the way for clinical application of such advanced technologies. This is represented by the large body of research performed using commercial products of companies in this business [18–21].

9.7 Valorization roadmap

In order to transfer the described products to the research market, and to make them available through formation of a spin-off start-up, several steps need to be taken. Conceptualization of the products and development of an initial product have been completed through this PhD. Furthermore, validation of the products has been performed in specific setups, such as validation of the release of small molecules from the developed microgels, while further validation needs to be performed to assess suitability for a range of different setups and requirements. The remaining steps for effective valorization of the products include optimization of the technology in a laboratory setup, formation of the spin-off, generating awareness and production through collaborations with industrial partners, and development and

optimization of further products. These steps are schematically presented in figure 9.2.

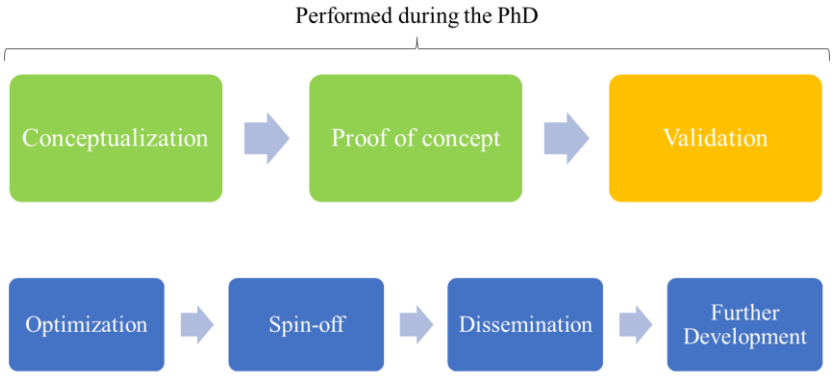

Figure 9.2. Suggested steps for valorization, completed steps are shown in green, steps that need to be taken are shown in blue

As demonstrated in figure 9.2, the first steps regarding product development for the base products of the spin-off are already taken within the context of this PhD program. Formation of the spin-off would be the next step. However, this step requires significant time and effort, as it includes securing investments which enable large scale production, advertising and further development of the products. The dissemination step, involving advertisement and publications using the products will be performed after the investments have been obtained, and will include spreading knowledge about the products through online advertising, conferences and publications, as well as targeted reach-out to laboratories conducting research in the field. After completion of these steps, it is expected that the spin-off would reach a stable revenue, which will enable further in-depth research on the products, and development of a range of solutions for a larger variety of applications within the bioprinting and biomedical research field.

9.8 References

1. Langer R, Vacanti J. "Advances in tissue engineering". J Pediatr Surg. 2016;51(1):8–12.
2. Edgar L, McNamara K, Wong T, Tamburrini R, Katari R, Orlando G. "Heterogeneity of Scaffold Biomaterials in Tissue Engineering.". Mater (Basel, Switzerland). 2016 May;9(5).
3. Murphy S V, Atala A. "3D bioprinting of tissues and organs.". Nat Biotechnol. 2014 Aug;32(8):773–85.

4. Amoli M, EzEldeen M, Jacobs R, Bloemen V, Salar Amoli M, EzEldeen M, Jacobs R, Bloemen V. "Materials for Dentoalveolar Bioprinting: Current State of the Art". Biomed . 2022 Dec 30;10(1):71.
5. Bittner SM, Guo JL, Mikos AG. "Spatiotemporal Control of Growth Factors in Three-Dimensional Printed Scaffolds.". Bioprinting (Amsterdam, Netherlands). 2018 Dec;12.
6. "X_PURE GELMA" [Https://www.rousselot.com/biomedical/products/x-pure-portfolio/x-pure-gelma]. [cited 2022 Sep 24].
7. "Methacrylated Hyaluronic acid (HA-MA)" [Https://www.nanosoftpolymers.com/product/methacrylated-hyaluronic-acid-ha-ma/]. [cited 2022 Sep 24].
8. "Innovative 3D Matrices for Breakthrough Research" [Https://advancedbiomatrix.com/].
9. "Cellink Bone" [Https://www.cellink.com/product/cellink-bone/]. [cited 2022 Sep 24].
10. Willing RP, Leopold AC. "Cellular expansion at low temperature as a cause of membrane lesions.". Plant Physiol. 1983 Jan;71(1):118–21.
11. Shiozaki A, Yamazato Y, Kosuga T, Kudou M, Shoda K, Arita T, Konishi H, Komatsu S, Kubota T, Fujiwara H, Okamoto K, Marunaka Y, Otsuji E. "Effect of low temperature on the regulation of cell volume after hypotonic shock in gastric cancer cells.". Int J Oncol. 2019 Oct;55(4):905–14.
12. Deo KA, Singh KA, Peak CW, Alge DL, Gaharwar AK. "Bioprinting 101: Design, Fabrication, and Evaluation of Cell-Laden 3D Bioprinted Scaffolds.". Tissue Eng Part A. 2020 Mar;26(5–6):318–38.
13. "3D Bioprinting Market Size & Share Report, 2022 - 2030" [Https://www.grandviewresearch.com/industry-analysis/3d-bioprinting-market]. 2021 [cited 2022 Sep 18].
14. "Global 3D Bioprinting Market" [Https://www.thebusinessresearchcompany.com/report/3d-bioprinting-global-market-report#:~:text=Rising governments and private funding to support 3D,healthcare attracted funding from government and private organizations.]. 2022 [cited 2022 Sep 19].
15. "Bio INX closes its first funding round" [Https://flanders.bio/en/news/bio-inx-closes-first-funding-round]. [cited 2022 Dec 13].
16. "Allevi Overview" [Https://pitchbook.com/profiles/company/97061-14#overview]. [cited 2022 Sep 24].
17. "Advanced BioMatrix Overview" [Https://pitchbook.com/profiles/company/223844-05#overview]. [cited 2022 Sep 24].
18. "Advanced Biomatrix Library" [Https://advancedbiomatrix.com/library/]. [cited 2022 Sep 24].
19. Gómez-Blanco JC, Mancha-Sánchez E, Marcos AC, Matamoros M, Díaz-Parralejo A, Pagador JB. "Bioink Temperature Influence on Shear Stress, Pressure and Velocity Using Computational Simulation". Vol. 8. 2020.
20. Pössl A, Hartzke D, Schmidts TM, Runkel FE, Schlupp P. "A targeted rheological bioink development guideline and its systematic correlation with printing behavior.". Biofabrication. 2021 Apr;13(3).
21. Schmidt SK, Schmid R, Arkudas A, Kengelbach-Weigand A, Bosserhoff AK. "Tumor Cells Develop Defined Cellular Phenotypes After 3D-Bioprinting in Different Bioinks". Vol. 8. 2019.

Curriculum Vitae

Mehdi Salar Amoli
Mehdi.salaramoli@kuleuven.be

Academic Background

- Feb 2019 – Feb 2023: PhD researcher, Surface and Interface Engineered Materials (SIEM), Campus Group T, KU Leuven
    - Topic: "Development of inks for tissue engineering of the dentoalveolar region through bioprinting", KU Leuven, Belgium
    - Supervisor: Prof. Dr. Veerle Bloemen, Co-supervisor: Prof. Dr. Reinhilde Jacobs
- 2017 – 2018: Master of science in "Biomaterials and Tissue Engineering" at bioengineering department, Imperial College London
    - Dissertation: Prof. Molly Stevens group," Development of non-viral gene delivery techniques using silicon nanoneedles"
    - Final qualification: UK Merit
    - Dissertation qualification: UK Distinction
- 2013-2017: Bachelor of science in "Biomaterials and Tissue Engineering" at bioengineering faculty, Amirkabir University of Technology.
    - Dissertation: Prof. Atefeh Solouk group, "Production and Morphology Evaluation of Bioglass /Gelatin /Chitosan Drug Loaded Scaffold for Osteochondral Tissue Engineering"
    - Score of final two years: 18.06/20 (A^+)
    - General score: 17.03/20 (A)
    - Dissertation mark: 19.5/20 (A^+)
- 2013: Position in konkoor (Iranian universities entrance exam): top 3 percent
- 2009-2013: Diploma: in mathematics
    - Score: 18.88/20 (A^+)

Conferences

- "Development of a photocrosslinkable pNIPAM-methylcellulose bioink for dentoalveolar bioprinting", Belgian symposium on tissue engineering, 2022
- "Development and characterization of pNIPAM-based microgels for drug delivery within dentoalveolar tissue engineering strategies", European Society for Biomaterials, 2022
- "Development, characterization and encapsulation of drug loaded microgels in bioinks aimed at dentoalveolar bioprinting", 3D Bioprinting International Conference, 2022
- "Development and characterization of colloidal pNIPAM-based microgels for delivery of growth factors in dentoalveolar tissue engineering strategies", Belgian society of tissue engineering symposium, 2021

- "3D printable hydrogel scaffold for regeneration of dental pulp", Belgian society of tissue engineering symposium, 2019
- "Intracellular siRNA delivery using silicon nanoneedle arrays", British society for gene and cell therapy, autumn conference, 2018

Journal Publications

- Anand R, Salar Amoli M, Huysecom AS, Amorim PA, Agten H, Geris L, Bloemen V. "A tunable gelatin-hyaluronan dialdehyde/methacryloyl gelatin interpenetrating polymer network hydrogel for additive tissue manufacturing", Vol 17, Biomedical Materials, 2022
- Salar Amoli M, Anand R, EzEldeen M, Amorim PA, Geris L, Jacobs R, Bloemen V. "The development of a 3D printable chitosan-based copolymer with tunable properties for dentoalveolar regeneration", Vol. 289, Carbohydrate Polymers, 2022
- Salar Amoli M, EzEldeen M, Jacobs R, Bloemen V. "Materials for Dentoalveolar Bioprinting: Current State of the Art". Vol. 10, Biomedicines, 2022.
- Gu Y, Ma H, Shujaat S, Orhan K, Coucke W, Salar Amoli M, et al. "Donor- and recipient-site morbidity of vascularized fibular and iliac flaps for mandibular reconstruction: A systematic review and meta-analysis". Vol. 74, J Plast Reconstr Aesthetic Surg, 2021

Patents

- Iranian national patent No.73268
    - Topic: Air purifier from micron haze using 3-layers and washable filters
- Iranian national patent No.68668
    - Topic: Designing and manufacturing dual purpose washing resources

Teaching

- 2021-2022, Supervision of MSc Student, Mr. Thomas Van Laeken, "Development of poly-n-isopropylacrylamide based hydrogel for dentoalveolar bioprinting"
- 2020-2021, Supervision of MSc Student, Ms. Huimin Yang, "Development and Characterization of PNIPAM-methylcellulose Microgel and the Evaluation of drug encapsulation"
- 2021, MSc level, Lecture on "Design of experiments"
- 2020-2021, BSc level, Thermodynamics (B-KUL-T2THEE) exercise sessions, Teaching and examination within the Faculty of Engineering Technology Campus Groep T
- 2019-2020, BSc level, Thermodynamics exercise sessions, Teaching and examination within the Faculty of Engineering Technology Campus GroepT

Experiences

- Utrecht summer school of biofabrication 2019, Attendee, winner of best idea presentation
- Official member of Iranian National Elite Foundation since 2013
- Internship course at Iran's Polymer and Petrochemical Institute working on a polymeric biosensor for early detection of Alzheimer's disease (2016).
- IELTS test band score 8 (Listening 8, Reading 9, Speaking 8, Writing 7.5)